CHARACTERIZATION OF THE EARLY CELLULAR MECHANISMS PROMOTING MYOCARDIAL FIBROSIS

by

Mryanda Janet Sopel

Submitted in partial fulfilment of the requirements
for the degree of Doctor of Philosophy

at

Dalhousie University
Halifax, Nova Scotia
July 2012

DALHOUSIE UNIVERSITY

DEPARTMENT OF PATHOLOGY

The undersigned hereby certify that they have read and recommend to the Faculty of Graduate Studies for acceptance a thesis entitled "CHARACTERIZATION OF THE EARLY CELLULAR MECHANISMS PROMOTING MYOCARDIAL FIBROSIS" by Mryanda Janet Sopel in partial fulfillment of the requirements for the degree of Doctor of Philosophy.

Dated: July 13, 2012

External Examiner: _____

Research Co-Supervisors: _____

_____

Examining Committee: _____

_____

Departmental Representative: _____

DALHOUSIE UNIVERSITY

DATE: July 13, 2012

AUTHOR: Mryanda Janet Sopel

TITLE: CHARACTERIZATION OF THE EARLY CELLULAR MECHANISMS PROMOTING MYOCARDIAL FIBROSIS

DEPARTMENT OR SCHOOL: Department of Pathology

DEGREE: PhD CONVOCATION: October YEAR: 2012

_____

Signature of Author

For my mother and sister who were my rocks without even knowing it.

If your face is all swollen from the beatings of life, just smile and pretend like you're a fat man.

-- Nigerian Proverb

If it was going to be easy, someone else would have already done it.

-- Dr. Jean-Francois Légaré

Table of Contents

LIST OF TABLES

List of Figures

ABSTRACT

Myocardial fibrosis is a common pathological finding in patients with cardiovascular disease and is believed to be a major contributing factor in the development of end stage organ failure. Early events that promote the development of myocardial fibrosis are not well understood. Rapid cellular infiltration into the cardiac tissue is evident in fibrosis but the infiltrating populations and their functions have yet to be completely elucidated. The aim of this thesis was to characterize the phenotype and function of this cellular population in a model of hypertension mediated myocardial fibrosis. Furthermore, we intended to explore therapies that target this population and ameliorate fibrosis. We characterized a novel population of infiltrating cells as circulating fibroblast progenitor cells, termed fibrocytes. We determined that this population does not appear to specifically migrate in response to previously established chemotactic signals (CCL2 or CXCL12). We found that fibrocytes respond to fibrogenic stimuli (AngII and CTGF) by increasing the expression of collagen and CTGF, an early molecular mediator of fibrosis, while also promoting fibrocyte differentiation. Using an anti-hypertension treatment, we found that hypertension as a physiologic stimulus likely promotes cellular infiltration and corresponding fibrosis. We also established that treatment with activated protein C (aPC) conferred protection against the development of myocardial fibrosis, potentially by inhibiting fibrocyte recruitment and/or activation. Lastly, to assess fibrocyte involvement in the progression of human myocardial fibrosis we assessed fibrocytes in levels in the circulation of patients with ischemic heart disease compared to healthy controls. We found that patients with ischemic heart disease had an increase of circulating cells that have the potential to become fibrocytes compared to healthy controls and therefore likely contribute to myocardial fibrosis. From this data, we propose that fibrocytes are a key effector cell that directly promotes pathologic fibrosis within the injured myocardium. Understanding their migration and function is therefore essential to the development of future therapies targeting this cell type to inhibit their role in fibrosis.

LIST OF ABBREVIATIONS AND SYMBOLS USED

α	Alpha
A	Appendix
ABC	Avidin-Biotin Complex
ACE	Angiotensin Converting Enzyme
ACK	Ammonium Chloride
AngI	Angiotensin I
AngII	Angiotensin II
ANOVA	Analysis of Variance
AP-1	Activator Protein-1
aPC	activated Protein C
APC	Allophycocyanin
ARB	Angiotensin II Receptor Blocker
AT1	Angiotensin II Type 1 Receptor
AT1R	Angiotensin II Type 1 Receptor
AT2R	Angiotensin Type 2 Receptor
β	Beta
Bax	Bcl-2 Associated X
Bcl-1	B-Cell Lymphoma 2
bFGF	basic Fibroblast Growth Factor
BSA	Bovine Serum Albumin
BM	Bone Marrow
°C	Degree Celsius
CABG	Coronary Artery Bypass Grafting

CD	Cluster of Differentiation
CDHA	Capital Distric Health Athority
cDNA	complementary Diribonucleotide Acid
CFSE	Carboxyfluorescein Succinimidyl Ester
cm	Centimeter
CNN2	CYR61/CTGF/NOV-2
CO_2	Carbon Dioxide
Coll	Collagen
Col	Collagen
CPB	Cardiopulmonary Bypass
CTGF	Connective Tissue Growth Factor
CTnI	Cardiac Troponin I
CVICU	Cardiovascular Intensive Care Unit
Cy	Cyanine
d	Day
DAB	3,3' Diaminobenzidine
DIC	Differential Interference Contrast Microscopy
DPBS	Dulbecco's Phosphate-Buggered Saline
dUTP	Deoxyuridine Triphosphate
ECL	Enhanced Chemiluminescence
ECM	Extracellular Matrix
ED1	Antibody Clone for anti-CD68
EDTA-K_2	Potassium Ethylenediaminetetraacetic Acid
eGFP	enhanced Green Fluorescent Protein

ELISA	Enzyme-Linked Immunosorbent Assay
EMT	Endothelial-Mesenchymal Transition
EPC	Endothelial Progenitor Cell
EPCR	Endothelial Protein C Receptor
ERK	Extracellular Signal-Regulated Kinases
FACS	Flow Associated Cell Sorting
FBS	Fetal Bovine Serum
F_c	Fragment Crystallizable Region
FC	Fibrocyte
FG	Fast Green
Fig.	Figure
Fitc	Fluorescein Isothiocyanate
FSC	Forward Scatter
g	Gram
	Gravity Acceleration
G-CSF	Granulocyte Colony-Stimulating Factor
GFP	Green Fluorescent Protein
h	Hour
H&E	Hematoxylin and Eosin
HIF1	Hypoxia Inducible Factor 1
HPV	High Powered Field of View
HPRT	Hypoxanthine-Guanine Phosphoribosyltransferase
hr	Hour
HRT	Heart

HTN	Hypertension
HUVEC	Human Umbilical Vein Endothelial Cells
ICAM	Intercellular Adhesion Molecule-1
IgG	Immunoglobulin G
IHD	Ischemic Heart Disease
IL-1	Interleukin-1
JNK	c-Jun N-Terminal Kinase
kg	Kilogram
LDHb	Lactate Dehydrogenase b
LFA-1	Lymphocyte Function-Associated Antigen
LSAB	Labeled Streptavidin Biotin
MAP	Mitogen-Activated Protein
MCP-1	Monocyte Chemotactic Protein-1
MF	Myocardial Fibrosis
mg	Milligram
MHC	Major Histocompatibility Complex
min	Minute
mL	Millilitre
mm	Millimeter
mM	Millimolar
MMP	Matrix Metalloproteinase
mRNA	messenger Ribonucleic Acid
NANT	Non-Adherant Non-T Cell
NF-κB	Nuclear Factor κB

NFAT	Nuclear Factor of Activated T cells
ng	Nanogram
nM	Nanomolar
OCT	Optimal Cutting Temperature Compound
PBMC	Peripheral Blood Mononuclear Cell
PCI	Percutaneous Coronary Intervention
PDGF	Platelet Derived Growth Factor
PDGFR	Platelet Derived Growth Factor Receptor
PE	Phycoerythrin
PerCP	Peridinin Chlorophyll Protein
PFA	Paraformaldehyde
PMN	Polymorphonuclear
PMSF	Phenylmethanesulfonyl Fluoride
PVDF	Polyvinylidene Fluoride
qRT-PCR	quantitative Reverse Transcription-Polymerase Chain Reaction
qPCR	Quantitative Polymerase Chain Reaction
RAG	Recombination Activating Gene
RAS	Renin-Angiotensin System
REB	Research Ethics Board
RIPA	Radioimmunoprecipitation Assay Buffer
RNA	Ribonucleic Acid
ROS	Reactive Oxygen Species
RPMI	Roswell Park Memorial Institute 1640
RT	Room Temperature

S	Supplemental Figure
SAP	Serum Amyloid Protein
SDF-1α	Stromal Derived Growth Factor-1
SDS-PAGE	Sodium Dodecyl Sulfate Polyacrylamide Gel Electrophoresis
SEM	Standard Error from the Mean
SMA	α-Smooth Muscle Actin
SR	Sirius Red
SSC	Side Scatter
TGFβ	Transforming Growth Factor β
TIMP	Tissue Inhibitors of Metalloproteinases
TNF-α	Tumor Necrosis Factor-α
Tub1a	Tubulin α 1a
TUNEL	Trerminal Deoxynucleotide Transferase-Mediated dUTP Nick-End Labeling
U	Unit
μm	Micrometer
μg	Microgram
μM	Micromolar
VCAM	Vascular Cellular Adhesion Moleculte
VLA	Very Late Antigen
vWF	von Willebrands Factor
WBC	White Blood Cell
wk	Week
wt	Weight

WT	Wild Type

ACKNOWLEDGEMENTS

I would like to acknowledge the contribution of my supervisor, Dr. Jean-Francois Légaré. I am grateful for the opportunity he has presented me to not only persue the work presented in this thesis, but also establish usefull collaborations and expose me to many facets of science and medicine. He has always pushed me when necessary, shown me when to give up and always kept me focused on what was truly important. He has always provided me with a keen insight on the bigger picture in science, work and life. I truly could not have asked for a better mentor.

I would also like to thank the other members of my supervisory committee. Many thanks in particular to my co-supervisor Dr. Tim Lee, whos guidance and wisdom from years of a successful career is nothing but an inspiration. He may actually teach me what proper sentence structure is one of these days. Thanks are also required for my committee member and collaborator, Dr. Robert Liwski. I've never met a man with so many ideas; it is a skill that I'm still trying to develop. Dr. Liwski was always supportive of my work and willing to help. Dr. Kishore Pasumarthi was also a great support with suggestions and kind words of encouragement. My entire supervisory committee has always been dedicated to my success in this degree and has provided enormous support and guidance.

The present and past members of the Atlantic Centre for Transplantation Research have been an amazing group of people to be surrounded by on a daily basis. It was from this group that I learned so much about both the basis of what we do and shared technical skills. In particular, I'd like to thank Tanya Myers. She was more than a technician for me for this degree, she was my teacher, my saviour on many occasions, and also a wonderful friend. Nicole Rosin and Alec Falkenham, my colleagues and co-conspirators from the Légaré lab, were amazing for bouncing ideas off of, working together as a team and providing me endless laughter and bickering, to which I credit for our productivity as a group. I'd like to thank Alison Gareau, Micheal Hart-Matyas and all the other graduate students with whom I've shared an office. They provided me with many laughs, much friendship and plenty of support, all inspite of my loud voice and bad humour. Lastly I'd like to thank each and every member that I've worked with in this lab, you've all had a wonderful impact on me during my time here and I can never thank you enough for making the last 4 years so enjoyable.

Lastly, I'd like to thank my entire family and all my friends for their continued support. While it may have seemed to them that I was never going to finish, they never stopped encouraging and supporting me. For my partner, Dave, I can't express how grateful I am that he endured all the madness that came with this degree. His love, support, humor and the healthy level of distraction he provided made my life that much easier.

CHAPTER 1 - INTRODUCTION

1.1 Overview

Cardiovascular disease remains one of the highest causes of morbidity and mortality in Canada despite advancements in disease mechanisms knowledge, health awareness campaigns and novel therapeutic interventions (1). Though there is a strong push for awareness and prevention within public health groups to adress current risk factors, ongoing research is required to understand the underlying patho-physiologic mechanisms responsible for progressive cardiovascular disease and to develop novel therapeutics to improve the lives of individuals with cardiovascular disease.

A common pathologic feature found in many cardiovascular diseases is the formation of scar tissue within the heart, a process termed myocardial fibrosis. Myocardial fibrosis occurs when an excess of structural proteins are deposited within the myocardium. This deposition is believed to occur in response to myocardial injury in an effort to maintain the structural and functional integrity of the heart. However, deposition of structural proteins, also called extracellular matrix (ECM) proteins, can eventually replace areas of functional, healthy tissue (2). This increases the total stiffness of the heart and eventually impairs organ function (3). If fibrosis is extensive, the heart may be unable to provide sufficient blood flow to the body to meet its physiologic needs resulting in heart failure. There currently is no available therapy specifically targeted to inhibit this fibrotic process. Despite extensive research, there is a paucity of knowledge regarding the mechanisms driving myocardial fibrosis, particularly surrounding the early events responsible for the initiation of fibrosis. Therefore, further studies are required within this field to understand the exact mechanisms promoting myocardial fibrosis.

It has long been appreciated that there is a distinct cellular component involved in the development of myocardial fibrosis. A non-cardiomyocyte population is evident within a fibrotic heart in which the area affected by the accumulation is usually proportional to the area affected by fibrosis (4). These cells are believed to accumulate by the infiltration, activation and proliferation of circulating and resident cells (5). Typically, this represents a heterogenous population of cell types that are responsible for secreting the pro-fibrotic factors and ECM proteins responsible for driving the reparative process (2). Without resolution of the injurious stimuli and hemodynamic stress, the accumulating cells are maintained by a self-sustaining pro-fibrotic feedback loop that promotes pathologic fibrosis within the heart (2, 6).

Prior to the initiation of the work presented in this thesis, the prevailing paradigm suggested a biphasic response of inflammation and corresponding fibrosis (mediated by infiltrating leukocytes and activated mesenchymal cells respectively) was responsible for propagating myocardial fibrosis. There is general agreement that during the later stages of this response myofibroblasts, or activated fibroblasts, are the predominant ECM producing cell type responsible for secreting structural protein in reparative and fibrotic physiologic responses (6). In contrast, the phenotype of the early cell influx is less clear. In the absence of ischemia, the early infiltrating cells in a fibrotic myocardium have been suggested to be monocyte-derived macrophages; however, the exact phenotype of the inviltrating population has not been clearly determined. Indeed cells infiltrating the myocardium are primarily mononuclear in appearance, lacking polymorphonuclear cells

(7, 8). However, cells deriving from a monocyte lineage have been shown to differentiate into a heterologous population of varying phenotypes and biologic functions (9, 10). To date, no conclusive evidence has been provided that the paradigm of leukocyte mediated inflammation and mesenchymal cell mediated fibrosis is correct. The evidence presented here suggests an effector cell that bridges these two responses.

1.2 Project Hypothesis and Aim

It was my hypothesis that a circulating progenitor leukocyte, from a myeloid lineage, infiltrates the myocardium prior to the development of myocardial fibrosis and orchestrates the impending fibrotic response. To prove or disprove this hypothesis I investigated the early cellular and molecular mediators involved in promoting the development of myocardial fibrosis. To accomplish this we used a well-established hypertensive model of myocardial fibrosis secondary to Angiotensin (Ang)II infusion. This model allowed us to dissect the mechanisms promoting fibrosis in the absence of additional confounding inflammation evident in ischemic injury models of myocardial fibrosis.

1.3 Renin-Angiotensin System

Much of the data presented in this thesis was obtained using a model of myocardial fibrosis secondary to AngII infusion. This is a well-established hypertensive model of myocardial remodeling characterized by cellular infiltration, myocardial hypertrophy and excess ECM deposition (7, 11, 12). This model allowed us to analyze the mechanisms driving fibrosis in the absence of confounding variables introduced in other models of myocardial fibrosis secondary to ischemic injury. Furthermore, the pathology evident in

the myocardium of AngII infused animals mimics that found in patients with hypertensive and/or hypertrophic cardiomyopathy (7, 11, 12).

The Renin-Angiotensin System (RAS) is a neurohormonal cascade that regulates vascular tone and homeostasis in health but can become dysregulated and promote disease. Angiotensinogen is the only known AngII precursor and is primarily released by the liver into the circulation (13). Circulating Angiotensinogen is enzymatically cleaved to form the inert decapeptde Angiotensin I (AngI) by interacting with circulating renin. Renin is a protease largely produced in the kidney by juxtaglomerular cells (14-16). Once generated, AngI is converted into AngII by AngII Converting Enzyme (ACE). ACE is constitutively expressed by endothelial cells allowing for efficient generation of AngII in the circulation (17). AngII is the main effector molecule of the RAS and elicits its biologic effects by signaling through the AngII receptor type 1 and type 2 (AT1R and AT2R respectively). AT1R signaling mediates the most notable physiologic effects of AngII including vasoconstriction, hormone regulation, renal function and electrolyte and water balance (18). Furthermore, continuous signlaning through the AT1R is believed to promote the fibrotic effects of AngII stimulation (5). The function of AT2R signaling is not as well understood, though AngII-AT2R signaling is believed to be important in embryonic development and is thought to have opposing, and thus regulatory, effects to AT1R (18). In circulation, AngII has a half-life of approximately 15 sec in which it must interact with its receptors before it is broken down (19).

The RAS has been widely implicated in the progression of many cardiovascular diseases including hypertension, arteriosclerosis and heart failure (5, 20, 21). Inhibition of the RAS system using ACE inhibitors and AngII receptor blockers (ARBs) has been shown to significantly improve clinical outcomes and myocardial remodeling in patients (11, 22). Furthermore, exogenous administration of AngII to rodents is sufficient to induce hypertension, myocardial fibrosis and eventual heart failure (7, 23, 24). Taken together, this evidence supports the role of the RAS system, specifically AngII, in the initiation and progression of cardiovascular disease, myocardial fibrosis and heart failure.

While the exact mechanisms by which AngII is believed to be fibrogenic to the myocardium is still being completely elucidated, it is believed to involve both systemic and local myocardial signaling. Systemically, the vasopressor function of AngII is capable of eliciting chronic hypertension and pressure-overload when circulating levels are elevated for a prolonged period (25). Chronic hypertension confers hemodynamic stress unto the myocardium and can induce cardiomyocyte death and stimulate myocardial fibrosis (26, 27). At the organ level, AngII is believed to promote fibrosis by directly stimulating resident and infiltrating cells within the heart. AngII-ATIR signaling is capable of activating pro-inflammatory transcription factors including NF-κB, NFAT and AP-1 that initiate and sustain expression of pro-inflammatory mediators (28-33). AngII also elicits the expression of mitogens and growth factors that promote hypertrophy and excess production of ECM proteins with decreased degradation that, together, contribute to progressive fibrosis (34-36). This data supports a direct role for AngII in the stimulation of myocardial fibrosis

1.4 Myocardial Fibrosis

Fibrosis occurs in the heart when there is a shift in the balance of ECM protein towards production rather than degradation (37). This process is initially beneficial, acting as a repair mechanism to counteract the detrimental effects of tissue injury and increased organ load but, without regression, can become pathological (2).

1.4.1 Extracellular Matrix

1.4.2 ECM in Structure and Function

The ECM is an important, dynamic component of the myocardium and contributes to overall organ structure, function, cell-cell adhesion and cell signaling (38). The ECM consists of fibrilar and non-fibrilar proteins including collagen, proteoglycans, elastin, and accessory proteins (39). Together, these proteins provide dynamic scaffolding for the resident cells of the heart. Collagen is the predominant ECM protein in the heart, particularly collagen type I and IV, and is found as a weave structure surrounding the muscle fibers in normal cardiac tissue (40). The surrounding collagen maintains cardiomyocyte arrangement, transmits force and resists excess cardiomyocyte stretch beyond physiologic capacity (41, 42). Glycoproteins, including fibronectin and laminin, crosslink other ECM proteins, including collagen, and interact with cardiomyocytes to provide organizational support within the structure of the heart (43-45). Resident cells interact with the various ECM proteins using integrins present in their cellular membrane (44, 46, 47).

1.4.3 ECM in Dynamic Response to Injury

ECM distribution and protein content of the myocardium is drastically altered in pathologic conditions. Collagen, glycoprotein and accessory protein content largely increase in the myocardium during the development and progression of myocardial fibrosis (42). Excess collagen is produced by fibroblasts and myofibroblasts to provide increased structural support to compensate for a loss of cardiomyocytes seen in chronic injury (48-50). Increased tensile strength is also provided by various components of the ECM, mostly adaptor proteins, which promote the crosslinking of the structural proteins and regulate matrix stability (51, 52). Additionally, the expression and function of pro-fibrotic factors, including transforming growth factor-β (TGF-β), can be altered by ECM components (51-53). Accessory proteins and bioactive metabolites of ECM components, termed matrikines, also influence cellular recruitment and activation of both resident and infiltrating cells (54-56). Furthermore, the arrangement of ECM components, collagen in particular, are reorganized in myocardial fibrosis and can result in impaired cell-cell interactions, signaling and electrical conductance (40, 47, 57). Together, this data illustrates that the ECM is not only an inert scaffolding structure but is a dynamic player of the fibrotic process.

1.4.4 ECM Degradation and Maintenance

ECM composition is not static in health or disease and the protein components are constantly being produced and degraded. Matrix metalloproteinases (MMPs) and tissue inhibitors of metalloproteinases (TIMPs) are responsible for ECM maintenance and turnover (58). MMPs are responsible for the degradation of matrix proteins while TIMPs inhibit MMP activity and promote structural protein preservation. These components

form a regulatory system that tightly controls the balance of ECM production versus destruction. In myocardial remodeling there is an obvious shift towards ECM deposition as indicated by the scarring evident within myocardial tissues; however, protein degradation also contributes to the disease process by propagating ECM reorganization and cell migration.

Taken together, alterations of the ECM homeostasis is the fundamental basis of the processes that lead to myocardial fibrosis. Degradation of the matrix is essential for cell migration and infiltration to repair and compensate for the loss of cardiomyocytes. Increased ECM protein deposition is required to provide additional structural support lost after cardiomyocyte death, as regeneration of cardiomyocyte cells is significantly limited. However, without the resolution of the injurious stimui, ECM remodeling continues and the stiffness of the myocardium increases until it can no longer function sufficiently and organ failure is reached. Therefore, a potential therapeutic avenue for inhibiting this self-sustaining system would involve targeting the cells that secrete the fibrotic growth factors, ECM proteins and matrix regulating enzymes. Further investigations are required to understand the functional properties of both the infiltrating and resident cells that contribute to this process and how they are regulated.

1.5 Effector Cells

Myocardial fibrosis is associated with a significant cellular component that is responsible for promoting the fibrotic process. Rapid cellular infiltration and/or proliferation is evident early on in the development of myocardial fibrosis (59-61). This accumulating

cell population consists of cells that secrete ECM proteins and molecular mediators that promote fibrosis. The effector functions of the accumulating cell types are therefore essential to the propagation of the fibrotic process.

1.5.1 Monocytes/Macrophages

Monocytes are a mononuclear leukocyte cell type found in circulation that have long been shown to be a key mediator of the innate immune system and play a significant role in inflammation. Monocyte trafficking into tissues has been implicated in fibrotic processes (62). After entry into tissues, monocytes can undergo differentiation into a macrophage cell type. Macrophages are capable of orchestrating many aspects of a fibrotic response. Macrophages clear damaged/dead cells from injured tissue by phagocytosis (62). Macrophages also produce many pro-inflammatory cytokines and chemokines to recruit and activate other effector cells including more monocytes, fibroblasts and endothelial cells (63). Macrophages also secrete growth factors, including TGF-β, and enzymes that stimulate matrix remodeling, which together directly promote and modulate the ECM protein production and rearrangement (64-66). Furthermore, macrophages have been shown to directly promote tissue fibrosis in other organs and, as such, are also a candidate cell type in promoting myocardial fibrosis (67).

1.5.2 Fibroblasts

Fibroblasts are the predominant cell type responsible for producing and depositing ECM proteins. Fibroblasts are mesenchymal cells that are typically found within the endomysial collagen network between myocyte bundles in the heart (68). Fibroblasts are responsible for secreting cytokines and growth factors in order to coordinate many

physiological processes, including fibrosis (69). Fibroblasts can be activated to differentiate into a myofibroblast phenotype, largely identified by α-smooth muscle actin (αSMA), embryonic smooth muscle myosin heavy chain (SMemb) and extra domain-A (ED-A) fibronectin expression (70). Activation of fibroblasts within the myocardium only occurs after injury as myofibroblasts are not present in a healthy heart (71). Myofibroblasts secrete large volumes of ECM proteins and are capable of contraction to provide increased tissue tension (72). Fibroblast-myofibroblast differentiation occurs in response to mechanical stretch and stimulation with cytokines and growth factors (6, 73-78). In the injured myocardium, myofibroblasts can be found in large numbers around the injured and fibrotic tissue (79, 80). The origin of these myofibroblasts is largely believed to be from the activation of resident fibroblasts (81). However, myofibroblasts can also arise from endothelial-mesenchymal transitions (EMT) (82, 83). Resident pericytes associated with the vasculature also have the potential to transition into a myfibroblast phenotype (84). A population of bone marrow derived fibroblast progenitor cells, termed fibrocytes, can be mobilized in response to fibrosis and act as a reservoir external to the myocardium for myofibroblast generation (85, 86). In healthy wound healing, myofibroblasts undergo apoptosis after healing has occurred; however, in fibrosis, myofibroblasts persist in tissues promoting pathologic ECM protein deposition (6).

1.6 Chemokines

Chemokines are molecular mediators that induce target cells to migrate towards a positive gradient. This is a physiologic method to ensure that any cells required for a specific process is available at an appropriate time (87). Therefore, chemokine

expression regulates the kinetics involved in recruiting circulating effector cells into a fibrotic heart. Interestingly, chemokine signaling is typically pleitrophic in nature and there is a degree of redundancy built into the system to overcome dysfunctions that may arise (87). Understanding the expression patterns of various chemokines is therefore important in mapping the mechanisms required for recruiting effector cells into the myocardium.

1.6.1 CCL2/MCP-1

CCL2, also called Monocyte Chemotactic Protein (MCP)-1, has been implicated in inflammation and fibrosis. CCL2/MCP-1 is a potent chemoattractant for monocytes and subsets of progenitor cells (88, 89). Both resident cells, including endothelial, fibroblast and myocytes, as well as inflammatory cells, including monocytes, have been shown to express CCL2 (90). CCL2 signals through the CCR2 receptor found on the cell surface of target cells (91, 92). Beyond chemotaxis, CCL2 promotes fibroblast activation, proliferation and cytokine production (93). Interestingly, some evidence suggests that CCL2 stimulation may also confer a degree of protection for cardiomyocytes (94). Upregulation of CCL2 is promoted by increases in tissue ROS, pro-inflammatory cytokines and growth factors (95-98), all of which are found in myocardial injury and remodeling. Many studies have found a significant increase myocardial CCL2 expression in rodent models of myocardial fibrosis and in patients with cardiovascular disease (24, 99-101). Inhibition of CCL2 signaling in models of myocardial fibrosis resulted in reduced cellular infiltration, collagen deposition and improved cardiac function (24, 102-104). This data implies that CCL2 promotes aberrant fibrosis within the heart by recruiting and stimulating effector cells.

1.6.2 CXCL12/SDF-1α

CXCL12, also called Stromal Derived Growth Factor (SDF)-1α, is a classic example of a pleitrophic chemokine. Though it is constitutively expressed by the myocardium, CXCL12/SDF-1α expression is upregulated after myocardial infarction and in pressure-overload injury (105-108). However, there is no definitive evidence to determine whether it is beneficial or detrimental in the fibrotic process after injury. CXCL12 signals almost exclusively through its receptor, CXCR4, and is a potent chemoattractant for hematopoietic stem cells (109). A body of literature supports a protective role for CXCL12, particularly after myocardial infarction (107, 110-113). CXCL12 is believed to promote the recruitment of endothelial progenitor cells, which in turn, support an increase angiogenesis to improve perfusion to injured tissues (108, 114, 115). Evidence also suggests that CXCL12 is protective for cardiomyocytes against apoptosis by inhibiting pro-apoptotic signaling (110, 116). Some also believe that CXCL12 is key in promoting cardiac regeneration by recruiting progenitor cells that can differentiate into cardiomyocytes (115), though regeneration is not always evident with CXCL12 treatment in models of myocardial infarct (117). Alternatively, there is evidence suggesting that CXCL12 may have a negative inotropic effect on cardiomyocytes promoting impaired contraction (118). Furthermore, another study found that an increase in CXCL12 aggravates myocardial remodeling and decreases organ function (119). Whether protective or fibrogenic, CXCL12 appears to play a role in myocardial fibrosis, though the exact role is yet to be clearly elucidated.

1.7 Cytokines and Growth Factors

Soluble factors within the myocardial environment influence the cellular components of the fibrotic process. Cytokine and growth factor expression is essential in orchestrating cellular migration, activation, differentiation and apoptosis (120). The sources of these molecular mediators are varied and there is considerable redundant expression by different cell types. However, the production of cytokines and growth factors is a key effector function of recruited and/or activated cells that drive the pathologic process. Various cytokines and growth factors are also responsible for the maintenance of the effector population by providing survival, activation and proliferation signals to these cells. This illustrates the essential function that cytokines and growth factors provide in promoting pathologic fibrosis.

1.7.1 Pro-inflammatory Cytokines

1.7.1.1 Interleukin-1

Interleukin-1 (IL-1) is a pro-inflammatory cytokine produced early in the myocardial repair process. Serum levels of IL-1 are elevated in patients after a myocardial infarct and in heart failure (121, 122). Expression of IL-1 is induced by endogenous 'danger signals' released by damaged cells, mechanical stretch, and cytokine stimulation (123-126). Most resident cells and infiltrating cells are capable of IL-1 production (123, 127-129). IL-1 signaling promotes an inflammatory response by activating cells and inducing the expression of other pro-inflammatory mediators (125). IL-1 promotes the degradation and deposition of ECM proteins by inducing MMP activity, inhibiting TIMP expression and modestly promoting collagen synthesis (125). IL-1, in combination with

Tumor Necrosis Factor (TNF)-α, has a negative inotropic effect on cardiomyocyte contractility (130). IL-1 therefore has a key role in the initial inflammatory phase of myocardial injury and promotes further inflammation, EMC remodeling and decreased cardiac function.

1.7.1.2 Tumor Necrosis Factor-α

TNF-α is another pro-inflammatory cytokine implicated in myocardial fibrosis and organ failure. Elevated circulating TNF-α levels are detectable in patients with cardiovascular disease, including heart failure (131, 132). In fact, TNF-α is believed to be a viable biomarker of cardiovascular disease that can predict the degree of functional impairment (131, 133, 134). Hypoxia, endogenous 'danger signals', mechanical stretch, and other molecular mediators promote TNF-α expression, similar to IL-1 (123, 125, 135-137). TNF-α elicits similar cellular responses as IL-1, including the propagation of inflammation, promoting ECM remodeling, and acting as a negative inotrope to depress cardiac function (138). However, TNF-α appears to be a more potent fibrotic mediator as the infusion of exogenous TNF-α or over-expression of cardiac TNF-α is sufficient to promote myocardial fibrosis, hypertrophy and eventual organ failure (139). TNF-α appears to be an essential early mediator driving pathologic fibrotic responses within the myocardium.

1.7.2 Pro-Fibrotic Growth Factors

1.7.2.1 Transforming Growth Factor-β

Transforming Growth Factor (TGF)-β is a highly pleotropic cytokine that has long been shown to be a critical component of both healing and pathologic fibrosis. TGF-β is

secreted as a latent form that must be proteolytically activated (53). The latent form of TGF-β is constitutively expressed and associated with the supporting matrix of organs, which functions as a reservoir for this cytokine (53). Latent TGF-β is cleaved by proteases that are associated with matrix remodeling, thus allowing the activation of this potent mediator when the structural foundation of tissues are disturbed, as is seen in injury (53, 140). Activated TGF-β classically signals through a series of adaptor proteins, called SMAD proteins, which form complexes and translocate to the nucleus to inhibit or promote gene expression. The pleiotrophic effects of TGF-β signaling are determined by the exact composition of the SMAD signaling complex, the cell type stimulated and the composition of the environmental milieu (141). TGF-β promotes chemotaxis of circulating monocytes and promotes their activation into a pro-inflammatory cytokine producing cell (142). However, activated macrophages within tissues are largely inhibited by TGF-β stimulation and exhibit reduced pro-inflammatory mediator expression (143). TGF-β is a potent activator of fibroblasts. Fibroblasts stimulated with TGF-β undergo maturation into a myofibroblast phenotype and significantly increase their ECM protein expression (144). TGF-β activation stimulates hypertrophic growth of cardiomyocytes (145). Increased TGF-β activation also promotes the expression of Connective Tissue Growth Factor (CTGF), another pro-fibrotic factor, which contributes to the pro-fibrotic milieu (146). TGF-β is believed to work synergistically with other growth factors, including CTGF and Platelet Derived Growth Factor (PDGF), to enhance ECM protein production and wound contraction (147). TGF-β is upregulated in models of myocardial injury and patients with cardiovascular disease (148-151). It directly contributes and further propagates the ECM deposition,

hypertrophy and overall organ dysfunction in cardiomyopathies. Furthermore, it's believed that TGF-β is a key regulatory factor that mediates the transition from an inflammatory reaction to an eventual fibrotic process by dampening the immune system and promoting a fibrotic milieu (152).

1.7.2.2 Connective Tissue Growth Factor

Connective Tissue Growth Factor (CTGF), or CNN2, is a fibrogenic growth factor that has a complex role in the initiation and progression of myocardial fibrosis. CTGF is believed to be a matricellular protein that influences the activities of growth factors found within the ECM (153). Though intensely studied, no specific receptor has yet to be found for CTGF; however, CTGF is still capable of inducing intracellular signaling most likely via interactions with integrins expressed on the cell surface (154, 155). CTGF is largely believed to be a downstream mediator of TGF-β signaling and can be induced by both SMAD-dependent and independent signaling (156-158). Evidence also suggests that CTGF expression can be induced via TGF-β-independent mechanisms as well (159, 160). CTGF stimulation by itself is only a weakly fibrogenic stimulus (76, 161). However, CTGF stimulation in the presence of TGF-β significantly promotes fibroblast activation and ECM protein production beyond the levels induced by TGF-β alone (162). As such, CTGF is believed to be a co-factor for TGF-β promoting synergistic fibrotic effects. Significant CTGF expression has been found shortly after myocardial infarcts, in hypertensive heart disease and in patients with heart failure (159, 163, 164). In fact, CTGF expression was found elevated for over 180 days after a myocardial infarct suggesting a key role for CTGF in long-term reactive fibrosis (163). Measuring circulating serum levels of CTGF has been proposed as a prognostic tool to monitor the

extent of myocardial fibrosis in patients with cardiovascular disease (159, 165). CTGF is clearly involved in driving the fibrotic process, coupled with TGF-β, though the exact mechanisms have yet to be clearly established.

1.7.2.3 Platelet Derived Growth Factor

Platelet Derived Growth Factor (PDGF) is a growth factor thought to be both protective and fibrogenic. PDGF is a group of isoforms that includes PDGF-A, -B, -C, and –D that are required to form dimers in order to signal through one of its two specific receptors, PDGFRα and PDGFRβ (166). Differential expression of the isoforms has been demonstrated in fibrotic processes but isoform-specific effects are not clear (167). Constitutive expression of PDGF is detectable within the healthy myocardium, which is believed to be responsible for appropriate ECM maintenance (167). PDGF is upregulated in injury and is partially responsible for recruiting effector cells including leukocytes, endothelial cells and fibroblasts (168-170). Similar to CTGF, PDGF functions with TGF-β in a synergistic fashion to promote fibroblast maturation into myofibroblasts, proliferation, extensive upregulation of ECM protein production, and matrix contraction (168, 171, 172). Overexpression of PDGF within the heart promotes excess collagen deposition, hypertrophy and dysfunction of the myocardium (173). This data supports a fibrotic and hypertrophic role for PDGF when upregulated after myocardial infarction and in pressure-overload injury (174).

PDGF is also believed to be protective. Therapeutic drugs used for cancer treatment that block PDGF receptor availability have been associated with significant cardiomyopathies

in patients indicating PDGF signaling is beneficial (175). Furthermore, PDGF stimulation promotes angiogenesis and maturation of newly formed blood vessels (176). PDGF receptor inhibition in cardiac pressure-overload is associated with impaired vascularization, focal ischemic injury and impaired cardiac function (174). There is additional evidence that suggests that PDGF is protective against apoptosis in cardiomyocytes (177). Whether PDGF promotes pathologic fibrosis or protects against it is likely a response mediated by other factors, including TGF-β, within the surrounding milieu that would shift the balance to one response or the other.

1.7.3 Role of Molecular Mediators Regarding Effector Cell Activation and Function

The outlined molecular mediators above act as chemical communication signals to initiate and propagate the fibrotic process. They do so by acting on the cells present within the microenvironment where they are being produced. Leukocytes and fibroblasts are both activated by pro-inflammatory cytokines (178). Growth factors are particularly potent stimulators of fibroblasts that promote their differentiation and ECM protein production. Furthermore, effector cells, including leukocytes and fibroblasts, secrete cytokines and growth factors as a means of promoting fibrosis. Measuring these mediators within the cardiac milieu allows us to assess the fibrotic process at an organ level. Alternatively, identifying the cell type producing these mediators allows us to dissect the key cellular mediators driving fibrosis and the mechanisms by which they do so. Studying the expression of theses mediators is fundamental to understand the fibrotic process and the cells driving it.

1.8 Cardiovascular Disease in Patients

Our animal model is a good tool to dissect the specific mechanisms driving fibrosis but does not represent the multifactorial nature of myocardial fibrosis development in patients. While hypertension is a common contributing factor to myocardial injury, the development of coronary artery disease leading to ischemic heart disease is also very prevalent within our population. Coronary artery disease develops when the coronary arteries of the heart have a progressive build up of atherosclerotic plaque narrowing the lumen (179). As the disease progresses it will significantly impair the blood flow to the myocardial tissues (179). Without sufficient oxygenated blood, the myocardial tissue downstream of the afflicted vessel will succumb to ischemic damage. Ischemic injury promotes a significant inflammatory and fibrotic response within the myocardium (180). Patients diagnosed with coronary artery disease are also at risk for a complete vascular occlusion (acute myocardial infarct) and end-stage heart failure (181). Therefore, patients exhibit a multitude of contributing factors that promote the development of myocardial fibrosis that cannot be fully accounted for in animal models. However, we maintain that many of the basic mechanisms promoting fibrosis determined using animal models, including many of the effector cell types driving the response, are still pertenant to the disease process in humans.

1.9 Current Treatment Modalities for Cardiovascular Disease

Due to the prevalence of cardiovascular disease within our society, a large arsenal of pharmaceuticals is currently available and widely used. Many of these drugs specifically target molecular mediators or physiologic signaling pathways that drive progressive cardiovascular disease. Of these drugs, many target cholesterol levels (statins),

sympathetic nervous system activation (β-blockers), the clotting cascade (anti-coagulants) and vascular tone (RAAS inhibitors, diuretics, calcium channel blockers) (182). Many of these drugs are used in combination to inhibit multiple biologic mechanisms that promote aberrant cardiac events (182). Even with these diverse therapeutic options, individuals with heart failure still have a 5 y mortality rate that approaches 60% on average indicating an ongoing demand for novel pharmacological therapies to improve patient outcomes (183).

Surgical techniques are also implemented to alleviate physical manifestations of cardiovascular disease. These interventions are largely used to treat myocardial infarcts and/or coronary artery disease, where stenoses or occlusion occur in coronary vessels inducing ischemic injury to the downstream myocardial tissues. Percutaneous Coronary Intervention (PCI) is a minimally invasive technique that allows the opening of constricted vessels by using balloon angioplasty (184). Typically an expandable wire mesh tube, known as a stent, is then placed within the affected vessel in an attempt to maintain the increased luminal diameter and increase blood flow. Alternatively, Coronary Artery Bypass Grafting (CABG) surgery is a highly invasive technique that involves the grafting of patent vessels isolated from elsewhere in the body to the aortic root and also downstream of the diseased vessel (184). This effectively bypasses the diseased vessel allowing the revascularization of the ischemic tissue originally supplied by the narrowed or occluded vessel. Both PCI and CABG surgery allow for revascularization of tissue and improved perfusion of the myocardium. Though these techniques are critical for preventing further tissue injury in patients with ischemic heart disease they are not

believed capable of repairing tissue that has already undergone signficant remodeling. However, new avenues of therapy are currently being trialed, including stem cell therapy, which promote cardiac regeneration and repair rather than inhibiting precursor events (185). Treatments that promote cardiac regeneration would be useful in those patients whom present with myocardial injury late or do not respond to current treatments.

Taken together, it is clear that current therapies for patients with cardiovascular disease are largely successful in inhibiting the precursor events the can lead to heart failure. However, we are not yet capable of completely abrogating myocardial fibrosis and the associated tissue remodeling seen in cardiovascular disease or repairing an already injured myocardium. New techniques are still needed to address these issues. One particular avenue to approach design of novel therapeutics is to target the cellular mediators of fibrosis. By identifying the exact cell types responsible, how they traffic to the tissue and their biologic function, these can then be targeted to decrease pathologic fibrosis.

1.10 Project Rationale

Though there has been intense study of myocardial fibrosis and remodeling, there is a paucity of evidence relating to the specific mechanisms that occur early in the pathologic response initiating myocardial fibrosis. Specifically, there is limited evidence available regarding the exact phenotype of the initial infiltrating effector cell type(s) and their migration kinetics in models of myocardial fibrosis in the absence of ischemia. Furthermore, the mechanisms by which these infiltrating cells are recruited into the

myocardium and how they promote fibrosis are unclear. My original hypothesis for this project was that a circulating progenitor leukocyte, of myeloid lineage, infiltrates the myocardium prior to the development of myocardial fibrosis and orchestrates the resulting fibrotic response. From that hypothesis I projected that any therapeutic interventions that inhibit this effector cell infiltration would confer protection in the presence of fibrotic stimuli. Lastly, I anticipated that the cell type identified in an animal model of myocardial fibrosis would also contribute to myocardial fibrosis in patients with ischemic heart disease.

1.11 Objectives

1) Characterize the phenotype of the initial infiltrating cells in a rodent model of myocardial fibrosis.

2) Identify the mechanisms responsible for recruiting the infiltrating cell type.

3) Characterize the pro-fibrotic molecular stimuli that promote myocardial fibrosis.

4) Identify therapeutic avenues to inhibit cellular infiltration and protect against myocardial fibrosis.

5) Determine if the identified infiltrating cell type is involved in clinical cases of cardiovascular disease potentially promoting myocardial fibrosis.

CHAPTER 2

MYOCARDIAL FIBROSIS IN RESPONSE TO ANGIOTENSIN II IS PRECEDED BY THE RECRUITMENT OF MESENCHYMAL PROGENITOR CELLS

MJ Sopel*, NL Rosin, TDG Lee, JF Légaré**

Laboratory Investigation. 2011. 91(4):565-578

* Author contributions are clearly outlined in Appendix 2.

2.1 Abstract

Background: Myocardial fibrosis is characterized by significant extracellular matrix (ECM) deposition. The specific cellular mediators that contribute to the development of fibrosis are not well understood. Using a model of fibrosis with Angiotensin II (AngII) infusion, our aim was to characterize the cellular elements involved in the development of myocardial fibrosis. *Methods:* Male C57Bl/6 and Tie2GFP mice were given AngII (2.0mg/kg/min) or saline (control) via mini osmotic pumps for up to 7d. Hearts were harvested, weighed and processed for analysis. Cellular infiltration and collagen deposition were quantified. Immunostaining was performed for specific markers of leukocytes (CD45, CD11b), myofibroblasts (SMA), endothelial cells (vWF), and hematopoietic progenitor cells (CD133). Bone marrow origin of infiltrating cells was assessed using GFP^+ chimeric animals. Relative qRT-PCR was performed for pro-fibrotic cytokines (TGF-β1, CTGF) as well as the chemokine SDF-1α. Myocardial infiltrating cells were grown *in vitro*. *Results:* AngII exposure resulted in multifocal myocardial cellular infiltration, which preceded extensive ECM deposition. A limited number of myocardial infiltrating cells were positive for leukocyte markers but were significantly positive for myofibroblast (SMA) and endothelial cell (vWF) markers. However, using Tie2GFP mice, where endothelial cells are GFP^+, myocardial infiltrating cells were not GFP^+. Transcript levels for SDF-1α were significantly elevated at 1d of AngII exposure suggesting that hematopoietic progenitor cells may be recruited. This was confirmed by positive CD133 staining of infiltrating cells and evident GFP^+ cellular infiltration when exposing GFP^+ bone marrow chimeras to AngII. Furthermore, a significant number of $CD133^+/SMA^+$ cells were grown *in vitro* from the myocardium of AngII exposed animals

($p<0.01$). *Conclusions*: Myocardial ECM deposition is preceded by the infiltration of the myocardium with hematopoietic cells that express mesenchymal markers. This data suggest that mesenchymal progenitor cells are recruited, and may have a primary role, in the initiation of myocardial fibrosis.

2.2 Introduction

Myocardial fibrosis is a common pathological feature seen in many patients with heart disease and is hypothesized to be the final common pathway that ultimately results in irreversible organ failure (5). Pathologically, fibrosis is characterized by the accumulation of extracellular matrix (ECM) proteins within the myocardium. While initially ECM deposition can be beneficial and occur in response to injury, the repair response can become exacerbated (5). The lack of resolution of this ECM deposition in tissue is the hallmark of fibrosis (2). The accumulation of ECM proteins within the myocardium enhances cardiac stiffness and can eventually impair cardiac function leading to the development of heart failure (5). The exact mechanisms responsible for myocardial fibrosis remain to be clearly defined, despite intense study.

Recent evidence has implicated Angiotensin II (AngII) in the progression of myocardial fibrosis. AngII has been suggested to be a potent pro-fibrotic molecule (5). Increased serum levels of AngII are seen in patients with cardiovascular diseases that are associated with myocardial fibrosis, including atherosclerosis, hypertension, cardiac hypertrophy and heart failure (5, 20, 21). Clinical trials looking at the inhibition of the renin-angiotensin system, and more specifically AngII receptor blockers (ARB), demonstrate

significant benefit in the prevention of cardiovascular events, including the cardiac remodeling seen with myocardial fibrosis (11, 186). Moreover, AngII given exogenously to rodents has been shown to result in cellular changes within the myocardium, hypertrophy and eventual fibrosis, similar to that seen in humans (7, 11, 12, 187). Taken together, this evidence strongly supports a role for AngII in the development of myocardial fibrosis. The direct mechanisms responsible, and the effector cells involved, have yet to be fully characterized.

Rapid myocardial cellular infiltration is evident in animals infused with AngII which suggests that the cellular component has an effector function in the development of myocardial fibrosis (61). It is unclear, however, what cell types participate in this infiltration. The cellular accumulation has been primarily described as mononuclear in appearance, lacking polymorphonuclear cells. This has led some investigators to suggest that these cells are of the monocyte/macrophage lineage (12, 187-190). One should note that cells that stain positive for monocyte/macrophage markers do not account for all the infiltrating cells (12, 187, 188). This observation suggests a role for a yet to be described cell type.

The predominant characteristic of fibrosis, ECM deposition, is generally thought to result from the activities of fibroblasts and myofibroblasts rather than macrophages. Cardiac fibroblasts are activated in response to hypertrophic stimuli, including AngII (191-194). Furthermore, fibroblasts proliferate and increase the production of ECM proteins in response to AngII exposure *in vitro*. However, the *in vivo* data available to support this

response to AngII is limited (5, 191-194). Finally, if myofibroblasts make up a component of the cells that accumulate in the myocardium after AngII exposure, their origin remains to be determined. Myofibroblasts can arise from the activation and proliferation of resident fibroblasts or from several different sources including endothelial-mesenchymal transitions and blood borne mesenchymal progenitor cells (referred to as fibrocytes) (2, 85, 195-197).

The data presented in this study characterizes early cellular migration to the myocardium in response to AngII. We identify a novel population of hematopoietic progenitor cells with mesenchymal properties as an infiltrating cellular population involved in AngII mediated myocardial fibrosis and as such, suggest alternative mechanisms in the initiation of fibrosis.

2.3 Materials and Methods

2.3.1 Animals

All work was approved by Dalhousie University's *University Committee on Laboratory Animals*. Male C57BL/6, enhanced green fluorescent progein (eGFP) and Tie2-GFP mice ranging from 7 to 8 wk of age were purchased from Jackson Laboratory (Bar Harbour, ME) and were housed within the Medical Sciences Animal Care Facility at Dalhousie University. Mice were provided food and water *ad libitum* for 1 wk prior experimentation.

2.3.2 AngII Infusion

Animals were anesthetized with isoflurane (Baxter Healthcare Corp., New Providence, NJ) in oxygen delivered by a Fortec vaporizer. When surgical levels of anesthesia were reached a 1-2 cm mid-scapular skin incision was made and a mini osmotic pump (Alzet, Palo Alto, CA) was inserted subcutaneously. The incision was closed using 7mm wound clips. Animals were randomly assigned to receive AngII (2.0 μg/kg/min, Sigma Aldrich, Oakville ON), AngII and Losartan (ARB; 6.9 μg/kg/min, Sigma Aldrich) or a vehicle control of saline. The pumps remained in for 1, 3 or 7d during which the animals were provided with food and water *ad libitum* and observed for signs of morbidity. Prior to euthanization, blood pressure measurements were taken via the Coda2 non-invasive cuff system (Kent Scientific, Torrington, CT) for a minimum of 5 consecutive measurements.

2.3.3 GFP^+ Bone Marrow Chimera

Generation of GFP-bone marrow (BM) chimeric animals were generated as previously described (198). Briefly BM cells were harvested from 8 week old eGFP-transgenic mice with a C57/Bl6 background (198). After irradiation with a two doses of 5.5 Gy, four hours apart, the unfractionated GFP^+ BM cells ($5x10^6$ cells in 150ul of sterile phosphate – buffered saline) were injected via the tail vein into irradiated C57/Bl6 mice. Engraftment was evaluated 8 weeks later by collecting peripheral blood cells and looking at the frequency of GFP^+ cells among peripheral nucleated cells (data not shown) (88, 198). Only animals with demonstrated engraftment (>60% of white blood cells were GFP^+) were used for the 2 treatment groups (saline control or AngII infusion as per protocol). Immunofluorescence was used to enhance localize GFP^+ cells within the myocardium. Antigens were retrieved on sections of formalin fixed and paraffin embedded GFP

chimeric tissues and then non-specific protein binding was blocked with 10% normal goat serum. The tissues were then incubated with the rabbit anti-eGFP primary antibody (Abcam, Cambridge, MA) followed by incubation with an alexa488 conjugated goat anti-rabbit. Tissues were thoroughly washed and cover slipped. Fluorescent microscopy was performed; pictures were captured and analyzed in Adobe Photoshop 5.0. Cover slips were removed and the tissues were then stained with a hematoxin and eosin (H&E) stain to assess basic histology of tissues for comparison to GFP positivity. Light microscopy was performed; pictures were captured and analyzed in Adobe Photoshop 5.0.

2.3.4 Tissue Harvest

Hearts from experimental animals were harvested and weighed. Cardiac mass index was measured by calculating the heart:body weight ratio. The hearts were lastly divided along the short axis into 3 portions including the base, middle and apical sections. The base portion was processed for histological examination while the other two portions were snap frozen immediately for molecular analysis.

2.3.5 Cell Isolation and Culture

Hearts from untreated mice (n=3) or mice infused with AngII for 3d (n=3) were harvested under sterile conditions and used for cell isolation. Briefly, hearts were initially mechanically minced and then enzymatically digested in a Collagenase solution (50μg/mL Collagenase II, Cedar Lane, Burlington, ON) in Roswell Park Memorial Institute 1640 (RPMI) media (Gibco, Life Technologies, Burlington ON) at 37°C with agitation for 45min. The cell isolates were washed twice with complete RPMI (10% heat-inactivated fetal calf serum, 2mM L-glutamate, 100μg/ml streptomycin and 100U/ml

Penicillin) and then plated on T-25 flasks coated with 0.1% gelatin. Cellular isolates were incubated at 37°C with 5% CO_2 for 3d, after which all non-adherent cellular debris was removed and fresh media was supplied. In all groups, digital images taken using an inverted microscope for cell counting. Areas of cell growth were randomly selected (6/flask containing cells isolated from 1 heart) for cell counts. Adherent cells from naïve hearts were then serum starved for 24hr and then exposed to AngII (100nM) in serum free RPMI for 2d. Digital images were again taken to asses cell growth.

For immunofluorescence, cultured myocardial cells initially grown on 0.1% gelatin coated cover slips were fixed with 4% paraformaldehyde for 30min. Non-specific protein binding was blocked with a Mouse on Mouse Block kit (Vector, Burlington CA) and normal goat serum. The cells were incubated with the primary antibodies of rabbit ant-CD133 (Abcam) and mouse anti-α-smooth muscle actin (SMA, Sigma Aldrich). This was followed by incubation with an Alexa488 conjugated goat anti-mouse secondary and an Alexa555 conjugated goat anti-rabbit secondary. Cells were thoroughly washed and mounted on slides. Fluorescent microscopy was performed and digital images were acquired and analyzed in Adobe Photoshop 5.0. Furthermore, differential interference contrast microscopy was performed and digital images were acquired.

2.3.6 Histological Analysis

Hearts were processed for histological assay by: a) fixing with 10% formalin for 24hr; b) protecting with sucrose/OCT followed by snap freezing; or c) fixing with 4% paraformaldehyde for 24hr. Formalin fixed tissues were paraffin embedded and were

serially sectioned on a microtome (5μm). Frozen and paraformadehyde fixed tissues were OCT embedded and serially sectioned on a cryostat (8μm). Basic myocardial histology and cellular infiltration were examined using heart cross-sections stained with H&E. Cellular changes were quantified by using an overlaid 500 x 500 pixel grid over heart sections, which were captured at 5x magnification. Grids that contained any cellular infiltration or areas of excess ECM deposition were tallied as well as total grids encompassed by the heart. The percent of grids affected were then calculated.

Immunohistochemistry for SMA (Sigma Aldrich), von Willebrand Factor (vWF; Chemicon, Temecula, CA), KI-67 (DakoCytomation, Mississauga, ON) and CD133 (Abcam) was performed on paraffin embedded tissues which required deparaffinization and antigen retrieval prior to staining. Immunohistochemistry was performed for CD45 (BD Biosciences, San Jose, CA) and CD11b (AbD Serotec, Raleigh, NC) on frozen tissue which did not require antigen retrieval prior to staining. Briefly, endogenous peroxidases were quenched with 3% hydrogen peroxide; endogenous biotin was blocked (DAKO Biotin Blocking System, DakoCytomation, Mississauga, ON); and non-specific staining was blocked with normal goat serum or normal horse serum. Sections were incubated with the individual primary antibodies and followed by a specific biotin-conjugated secondary antibody. The antibody complexes were then conjugated to an Avidin-biotin complex (Vecstastain ABC kit; Vector) and developed using 3,3' diaminobenzidine as the chromogen (DAB, DakoCytomation). Light microscopy was performed; pictures were captured and analyzed in Adobe Photoshop 5.0. Immunofluorescent staining was also performed for vWF on paraformaldehyde fixed tissues. Briefly, the tissues were

incubated with normal goat serum to block non-specific binding. The slides were incubated with the primary antibody followed by a Cy3 conjugated secondary. Fluorescent microscopy was performed; pictures were captured and analyzed in Adobe Photoshop 5.0

2.3.7 Collagen Deposition

Collagen detection was accomplished using Sirius red and fast green stains, and quantified using a modified technique originally described by Underwood and colleagues *(199)*. Image analysis software (IPTK 5.0, Reindeer Graphics, Asheville, NC) was used to quantify collagen in the heart sections. Briefly, slides were examined under a microscope with the 10X objective and areas of collagen deposition were captured with a digital camera. The image analysis software was used to quantify the amount of tissue positive for Sirius red. Sections from individual animals were averaged and experimental groups compared to control animals.

2.3.8 Relative Quantitative Polymerase Chain Reaction (qRT-PCR)

Using the TRIzol reagent (Gibco), RNA was isolated from the snap frozen myocardium as per the manufacturer's protocol. First strand cDNA was synthesized from 1 μg of total RNA using iScript cDNA Synthesis Kit (Biorad. Hercules, CA).

Relative quantitative RT-PCR (qRT-PCR) was completed using 12.5 ng of input cDNA with 0.5 μM of each of the forward and reverse primers and 1x iQ SYBR Green Supermix (Bio-Rad) was subjected to qRT-PCR using iQ Multicolour Real-Time PCR Detection System thermocycler (Bio-Rad). Standard curves, for efficiency, and no-

template control samples were run along with the samples during thermocycling. A melting curve was performed after thermocycling was complete to ensure target specificity. The primers were designed against the mRNA sequence of connective tissue growth factor (CTGF) (forward: 5'-TCAACCTCAGACACTGGTTTCG-3'; reverse: 5'-TAGAGCAGGTCTGTCTGCAAGC-3'), stromal derived factor (SDF)-1α (forward: 5'-GTAGAATGGAGCCAGACCATCC-3'; reverse: 5'-ATTCGATCAGAGCCCATAGAGC-3'), transforming growth factor (TGF)-β1 (forward: 5'-GACTATCCACCTGCAAGACTATCG-3'; reverse: 5'-GACTATCCACCTGCAAGACTATCG-3') and 18S ribosomal RNA (forward: 5'-TCAACTTTCGATGGTAGTCGCCGT-3'; reverse: 5'-TCCTTGGATGTGGTAGCCGTTTCT-3'). Expression was normalization to the 18S ribosomal gene using the Pfaffl method.

2.3.9 Statistical Analysis

One-way ANOVA tests were completed on all quantitative data using the Dunnet post-test to compare the experimental groups to the saline control. Our level of significance was set as $p \leq 0.05$. All statistical calculations were computed using GraphPad Prism 4 software.

2.4 Results

2.4.1 Effect of AngII on Animals

Animals were assigned to 3 experimental groups and infused with: a) AngII (2.0 μg/kg/min, n=35); b) AngII with Losartan (ARB, 6.9 μg/kg/min, n=4); or c) saline (control, n=17). Myocardial hypertrophy was measured via a cardiac mass index. AngII

exposure resulted in a significant increase in cardiac mass index at 7d ($p < 0.01$) compared to control animals (Fig. 2.1). Infusion of an ARB abolished the hypertrophic effect of AngII at 7d (Fig. 2.1) confirming that AngII effects are dependent on the interaction with its receptor (AT1R). AngII exposed animals showed a significant increase in their systolic, diastolic and mean arterial pressures after 7d of exposure when compared to control animals ($p < 0.01$; Fig. 2.1).

2.4.2 Myocardial Collagen Deposition

Hearts were harvested after 1, 3 and 7d and the degree of myocardial collagen deposition was quantified in heart sections stained with Sirius red. AngII exposure resulted in multi-focal areas of extensive collagen deposition after 3 and 7d when compared to control animals (Fig. 2.2). Quantification of collagen accumulation in AngII exposed animals confirmed these findings at 3 and 7d post AngII infusion compared to background collagen levels seen in control animals ($p < 0.01$; Fig. 2.2). Co-treatment of mice with AngII and an ARB resulted in base-line levels of collagen deposition suggesting that the fibrotic effects of AngII require AT1R signaling. The transcript levels of the pro-fibrotic factor transforming growth factor (TGF)-β1, analyzed by qRT-PCR, was significantly elevated above saline levels after 1 and 3d of exposure (4 and 5 fold increase respectively, $p < 0.01$, Fig. 2.2). Similarly the transcript levels of the pro-fibrotic factor connective tissue growth factor (CTGF) downstream of TGF-b1, analyzed by qRT-PCR, was also significantly elevated above saline levels after 1 and 3d of exposure (19 and 13 fold increase respectively, $p < 0.01$, Fig. 2.2), but were at baseline levels in animals receiving AngII and an ARB (Fig. 2.2). The significant increase in both TGF- β1 and

CTGF transcript levels at 1d appears to temporally precede the increase in collagen deposition seen at 3 and 7d.

2.4.3 Cellular Infiltration

Hearts stained with H&E suggested that AngII exposure resulted in progressive myocardial changes over the 7d period. Multifocal areas of cellular infiltration and myocyte loss were evident, particularly at 3 and 7d, in the myocardium of AngII exposed animals (Fig. 2.3). We have adapted a grid-scoring method to quantify cellular infiltration within AngII exposed myocardiums confirming that significant myocardial cellular infiltration is evident as early as 1d exposure and progressively increased at 3 and 7d ($p < 0.01$ at 1, 3 and 7d; Fig. 2.3). In contrast, hearts from saline control animals and animals co-treated with AngII and an ARB exhibited normal myocardial histology with no significant cellular infiltration (Fig. 2.3).

Cells seen infiltrating the myocardium were mononuclear in appearance with no evident polymorphonuclear cells. Immunohistochemistry was used to identify these cells using cell specific markers. At 7d, less than 20% of the infiltrating cells were positive for a leukocyte specific marker (CD45; Fig 2.4), which also corresponded with staining patterns for macrophage-specific markers (CD11b; Fig 2.4) and negative peroxidase stain (data not shown). In contrast, immunohistochemistry for myofibroblasts/smooth muscle cells (SMA) and endothelial cells (vWF) showed a large number of the infiltrating cells stain positively in areas of ECM deposition (Fig. 2.4).

The evident vWF staining is indicative of endothelial cell accumulation suggestive of neo-angiogenesis. To confirm the presence of endothelial cells we used a transgenic mouse (Tie2-GFP) that expresses green fluorescent protein (GFP) under the endothelial specific promoter Tie2. In the myocardium of Tie2-GFP mice exposed to AngII, few GFP positive cells were visible within areas of myocardial cellular infiltration and little co-localization with vWF positive staining was evident (Fig. 2.5.). This data suggests that the infiltrating cells were not differentiated endothelial cells.

2.4.4 Origin of Myocardial Infiltrating Cells

Based on KI-67 staining, infiltrating cells appear to undergo significant proliferation suggesting that they may be undifferentiated cells with a high proliferative index (Fig. 2.6). The transcript levels for a well-known chemokine for hematopoietic progenitor cells, SDF-1α, was significantly increased within 1d of exposure to AngII and remained elevated over the 7d exposure period (Fig. 2.7). We used immunohistochemistry for a hematopoietic progenitor cell marker, CD133, to identify and localize any hematopoietic progenitor cells *in vivo*. A large population $CD133^+$ cells was evident within areas of myocardial infiltration in AngII exposed myocardiums at 3 and 7d of exposure, which corresponded to the expression of SMA^+ marker (Fig. 2.7). The bone marrow origin of these myocardial-infiltrating cells was then confirmed using GFP^+ chimera mice. GFP^+ chimera (n=5) mice were exposed to AngII or saline infusion and heart tissue examined at 3d. Virtually all infiltrated cells were positive for GFP when compared to saline control (Fig. 2.8).

2.4.5 Isolation of $CD133^+/SMA^+$ Cells and Growth *In Vitro*

Using whole heart homogenate, we were able to grow primary cultures of adherent cells in an effort to characterize the origin of myocardial infiltrating cells seen in animals exposed to AngII. Myocardial cell isolates were taken from both AngII exposed and untreated animals. After 3d in culture, a distinct adherent cell population with spindle shape morphology was evident in flasks containing isolates from AngII treated myocardiums (Fig. 2.9). This was in contrast to very few adherent cells seen in cultures of untreated heart homogenates (Fig. 2.9). When quantified, there were significantly more adherent cells in cultures from AngII treated as compared to untreated hearts (60 cells/HPV and 8 cells/HPV respectively, $p < 0.01$, Fig. 2.9). Dual labeling for CD133 and SMA using immunofluorescent labels was used to further characterize the cultured cells. Cells from untreated hearts were single positive $CD133^-SMA^+$ whereas 81 ± 3% of cells from an AngII exposed hearts appeared to be double positive $CD133^+SMA^+$ (Fig. 2.9). In an additional set of experiments, cells cultured from untreated hearts were treated with AngII (100nM) for 2d but failed to show a significant expansion in the number of $CD133^+$ cells, further supporting that their origin is not from resident cells (Fig. 2.9).

2.5 Discussion

We have shown that AngII exposure results in significant ECM deposition that is characteristic of myocardial fibrosis. This collagen deposition was correlated with an increase in key pro-fibrotic factors, TGF-β1 and its down stream mediator CTGF, shortly after AngII infusion. We have provided evidence that early cellular infiltration into the myocardium precedes significant ECM deposition, potentially providing pro-fibrotic stimuli to initiate fibrosis. Despite the fact that the AngII infusion model is a well-

established model for hypertrophy, fibrosis, and hypertension, there has been little work done to characterize the cellular component of the response. The current paradigm asserts that fibrosis is the response to an initial stimulus that induces local inflammation and the recruitment of inflammatory cells. These cells then stimulate a fibrotic response. This theory has been supported by the identification of mononuclear cells, positive for macrophage markers, in the infiltrating cell population (12, 187-190). However, cell phenotypes and marker expression are dynamic and cells can alter their molecular expression to respond appropriately to stimuli in their environmental milieu. There is a circulating monocyte/macrophage precursor population that expresses specific markers for this cell type but are a phenotypically heterogeneous population (9, 10). Furthermore, precursors from the monocyte/macrophage lineage have been found to differentiate into non-immune cell types when presented with the appropriate stimuli (10, 200, 201). It is plausible that macrophage marker expression in tissue could have a temporal relationship to the degree of cell differentiation. We found very few cells expressing leukocyte or macrophage markers within the myocardium of mice early after AngII infusion which has been supported by others (24). This data suggests that fully differentiated leukocytes, specifically macrophages, may not represent the primary infiltrating cell. This data casts doubt on the prevailing paradigm that acute inflammation is the primary mechanism promoting fibrosis. However, there is an important distinction to be made between the present study, which uses a model of AngII-mediated fibrosis, compared to ischemic models that have been associated with fibrosis. In models of ischemia, in which there has been myocardial injury or infarction, inflammation has been shown to play a key role in healing and likely participates in the development of fibrosis but its contribution to date

has been poorly defined (152, 202, 203). The complex interactions between ischemia and the development of fibrosis were not explored in this study.

We have shown that AngII exposure results in significant positive staining for markers of mesenchymal cells, including SMA and vWF, by early myocardial infiltrating cells. SMA is a structural protein largely found in smooth muscle cells and myofibroblasts (204). The diffuse staining pattern of SMA would correspond with a myofibroblast-like cell population which are believed to be the primary cell responsible for ECM deposition (204). vWF, however, is a glycoprotein that is largely concentrated on the sub-endothelial matrix and as such, is often used as a histological marker for endothelial cells (205). Extensive staining with vWF is indicative of endothelial cell accumulation and/or neo-angiogenesis. However, our findings using Tie2GFP mice, in which endothelial cells express GFP, suggest that areas of myocardial cellular infiltration do not represent terminally differentiated endothelial cells.

We also found that a significant proportion of the infiltrating cells within the myocardium were positive for CD133. CD133 is known as a marker of hematopoietic stem cells found largely in the bone marrow and circulation (206). The presence of CD133 positive cells within the myocardium of AngII exposed animals suggests a role for undifferentiated hematopoietic progenitor cells in the fibrotic response. The hematopoetic (BM) origin of infiltrating cells was confirmed using BM chimera in which virtually all infiltrating cells were GFP^+. This hypothesis is supported by the fact that SDF-1α, a common chemokine for hematopoietic progenitor cells (207), was

significantly up-regulated within the myocardium of AngII exposed animals as early as day 1. This provides a potential mechanism to allow recruitment of circulating progenitor cells out of the blood into the tissue. Furthermore, we have shown that a large proportion of cells accumulating within AngII exposed myocardium were positive for a proliferation marker, KI-67, suggesting a high proliferative index. Terminally differentiated cells, including myocytes and leukocytes, typically do not undergo proliferation. Collectively, our data suggest that AngII results in the early recruitment of a hematopoietic progenitor cell into the myocardium.

The co-localization of a mesenchymal marker (SMA) and a hematopoietic progenitor marker (CD133) within areas of myocardial cellular infiltration suggests that these cells could represent fibroblast precursor cells, sometimes referred to as "fibrocytes". Fibrocytes are thought by some to be derived from an early monocyte precursor lineage (200). They are characterized by the co-expression of a hematopoietic marker (CD133/CD34), a leukocyte marker (CD45/CD11b) and a mesenchymal marker (SMA/Coll1) (208). Expression levels of these markers vary depending on the level of differentiation from early progenitor markers to late myofibroblast markers (208). However, the co-localization of a hematopoietic marker (CD133, CD34) and a mesenchymal marker (SMA, Coll1), as we demonstrated in primary isolated cells *in vitro*, is sufficient to confirm a fibrocyte phenotype (209). Our *in vitro* data demonstrated that these $CD133^{+}SMA^{+}$ cells can be grown easily in primary cultures from the myocardium of AngII exposed animals when compared to untreated animals where $CD133^{+}SMA^{+}$ could not be identified by 3d in culture. Furthermore exposure of primary

cultures from untreated animals to AngII did not yield expansion of $CD133^{+}SMA^{+}$ cells supporting our GFP chimera data that the origin of these cells is likely from the bone marrow as opposed to locally proliferating cells.

Fibrocytes have been implicated in liver, kidney, lung and skin fibrosis (196, 210, 211). Furthermore, others have shown that AngII exposure leads to the recruitment of fibrocytes into renal tissue in a model of kidney fibrosis (211). Importantly, fibrocytes can be recruited in response to SDF-1α gradients (196). However, until recently few investigators have suggested a major role for fibrocytes in cardiac fibrosis. Haudeck et al. in a recent publication was able to show that fibroblast precursors can be seen in animals exposed to AngII who develop myocardial fibrosis (24). The identified fibroblast precursors exhibited leukocyte markers (CD45), fibroblast markers (SMA) and progenitor cell markers (CD34) which, are all in keeping with the phenotype of fibrocytes we have shown in the present manuscript ($CD133^{+}/SMA^{+}$) (24). Our findings complement this recent work supporting the role of fibrocytes and confirming *in-vivo* (GFP chimera) and *in-vitro* ($CD133^{+}SMA^{+}$ primary cultures) that these cells appear to be fibroblast progenitor cells originating from the bone marrow.

Taken together, our findings supports the hypothesis that fibrocytes are the hematopoietic progenitor cell type that is recruited to the myocardium early after AngII exposure. We are proposing that fibrocytes, as opposed to solely inflammatory cells, are a key effector cell in the initiation of myocardial fibrosis. The regulation of fibrocyte recruitment is just beginning to be characterized and is potentially different from that of leukocytes. Thus,

additional investigation into the role and regulation of fibrocytes is required to further characterize their role in myocardial fibrosis.

2.6 Acknowledgements

We would like to thank Tanya Myers and Mary Li for their skillful technical assistance.

The present work was supported in part by a grant from the Nova Scotia Health Research Foundation (#42311).

A

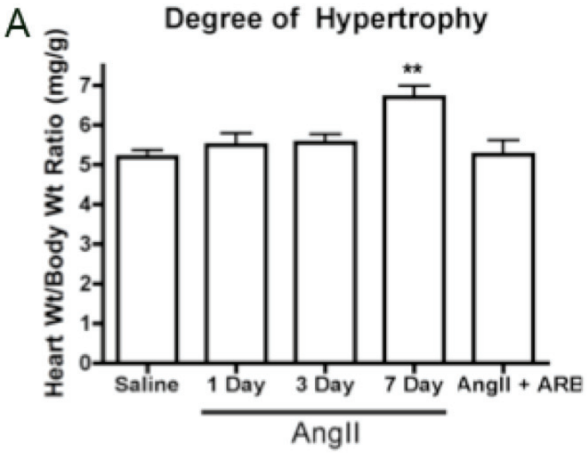

B

Experimental Group	Systolic Pressure (mmHG)	Diastolic Pressure (mmHG)	Mean Arterial Pressure (mmHG)
Saline	120.0 ± 6.3	89.4 ± 4.9	99.3 ± 5.1
AngII – 7Days	145.9 ± 4.3**	115.0 ± 4.7**	124.0 ± 4.4**

Figure 2.1 The Effects of AngII on Animals

AngII exposure induced an increase in the cardiac mass index (heart weight:body weight ratio) at 7d (A); Hemodynamic measurements were taken via tail cuff and AngII exposure at 7d increased systolic, diastolic and mean arterial pressure (B). $^{**}p<0.01$

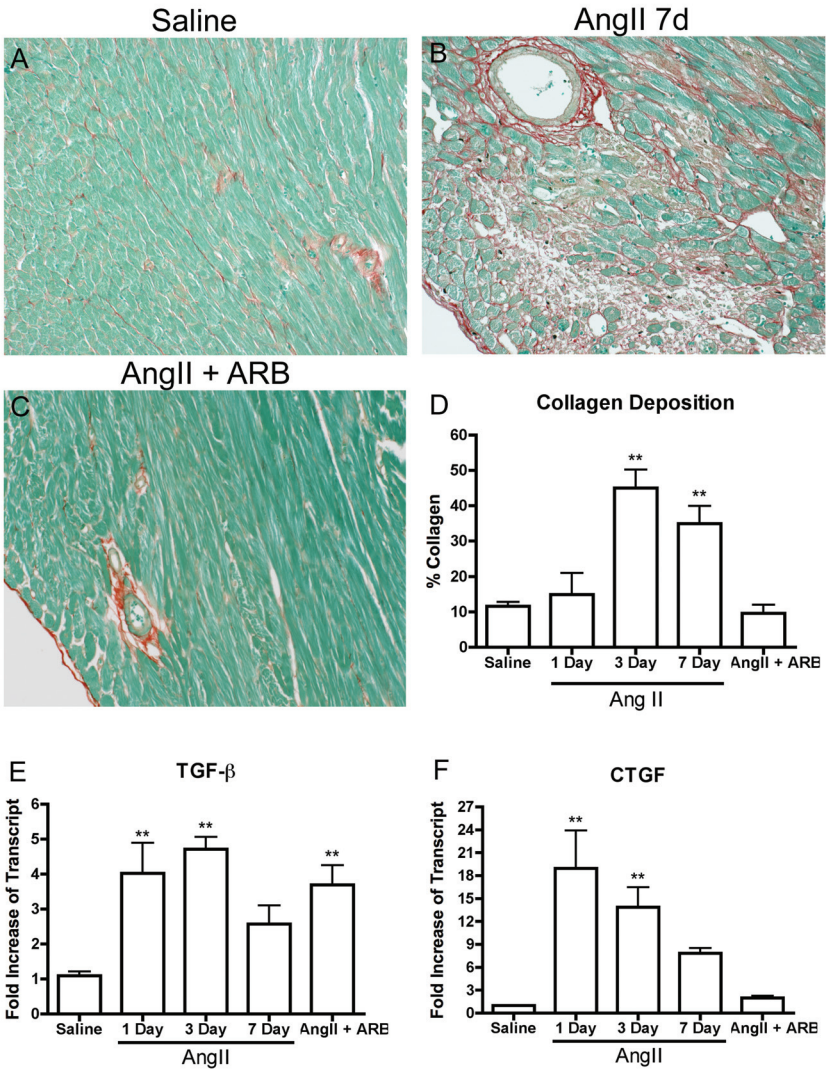

Figure 2.2 Collagen Deposition

To evaluate collagen deposition heart sections were stained with Sirius red and fast green. Representative sections are shown from control animals (A), 7d AngII exposed animals (B), and 7d AngII exposed animals + ARB (C). Collagen in the heart sections was quantified using image analysis software. AngII exposure resulted in significant collagen deposition at 3 and 7d and appeared dependent on AngII receptor mechanism (D). Using

qRT-PCR, we measured myocardial expression of TGF-β1 (E) and CTGF (F) mRNA transcript levels relative to the 18s ribosomal gene expression. Relative mRNA transcript levels for both TGF-β1 and CTGF were significantly increased in AngII infused animals at 1 and 3d, $**p<0.01$. Images were captured at 25X.

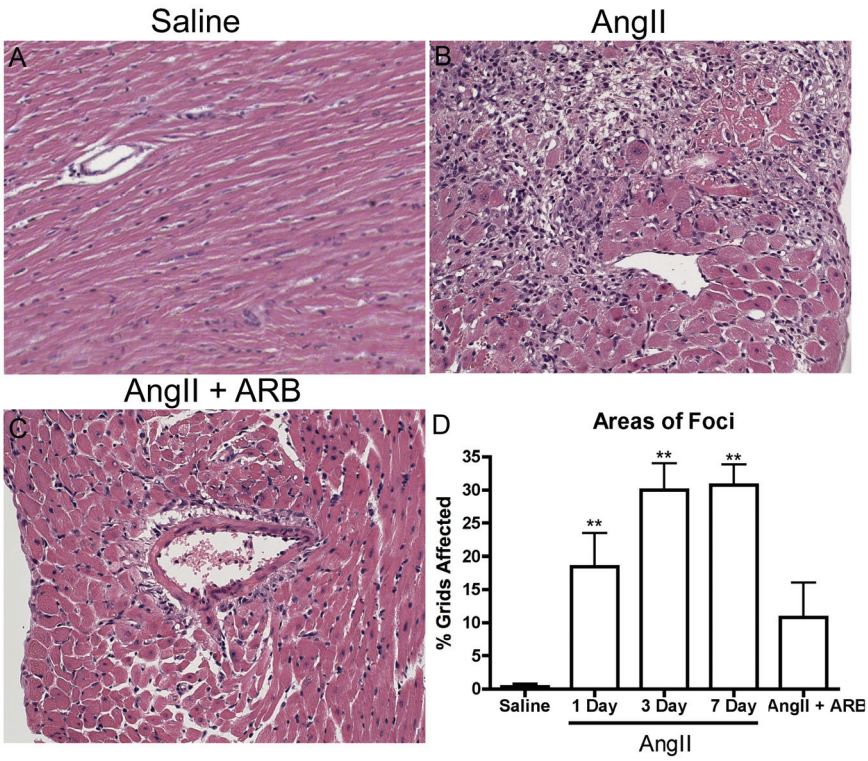

Figure 2.3 Heart Morphology

Representative sections of hearts stained with H&E from animals: saline control (A) AngII for 7d (B) and 7d AngII exposed animals + ARB (C). AngII infused animals resulted in areas of marked mononuclear cell accumulation, which preceded cardiomyocyte loss and replacement by extracellular matrix. The percent area of the myocardium affected by foci of myocardial cellular infiltration and ECM deposition was quantified to confirm visual assessments (D), $^{**}p<0.01$. Images were captured at 25X.

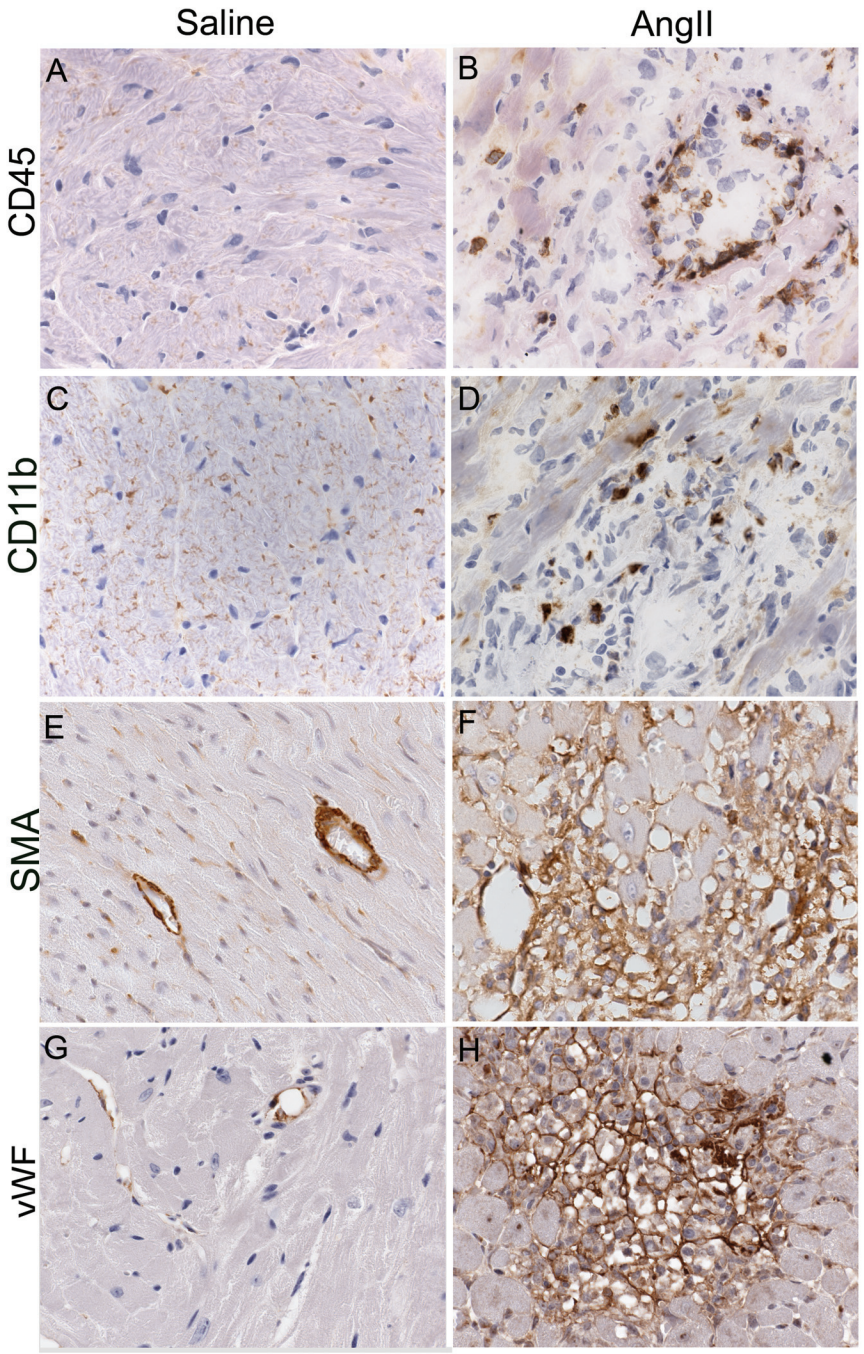

Figure 2.4 Immunocytochemistry

Immunostaining for a pan-leukocyte marker (CD45, A, B), monocyte/macrophage marker (CD11b, C, D), myofibroblasts (SMA, E, F), and endothelial cell associated marker (vWF, G, H). Representative sections are shown from control animals (A, C, E,

G), and 7d AngII exposed animals (B, D, F, H). AngII exposure is associated with myocardial infiltration with some $CD45^+$ and $CD11b^+$ cells but marked SMA^+ and vWF^+ cells. Images were captured at 63X.

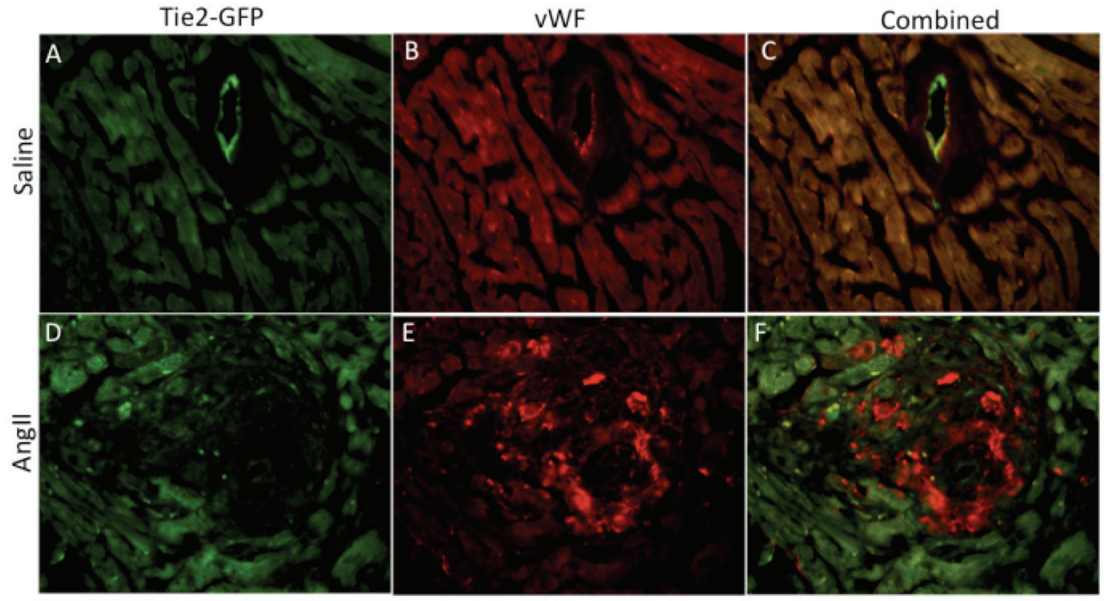

Figure 2.5 Endothelial Cell Localization

Fluorescence of natural green fluorescence protein (GFP) expression in a Tie2-GFP mouse (A, D), immunofluorescence of vWF staining with a red Cy3 secondary (B, E) and the combined image of both the GFP and vWF fluorescence with yellow coloration indicating overlapped expression (C, F). Representative images from control animals (A-C) and 7d AngII animals (D-F) are shown. Images were captured at 63X.

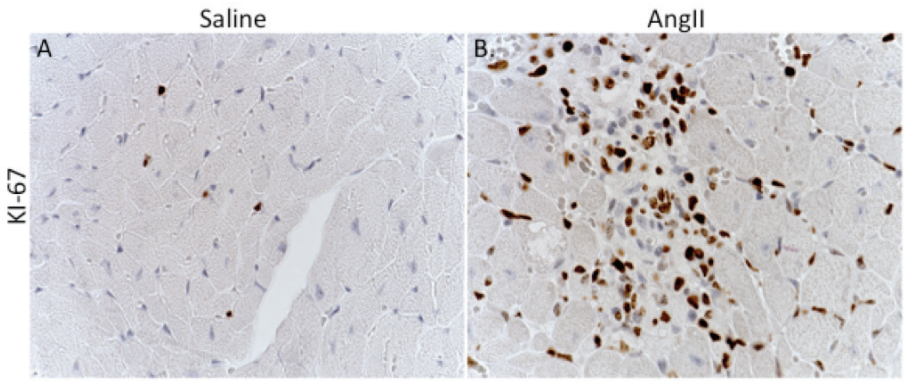

Figure 2.6 Cellular Proliferation

Representative images of immunocytochemistry for the proliferation marker KI-67 in control animals (A) and 7d AngII animals (B). Images were captured at 63x.

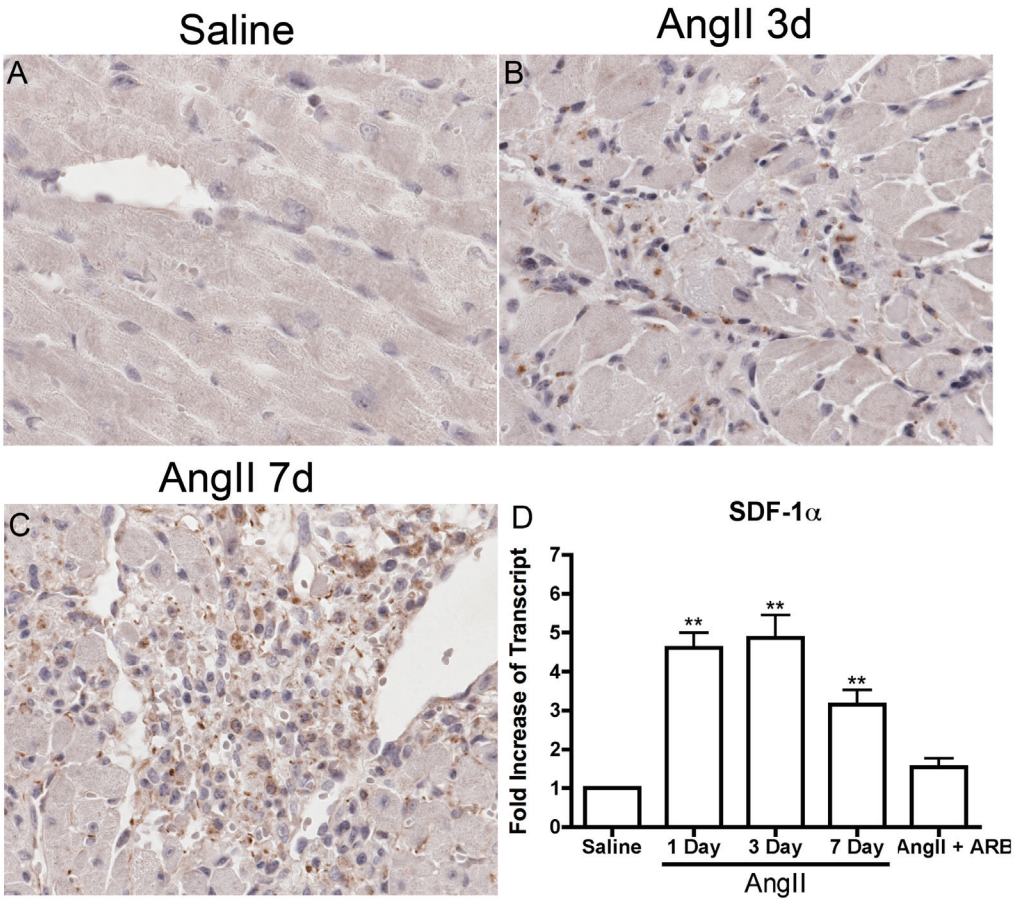

Figure 2.7 Hematopoietic Progenitor Cells

Immunostaining for the hematopoietic progenitor cell marker CD133. Representative sections are shown from control animals (A), 3d AngII exposed animals (B), and 7d AngII exposed animals (C). AngII exposure is associated with myocardial infiltration by a $CD133^{+}$ population increasing from 3 to 7d. Using qRT-PCR, transcript level of SDF-1α (D) was measured and normalized to 18S ribosomal gene expression. Relative transcript levels of SDF-1α was significantly increased in AngII infused animals. **p<0.01. Images were captured at 63X.

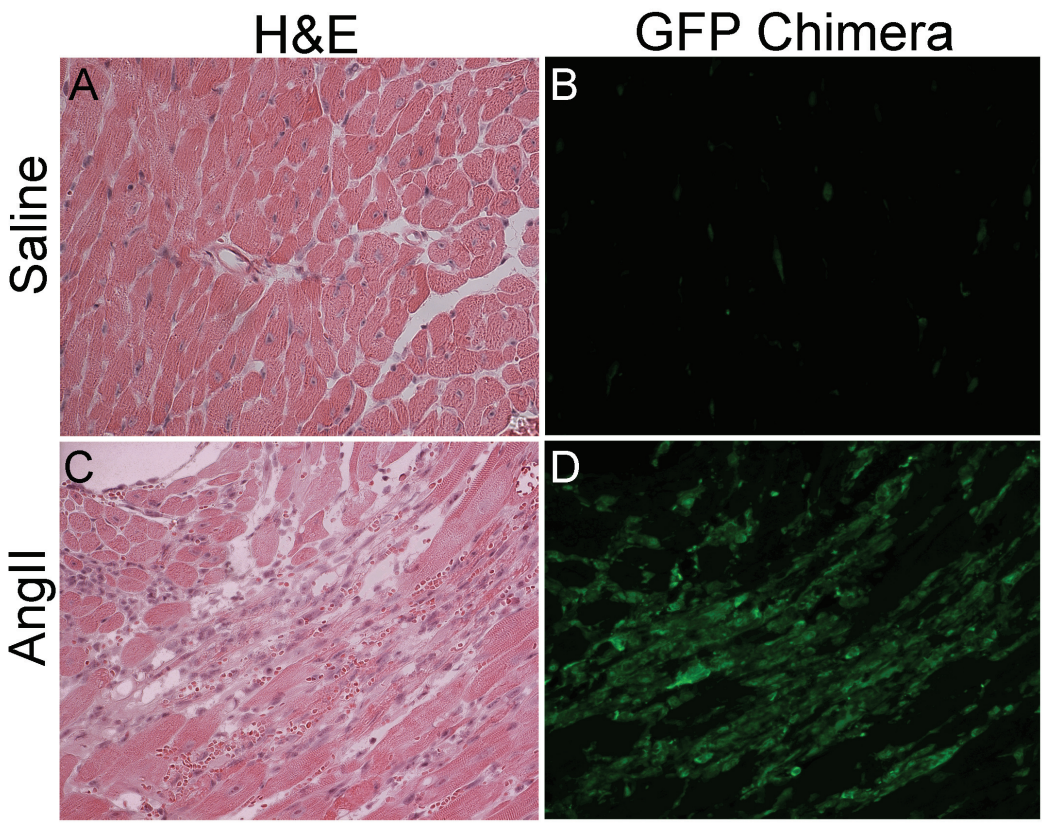

Figure 2.8 GFP Chimera Experiments

Representative sections of heart tissue taken from GFP^+ BM chimeric animals that were assigned at random: saline control treatment for 3d (A,B) or AngII for 3d (C,D). AngII infusion resulted in areas of marked cellular accumulation seen in H&E (C) when compared to control (A). Furthermore, all areas of cellular infiltration in AngII animals were strongly positive for GFP^+ immunofluorescence (D) when compared to saline control (B) suggesting that virtually all infiltrating cells are of BM origin. Images were captured at 25X.

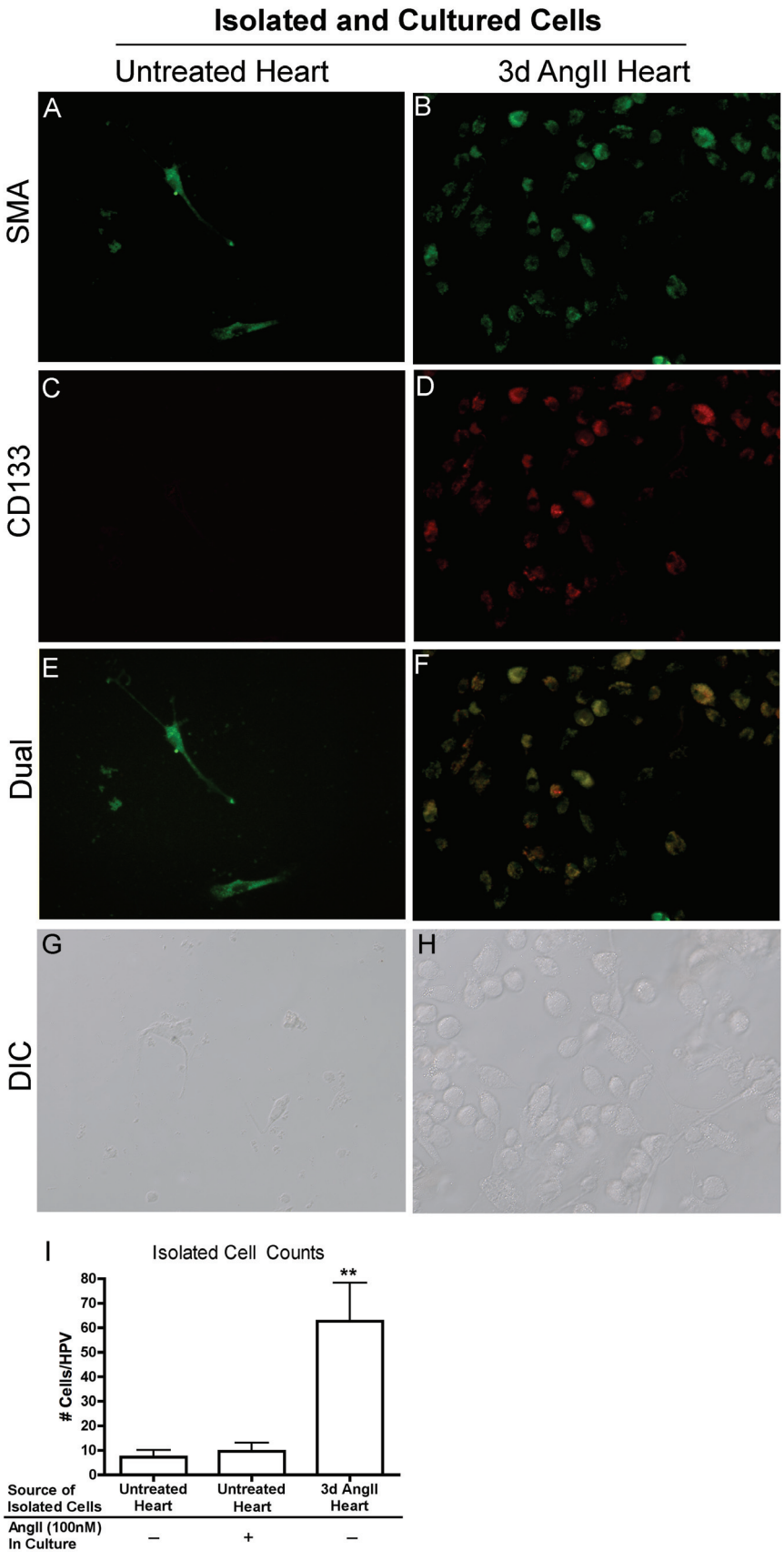
Isolated and Cultured Cells
Untreated Heart
3d AngII Heart
A
B
SMA
C
D
CD133
E
F
Dual
G
H
DIC
I
Isolated Cell Counts
**
80
70
60
50
40
30
20
10
0
Cells/HPV
Source of Isolated Cells
Untreated Heart
Untreated Heart
3d AngII Heart
AngII (100nM) In Culture
–
+
–

Figure 2.9 Isolated Cells

Cells were isolated out of the myocardium of untreated and 3d AngII exposed animals. Photomicrograph were taken of adherent cell populations obtained from untreated (A,C,E,G) and AngII exposed (B,D,F,H) myocardium after 3d in culture at 40x magnification. Representative pictures illustrate the increase in adherent cells in cultures from AngII exposed myocardiums (G,H). Cell counting (6 high power field (HPV) 10X/animal) was used to quantify the degree of cell growth by adherent cells between untreated naïve cells, untreated cells exposed to AngII (100nM) and cells from AngII exposed myocardium (I). Dual labeling immunofluorescence was used to demonstrate co-localization of SMA (green; A,B), CD133 (red: C,D), and overlaid to show co-localization of markers (yellow) (E,F) captured at 40x magnification. **$p<0.01$.

CHAPTER 3

FIBROBLAST PROGENITOR CELLS ARE RECRUITED INTO THE MYOCARDIUM PRIOR TO THE DEVELOPMENT OF MYOCARDIAL FIBROSIS

MJ Sopel*, A Falkenham, A Oxner**, I Ma**, TDG Lee, JF Légaré**

International Journal of Experimental Pathology. 2012. 93(2):115-124

* Author contributions are clearly outlined in Appendix 2.

3.1 Abstract

Introduction: Using an established model of myocardial hypertrophy and fibrosis after Angiotensin II (AngII) infusion, our aim was to fully characterize the early cellular element involved in the development of myocardial fibrosis. *Methods:* Male Lewis rats were infused with saline or AngII (0.7mg/kg/d) for up to 7d. Collagen deposition and cellular infiltration were characterized by histological stains. Infiltrating cells were grown *in vitro* and processed by flow cytometry and immunostaining. Chemokine expression was measured using qRT-PCR. *Results:* AngII infusion resulted in multifocal myocardial cellular infiltration (peak at 3d) that preceded collagen deposition. Monocyte chemotactic protein (MCP)-1 transcripts peaked after 1d of AngII exposure. Using a triple labeling technique, the infiltrating cells were found to express markers of leukocyte ($ED1^+$), mesenchymal cells (α-smooth muscle actin $(SMA)^+$), and hematopeotic progenitor cells ($CD133^+$) suggesting a fibroblast progenitor phenotype. *In vitro*, $ED1^+/SMA^+/CD133^+$ cells were isolated and grown from AngII exposed animals. Comparatively, few cells were cultured from untreated control hearts and they were found to be $ED1^-/SMA^+/CD133^-$. *Conclusions*: We provide evidence that myocardial ECM deposition is preceded by infiltration into the myocardium by cells that express hematopoietic (ED1, CD133) and mesenchymal (SMA) cell markers, a characteristic phenotype of fibroblast precursor cells, termed fibrocytes. This suggests that fibrocytes may have effector functions in the initiation of myocardial fibrosis rather than presumed leukocytes.

3.2 Introduction

Myocardial fibrosis is a pathophysiological process characterized by the deposition of extracellular matrix (ECM) proteins within myocardial tissue and is a common pathological feature of many cardiovascular diseases including hypertrophy and hypertension (2). The accumulation of ECM proteins within the myocardium enhances cardiac stiffness and eventually impairs cardiac function, leading to what is known as diastolic heart failure (5). Despite intense study, the mechanisms involved in the initiation and progression of myocardial fibrosis have yet to be fully characterized and is often suggested to be secondary to a primary inflammatory response (212, 213).

Recent work suggests that Angiotensin II (AngII), a part of the renin-angiotensin system, may play a key role in the development of myocardial fibrosis (5). This is supported by clinical evidence that patients with cardiovascular diseases and associated myocardial fibrosis have increased serum levels of AngII (5, 20, 21). Inhibition of the renin-angiotensin system, and more specifically using AngII receptor blockers, has demonstrated a significant clinical benefit in the prevention of cardiac remodeling including myocardial fibrosis (11). Using rodent models, in which AngII is given exogenously, several groups have demonstrated the development of myocardial hypertrophy and fibrosis (7, 11, 214). Taken together, this evidence strongly supports a role for AngII in the development of myocardial fibrosis; however, the direct mechanisms responsible and the effector cells involved have yet to be completely elucidated.

It has previously been described that exposure to AngII, as well as other fibrotic stimuli, results in rapid cellular infiltration that precedes the development of myocardial fibrosis (59, 61, 214). This temporal relationship suggests that the cellular component of a fibrotic response have an effector role in the stimulation of myocardial fibrosis. Until recently, much of the evidence has suggested that this cellular infiltration was mononuclear and consistent of cells from the monocyte/macrophage lineage, as demonstrated by positive immunocytochemical staining for specific molecules present on myeloid cells, ED1/CD11b (7, 156). Such evidence supported the paradigm that AngII mediates the development of myocardial fibrosis by promoting the recruitment of leukocytes (largely macrophages), that could then initiate a fibrotic response (5).

However, the exact phenotype of the initial infiltrating cells has thus far been poorly defined. We believe that these cells are the first direct responder to increased circulating levels of AngII and as such, could reasonably be assumed to mediate downstream effects. In this study, we provide evidence that the early cellular populations recruited to the myocardium, using a well described model of AngII exposure known to result myocardial hypertrophy and fibrosis, are not inflammatory leukocytes but are circulating progenitor cells that express hematopoietic and mesenchymal markers. This information will offer a broadened understanding of the process of myocardial fibrosis as well as alternative avenues of intervention.

3.3 Materials and Methods

3.3.1 Animals

All work was approved by Dalhousie University's *University Committee on Laboratory Animals* following the guideline of the Canadian Council on Animal Care. Male Lewis rats (Charles River Laboratories, St. Constant, QC) weighing 300-375g were housed in the Carlton Animal Care Facility, Dalhousie University, and provided food and water *ad libitum*. Animals were anesthetized with a ketamine (100mg/kg)/xylazine (5mg/kg) cocktail and a 1-2cm mid-scapular skin incision was made using aseptic techniques. Osmotic minipumps (Durect Corporation, Cupertino, CA) containing either saline (control group, n=24) or AngII (0.7 mg/kg/d; Sigma-Aldrich Canada Ltd., Oakville, ON, n=34) dissolved in saline, were placed subcutaneously. The incision was closed using 4-0 nylon sutures and animals were allowed to recover. Rats were sacrificed 4h, 1d, 2d, 3d, or 7d following implantation of the minipumps. The hearts were harvested and weighed to calculate the cardiac mass index (heart:body weight ratio). The heart tissue was processed for analysis.

3.3.2 Hemodynamic Measurements

Blood pressure was assessed using a non-invasive tail cuff system (Kent Scientific, Torrington, CT). Animals were subjected to 5 days of measurements prior to the initiation of the 7d experiment to allow for acclimatization and prevent artificial elevation of blood pressure. Blood pressures were measured prior to and daily after implantation of mini-osmotic pumps for a minimum of 5 consecutive readings per animal.

3.3.3 Cell Isolation and Culture

Hearts from untreated, naïve rats (n=4) or rats infused with AngII for 3d (n=6) were harvested under sterile conditions and used for cell isolation. Briefly, hearts were initially mechanically minced and then enzymatically digested in a Collagenase solution (50μg/mL Collagenase II, Cedar Lane, Burlington, ON) in Roswell Park Memorial Institute 1640 (RPMI) media (Gibco, Life Technologies, Burlington ON) at 37°C with agitation for 45min. The cell isolates were washed twice with complete RPMI (10% heat-inactivated fetal calf serum, 2mM L-glutamate, 100μg/ml streptomycin and 100U/ml Penicillin) and then either poured through a 70μm pore filter to generate a single cell suspension for flow cytometry or directly plated on T-75 flasks coated with 0.1% gelatin for culture. Of the whole homogenate samples, a small but equal proportion of each sample was plated onto a 0.1% gelatin coated coverslip. Cellular isolates were incubated at 37°C with 5% CO_2 for 3d, after which all non-adherent cellular debris was removed and fresh media was supplied. In all groups, digital images were taken using an inverted microscope for cell counting. Areas of cell growth were randomly selected (6/flask containing cells isolated from 1 heart) for cell counts. Cells grown in T-75 flasks were dissociated from the flask using 0.05% trypsin in serum free RPMI and were prepped for analysis by flow cytometry. Cells grown on coverslips were fixed in 4% paraformaldehyde and stored at 4°C until stained.

3.3.4 Flow Cytometry

Cells isolated out of the heart were analyzed by flow cytometry either directly after isolation from the heart (naïve n=2; AngII n=2) or after expansion in culture (naïve n=2; AngII n=4). A single cell suspension was isolated from whole heart homogenate directly

after isolated. Cells were permeabilized for intracellular staining using Cytofix/Cytoperm kit (BD Bioscience, San Jose, CA) as per manufacture's protocol. Non-specific protein interactions were blocked by incubating the cells with goat IgG. Cells were incubated with polyclonal rabbit anti-CD133 (Abcam, Cambrdge, MA), monoclonal mouse anti-CD68 (ED1, AbD Serotec, Oxford, UK), and polyclonal rabbit anti-Collagen 1a (Coll1a; Rockland, Gilbertsville, PA). The cells were incubated with host specific secondary antibodies conjugated with PerCP, Fitc, and PE respectively. Positive, isotype, secondary only and negative controls were completed along side experimental staining for compensation purposes and to control for non-specific binding. Samples were fixed in a 0.4% Formaldehyde solution and stored at 4°C until analysis. Samples were analyzed using a FACScalibur Flow Cytometer (BD Bioscience).

Expression of CD133 was assessed in isolated cells cultured for 3d to determine if their phenotype had changed during culture. Cells were permeabilized and blocked with goat IgG. Cells were then incubated with anti-CD133 followed by an incubation with a FITC-conjugated secondary. Isotype, secondary only and negative controls were completed along side experimental staining. Samples were fixed and stored at 4°C until analysis. Samples were analyzed using a FACScalibur flow cytometer (BD Bioscience).

3.3.5 Histology

Hearts were fixed in 4% Formaldehyde for 24h and incubated in a series of increasing percents of ethanols to dehydrate tissues which was followed by an incubation in a clearing agent, xylene. Hearts were then embedded in paraffin wax and serially sectioned (5μm). Basic myocardial histology and cellular infiltration were examined using heart cross-sections stained with hematoxylin and eosin (H&E). A blinded observer analyzed

heart sections for cell and nuclear morphology at a 63x magnification. Light microscopy was performed using a Zeiss Axiovision 4.6 digital image analysis program (Carl Zeiss, Toronto, ON). Pictures were captured using an AxioCam HRc camera (Carl Zeiss) and analyzed in Adobe Photoshop 5.0.

3.3.6 Collagen Deposition

Collagen staining was accomplished using Sirius red and quantified as previously described (214). Picrosirius red staining is a well-described histochemical stain for fibrillar Type I and Type III collagen which are believed to be the main types of collagen seen with myocardial fibrosis (60). Briefly, slides were examined under a microscope with the 10X objective and areas of collagen deposition were captured with a digital camera. The image analysis software was used to quantify the amount of tissue positive for Sirius red. Images from areas containing the most collagen staining were taken from a cross-section from individual hearts, with a minimum of 4 animals/experimental group, at a 10x magnification. Images were analyzed for collagen content to compare areas of fibrosis between different experimental groups. Percent collagen content calculated then averaged and experimental groups compared to control animals.

3.3.7 Immunohistochemistry

Immunohistochemistry was performed to assess the phenotypes of infiltrating cells. Briefly, slides were processed in a standard fashion as previously described (214). Sections were incubated with a relevant primary antibody against CD68 (ED1, AbD Serotec), α-smooth muscle actin (SMA; 1A4, Sigma-Aldrich Canada Ltd.), or CD133 (Abcam), and was developed using the LSAB technique, as per manufacturer's protocol

(DakoCytomation, Burlington, ON). Light microscopy was performed using a Zeiss Axiovision 4.6 digital image analysis program (Carl Zeiss). Pictures were captured using an AxioCam HRc camera (Carl Zeiss) and analyzed in Adobe Photoshop 5.0. Among the images analyzed, one image of maximal $ED1^{+}$ myocardial infiltration from a minimum of 4 animals/experimental group captured at 25x were used for quantification. A blinded observer counted ED+ cells and the resulting tallies were averaged and experimental groups were compared to control groups.

3.3.8 Immunofluorescence

Triple labeling, using a combination of immunofluorescent probes and immunohistochemistry was performed to identify cells expressing multiple cell markers in paraffin-embedded heart samples. Briefly, slides were processed in a standard fashion as previously described (214). Tissues were incubated with anti-CD133 (AbCam) and developed using the LSAB technique (DakoCytomation). The tissues were then incubated with primary antibodies of anti-CD68 (ED1, AbD Serotec) and anti-SMA (C04018, Biocare Medical, Concord, CA) followed by host specific secondary antibodies conjugated with Alexa488 and Cy3 respectively. Images were taken of AxioCam HRc campera (Carl Zeiss) using light microscopy to visualize the CD133 and fluorescent microscopy at the 488 and 535 wavelengths to assess fluorescent staining. The micrograph of the CD133 staining was analyzed using Adobe Photoshop 5.0 and the positive brown staining was selected and a colored mask representing the positive cells was generated. The two fluorescent images and the colored mask were overlaid to assess co-localization.

Isolated cells that were paraformaldehyde fixed on coverslips were stained using an altered protocol from those described above. Antigen retrieval was not required for formaldehyde fixed samples. Non-specific protein binding was blocked by incubating the tissues with a 10% normal goat serum. Samples were then incubated with the primary antibodies anti-CD68 (ED1, AbD Serotec), anti-CD133 (Abcam) and anti-SMA (Biocare Medical), which were followed by an incubation with host specific secondary antibodies conjugated with Alexa488 Cy3 and Cy5 respectively. Lastly, tissues were incubated with Hoescht (Invitrogen, Burlington, ON). Tissues were thoroughly washed and wet mounted. Fluorescent microscopy was preformed using an AxioCam HRc camera (Carl Zeiss). Pictures were taken at the 488 and 535, 650 and 350 wavelengths and resulting images were overlaid. Images were analyzed in Adobe Photoshop 5.0.

3.3.9 Relative Quantitative RT-PCR (qRT-PCR)

We used relative quantitative RT-PCR to analyze mRNA transcript levels within myocardial tissue as we previously described (215). Briefly, using the TRIzol reagent (Invitrogen, Burlington, ON), RNA was isolated from snap frozen heart tissue, as per manufacturer's protocol. Isolated total RNA (2μg) was used to synthesize cDNA using oligo(dT)20 in SuperScript III First Strand Synthesis SuperMix kit (Invitrogen) as per the manufacturer's protocols. 25ng of input cDNA with 0.5μM of each of the forward and reverse primers for MCP-1 or reference gene and 1x iQ SYBR Green Supermix (Bio-Rad Laboratories, Mississauga, ON) was subjected to qPCR using iQ Multicolour Real-Time PCR Detection System thermocycler (Bio-Rad). Standard curves, for efficiency, and no-template control samples were run along with the samples during thermocycling. A melting curve was performed after thermocycling was complete to ensure target

specificity. Expression and normalization of the target gene, MCP-1, were calculated relative to the three housekeeping genes (Tub1a, LDHb, HPRT) using qBase v.1.3.5, as described previously (216). The primers used were designed against the mRNA sequence of specified genes using Primer3 (version 0.4.0, Table 3.1).

3.3.10 Statistical Methods

Data are reported as mean ± SEM. Continuous variables were analyzed with GraphPad Prism (La Jolla, CA) by comparing each experimental group to a control group using an unpaired two-tailed t-test. Upregulation of MCP-1 mRNA by qRT-PCR was compared to baseline gene expression and analyzed by a one-sample t-test. Statistical significance was defined as a $p \leq 0.05$.

3.4 Results

3.4.1 Hemodynamic Measurements

The blood pressures of both AngII (n=4) and saline (n=2) infused animals were measured over the 7d infusion period (Fig. 3.1). An elevation of blood pressure was evident as early as 1 day of AngII infusion, compared to saline controls. Blood pressure levels remained elevated in AngII infused animals over the 7 days of infusion, supporting AngII infusion as a model of hypertension.

3.4.2 Myocardial Collagen Deposition

AngII infusion is an established model of myocardial hypertrophy and fibrosis (11). Using this model, AngII exposure (7d) resulted in significant myocardial hypertrophy (heart weight:body weight) when compared to saline control ($p<0.05$; Table 3.2). Sirius

red staining of the myocardium of AngII infused rats revealed multi-focal areas of extensive collagen deposition throughout the ventricles of the heart (Fig. 3.2, S3.1). Saline infused rats showed limited, background levels of collagen content within the interstitium. Quantification of collagen deposition by digital image analysis confirmed a significant increase in collagen content in areas of the hearts from 3d and 7d AngII infused animals as compared to control animals ($p<0.05$, Fig. 3.2, S3.1).

3.4.3 Myocardial Histology

Infusion of AngII is also known to be associated with cellular and structural changes as well. Hearts from saline control animals demonstrated normal myocardial morphology (Fig. 3.3). In contrast, heart tissue from AngII exposed animals exhibited multi-focal areas of cellular infiltration, cardiomyocyte loss, and extensive extracellular matrix deposition. These changes could be seen throughout the left and right ventricles and were evident in both perivascular and interstitial tissues. The prominent feature of these changes were dense areas of cellular infiltration that could be seen as early as 1d following the onset of AngII infusion and progressed over the 7 days (Fig. 3.3).

To investigate factors in the environmental milieu that may be recruiting the infiltrating cells we used relative qRT-PCR to assess the transcript levels of chemotactic factors. Specifically we assessed the transcript levels of MCP-1, a chemotactic cytokine for monocytes/macrophages and some progenitor cell types. Myocardial expression of MCP-1 mRNA was quantified following 4h, 1d, 2d and 3d of AngII infusion (Fig. 3.3). There was a significant increase in MCP-1 mRNA expression compared to the baseline

expression of the three normalized housekeeping genes in the myocardium of animals exposed to AngII for 1d, 2d and 3d ($p < 0.05$). Furthermore, peak expression of MCP-1 mRNA occurred following 1d of AngII infusion with an increase of approximately 20 fold above the baseline expression of the housekeeping genes.

3.4.4 Myocardial Infiltrating Cells

We next characterized the phenotypes of the infiltrating cells by assessing cell morphology and cell specific marker expression. The infiltrating cells were mononuclear in nature with no evident polymorphonuclear (PMN) cells at any time point from 1-7d. Immunohistochemical staining for cell specific markers was used to characterize the infiltrating cell types within the myocardium. A portion, approximately 50%-75%, of the cellular infiltrate at 3d and 7d were positive for a monocyte/macrophage marker, ED1 (Fig. 3.4). Quantification confirmed an increase of $ED1^+$ cells at day 1, 3 and 7 in AngII infused animals with peak infiltration seen at 3d ($p<0.01$, Fig. 3.4). Additionally, infiltrating cells at 3d and 7d were largely positive for a myofibroblast marker, SMA (Fig. 3.4); however, due to the diffuse nature of SMA staining, quantification of SMA^+ cells was not performed. Similarly, we investigated the presence of a progenitor cell population within the myocardium of AngII stimulated animals by staining for a hematopoietic progenitor cell marker, CD133. No CD133 positive staining cells were evident in saline control animals (Fig. 3.4). In AngII infused animals, the infiltrating cell population at 3d and 7d appeared largely positive for CD133 suggesting that the infiltrating cells potentially express all three markers.

A correlation between the areas staining positive for ED1, SMA and CD133 suggested that many infiltrating cells might be co-expressing these markers. We used triple immuno-labeling to characterize cell expression of ED1, SMA and CD133. We found that, in the myocardium of AngII infused animals, that a significant population of $ED1^+$ cells were also positive for SMA and CD133 (triple positive) (Fig. 3.5). No double or triple labeling was apparent in the myocardium of saline control animals (data not shown). The expression of both hematopoetic (ED1, CD133) and mesenchymal (SMA) markers is not a generally accepted phenotype of mature macrophages though is a phenotype found in a specific mesenchymal progenitor cell type originating from a circulating $CD14^+$ population (11, 200, 217).

3.4.5 *In Vitro* Culture and Characterization of Infiltrating Cells

Infiltrating cells were isolated from the myocardium of 3d AngII infused rats and evaluated by FACS analysis for expression of ED1, SMA and CD133. Using this approach cells isolated from AngII exposed animals had a large of population of cells that were $ED1^+/SMA^+/CD133^+$ (>4 fold) when compared to saline control animals (Fig. 3.6).

We then proceeded to culture isolated cells *in vitro* to confirm the phenotype of these cells. After 3 days of culturing heart homogenates, an adherent spindle shaped cellular population was evident in cultures from the myocardium of AngII treated animals when compared to the few cells obtained from the myocardiums of untreated animals (Fig. 3.7). When quantified, 136 ± 22 cells per high powered view (hpv) could be identified in cultures from AngII exposed animals compared to 2 ± 1 cells per hpv in cultures from untreated, naïve animals ($p<0.01$, Fig. 3.7). Triple label immunofluorescence was used and confirmed that cultured cells from AngII exposed animals were positive for ED1,

SMA and CD133 (Fig. 3.7). In contrast, cells seen in cultures from naïve animals were only SMA^+ (Fig. 3.7). CD133 expression was assessed by flow cytometry and suggested that 63% ± 5% of cells seen in cultures from AngII exposed animals were positive (Fig. 3.7). Taken together, this data supports our *in vivo* findings that infiltrating cells are largely of a mesenchymal progenitor cell population referred to as fibrocytes.

3.5 Discussion

Despite the fact that AngII infusion in rodents is a well-established model to study hypertension, hypertrophy and fibrosis, there is limited evidence regarding the exact cell types responsible for the fibrotic response. Previous work has suggested that an increase in circulating AngII initiates an inflammatory response within the myocardium that recruits leukocytes. These inflammatory cells are thought to be activated and produce pro-fibrotic factors (5). Support for this theory includes the identification of mononuclear cells within the infiltrating cell population, some of which stain positive for ED1 and CD11b, which are indicative of a monocyte/macrophage cell type (7, 156). However, cell phenotypes are dynamic and cells can alter their molecular expression to respond appropriately to stimuli in their environmental milieu. For example, circulating myeloid precursor cells express specific markers of monocytes/macrophages, but are a phenotypically heterogeneous population and can differentiate into non-immune cell types when presented with the appropriate stimuli (9, 10). Previously, it has been assumed that, due to ED1/CD11b positive cellular staining, macrophages are the cell type predominantly recruited early during AngII induced myocardial fibrosis (7). However, these cells have not been shown to be mature macrophages and therefore could be an early myeloid precursor cell type. In fact, we have shown that the number of $ED1^+$ cells

peaks at 3d of AngII infusion, while cellular infiltration is still largely evident after 7d infusion. Furthermore, we have provided evidence that the majority of $ED1^+$ cells are also positive for SMA, which is not an accepted phenotype of mature macrophages. A cell population that is $ED1^+SMA^+$ is indicative of a progenitor cell type and, in fact, we found that many of the infiltrating cells expressed the hematopoietic progenitor cell marker CD133. This evidence would suggest that a mesenchymal progenitor cell type are the primary responders to potent fibrotic stimuli and potentially initiate the fibrotic response within the myocardium.

We interpret these findings to suggest that infusion of exogenous AngII stimulates the recruitment of a fibroblast precursor cell type, called fibrocytes, within the myocardium. Fibrocytes are thought to be derived from an early monocyte precursor lineage and, as such, express myeloid markers supporting findings by others that have identified cells populations expressing markers of monocytes/macrophages (200). The important phenotypic distinction is that fibrocytes are characterized by the co-expression of hematopoietic markers (CD133/CD34), leukocyte markers (ED1/CD11b) and mesenchymal markers (SMA/Col-1a) (208, 217). Expression levels of these markers vary depending on the level of differentiation from early progenitor cells to late myofibroblast cells, which could potentially explain why we found less $ED1^+$ cells at 7d AngII infusion (208). This may also explain why only 63 ± 5% of isolated cells were positive for CD133. Work from our group has recently described the early migration of $CD133^+/SMA^+$ fibroblast progenitor cells in mice myocardium after AngII exposure,

supporting our findings (214). However, the present manuscript is the first to describe the migration of fibrocytes in rat myocardium.

Fibrocytes are thought to be recruited out of the circulation by gradients of SDF-1α/CXCL12, CCL21 and, importantly, MCP-1/CCL2 (85, 196, 201, 218). This is of significance because we found an increase in transcript levels of MCP-1 within the myocardium, as early as 4h of AngII infusion, which could act as a possible mechanism for recruiting fibrocytes into the myocardium. Supporting our findings, recent work by Haudek *et al.* using MCP-1 KO animals was able to show that MCP-1 was responsible for the recruitment of $CD34^{+}/CD45^{+}$ fibroblast precursor cells to the myocardium in response to AngII (24). Furthermore, inhibition of migration of these cells resulted in a reduction in the development of fibrosis confirming that fibrocytes likely play an effector role in the development of fibrosis (24). Though we did not identify the cellular origin of the MCP-1, others have found that local endothelial cells, vascular smooth muscle cells, fibroblasts and myocytes can produce MCP-1 in response to a variety of stimuli, possibly including the increase in circulating AngII and/or an increase in hemodynamic pressure evident in this model (90). While fibrocytes have been implicated as an effector cell in several models of tissue fibrosis, including after AngII exposure, this has not been well established in models of myocardial fibrosis (24, 60, 214, 219, 220).

We are proposing that fibrocytes, a progenitor cell type, are a key effector cell in the initiation of AngII induced myocardial fibrosis. We are not suggesting that inflammatory

cells play no role in this process. However, given that fibrocytes have the capacity to produce pro-inflammatory mediators as well as contribute to fibrosis by producing collagen and fibronectin, we suggest that fibrocytes may act as a bridging cell type from an early inflammatory response to a corresponding fibrotic response later (220-222). Our findings, in addition to recent work from others, are providing a body of evidence in which bone marrow derived progenitor cells (fibrocytes) may represent a significant source of cells capable to migrate into tissues and differentiate into myofibroblasts (24, 60, 88, 214). Our findings also suggest that local activation of resident fibroblasts may not be the primary source of cells responsible for the development of fibrosis after AngII exposure and open the way for potential therapeutic modalities able to limit the recruitment of fibrocytes. In the present study, our findings demonstrate that the majority of the infiltrating cells expressed $ED1^{+}/SMA^{+}$ and $CD133^{+}$, suggesting that the majority were bone marrow in origin. Clearly, future work that will characterize the regulation of fibrocyte recruitment may allow us to intervene pharmacologically and inhibit this recruitment to the myocardium and potentially prevent excessive myocardial fibrosis associated with many cardiovascular conditions.

3.6 Acknowledgements

This work was supported in part by a grant from the Nova Scotia Health Research Foundation (#42311). Furthermore, we would like to thank Mary Li and Tanya Myers for their skillful technical assistance.

Table 3.1: Primer Sequence of the Target Genes

Gene Symbol	Forward Primer	Reverse Primer	Base Pairs
MCP-1	atctgtgctgaccccaataagg	gtggttgtggaaaagagagtgg	196
Tub1a	aaccatgcgtgagtgtatctcc	aactgtgggttccaggtctacg	226
HPRT	aaaggacctctcgaagtgttgg	ctttactggccacatcaacagg	213
LDHb	gtcatcaaccagaagctgaagg	agggaagaagcaaactgtgacc	194

Forward and reverse primers (5’ - 3’ orientation) for the specific genes have a product length of the corresponding base pairs

Table 3.2: Hypertrophic Assessment

	Saline	3d AngII	7d AngII
Heart Weight:Body Weight Ratio (mg/g)	2.7 ± 0.1	3.0 ± 0.1	3.2 ± 0.2*

*p<0.05 when compared to saline control

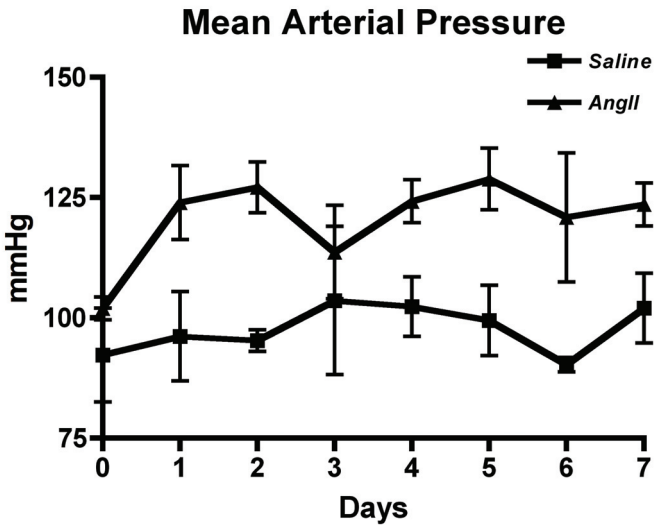

Figure 3.1 Mean Arterial Pressure

Mean arterial pressure measurements from animals infused with AngII (triangle) and saline (square) over a 7d period.

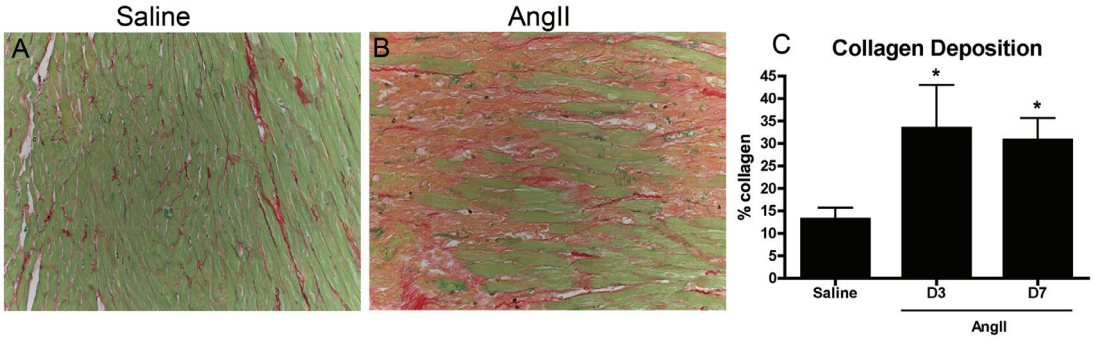

Figure 3.2 Sirius Red Stain for Collagen

To evaluate collagen deposition in the experimental groups heart sections were stained with Sirius red and fast green. Representative sections are shown from control animals (A) and 7d AngII exposed animals (B). Collagen in most afflicted areas of the heart sections was quantified using image analysis software (C), *$p<0.05$. Images were captured at 10X.

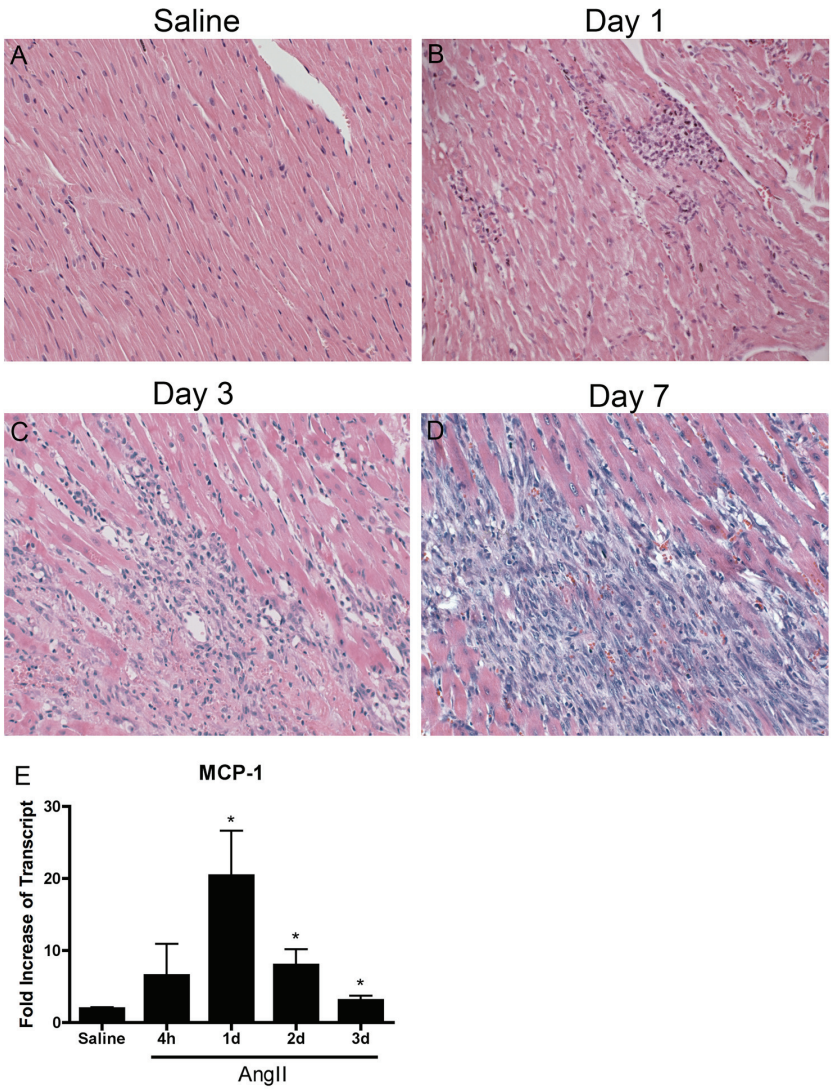

Figure 3.3 Cellular Infiltration

Hearts stained with H&E from control animals receiving saline (A), AngII for 1d (B), AngII for 3d (C) or AngII for 7d (D). AngII infused animals revealed areas of marked cellular accumulation, cardiomyocyte loss and replacement by extracellular matrix. Images were captured at 25X. qRT-PCR was used to assess myocardial expression of MCP-1 transcript levels relative to 3 housekeeping genes (E). Relative expression of MCP-1 mRNA was significantly increased in AngII infused animals 1d, 2d, and 3d, *$p<0.05$.

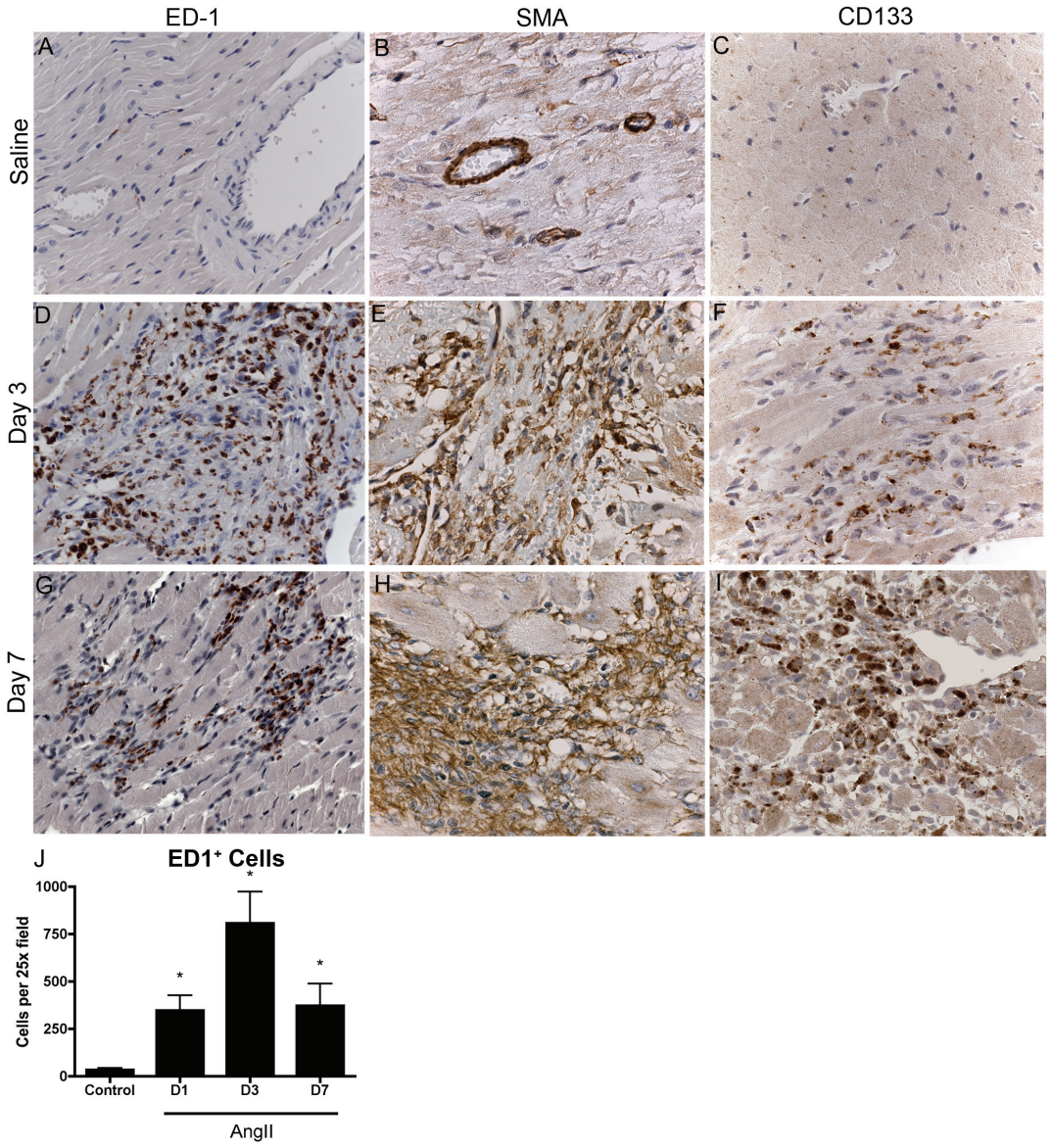

Figure 3.4 Immunohistochemistry Staining

Immunohistochemistry for ED1 (A, D, G), SMA (B, E, H), and CD133 (C, F, I) was used to identify the cellular infiltrate in heart sections. Representative sections from control animals receiving saline (A, B, C), AngII for 3d (D, E, F) and AngII for 7d (G, H, I) are shown. $ED1^{+}$ cellular infiltration was quantified by counting 3 fields (HPF), n=4 per group, *$p<0.01$. Images were captured at 63X.

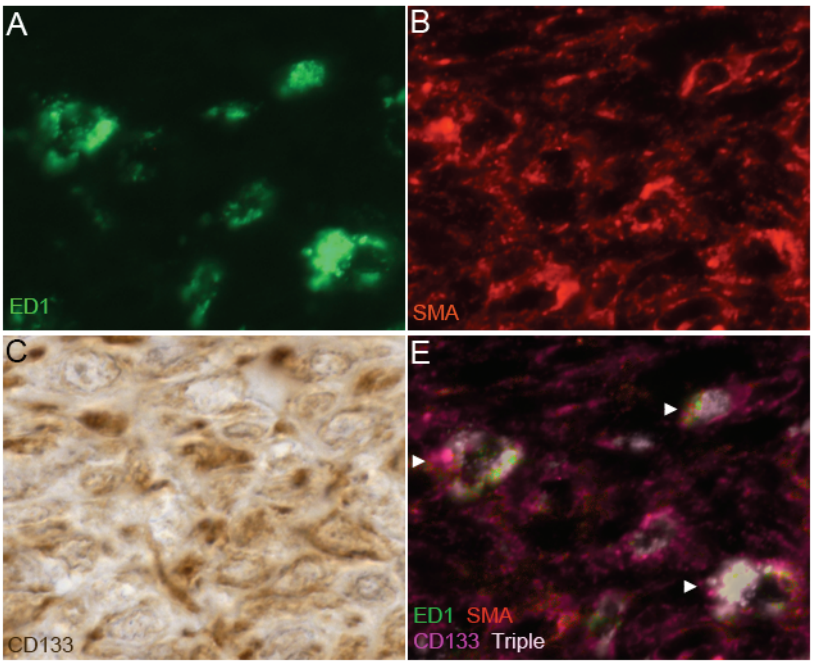

Figure 3.5 Triple Labeling for ED1, SMA and CD133 *In Vivo*

immunofluorescent labeling for ED1 (green; A) and SMA (red; B) followed by immunohistochemistry for CD133 (brown; C). Triple labeling of cells is indicated in the composite image of the three stains where a representative coloured mask (purple) of CD133 positivity was generated and overlaid the dual staining image of ED1 and SMA. Triple positive cells are indicated by a white overlay coloring (arrows). Images were captures at 63X.

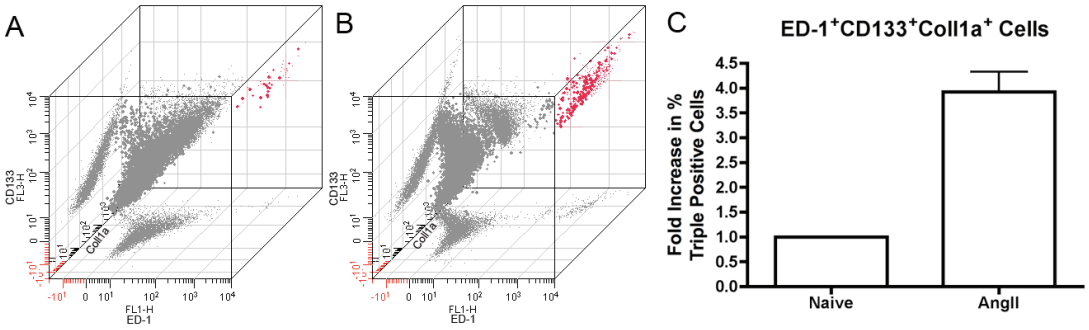

Figure 3.6 Isolation of Infiltrating Cells

A single cell suspension of cells directly isolated out of naïve and AngII exposed hearts were labeled for flow cytometry for ED1, Coll-1a and CD133. Representative 3-axis dot plot of flow cytometry data from naïve (A) and AngII (B) exposed animals are shown with ED-1 expression on the x axis, CD133 expression on the y axis and Coll1a expression on the z axis. Triple positive cells are displayed in red. Percent positive triple labeled cells normalized to naïve controls was determined (D).

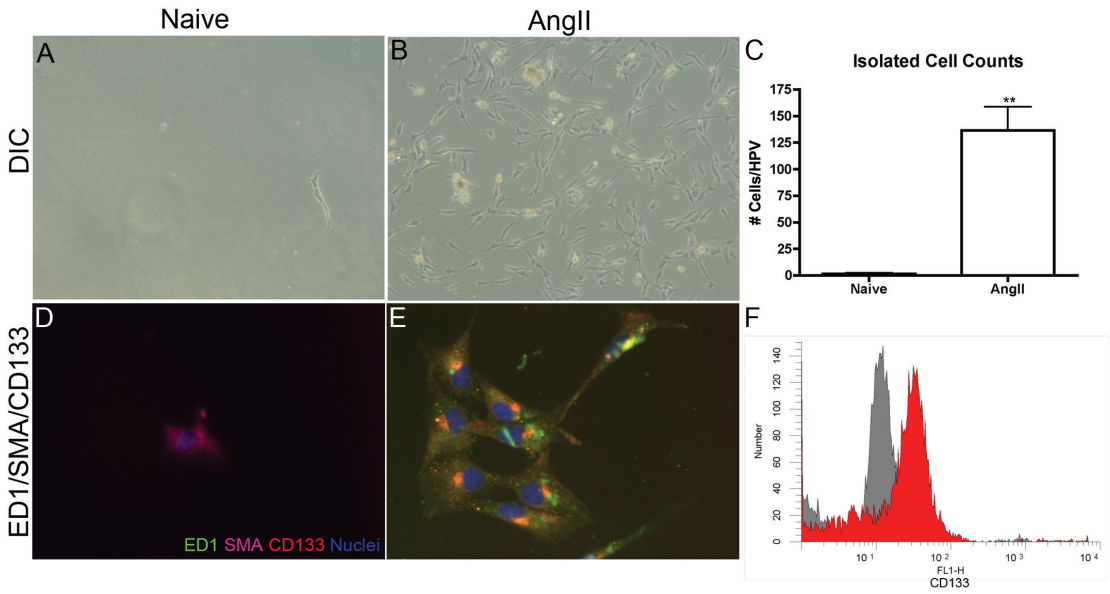

Figure 3.7 *In Vitro* Culture of Infiltrating Cells

Infiltrating cells were cultured from whole heart homogenates form naïve, untreated and 3d AngII infused mice. Photomicrographs were taken of adherent cell populations isolated from naive (A) and 3d AngII exposed (B) animals using differential interference contrast (DIC) microscopy (10x). Cell counting (6 high power fields of view (HPV) per plate) was used to quantify the number of adherent cells between the two groups (C). Triple labeling immunofluorescence was used to demonstrate co-localization of ED1 (green), SMA (red), and CD133 (purple) along with Hoeschst (blue) as a nuclear stain. Images were overlaid to show co-localization of markers in cells from untreated (D) and AngII exposed (E) myocardiums (40x). A representative histogram of the CD133 expression (red) compared to the negative control (grey) determined by flow cytometry (F). *$p<0.05$.

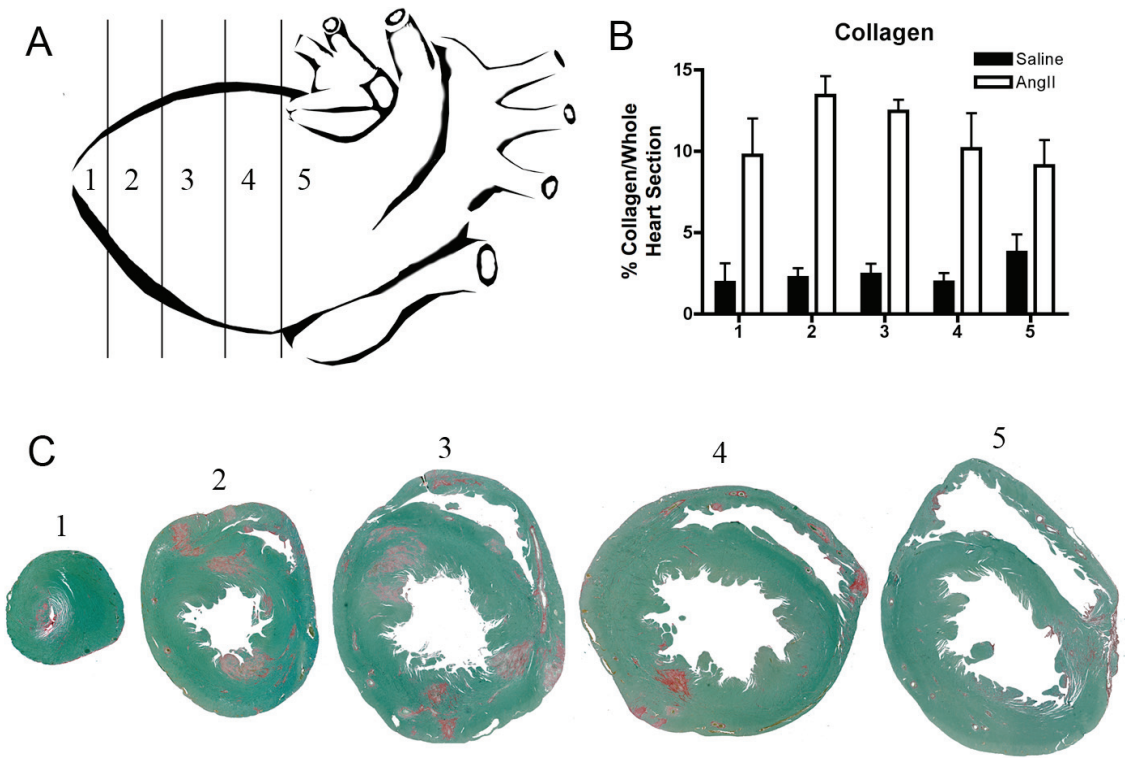

Figure S3.1 Whole Heart Analysis of Collagen Content

Hearts from 7d AngII animals (n=4) and saline control animals (n=2) were dissected into 5 sections as illustrated (A) and processed for histological examination. 5μm sections were cut from 2 depths of each section isolated and were stained with Sirius red to assess collagen content. Images were captured at 2.5x magnification and compiled into 1 cross section image that was digitally analyzed to quantitate collagen content from each portion of the heart (B). Areas of collagen deposition are evident throughout the entire ventricles of AngII infused animals after 7d (C).

CHAPTER 4

FIBROBLAST PROGENITOR CELL MIGRATION TO THE ANGII EXPOSED MYOCARDIUM IS NOT CXCL12- OR CCL2-DEPENDENT

A Falkenham, MJ Sopel*, NL Rosin**, TDG Lee, T Issekutz**, JF Légaré**

Submitted to Circulation Research, April 2, 2012 – Rejected June 5, 2012

Resubmitted to American Journal of Pathology, July 18, 2012

* Author contributions are clearly outlined in Appendix 2.

4.1 Abstract

Introduction: Fibroblast progenitor cells (fibrocytes) are believed to be important to the development of myocardial fibrosis (MF) and suggested to migrate to the heart via the chemokines CXCL12 and CCL2. *Objective:* If CXCL12 and CCL2 are necessary for fibrocyte migration, disrupting their chemotactic pathways in a model of MF will reduce fibrocyte infiltration in the heart and subsequently reduce fibrosis. *Methods:* C57/Bl6 and $CCR2^{-/-}$ mice were treated with saline, AngII, or AngII plus the CXCR4 antagonist AMD3100 via osmotic mini-pump. Tissues were analyzed for cellular infiltrate and collagen deposition. *Results:* AngII exposure resulted in cellular infiltration in the myocardium. Unexpectedly, AngII+AMD3100 exposure led to approximately 2.5-fold increase in cellular infiltrate and 2.4-fold increase in collagen deposition compared to AngII alone. Furthermore, the majority of infiltrating cells were fibrocytes. This effect appeared to be due to CXCR4 antagonism mobilizing progenitor cells into circulation. $CCR2^{-/-}$ mice also failed to demonstrate a reduction in infiltrate and fibrosis at 3d compared to WT mice. $CCR2^{-/-}$ mice did, however, demonstrate significant reductions in infiltrate and fibrosis in the myocardium relative to WT mice at 28d. *Conclusions:* CXCL12 and CCL2 do not have prominent roles in fibrocyte recruitment in AngII-mediated MF, as previously thought. Furthermore, the inability to show reductions in infiltrate and fibrosis in $CCR2^{-/-}$ mice at 3d suggests that the reductions observed at 28d are via an alternative mechanism to chemotaxis. The roles of these cytokines have yet to be fully characterized in the development of MF and require further investigation.

4.2 Introduction

Stem cell therapies for cardiovascular disease are suggested to have the potential to repair injured tissue and return lost function to the heart (223). Unfortunately, there remains little evidence of improved clinical outcomes from these therapies (224-226). This is believed to be due to our inability to ensure that stem cells differentiate into the desired cell type, which for the heart is a cardiomyocyte (224). Recently, we and others have identified a subset of stem cells, termed fibrocytes, which could be detrimental in regenerative therapies (214, 227, 228). Fibrocytes differentiate into myofibroblasts and produce extracellular matrix proteins, thus contributing to myocardial fibrosis rather than myocardial regeneration (24, 60, 214, 229). As such, mechanisms that favour fibrocyte migration may explain some of the difficulties investigators have experienced with stem cell therapies to date. Interrupting fibrocyte migration has been suggested as a potential therapeutic target for reducing myocardial fibrosis (24, 229-231).

There is a body of evidence demonstrating that the CXCL12-CXCR4 or CCL2-CCR2 axes are involved in the development of fibrosis, the exact mechanism by which they are involved remains unclear. There is evidence to suggest that fibrocytes migrate from the bone marrow into tissue through a chemotactic gradient of the chemokine CXCL12 (also known as stromal-derived factor-1) (230, 231). Myocardial CXCL12 has been shown to be upregulated in response to a variety of cardiac insults (219, 232-234). The expression of the primary CXCL12 receptor, CXCR4, on fibrocytes gives credence to a link between CXCL12 production and fibrocyte recruitment to the heart (196, 230, 231). The fact that a CXCR4 antagonist in models of pulmonary fibrosis inhibits fibrocyte recruitment and

decreases fibrosis, suggests that CXCL12 may be the key chemokine involved in fibrocyte recruitment to the myocardium (231).

Alternatively, the chemokine CCL2 (also known as monocyte chemotactic protein-1) has also been suggested as the key chemokine involved in organ fibrosis (24, 201, 229, 235-237). Kidney, lung, and liver models using knockouts for the CCL2 receptor, CCR2, show marked reductions in fibrosis compared to wild type mice (235, 237, 238). Xu et al., using a model of AngII-mediated myocardial fibrosis, demonstrated reduced cellular infiltrate to the heart and provided suggestive evidence that these cells were of a fibrocyte phenotype (229).

As both chemokines appear to have prominent roles in fibrocyte recruitment, our aim was to investigate whether we could manipulate the CXCL12-CXCR4 and CCL2-CCR2 axes to decrease fibrocyte recruitment in the early development of myocardial fibrosis. Using the CXCR4 antagonist AMD3100 in combination with $CCR2^{-/-}$ mice, we examined the dual inhibition of these two chemotactic pathways in a model of myocardial fibrosis.

4.3 Materials and Methods

4.3.1 Animals

Animal work was in accordance with the Canadian Council on Animal Care and approved by the Dalhousie *University Committee on Laboratory Animals*. Male C57BL/6 mice (8-10wk old) were purchased from Jackson Laboratory (Bar Harbour, ME, USA) and housed in the Carleton Animal Care Facility at Dalhousie University. CCR2

knockout mice on a C57BL/6 background were provided by Thomas Issekutz from a routinely genotyped colony. Mice were provided food and water *ad libitum* for 1wk prior to experimentation.

4.3.2 Saline/AngII/AMD3100 Infusion

Animals were anaesthetised with isoflurane (Baxter Healthcare, New Providence, NJ, USA) in oxygen delivered by a Fortec vaporizer. Upon reaching surgical levels of anaesthesia, a 1 cm mid-scapular incision was made and a mini-osmotic pump (Alzet, Palo Alto, CA, USA) was inserted subcutaneously. The incision was closed with 7 mm wound clips. Animals were randomly assigned treatments of vehicle control (saline), AngII (2.8 mg/kg/d; Sigma Aldrich, Oakville, ON, Canada), AMD3100 (11.4mg/kg/d; Tocris Bioscience, Ellisville, MO, USA), or AngII + AMD3100. The pumps remained in for 6hr, 12hr, 1d, 3d or 28d, during which, the animals were provided food and water *ad libitum* and observed for morbidity. In the time comparison groups, AngII (2.1 mg/kg/d) was infused for 3 or 28d. Animals were weighed and blood pressure measurements were taken using the Coda2 non-invasive tail cuff system (Kent Scientific, Torrington, CT, USA) for minimum of five measurements per animal.

4.3.3 Tissue Harvest

Experimental hearts were harvested and weighed. Cardiac mass index was calculated as heart:body weight ratio, as previously described (214). The base portion was processed for histology and the rest of the heart was vertically bisected and snap frozen for molecular analysis. Due to overlapping experimental groups previously published, some

historical samples from AngII and saline infused animals were used for this study to compare to new experimental groups (214, 227).

4.3.4 Cell Isolation

Naive blood was collected via cardiac puncture with heparinized-saline infusion and leukocytes were subsequently isolated for cell migration and cell culture. In brief, approximately 1mL of blood was collected per animal and diluted to 10mL with heparinized saline. The diluted blood was then centrifuged at 1847g for 10min at room temperature (RT) with low break. The buffy coat was transferred to a conical tube containing 5mL of ammonium chloride (ACK) lysis buffer, mixed thoroughly, and incubated at RT for 5min. ACK was neutralized by washing the cells with 10mL of cold DPBS (Gibco Life Technologies, Burlington, ON, Canada). Cells were centrifuged at 400g for 5min at 4°C and resuspended in complete RPMI (10% heat-inactivated fetal bovine serum, 2mM L-glutamate, 100 μg/ml streptomycin and 100 U/mL penicillin). Cells were then either used for migration studies or grown in flasks containing complete RPMI for 3d, prior to being lifted from the flasks using trypsin. Cultured cells were subsequently used for flow cytometry.

4.3.5 Cell Migration

Cell migration studies were conducted as previously described with modification (105). In brief, we used a modified Boyden chamber system with transwell migration inserts in 24-well plates (polycarbonate, 8 μm pore-size, Corning Life Sciences, PA). Chemokines were diluted to 100ng/ml in serum-free RPMI supplemented with 1% bovine serum

albumin (BSA) (91, 105). Following 2hrs of incubation at 37°C, cells were harvested for CD133 flow cytometry, as described below.

4.3.6 Flow Cytometry

Cultured fibrocytes were resuspended in Cytofix/Cytoperm (BD, Mississauga, ON, Canada) at the recommended dilution and incubated for 30min. Following washes with the Cytofix/Cytoperm wash (BD), F_c block (Miltenyi Biotec, Auburn, CA, USA) was added at the recommended dilution. Cells were incubated for 10min, after which conjugated antibodies for CD133 (FITC; Millipore, Billerica, MA, USA), CCR2 (PE; R&D Systems, Minneapolis, MN, USA), Vimentin (PerCP; Santa Cruz Biotechnology, Santa Cruz, CA, USA), and CXCR4 (APC; R&D) were added and incubated for 30min. Single label treatments were used for compensation. Matching isotype antibodies (Santa Cruz) served as controls. All incubations were carried out at 4°C. Data was acquired by four-colour flow cytometry using a BD FacsCalibur flow cytometer. Flow cytometry results were analyzed using WinList (Verity Software, Topsham, ME, USA).

4.3.7 Histologic Analysis

4.3.7.1 Paraffin

Hearts were processed in 10% buffered formalin for 24hr and paraffin-embedded. Serial-sections (5μm) were stained for histological and immunohistological analysis. Basic myocardial histology and cellular infiltrate were assessed using heart sections stained with hematoxylin and eosin (H&E). The area of the heart affected was calculated as previously described (214).

Fibrotic deposition was examined using heart sections stained with Sirius Red (SR) and the counter stain Fast Green (FG). Collagen content was semi-quantified by photographing representative SR/FG whole heart-sections at 5x magnification. Using Adobe Photoshop CS5, red pixels were positively selected and summed for a total number of red (collagen) pixels. Subsequently, non-background pixels were summed for a total number of heart pixels. The total collagen pixels were divided by the total heart pixels to provide a semi-quantitative measurement of the percent collagen content in the heart. All tissues were processed simultaneously for SR/FG and the same red colour palette was used to select red pixels.

Immunohistochemistry for smooth muscle cell actin (SMA; Sigma Aldrich), CD133 (Abcam, Cambridge, MA, USA), and KI-67 (DakoCytomation, Mississauga, ON, Canada) were performed on paraffin-embedded sections, which required antigen retrieval prior to staining. Briefly, endogenous peroxidases were quenched with 3% hydrogen peroxide, endogenous biotin was blocked with DAKO Biotin Blocking System (DakoCytomation), and non-specific staining was blocked with normal serum from the secondary antibody host. Sections were incubated with primary antibodies overnight at 4°C, followed by a specific biotin-conjugated secondary antibody. Secondary antibodies were conjugated to an avidin-biotin complex (Vecstatin ABC kit; Vector, Burlington, ON, Canada) and developed with 3,3' diaminobenzidine (DAB, DakoCytomation).

The proliferation index was calculated as the number of $KI67^{+}$ cells over the total number of infiltrating cells in a representative 5µm section of myocardium.

4.3.7.2 Frozen

Anesthetised mice were perfused with saline followed by 4% paraformaldehyde (PFA). The hearts were extracted and placed in 4% PFA overnight. The hearts were transferred to 30% sucrose and 10μm sections were cut on a cryostat for immunofluorescence. Immunofluorescence for CD45 (BD Biosciences, San Jose, CA, USA) and SMA was performed on frozen heart sections. In brief, sections were blocked with 10% serum from the secondary antibody host. Sections were then incubated with primary antibodies (same as above) overnight at 4°C. Following washes, sections were incubated with Cy2- and Cy3-conjugated secondary antibodies. Nuclei were stained with Hoechst. Slides were visualized using a Zeiss Axioplan II and photographed with an AxioCam HRC Colour Camera.

4.3.8 Relative Quantitative Polymerase Chain Reaction (qPCR)

RNA isolation, cDNA generation, and qPCR were performed as previously described (228). Primers were designed against mRNA sequences of CXCL12 (forward: 5'-ATTCGATCAGAGCCCATAGAG-3'; reverse: 5'-GTAGAATGGAGCCAGACCATCC-3') and CCL2 (forward: 5'-CCAGCCAACCACTGAAGC-3'; reverse: 5'-AGCTCTCCAGCCTACTCATTGG-3'). Expression was normalization to the 18S (forward: 5'-TCAACTTTCGATGGTAGTCGCCGT-3'; reverse: 5'-TCCTTGGATGTGGTAGCCGTTTCT-3') ribosomal gene using the Pfaffl method.

4.3.9 Statistics

Results are expressed as mean ± SEM. Multiple group comparisons were performed by one-way analysis of variance (ANOVA) followed by Bonferroni post-test for comparing means. One-sample t-tests were used for relative comparisons between experimental groups and standardized controls.

4.4 Results

4.4.1 AngII Exposure Increases Myocardial Transcription of CXCL12

Previous work in our laboratory using a well-established model of hypertension and hypertrophy with AngII infusion has demonstrated that fibrocyte infiltration in the heart precedes the development of myocardial fibrosis (214, 227, 228). Fibrocyte infiltration has been suggested to be in response to CXCL12 (196, 214, 230, 231). Using the AngII-mediated myocardial fibrosis model, we tested this hypothesis. qRT-PCR was used to detect changes in CXCL12 transcript in the myocardium. By 1d of AngII infusion, CXCL12 mRNA expression was significantly upregulated to 4.60 ± 0.39 fold greater than control ($p<0.01$) (Fig. 4.1a). The increase in CXCL12 transcript corresponds to the increased fibrocyte infiltration by 1d that we have previously described (214).

Migration to CXCL12 is dependent on the interaction with its receptor, CXCR4 (239). To confirm that fibrocytes could respond to CXCL12, we first had to confirm that they expressed CXCR4. Circulating blood PBMCs were cultured for 3d to obtain enriched fibrocytes as previously described (214). Cultured cells were labelled for a progenitor marker (CD133) and a mesenchymal marker (collagen-1) to confirm the fibrocyte

phenotype (co-expression), as well as being labelled for CXCR4. Nuclei are labelled blue (Hoechst). A representative photomicrograph is shown in Figure 4.1b with collagen fluorescing green, CD133 fluorescing orange, and CXCR4 fluorescing pink. The colocalization of these markers appears red, confirming that fibrocytes taken from the circulation and purified *in-vitro* can express CXCR4.

4.4.2 CXCR4 Antagonism with AngII Exposure Increases Cellular Infiltration in the Myocardium

As we have shown previously, AngII infusion resulted in significantly increased myocardial cellular infiltrate (Fig. 4.2b), which was absent in saline controls (Fig 4.2a). Using a previously described grid counting technique to quantify cellular infiltration, we observed that 29.99 ± 4.01 % of the myocardium was affected by cellular infiltrate in representative sections following AngII infusion (Fig. 4.2i). Unexpectedly, blocking the CXCL12-CXCR4 axis with AMD3100 led to an increase in cellular infiltration when compared to all other experimental groups (Fig 4.2c). Quantitatively, animals that received AngII+AMD3100 had 75.09 ± 2.90 % of the myocardium in representative sections being affected by cellular infiltrate (Fig. 4.2i) – a significant 3 fold increase in percentage of grids affected in the myocardium relative to AngII alone ($p<0.01$).

Consistent with what has previously been shown, AMD3100 infusion alone was insufficient to recruit cells to the myocardium (Fig. 4.2d) (240).

4.4.3 Increased Cellular Infiltration is Associated with Increased Fibrosis in the Myocardium

Fibrocytes are suspected of contributing to the deposition of extracellular matrix and as such, inhibiting their recruitment has been shown to reduce fibrosis (24, 229-231). In our model, we have demonstrated that AngII infusion leads to fibrocyte infiltration in the myocardium and that the simultaneous infusion of AngII and AMD3100 further increases this cellular infiltrate.

We semi-quantified the collagen in the myocardium after Sirius Red staining and found that in saline control animals, the myocardium was comprised of 2.11 ± 1.25% collagen in representative sections (Fig. 4.2e, j). Following AngII infusion, collagen content in the myocardium increased to 11.50 ± 1.12% of representative sections (Fig. 4.2f, j). Consistent with the increase in infiltrating cells, simultaneous infusion of AngII and AMD3100 appeared to increase collagen content in the myocardium compared to both control and AngII infusion (Fig. 4.2g) ($p<0.01$). When we semi-quantified collagen content following AngII and AMD3100 infusion, on average collagen constituted 28.05 ± 2.83% of the myocardium in representative sections (Fig. 4.2j), while AMD3100 infusion alone did not lead to significant changes in collagen content (Fig. 4.2h, j).

4.4.4 Infiltrating Cells are Phenotypical of Fibrocytes

Frozen myocardial tissue from animals infused with AngII and AngII + AMD3100 were stained for the pan-leukocyte marker CD45 and the mesenchymal marker SMA. Colocalization of these two markers is a phenotype characteristic of fibrocytes (196, 241). A representative photomicrograph from an AngII + AMD3100 heart is shown in Figure

4.4 with CD45 fluorescing green (Fig. 4.3a) and SMA fluorescing red (Fig. 4.3b). The colocalization of these markers appears yellow and is present on a large proportion of infiltrating cells (Fig. 4.3c). Thus, fibrocytes are present in the myocardium despite the blockade of CXCR4. Serving as a positive control, the fibrocyte phenotype was also observed in the myocardium of AngII-infused animals, as previously described (data not shown) (214, 228).

4.4.5 CXCR4 Antagonism Mobilizes Bone Marrow Cells

We believed that the increase in infiltrating cells in the myocardium may have been due to the mobilization of stem cells by CXCR4 antagonism. Antagonizing CXCR4 is known to mobilize hematopoietic stem cells into circulation and as such, is used in combination with G-CSF for increasing stem cell collection from peripheral blood (242). We confirmed this effect in our model by quantifying circulating blood leukocytes. Following AMD3100 infusion, the concentration of leukocytes in the circulation rose to 2.23 fold greater than saline control (Fig. 4.4a) ($p<0.05$). Flow cytometry confirmed that the increase in circulating leukocytes was associated with a corresponding increase in cells expressing the progenitor marker CD133 (Fig. 4.4b,c). This data provides evidence that AMD3100 increases the concentration of circulating progenitor cells. It also supports the idea that increased circulating progenitor cells are responsible for the increase in infiltrating cells in the myocardium, but that the mechanism is not dependent on CXCR4-mediated migration out of the blood.

4.4.6 Increased Cellular Infiltrate is Not Due to Proliferation or Increased Blood Pressure

Proliferation of infiltrated myocardial cells was assessed using KI67 immunohistochemical label, which was used to calculate a proliferation index. The proliferation index was based on the number of $KI67^+$ cells over the total number of infiltrating cells. In the AngII group, 56.9 ± 4.4% of infiltrating cells were found to be proliferative, as indicated by KI67 positivity. In the group receiving AngII + AMD3100 54.6 ± 2.1% were $KI67^+$. The high proliferative index in both groups is indicative of a progenitor cell phenotype rather than non-progenitor leukocytes. There was no statistically significant difference in the proliferation index between AngII and AngII + AMD3100 treated animals (Fig. S4.1).

AMD3100 did not have a significant effect on blood pressure with or without co-infusion of AngII (Fig. S4.2a). Hypertrophy also did not significantly differ between AngII and AngII + AMD3100 animals (Fig. S4.2b). Thus, the increase in infiltrating cells in the myocardium appears to be the consequence of increased cell mobilization from the bone marrow, not changes in blood pressure.

4.4.7 AngII Exposure Increases Myocardial Transcription of CCL2

The chemokine CCL2 has also been implicated in fibrocyte recruitment, particularly to the myocardium (24, 229). As such, we first assessed whether the CCL2 mRNA transcript was upregulated in the myocardium following AngII infusion. At 6hr of AngII exposure, CCL2 mRNA transcript was significantly increased: 7.83 ± 1.70 fold greater than control (Fig. 4.5a). Significantly increased CCL2 transcription was maintained until

12hr of AngII infusion: 12.26 ± 2.54 fold greater than control ($p<0.05$). When compared to CXCL12 (Fig 4.1), CCL2 expression appears to peak earlier with a several fold higher amount.

The primary receptor for CCL2 is CCR2. We next tested fibrocyte-enriched cultures for the presence of CCR2 using immunofluorescence. Cultured cells were once again labelled for the fibrocyte phenotype ($CD133^+$ and collagen-1^+) as well as CCR2. Nuclei are labelled blue (Hoechst). A representative photomicrograph is shown in Figure 4.5b with collagen fluorescing pink, CD133 fluorescing orange, and CXCR4 fluorescing green. The colocalization of these markers appears red. Purified fibrocytes were demonstrated to express CCR2 (Fig. 4.5b).

4.4.8 Ability of Fibrocytes to Migrate to CXCL12 and CCL2 *In Vitro*

To confirm progenitor cells could migrate to both chemokines, we examined the migration patterns of the circulating $CD133^+$ progenitor cell population using a transwell migration assay. Primary isolated peripheral blood mononuclear cells were used instead of cultured fibrocytes to better represent the actual population migrating in the circulation to the heart. $CD133^+$ cells migrated in significantly greater numbers to CXCL12 and CCL2 compared to media only controls (Fig. 4.6b) ($p<0.05$). Checkerboard analysis confirmed the increased number of cells was not due to chemokinesis (data not shown). We did not observe preferential migration to CXCL12 or CCL2 *in-vitro* by circulating CD133+ cells.

Flow cytometry was used to confirm that there were not two separate subsets of fibrocytes: one that expresses CXCR4 and one that expresses CCR2. Cultured fibrocytes were labelled for CD133, vimentin, CXCR4 and CCR2. $CD133^{+}$ $Vimentin^{+}$ cells (Fig. 4.6c) were gated on and assessed for CXCR4 and CCR2 positivity (Fig. 4.6d). Representative flow cytometry demonstrated that a large percentage (98.7%) of cultured fibrocytes co-express both receptors.

4.4.9 Fibrocyte Migration and Fibrosis in the Absence of CCR2

As $CD133^{+}$ cells appeared to migrate to both CXCL12 and CCL2, we investigated the *in vivo* migration of fibrocytes in the absence of the primary receptor for CCL2: CCR2. Others have previously suggested that $CCR2^{-/-}$ animals exhibit reduced cellular infiltration and fibrosis; however, these studies have been limited to time points 14d or longer (24, 229, 235, 238). As such, we examined whether the increased cellular infiltration and fibrosis observed with CXCR4 antagonism would be reduced in our early time point model of heart failure. Following 3d of AngII or AngII + AMD3100 infusion, representative sections from $CCR2^{-/-}$ mouse hearts were stained for H&E and Sirius Red. Despite the absence of CCR2, cellular infiltrate was still observed in AngII and AngII + AMD3100 myocardium (Fig. 4.7b, c, respectively). Through grid counts of the H&E stained sections, we found that there was no significant reduction in cellular infiltration at the 3d time point compared to wildtype (WT) mice (Fig. 4.7i) ($p<0.01$). Furthermore, there was significant fibrosis present in both AngII and AngII + AMD3100 animals (Fig. 4.7j). Thus, at this early time point, $CCR2^{-/-}$ mice failed to show a reduction in either cellular infiltrate or fibrosis compared to WT.

Given that others have demonstrated reductions in infiltrate and fibrosis between $CCR2^{-/-}$ and WT animals, we investigated potential differences in the experimentation that may account for differing results (229). We noted that in one group that used the AngII model of myocardial fibrosis, they used a lower dose of AngII and extended the infusion to 28d (229). We accounted for dose differences by lowering our AngII dose to 2.1mg/kg/d and infusing for 3d. Following 3d of AngII infusion, infiltrate and fibrosis were significantly elevated in both the $CCR2^{-/-}$ and WT animals; however, the differences between $CCR2^{-/-}$ and WT animals within experimental groups were not significant (data not shown). Thus, our findings at the lower dose were consistent with those at the higher dose.

In order to adjust for the difference in length of infusion, we administered the lower dose of AngII for 28d. We observed significant reductions in both cellular infiltrate and fibrosis in $CCR2^{-/-}$ mice relative to WT (Fig. 4.8e). Quantitatively, WT animals that received AngII had 18.27 ± 2.65% of the myocardium in representative sections being affected by cellular infiltrate (Fig. 4.8e). In contrast, $CCR2^{-/-}$ animals that received AngII had 8.90 ± 1.02% of the myocardium affected – an approximately 48.69% reduction in the percentage of grids affected in the myocardium relative to WT ($p<0.01$).

Consistent with the infiltrate findings, collagen content in WT myocardium remained significantly elevated over saline controls at 16.87 ± 1.50% of representative sections (Fig. 4.8f). Collagen content in $CCR2^{-/-}$ myocardium, however, was significantly reduced relative to WT, constituting just 8.61 ± 0.74% ($p<0.01$).

In both CCR2$^{-/-}$ and WT mice, the collagen appeared to have undergone maturation, increasing in density and colour, as seen by Sirius Red staining (Fig. 4.8c,d). While CCR2$^{-/-}$ animals exhibit reduced infiltrate and fibrosis at 28d of AngII infusion, these observations are not a consequence of modulating early fibrocyte migration, as demonstrated by the inability to show a change in either infiltrate or fibrosis compared to WT at 3d.

4.5 Discussion

Stem cell therapies to repair injured myocardium have gained a lot of credence since the discovery that progenitor cells can differentiate to myocardial cells, such as endothelial cells and cardiomyocyte-like cells (243, 244). The discovery of another progenitor cell type in myocardial injury – fibroblast progenitor cells (fibrocytes) – has balanced the scales between benefit and detriment in repairing the myocardium (24, 60, 214, 220, 229). Fibrocytes have been shown to migrate to the heart, differentiate into myofibroblasts, and produce ECM proteins, thus directly contributing to the development of fibrosis. A common link between many progenitor populations is the chemokine CXCL12. It is widely accepted that CXCL12 has an important role in stem cell movement and literature suggests the movement is directed to increased concentrations of CXCL12 (230, 231, 245).

CXCL12 upregulation is observed in many cardiovascular diseases (214, 232-234). We observed an increase in CXCL12 transcription in the heart following exogenous AngII

infusion – a hypertensive model of myocardial fibrosis (214). As our model represents the initial steps in the development of heart failure, we suspected CXCL12 and its receptor could potentially be used in a therapeutic setting for improving clinical outcomes; however, the role of CXCL12 in non-ischemic heart disease is not well understood. We previously showed that the development of fibrosis was associated with the recruitment of fibrocytes from the bone marrow (214). We sought to examine whether CXCL12 had a chemotactic role in fibrocyte recruitment to the myocardium. Song *et al* provide evidence for CXCL12 driving the recruitment of fibrocytes from circulation into injured tissue, using a model of bleomycin-induced lung fibrosis (231). They utilized a competitive antagonist against the CXCL12 receptor, CXCR4, in an attempt to inhibit fibrocyte recruitment. Using AMD3100, they observed a decrease in the number of fibrocytes in the lungs, suggesting CXCL12 is the chemokine responsible for fibrocyte migration into injured tissues. It is not clear that the population they were investigating expressed the fibrocyte-specific markers though. Thus, the role of CXCL12 in fibrocyte migration required further investigation.

Under the same premise, we hypothesized that CXCR4 antagonism with AMD3100 would inhibit the infiltration of fibrocytes into the myocardium, ultimately decreasing myocardial fibrosis. AMD3100 is a known stem cell mobilizer, due to its ability to interfere with attractive force of the CXCL12-CXCR4 axis in the bone marrow (242, 246). As such, administering AMD3100 increases the concentration of stem cells in circulation, as observed in our study. Provided CXCL12 is the primary chemokine involved in fibrocyte recruitment, the increased concentration of progenitor cells in

circulation in combination with CXCR4 antagonism should not lead to greater cellular infiltration in the myocardium. Unexpectedly, however, simultaneous infusion of AngII and AMD3100 was unable to decrease cellular infiltrate or myocardial fibrosis. Following 3d of continuous infusion, cellular infiltrate was significantly increased, which was associated with increased fibrotic deposition in the myocardium in animals receiving AngII+AMD3100. These effects did not appear to be a result of increased proliferation of infiltrating cells, as confirmed by an *in vivo* proliferation index. Infusion with AMD3100 alone did not result in infiltration or fibrosis, consistent with what others have shown (240). These results cumulatively suggest that CXCR4 antagonism in our model of AngII myocardial fibrosis is likely exacerbated secondary to the significant mobilization of fibrocytes to the circulation, but was unable to prevent progenitor cell recruitment.

One-time infusion of AMD3100 has been shown to increase the recruitment of the beneficial endothelial progenitor cells (EPCs) to the myocardium post-infarction. As such, Dai *et al.* chronically administered AMD3100 with the intention of increasing EPC recruitment for the duration of treatment (240). While there were increased progenitor cells in the myocardium, the cells did not differentiate to an endothelial phenotype and the increase in progenitor cells was associated with increased fibrosis. It follows that the unidentified progenitor cells in the infarct model may be fibrocytes and that a general effect of chronic AMD3100 infusion in heart disease is the recruitment of fibrocytes to the myocardium. While Dai *et al.* did not stain for mesenchymal markers, we have been able to show that following CXCR4 antagonism, the infiltrating cells express the fibrocyte phenotype, using markers for mesenchymal and haematopoietic origins. Using

CD45 and SMA colocalization, we identified fibrocytes in the myocardium following both AngII and AngII + AMD3100 infusion. We provide definitive evidence that fibrocyte migration to the heart in a model of myocardial fibrosis is not CXCL12 dependent. Furthermore, through CXCR4 antagonism, we are the first to show that increased fibrocyte recruitment leads to increased fibrosis.

Recently, a second chemokine has been implicated in fibrocyte migration: CCL2 (24, 201, 229). Using both knockouts for the chemokine and its receptor, investigators have been able to show decreased fibrocyte recruitment to the myocardium; however, these models differ in either AngII dosage or time of harvest, both of which may have implications on the interpretation of fibrocyte recruitment (24, 229). In this study, we have shown that fibrocytes simultaneously express both chemokine receptors, CXCR4 and CCR2, and can thus potentially migrate to both chemokines. We confirmed stem cell migration to both chemokines using *in vitro* transwell migration assays, but were unable to show preferential migration. We suspected CCL2 was mediating the recruitment of fibrocytes during CXCR4 blockade and to test this hypothesis, we administered AngII with and without AMD3100 in CCR2 $^{-/-}$ mice.

Our initial 3d harvests failed to show significant differences in infiltrate or fibrosis between CCR2 $^{-/-}$ and WT mice. This held true for both AngII and AngII + AMD3100 infusions. These results differ from what others have demonstrated at the 28d time point with AngII infusion (229). The inability to show differences in cell infiltration at 3d between CCR2$^{-/-}$ and WT mice suggested that the effects of CCR2 in this model are

primarily non-chemotactic. We examined this theory by comparing cellular infiltrate and fibrosis in the myocardium between an early time point (3d) and a late time point (28d). We observed similar reductions in fibrosis reported by others at the late time point (229). This confirmed that the reduction in infiltrate and fibrosis in $CCR2^{-/-}$ mice is not due to reduced fibrocyte migration.

While fibrocytes may be an important effector cell in the development of fibrosis, their presence alone does not dictate the development of fibrosis. In a model of pulmonary fibrosis, Murray et al. demonstrated that fibrocytes require the presence of stimulatory cells to have an effector role (247). Moore et al. also offer support for a CCR2 role in pulmonary fibrosis and consistent with our findings, the reduction in fibrosis was not a consequence of decreased cellular infiltrate or change in infiltrate composition (235). Sakai *et al.* also support a role of CCR2 in fibrogenesis, but demonstrate that the interaction between CCL2 and CCR2 is important in the production of pro-fibrotic factors, thus suggesting an alternate method by which CCR2 mediates fibrosis. Changes in key pro-inflammatory and pro-fibrotic cytokines have been noted in several different models of fibrosis that implicate the CCL2-CCR2 axis (235, 237, 238, 247).

We have shown that the chemokines CXCL12 and CCL2 do not play prominent roles in fibrocyte migration, as previously thought. While CXCL12 may have a role in the mobilization of stem cells, including fibrocytes, inhibition of its receptor, CXCR4, may lead to worsened fibrotic conditions, specifically in the myocardium. Likewise, the role of CCR2 signalling appears to be important in the maintenance of fibrocytes and fibrosis

in the heart, but these effects do not appear to be migration-dependent. CCR2 continues to be a potential therapeutic target in fibrotic conditions; however, the mechanism by which CCR2 inhibition reduces early cellular infiltrate and fibrosis has yet to be characterized.

4.6 Acknowledgements

We thank Tanya Myers and Maria Vaci for excellent technical support.

4.7 The Sources of Funding

The present work was supported in part by a grant from the Canadian Institute of Health Research (#44122).

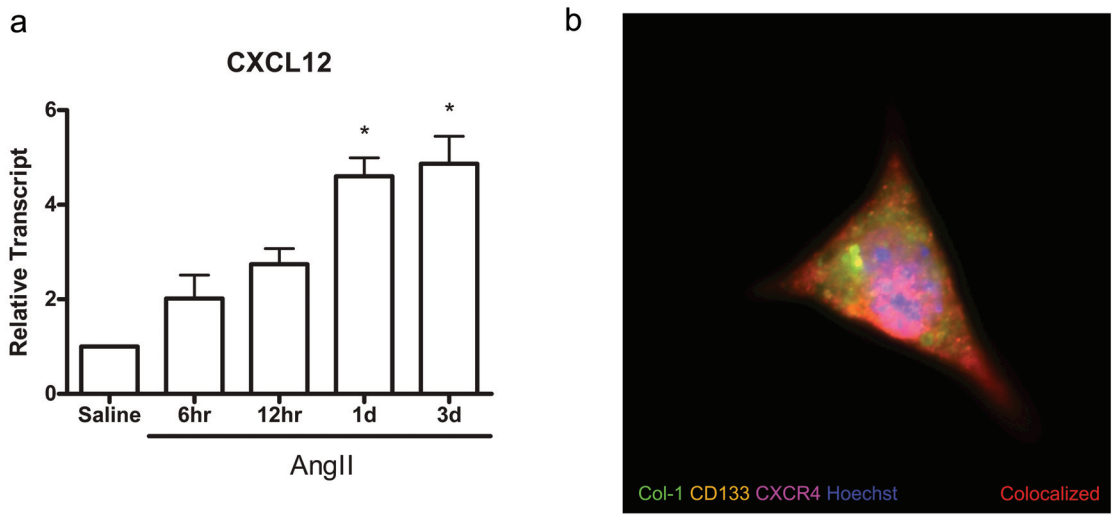

Figure 4.1 AngII Increases Myocardial CXCL12 mRNA

(A) Using qPCR, we measured myocardial expression of CXCL12 transcript levels relative to 18s ribosomal gene expression. Relative mRNA transcript levels for CXCL12 were significantly increased in AngII-infused animals at 1 and 3 days (**p<0.01). (B) Representative immunofluorescence is shown for the expression of CXCR4 on fibrocytes cultured from circulating leukocytes. The colocalization of collagen-1 (green), CD133 (orange), and CXCR4 (pink) overlaid as red on the fibrocytes. Nuclei were labelled blue with Hoechst. Images were captured at 100x.

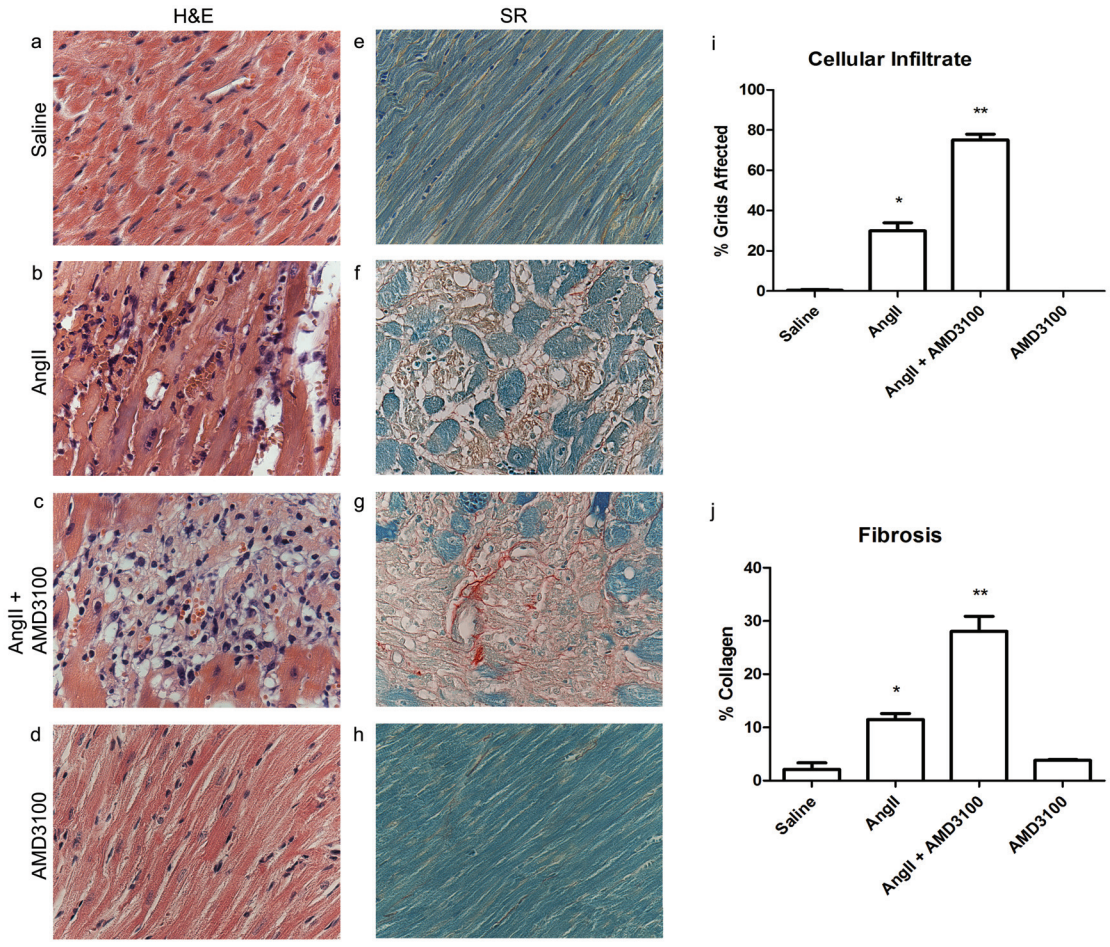

Figure 4.2 CXCR4 Antagonism Increases Cellular Infiltrate and Fibrosis

Representative sections of 3d hearts stained with H&E (A, B, C) and SR (D, E, F): saline control (A, E), AngII (B, F), AngII + AMD3100 (C, G), and AMD3100 (D, H). AngII-infusion led to significant cellular infiltrate in the heart (*p<0.01), which was exacerbated by CXCR4 antagonism (**$p<0.01$). The significant increase in cellular infiltrate (I) was associated with significantly increased collagen content (J), as semi-quantified by digital image analysis n=5). Images were captured at 40x.

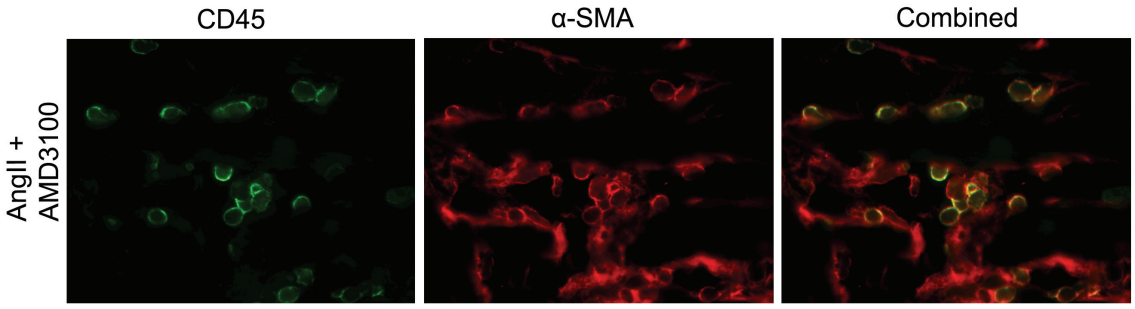

Figure 4.3 Infiltrating Cells are Predominantly Fibrocytes

Myocardial sections were labelled for the leukocyte marker CD45 (green) and the mesenchymal marker α-SMA (red). The overlay of these markers showed colocalization (yellow) of infiltrating cells in the myocardium of AngII + AMD3100 infused animals. Fibrocytes were found in the myocardium of AngII infused animals as well (data not shown). Images were captured at 63x.

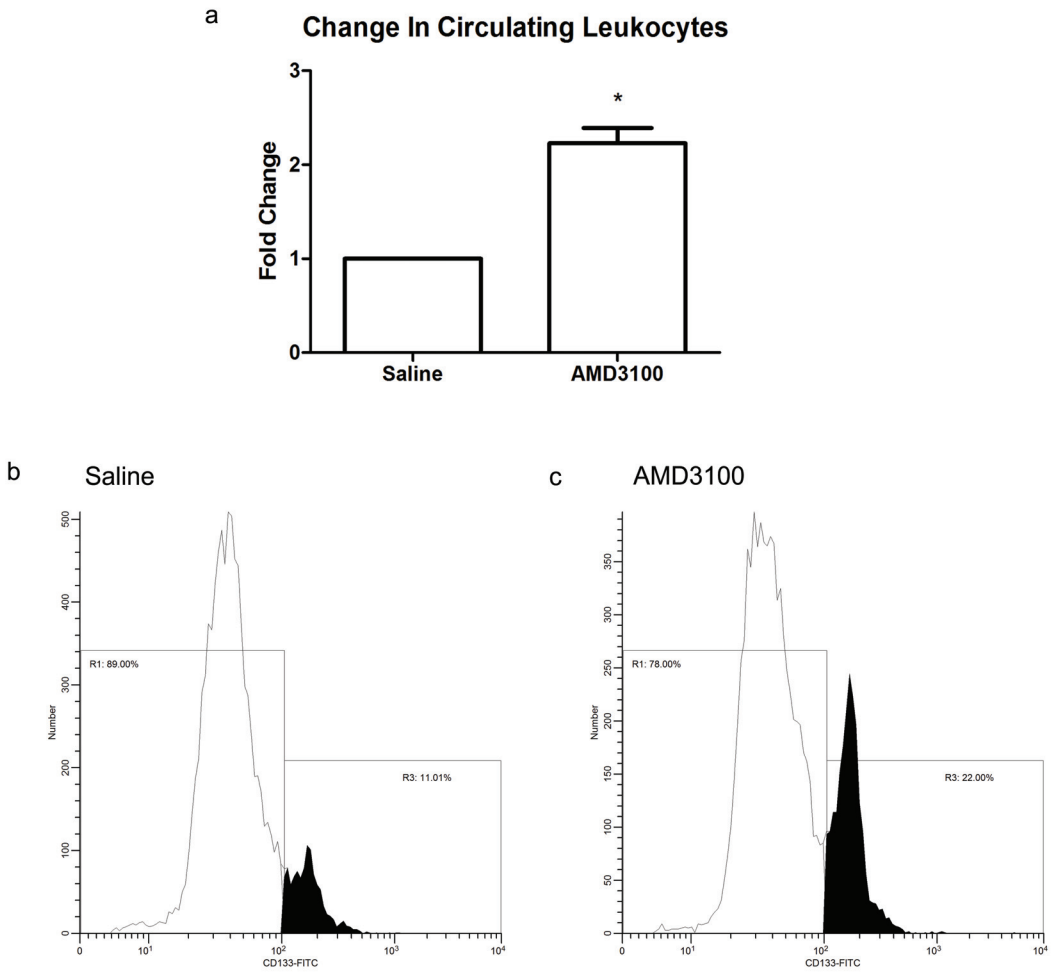

Figure 4.4 CXCR4 Antagonism Increases Circulating CD133$^+$ Leukocytes

A Following AMD3100 infusion, circulating leukocyte counts were significantly elevated compared to saline infusion. Circulating leukocytes were labelled for the progenitor marker CD133 (n=4). (B) Representative flow cytometry demonstrated that there was an increase in CD133$^+$ cells in circulation following AMD3100 infusion.

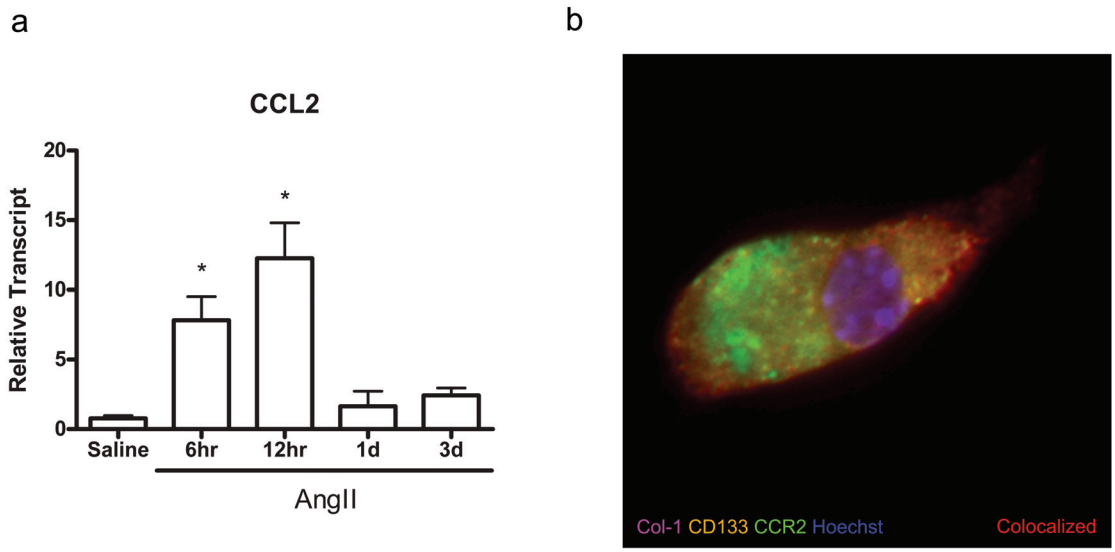

Figure 4.5 AngII Increases Myocardial CCL2 mRNA

A Using qPCR, we also measured myocardial expression of CCL2 transcript levels relative to 18s ribosomal gene expression. Relative mRNA transcript levels for CCL2 were significantly increased in AngII-infused animals by 6hrs and remained significantly elevated at 12hrs. (**$p<0.01$). B Representative immunofluorescence is shown for the expression of the primary CCL2 receptor, CCR2, on fibrocytes cultured from circulating leukocytes. The colocalization of collagen-1 (pink), CD133 (orange), and CXCR4 (CCR2) overlaid as red on the fibrocytes. Nuclei were labelled blue with Hoechst. Images were captured at 100x.

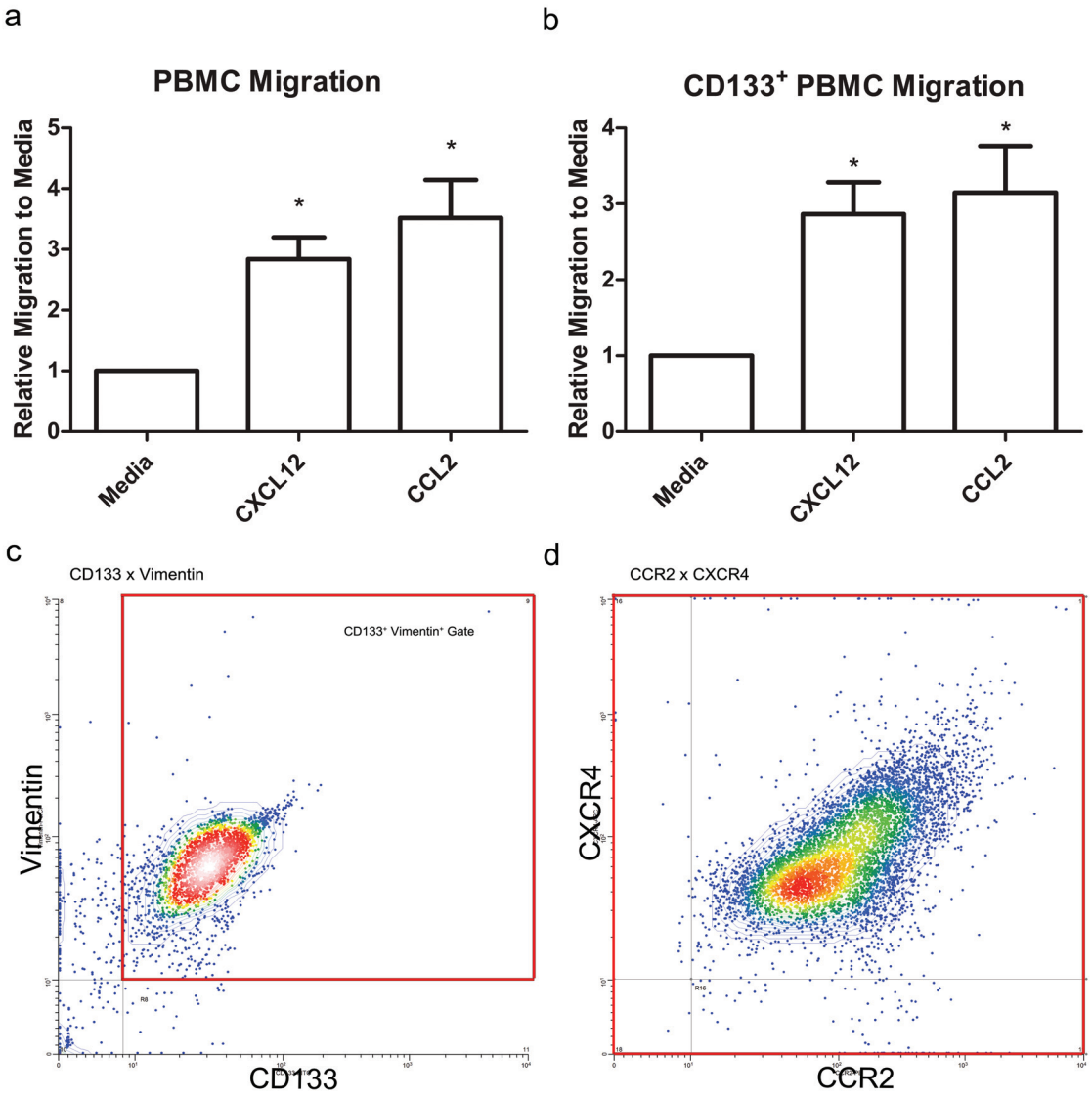

Figure 4.6 CD133$^+$ Cells Non-Preferentially Migrate to CXCL12 and CCL2

In vitro migration assays using PBMCs (n=4) (A) demonstrated that a population of CD133$^+$ circulating leukocytes (n=4) (B) migrate to both CXCL12 and CCL2 (*$p<0.05$). Representative flow cytometry confirmed that cultured fibrocytes (C: CD133$^+$ Vim$^+$) predominantly co-express the receptors CXCR4 and CCR2 (D), suggesting that it is the same population that is migrating to both chemokines.

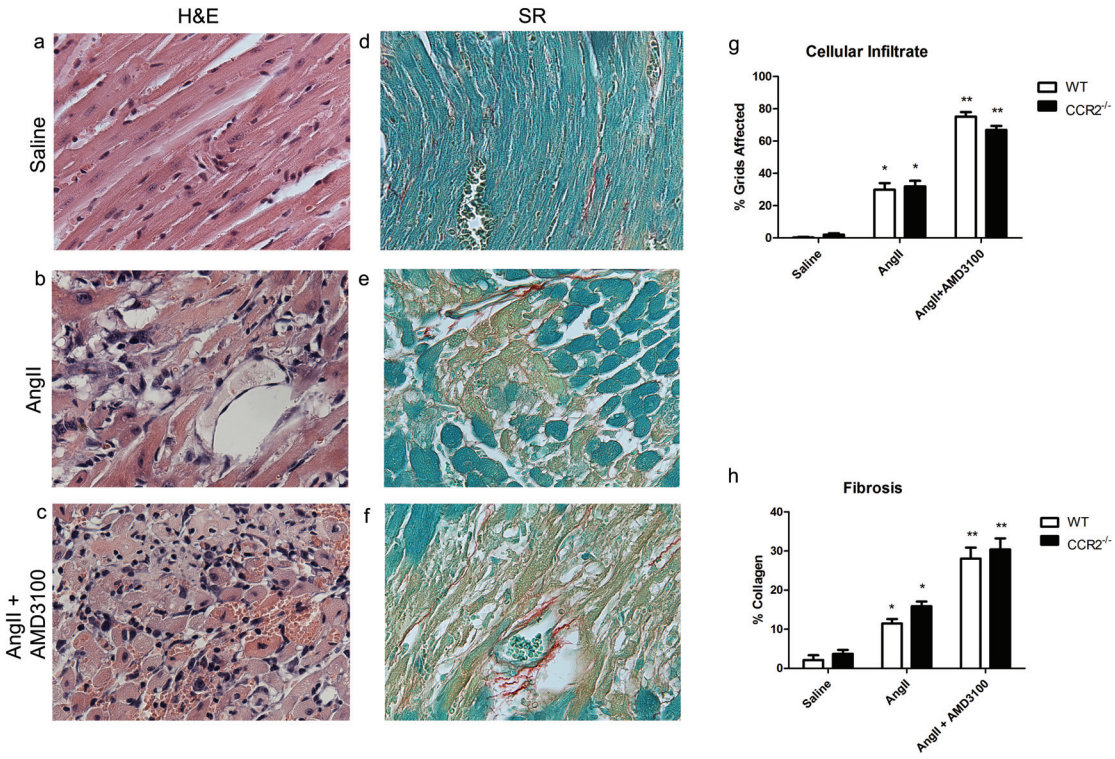

Figure 4.7 CCR2$^{-/-}$ do not Exhibit Reduced Infiltrate and Fibrosis in the Heart Following 3d of High-Dose AngII Infusion

Representative sections of 3d hearts stained with H&E (A, B, C) and SR (D, E, F) are shown: saline control (A, D), AngII (2.1mg/kg/d) (B, E) and AngII + AMD3100 (C, F). Myocardial infiltrate and fibrosis were compared between CCR2$^{-/-}$ and WT mice. AngII led to significant cellular infiltrate and fibrosis compared to saline controls (p<0.01, n=3), which was again exacerbated by CXCR4 antagonismm (*p<0.01, n=3). Despite the absence of CCR2, infiltrate (G) and fibrosis (H) were not significantly reduced at the 3d time point relative to WT experimental groups. Images were captured at 40x.

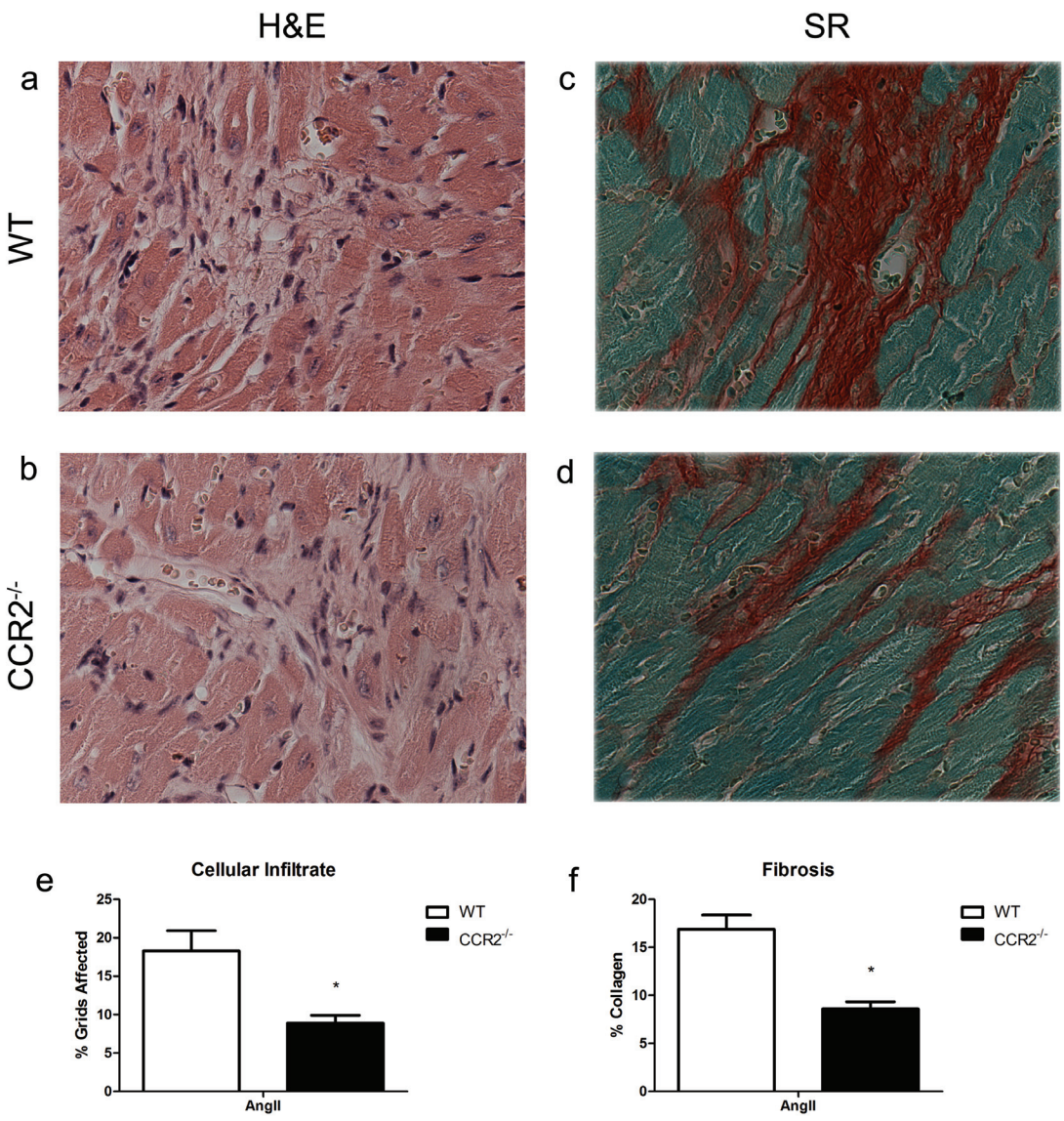

Figure 4.8 CCR2-Dependent Reduction in Infiltrate and Fibrosis are Time-Dependent

Representative sections of hearts stained with H&E (A, B) and SR (C, D) following 28d of AngII infusion: A, C WT and B, D CCR2$^{-/-}$. Both WT and CCR2$^{-/-}$ mice demonstrated reductions in infiltrate (E) and fibrosis (F) relative to their dose-matched (2.1mg/kg/d) 3d counterparts; however, CCR2$^{-/-}$ showed a greater reduction in both features relative the time-matched WT counterpart. (**$p<0.01$, n=4-5). Images were captured at 40x.

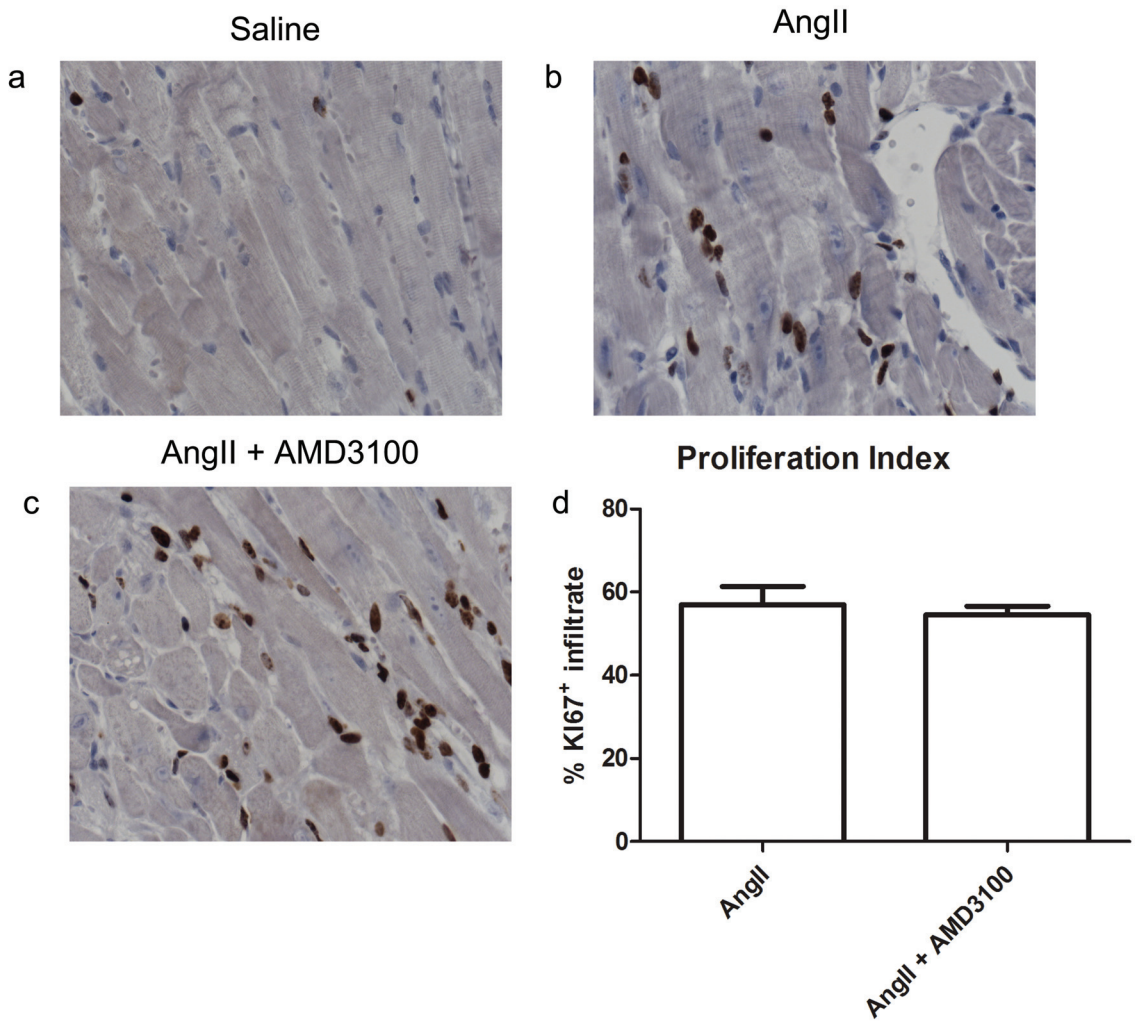

Figure S4.1: Increased Cellular Infiltrate is not due to Proliferation

KI67 labelling was used to assess proliferation in representative sections of myocardium for each experimental group (n=3). AngII and AngII + AMD3100 infused animals both showed large proliferating populations, which were absent in saline controls. The myocardial proliferation between the AngII and AngII + AMD3100 infused animals did not differ significantly.

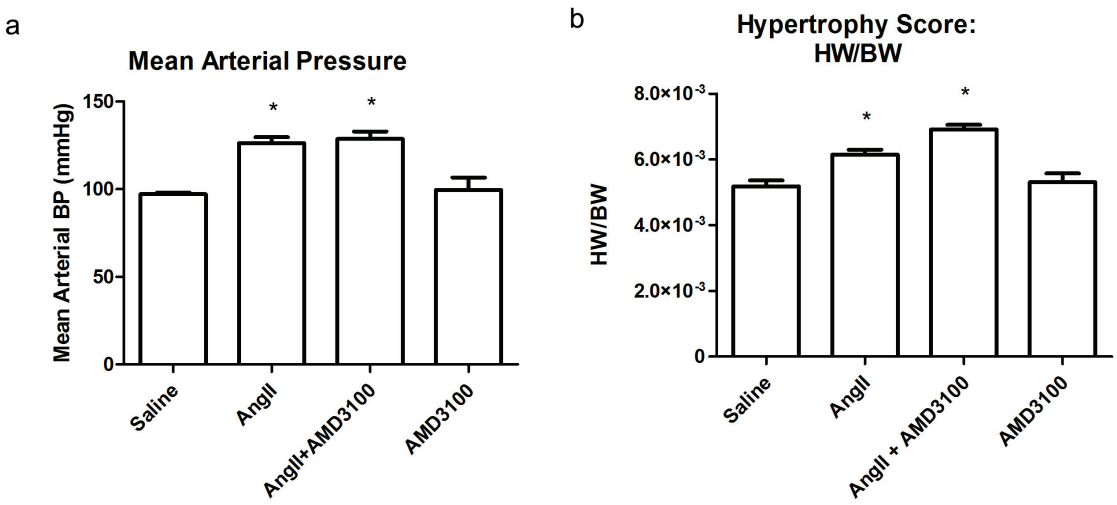

Figure S4.2: Increased Infiltrate and Fibrosis is not Blood Pressure or Hypertrophy Dependent

A Tail cuff measurements at the 3d endpoint demonstrated that AngII infusion significantly increases mean arterial pressure; however, AMD3100 did not significantly affect blood pressure (n=4). B Hypertrophy scores for AngII and AngII + AMD3100 were also significantly elevated relative to saline controls (*$p<0.01$), but did not significantly differ between the experimental groups (n=5).

CHAPTER 5

THE REGULATION AND ROLE OF CONNECTIVE TISSUE GROWTH FACTOR IN ANGII INDUCED MYOCARDIAL FIBROSIS

NL Rosin, A Falkenham, MJ Sopel*, TDG Lee, JF Légaré**

Submitted to American Journal of Pathology, February 10th, 2012

In Revision – January 18th, 2012

* Author contributions are clearly outlined in Appendix 2.

5.1 Abstract

Introduction: Angiotensin II (AngII) exposure to rodents is a common model of fibrosis. We have previously shown that cellular infiltration of bone marrow-derived progenitor cells (fibrocytes) occurs prior to ECM deposition and is associated with the production of connective tissue growth factor (CTGF). *Methods and Results:* In this study, we characterized the role of CTGF in promoting fibrocyte accumulation and regulation after AngII exposure. In animals exposed to AngII using osmotic mini-pumps (2.0μg/kg/min), myocardial CTGF mRNA peaked at 6hr (21-fold; $p<0.01$) while TGFβ peaked at 3d (5-fold; $p<0.05$) compared to animals receiving saline. Early CTGF expression was well before fibrocyte migration (1d) into the myocardium or ECM deposition (3d). CTGF protein expression was evident by 3d of AngII exposure and appeared localized to the cardiomyocytes. Isolated cardiomyocytes responded to AngII with increased CTGF production (2.1-fold; $p<0.05$). The role of CTGF on isolated fibrocytes was evaluated in-vitro, which demonstrated the promotion of fibrocyte proliferation (2-fold; $p<0.05$) and collagen production (2.3-fold; $p<0.05$). *Conclusion:* We provide strong evidence that AngII exposure first results in the production of CTGF by cardiomyocytes (6hr) well before the accumulation of fibrocytes or TGFβ expression, suggesting that CTGF is not functioning downstream of TGFβ. We also provide evidence that CTGF contributes to proliferation of fibrocytes in the myocardium and enhances differentiation of fibrocytes into a myofibroblast phenotype capable of contributing to ECM deposition.

5.2 Introduction

Myocardial fibrosis is a common pathological feature of many cardiovascular disorders characterized by an over-abundant deposition of extracellular matrix (ECM) molecules in combination with a deficit in ECM degradation (3, 248). The excess ECM protein results in loss of contractility and increased stiffness, ultimately leading to organ dysfunction and end-stage heart failure (3, 249). Current understanding of the molecular mechanisms culminating in increased matrix deposition is incomplete, warranting further investigation into the pathways involved.

One molecule, Angiotensin II (AngII) has been implicated in the development of fibrosis in the myocardium as well as in other fibrotic disorders (2, 250). This hormone is a member of the renin-angiotensin system and as such is involved in blood pressure regulation but has also been correlated with conditions that lead to organ fibrosis (211, 251). The exogenous administration of AngII to rodents through a subcutaneous osmotic pump has become a well-established model resulting in myocardial fibrosis and functional deterioration (214, 252).

Recent evidence published by us, and others has demonstrated that AngII exposure leads to an influx in hematopoetic progenitor cells, termed fibrocytes, into the myocardium. This occurs before ECM deposition (24, 214, 219). Fibrocytes possess both hematopoietic markers (CD34, CD45 and CD133) and mesenchymal markers (Collagen type I, fibronectin and vimentin) (85, 253). Supporting evidence for the involvement of

fibrocytes has been described in fibrotic disorders of the lung, kidney, liver and skin (254-257). While there is increasing evidence confirming the importance of fibrocytes in fibrotic conditions, there remains a significant paucity of mechanistic information, such as the tissue microenvironment with which these cells interact and the cytokine signaling that elicit their contribution to ECM production.

The current paradigm concerning pro-fibrotic signaling suggests that one of the first molecules involved in fibrosis development after AngII exposure is transforming growth factor-β (TGFβ) (258, 259). TGFβ has been suggested to interact directly with cardiomyocytes, which then produce other growth factors, such as connective tissue growth factor (CTGF) (260). In fact, recent studies have suggested that both; the well described TGFβ downstream regulation through the SMAD signaling pathway and a SMAD-independent TGFβ signaling pathway mediate the upregulation of CTGF (156, 158). Transgenic rodent models selectively overexpressing CTGF in fibroblasts result in increased systemic tissue fibrosis (261). In addition, increased levels of CTGF have been correlated with the development of fibrotic pathologies, including dermal, renal, liver, pulmonary, and cardiac fibrosis (153, 214, 262). Due to its strong link to fibrotic diseases, CTGF has also been suggested as a biomarker for fibrosis (165, 262). Notwithstanding this evidence, a direct causal link between CTGF and fibrosis development after AngII exposure has yet to be established.

In the current study we have characterized the effects of AngII exposure *in vivo* on CTGF levels in the myocardium and its effects in relation to infiltrating fibrocytes. We have

shown for the first time that CTGF is the first pro-fibrotic cytokine to be upregulated by cardiomyocytes in response to AngII exposure. We also provide evidence that in response to CTGF, infiltrating fibrocytes are capable of contributing to the process of ECM deposition and thereby fibrosis development.

5.3 Materials and Methods

5.3.1 Animals

All work was performed accordance with the Canadian Council on Animal Care and approved by the local Committee on Laboratory Animals. Male C57Bl/6 and CAG-EGFP (006567) transgenic mice between 7 to 8wk of age were purchased from the Jackson Laboratory (Bar Harbour, ME) and were housed within the Carleton Animal Care Facility at Dalhousie University. Mice were provided food and water *ad libitum* for 1wk prior to experimentation.

5.3.2 GFP Chimeric Animals

Chimeric animals were generated by transplanting bone marrow constitutively expressing GFP into lethally irradiated mice, as previously described (198, 214). Bone marrow cells were harvested from 8wk old GFP transgenic mice in a C57Bl/6 background that ubiquitously express GFP under control of the CAG promoter. Recipient mice were irradiated with two doses of 5.5Gy and unfractionated GFP+ BM cells ($1x10^6$ cells) were injected via tail vein. Engraftment was evaluated 8wk after transplant by collecting peripheral blood cells and evaluating the frequency of GFP+ cells relative to the total peripheral nucleated cells. Only animals with engraftment greater than 60% GFP+ were used for further treatment.

5.3.3 AngII Infusion

Animals had mini osmotic pumps containing AngII or saline implanted under general anesthesia as previously reported (214). In short, animals were anesthetized with isoflurane (Baxter Healthcare Corp., New Providence, NJ) in oxygen at which point a 1-2 cm mid-scapular skin incision was made and a mini osmotic pump (Alzet, Palo Alto, CA) was inserted subcutaneously. Animals were randomly assigned to receive AngII (2.0 μg/kg/min, Sigma Aldrich) or a vehicle control of saline. The pumps remained in for 6 or 12hr, 1, 3 or 7d during which the animals were provided food and water *ad libitum* and observed for signs of morbidity.

5.3.4 Tissue Harvest

Hearts from experimental animals were harvested and weighed then divided into three sections along the vertical axis. The base section of the heart was processed for histological examination with the other two pieces snap frozen immediately for molecular analysis.

5.3.5 Cell Isolation and Culture

Peripheral blood mononuclear cells (PBMCs) and bone marrow (BM) cells were isolated from naïve or 3d AngII exposed mice. Briefly, blood was collected in heparin containing syringes via cardiac puncture and centrifuged. The PBMC containing layer was isolated, washed and residual red blood cells were lysed using ammonium chloride solution. BM cells were removed from the tibias and femurs by flushing with 10mL of dPBS (Invitrogen) after removal of the bone ends.

Hearts from mice infused with AngII for 3d were harvested under sterile conditions and used for cell isolation as previously described (214). Briefly, hearts were mechanically and enzymatically digested in a collagenase solution (50 mg/mL collagenase II, Cedarlane, Burlington, ON) in RPMI 1640 media (Gibco, Burlington, ON) at 37^{o}C with agitation for 45min. Cell isolates were washed in complete RPMI containing 10% heat-inactivated FBS, 2mM L-glutamine, 100mg/mL streptomycin and 100U/mL Penicillin. Cells were then plated in T25 flasks coated with 0.1% gelatin, incubated for 3d at 37^{o}C and 5% CO_2, at which point all non-adherent cellular debris was removed and media was replenished.

Neonatal cardiomyocytes were isolated from day old C57Bl/6 pups as reported previously (263). In short, pups were decapitated, hearts were excised and mechanically and enzymatically digested in 0.25% trypsin-EDTA for 20min. Cell isolates were washed in complete DMEM containing 20% FBS, 2mM L-glutamine, 100μM non-essential amino acids, 100mg/mL streptomycin and 100U/mL Penicillin and allowed to differentially adhere to a T75 flask for 2hr. Cardiomyocytes were then collected from the suspension and plated on 0.1% gelatin coated 6-well plates. Isolated fibrocytes and neonatal cardiomyoctes were treated with a) AngII, b) recombinant human CTGF (Cell Sciences, Canton, MA, USA) or c) PBS as vehicle control.

5.3.6 Histological Analysis

Hearts were processed for histological assay by: a) fixing with 10% formalin for 24hr; b) protecting with sucrose/OCT followed by snap freezing. Formalin fixed tissues were

paraffin embedded and were serially sectioned on a microtome (5μm). Basic myocardial histology and cellular infiltration were examined using heart cross-sections stained with hematoxylin and eosin (H&E). Immunohistochemistry for CTGF (Abcam, Cambridge, MA) and Ki-67 (DakoCytomation, Mississauga, ON) was performed on paraffin embedded tissues, which were deparaffinized and treated for antigen retrieval prior to staining. Briefly, endogenous peroxidases were quenched with 3% hydrogen peroxide; endogenous biotin was blocked (DAKO Biotin Blocking System, DakoCytomation); and non-specific staining was blocked with normal goat serum. Sections were incubated with primary antibody, followed by a specific biotin-conjugated secondary antibody. The antibody complexes were then conjugated to an Avidin-biotin complex (Vectastain ABC kit; Vector, Burlington CA) and developed using 3,3' diaminobenzidine as the chromogen (DAB; DakoCytomation). Light microscopy was performed; pictures were captured and analyzed in Adobe Photoshop 5.0.

5.3.7 Immunofluorescence Staining

Isolated cells were plated on coverslips overnight, fixed in 4% paraformaldahyde, permeabilized with 0.03% Triton X-100, blocked against non-specific antibody binding with 10% normal goat serum and stained for CD45 (BD Biosciences, Mississauga, ON), Collagen type 1 (Rockland Inc, Gilbertsville, PA), cardiac troponin I (CTnI; Abcam), GFP (Abcam), αSMA (Sigma Aldrich) or CD133 (Abcam). Antibodies were detected using anti-host specific Alexa fluorescently labeled secondary antibodies (Invitrogen) and nuclei were counterstained with Hoescht stain (Sigma Aldrich). Images were captured with a Zeiss Axiovert 200 inverted microscope with a Hamamatsu ORCA-R2 digital camera with an AttoArc 2 HBO 100W lamp.

5.3.8 Immunoblotting

Western blotting was performed on samples isolated from snap frozen heart sections. Sections were homogenized in RIPA buffer (150mM NaCl, 50mM Tris-HCL base, 0.1% SDS, 0.1% Triton X-100, 0.5% deoxycholic acid) with protease inhibitors added (1mM PMSF, 5ug/mL Aprotinin, 5ug/mL Leupeptin, 5ug/mL Pepstatin A and 2mg/mL Iodoacetamide). Samples were then denatured by boiling with Laemmli sample buffer. Protein was separated on a 12% SDS-PAGE gel and transferred to Immobilon PVDF membrane (Millipore, Bedford, MA). Membranes were incubated with 5% skim milk in buffer for 1hr before incubation with CTGF antibody overnight at 4^{o}C (Abcam). Blots were developed using horseradish peroxidase-linked goat anti-rabbit IgG (Vector Labs, Burlington, UK) and an Amersham ECL kit (GE Life Sciences, Buckinghamshire, UK). β-actin was used as an internal control (Sigma Aldrich, Oakville ON).

5.3.9 Flow Cytometry

Cell surface expression of CD45 and cytosolic expression of vimentin and CTnI was determined using flow cytometry. Briefly, isolated PBMCs and BM cells were incubated with a monoclonal rat anti-CD45 antibody (CL9446AP; Cedarlane Labs) followed by FITC-conjugated goat anti-rat IgG_{2b} (Cedarlane) secondary antibody. Cells were then permeabilized using a commercial kit (BD Biosciences) and incubated with PerCP conjugated monoclonal mouse vimentin antibody (RV202; Santa Cruz Biotechnology Inc, Santa Cruz, CA, USA). Isolated neonatal cardiomyocytes were incubated with polyclonal rabbit anti-CTnI followed by an Alexa-488 conjugated goat anti-rabbit IgG (Invitrogen) secondary antibody. Following antibody incubations cells were fixed in 1% formalin solution for storage prior to analysis. Cells were analyzed with a (BD

FACScalibur (BD Biosciences, Mississauga, ON, Canada) flow cytometer within 5d of labeling. Findings were confirmed using isotype controls (CD45: rat IgG_{2b} eBiosciences (San Diego, CA, USA), vimentin-PerCP: IgG_1-PerCP Santa Cruz, and CTnI: rabbit IgG Sigma Aldrich). A secondary-only control was used to confirm the absence of nonspecific binding of the secondary antibody.

5.3.10 Relative Quantitative Polymerase Chain Reaction (qPCR)

Total RNA was isolated from snap frozen heart sections using TRIzol (Invitrogen, Carlsbad, CA) according to the manufacturer's protocol. First strand cDNA was synthesized from RNA using iScript cDNA Synthesis Kit (Biorad, Hercules, CA). The qPCR was completed using iQ SYBR Green Supermix (Biorad) and the iQ Multicolour Real-Time PCR Detection System thermocycler (Biorad) was used for detection. Efficiency curves and no-template control samples were run with samples each thermocycling. Melt curves were run after cycling to ensure target specificity. Primers were designed against mRNA sequence of CTGF (forward: 5'-TCAACCTCAGACACTGGTTTCG-3'; reverse: 5'-TAGAGCAGGTCTGTCTGCAAGC-3'), TGFβ (forward: 5'-GGTCTCCCAAGGAAAGGTAGG-3'; reverse: 5'-CTCTTGAGTCCCTCGCATCC-3'), collagen 1α1 (forward: 5'-CAACAGTCGCTTCACCTACAGC-3'; reverse: 5'-GTGGAGGGAGTTTACACGAAGC-3') and 18S ribosomal RNA (forward: 5'-TCAACTTTCGATGGTAGTCGCCGT-3'; reverse: 5'-TCCTTGGATGTGGTAGCCGTTTCT-3'). Expression was normalization to the 18S ribosomal gene using the Pfaffl method.

5.3.11 Proliferation Assays

An MTT assay for assessment of relative cellular proliferation was carried out according to the manufacturer's instructions (Invitrogen). In brief, cells were plated in 96-well tissue culture plates and allowed to adhere overnight prior to stimulation. Cells were stimulated for 24hr at which point MTT reagent was added for 4hr, followed by SDS-HCL solution for 18hr to stop the reaction. Samples were mixed and absorbance was then read at 570nm.

Relative proliferation was also assessed by immuno-fluorescent staining of Ki67 proliferation marker in cells plated on gelatin-coated coverslips. Cells were allowed to reach 50% confluency, then stimulated for 24hr at which point cells were fixed using 4% para-formaldehyde for 10min at room temperature. Non-specific binding was blocked using secondary host serum then coverslips were incubated overnight at $4^{o}C$ with anti-Ki67 antibody. Bound antibody was detected using anti-host specific Cy3 fluorescently labeled secondary antibodies (Invitrogen) and nuclei were stained with hoescht dye. Images were captured with a Zeiss Axiovert 200 inverted microscope with a Hamamatsu ORCA-R2 digital camera with an AttoArc 2 HBO 100W lamp. Relative proliferation was assessed by counting the number of Ki67 positive nuclei relative to the total number of nuclei in 5 random fields of view at 20x magnification.

5.3.12 Statistical Analysis

Data is represented as mean ± SEM. One-way ANOVA tests were completed using the Bonferroni post-test to compare the experimental groups to the saline control. All qPCR

results were evaluated based on the Wilcoxin Signed Rank test to compare changes in relative expression. All statistical calculations were computed using GraphPad Prism4 software and significance was determined if $p \leq 0.05$.

5.4 Results

5.4.1 Bone-Marrow Derived Progenitors are Mobilized from the Bone Marrow and Infiltrate into the Myocardium after AngII Exposure

Previous work from our laboratory has demonstrated that AngII exposure results in significant multi-focal areas of cellular infiltration within the myocardium by 1d (214). This cellular infiltration is then followed by significant collagen deposition in areas of infiltration over 3-7d of AngII exposure. GFP chimeric mice that constitutively express eGFP under control of the actin promoter in bone marrow derived cells were used initially to compare animals exposed to AngII or saline control. Chimeric mice exposed to AngII for 3d were found to have a significant proportion of infiltrating cells positive for GFP in the myocardium when compared to saline control (Figure 5.1A, B, E, F), suggesting that bone marrow derived cells are the predominant cell type. Immunofluorecence was used to show that infiltrating cells also expressed αSMA (mesenchymal myofibroblast marker) colocalized with GFP in AngII exposed animals (Figure 1C, D, G, H). Taken together, these findings confirm our previous work suggesting that a significant proportion of myocardial infiltrating cells are fibrocytes known to express bone marrow and mesenchymal markers (214, 228). Flow cytometry was used to identify double positive fibrocytes in the circulation. The percentage of CD45+/vimentin+ double positive cells, indicative of fibrocytes in PBMC's, was significantly higher in animals exposed to AngII when compared to saline control (Figure

5.2A, B). Taken together, AngII infusion resulted in early mobilization of fibrocytes from the bone marrow into the circulation and significant migration to the myocardium within 3d of exposure.

5.4.2 CTGF is the First Pro-Fibrotic Cytokine seen in the Myocardium after AngII Exposure

Previous work by us, and others suggested that TGFβ and CTGF may be the predominant pro-fibrotic cytokines associated with AngII dependent myocardial fibrosis (214, 264). Increased numbers and additional time-points were added to historical data (214). The expression of CTGF within the myocardium relative to both housekeeping gene and saline control was significantly increased (23-fold) as early as 6hr after AngII exposure ($p < 0.01$), preceding myocardial cellular infiltration or ECM deposition shown to be significant by 1d and 3d respectively (214, 228). CTGF mRNA levels were then seen to drop off at 12hr before increasing again at 24 hr by 19-fold ($p < 0.01$) (Figure 5.3A). As the second wave of CTGF expression occurs there is a concurrent increase in TGFβ levels that reached significance at 24hr of AngII exposure (4-fold) and peaked at 3d compared to saline control ($p < 0.01$) (Figure 5.3B). The increase in CTGF expression when compared to TGFβ was earlier and several fold higher, suggesting a role for CTGF in the subsequent fibrosis development (Figure 5.3C). Upregulation of CTGF expression was confirmed by showing a significant increase in the presence CTGF protein relative to saline controls at 3d of AngII exposure by western blotting of cardiac extracts (Figure 5.3D-E). The majority of CTGF appeared to be localized to the cardiomyocytes and not the infiltrating cells suggesting that cardiomyocytes may be the primary source of early CTGF production (Figure 5.3F, G).

5.4.3 Neonatal Cardiomyocytes Produce CTGF in Response to AngII

Given our evidence that CTGF production was upregulated in the myocardium prior to fibrocyte migration and appeared to be localized to cardiomyocytes, we sought to confirm that cardiomyocytes produce CTGF after AngII exposure. To achieve this we conducted *in vitro* stimulation assays using isolated neonatal cardiac myocytes. The majority of isolated cardiomyocytes stained positive for CTnI, both by flow cytometry (97%) and immunofluorescence (94%) suggesting high purity (Figure 5.4A, B). Stimulation of isolated cardiomyocytes for 6 hr with AngII significantly increased the CTGF mRNA expression 2.1-fold compared to vehicle only control ($p < 0.05$) (Figure 4C). This finding confirms that cardiomyocytes producing significant amounts of CTGF directly in response to AngII; thus providing direct supporting evidence that cardiomyocytes are the initial cell responsible for CTGF expression.

5.4.4 Fibrocytes Isolated and Cultured *In Vitro* from AngII Exposed Myocardium also Contributes to CTGF Expression

While our findings suggest that CTGF is produced initially by cardiomyocytes, it may not explain our observation *in-vivo* of a second peak in CTGF mRNA expression that appears to coincide with the increase in fibrocyte accumulation in the myocardium at 24hr of AngII exposure. Therefore, we examined the possibility that infiltrating cells could also contribute to the high level of CTGF found in whole tissue after AngII exposure. Infiltrating fibrocytes (after AngII exposure) were isolated as previously described[9]. Fibrocyte purity was assessed by confirming co-expression of a mesenchymal marker collagen type I and a hematopoetic marker CD45 (Figure 5.5A). Using this approach, the mean purity of fibrocyte cultures was 50%. Control animals yielded less than 1%

fibrocytes (Figure 5.5B). Direct exposure of the isolated fibrocyte population to AngII resulted in a significant 2.6-fold increase in CTGF mRNA expression compared to saline control ($p < 0.05$) (Figure 5.5C). This suggests that a fibrocyte rich population in which no cardiomyocytes are present is also capable of CTGF up-regulation and expression. These findings may explain the observed second peak in CTGF mRNA we observed in the mycardium of AngII exposed animals after 12hr of AngII exposure.

5.4.5 Fibrocytes Proliferate in Response to CTGF

We next focused on a potential role for CTGF in fibrocyte accumulation and ECM deposition. On examination of histological sections from animals exposed to AngII for 3d we observed significant positive staining of Ki67, a proliferation marker, in areas of fibrocyte infiltration when compared to saline control (Figure 5.6A, B). This would suggest that fibrocyte accumulation is dependent on both influx from the circulation and from proliferation. Fibrocyte proliferation in the myocardium occurred concurrently the elevation of CTGF. As such, we investigated the effect of CTGF exposure on the proliferation of fibrocytes in an *in vitro* setting. Isolated fibrocytes exposed to CTGF resulted in significant proliferation as assessed by Ki67 positivity when compared to media control ($p < 0.05$) (Figure 6C). This was confirmed using a second proliferation assay, the MTT assay ($p < 0.05$) (Figure 5.6D). These data suggest that increased fibrocyte proliferation within the myocardium after AngII exposure (3d) is in part due to the increase in CTGF observed at this time.

5.4.6 Fibrocytes Differentiate to ECM Producing Cells Under the Influence of CTGF

To investigate the effect of CTGF on fibrocyte differentiation, fibrocytes were isolated as above and exposed to CTGF. There was a significant increase in the mRNA expression of Collagen type 1, α1 subunit (COL1A1), with a 2.3-fold increase compared to saline control (Figure 5.7A). This suggests that fibrocytes can, under appropriate conditions, become a source of ECM in the myocardium particularly after AngII exposure and the presence of CTGF. Given that we have demonstrated that AngII upregulates the expression of CTGF (Figure 5.5), this would create a positive feedback loop promoting a profibrotic environment.

Fibrocytes isolated from peripheral blood were enriched over 14d with or without CTGF exposure. Cells that were not exposed to CTGF over the duration had a significantly lower αSMA to CD133 ratio, compared to early isolates (1d). On the other hand, fibrocytes exposed to CTGF during the 14d enrichment did not show a significant reduction in αSMA:CD133 (Figure 5.7B). Taken together, this suggests that CTGF exposure may allow fibrocytes to maintain a higher mesenchymal protein expression and therefore favor differentiation of fibrocytes into ECM producing myofibroblast-like cells.

5.5 Discussion

5.5.1 Bone Marrow-Derived Progenitor Cells Mobilize and Migrate to the Myocardium

We have previously reported that fibrocytes, a bone marrow-derived fibroblast progenitor population, represent the majority of infiltrating cells seen to accumulate in the

myocardium after AngII exposure (214, 228). The effector role of fibrocytes has been suggested in many fibrotic pathologies including models focusing on cardiomyopathy (60, 219), cardiac hypertrophy (198), pulmonary fibrosis (254) and renal fibrosis (211). In the present study we demonstrate that following 3d of AngII exposure, cells that have migrated to the myocardium are bone marrow-derived and stain positive for the mesenchymal marker αSMA, confirming that the infiltrating cells are fibrocytes. We have also provided evidence that fibrocyte numbers increase in peripheral blood after AngII exposure supporting a hypothesis of mobilization of these progenitor cells from the bone marrow in response to AngII. Given these findings, we investigated the parameters that induce fibrocyte accumulation in the myocardium and the propagation of the fibrotic response.

5.5.2 Fibrotic Mediators: Interaction between CTGF and TGFβ

We observed significant increases in CTGF mRNA and protein in the myocardium well before the accumulation of fibrocytes, suggesting a link between CTGF production by cardiomyocytes and fibrocyte accumulation. Immunocytochemistry labeling for CTGF confirmed that cardiomyocytes were a significant cellular source of CTGF. Further support for this hypothesis came from experiments using primary cultured cardiomyocytes, which demonstrated that AngII exposure results in significant increase in CTGF mRNA expression. The importance of CTGF in fibrosis development has been suggested by others and a link between AngII and CTGF has been implicated by data showing that CTGF expression could be abrogated in animal models by angiotensin receptor blockade (265). These data suggest that the initial increase in CTGF expression

seen in our model after AngII exposure was a direct result of signaling through AngII receptors (AT1R) located on resident cardiomyocytes (266).

Traditionally, CTGF is believed to be regulated via TGFβ signaling. CTGF was first described as a TGFβ response factor in human endothelial cells (HUVECs) and was found to be expressed by cultured skin fibroblasts in response to TGFβ as early as 30 min after exposure (267, 268). The role of TGFβ as a key regulator of fibrosis development has previously been described and explains why in the AngII infusion model, there was an increase in TGFβ mRNA in the myocardium after 1d of exposure (258, 259). We provide evidence for the first time that in a mouse model of AngII exposure, CTGF is expressed first (6hr) within the myocardium by resident cardiomyocytes, well before the observed increase in TGFβ expression (1d). Our findings suggest that in this model of AngII-induced myocardial fibrosis, the initial increase in CTGF expression occurs independently of TGFβ signaling. There is evidence from *in vitro* models that CTGF regulation can occur through a SMAD2/3 dependent, TGFβ-independent pathway for CTGF expression (158).

During the course of AngII exposure, the initial increase in CTGF expression was followed by a reduction in CTGF mRNA at 12hr. At 24hr, CTGF expression in the heart rebounded. This coincided with increased infiltration of fibrocytes into the myocardium, which implicated fibrocytes in the production of the second wave of CTGF (214). We

demonstrated that fibrocytes enriched in culture upregulate CTGF expression in response to AngII exposure, providing convincing evidence that fibrocytes could be contributing to the increased expression of CTGF in the myocardium observed at 24hr of AngII exposure. This second wave of CTGF expression also coincided with increased TGFβ expression, suggesting that this second increase in CTGF expression could be TGFβ dependent. Supporting this claim, TGFβ-dependent CTGF expression has previously been shown in skin fibroblast cultures (267, 268).

A third mechanism by which CTGF expression is modulated is through an autoregulatory feedback pathway in which CTGF can upregulate its own expression (261). Furthermore, CTGF can upregulate TGFβ expression, which is consistent with our observations that increased TGFβ expression occurred concurrently with increased CTGF expression (269).

Cumulatively, our results suggest that multiple cell types and feedback mechanisms likely contribute to the increased CTGF expression in the myocardium after AngII exposure. The early response to AngII is mediated by CTGF produced by cardiomyocytes directly through AngII receptor signaling. The secondary increase in CTGF expression, however, is mediated by combined direct AngII receptor signaling and TGFβ-dependent signaling by cardiomyocytes, resident fibroblasts and fibrocytes.

5.5.3 CTGF Regulation of Fibrocyte Proliferation and ECM Production

The timing of CTGF expression in the myocardium suggested that CTGF plays an important role in the early environment that leads to myocardial fibrosis following AngII exposure. As fibrocytes are the predominant infiltrating cell type in the myocardium after AngII exposure (214) and many fibrotic conditions feature CTGF upregulation, it followed that CTGF may promote fibrosis by acting on fibrocytes. In our AngII model, we demonstrated that fibrocytes in the myocardium were highly proliferative. Thus, we believed CTGF might promote fibrosis through fibrocyte proliferation. Several studies provide evidence supporting this theory by demonstrating that CTGF increases proliferation in cultured fibroblasts (270, 271). We therefore investigated the effects of CTGF on isolated fibrocytes in culture. Consistent with our *in vivo* findings, CTGF exposure led to increased fibrocyte proliferation *in vitro*. This suggests that the increase in CTGF production in the myocardium after AngII exposure contributed to the observed increase in fibrocyte accumulation within the myocardium through increasing fibrocyte proliferation.

Fibrocytes are progenitor cells that under certain conditions are capable of differentiation into collagen producing myofibroblasts. We sought to investigate the effect of CTGF on the maturation and differentiation of fibrocytes. We have provided evidence for the first time that fibrocyte enriched cell culture exposed to CTGF resulted in a significant increase in COL1A1 mRNA supporting the differentiation of fibrocytes toward an ECM producing phenotype. In support of our observation, some investigators have shown increased expression of ECM proteins by fibroblasts after exposure to CTGF (85, 272).

Furthermore, there is also evidence suggesting that inhibiting CTGF *in vitro* is sufficient to reduce collagen type 1 and αSMA protein production by stimulated fibroblast cell lines and primary isolated fibroblasts, thus supporting a role for CTGF in promoting and maintaining fibroblast differentiation and phenotype (271-273)

Taken together, our results suggest that CTGF is involved in the regulation of myocardial fibrosis after AngII exposure. We have provided two mechanisms by which CTGF contributes to the pro-fibrotic microenvironment: (1) increased fibrocyte proliferation contributing to fibrocyte accumulation and (2) promoting fibrocyte differentiation into ECM producing cells.

5.5.4 Mechanism of Action of CTGF

There has not yet been a CTGF receptor identified and, as such, the molecular mechanisms of action continue to be investigated. Although the exact molecular mechanisms of CTGF signaling is beyond the scope of the current manuscript, there are a number of possible pathways that may be involved in regulation of ECM production and cellular proliferation in response to CTGF. Separate domains of CTGF have been suggested to be responsible for regulating proliferation or differentiation, supporting this hypothesis (271). One possible pathway that is likely involved is the mitogen-activated protein (MAP) kinase cascades, specifically p38, which is involved in regulating proliferation and collagen type 1 expression (274). In fact, p38 positively regulates COL1A1 expression by primary fibroblasts and is significantly phosphorylated after cells are exposed to CTGF (275). Moreover, exposure to CTGF results in reduced

phosphorylation of MAP kinases, ERK1/2 and JNK, which have been suggested to repress COL1A1 expression, resulting in increased COL1A1 expression when CTGF is present (275, 276). Taken together, these studies suggest that activation of the p38 MAP kinase pathway in combination with repression of the ERK1/2 and JNK pathways could control COL1A1 expression and proliferation of fibrocytes in response to CTGF.

Anti-fibrotic intervention through blockade of CTGF has shown positive results in animal models of skin, kidney and lung fibrosis (277-279). Potential strategies for interrupting the effects of CTGF were thoroughly reviewed by Brigstock and have included monoclonal antibody, antisense oligonucleotide and siRNA interventions. Preliminary results published from recent stage 1 clinical trials suggested that a humanized anti-CTGF antibody decreased kidney failure in a cohort of patients with diabetic nephropathy (280). These therapeutic strategies, however, have not yet been successfully deployed in models of myocardial fibrosis (281). We have provided support for a pro-fibrotic role for CTGF in the development of myocardial fibrosis after AngII exposure. While CTGF appears to contribute to the proliferation of fibrocytes after AngII exposure, it may not regulate the initial influx of fibrocytes into the myocardium. Consequently, CTGF inhibition may not entirely block the development of myocardial fibrosis. At the same time, CTGF may still present a therapeutic target for reducing fibrosis in cardiac diseases, although its inhibition requires further evaluation.

5.5 Acknowledgments

We are grateful to Ms. Tanya Myers for excellent technical expertise.

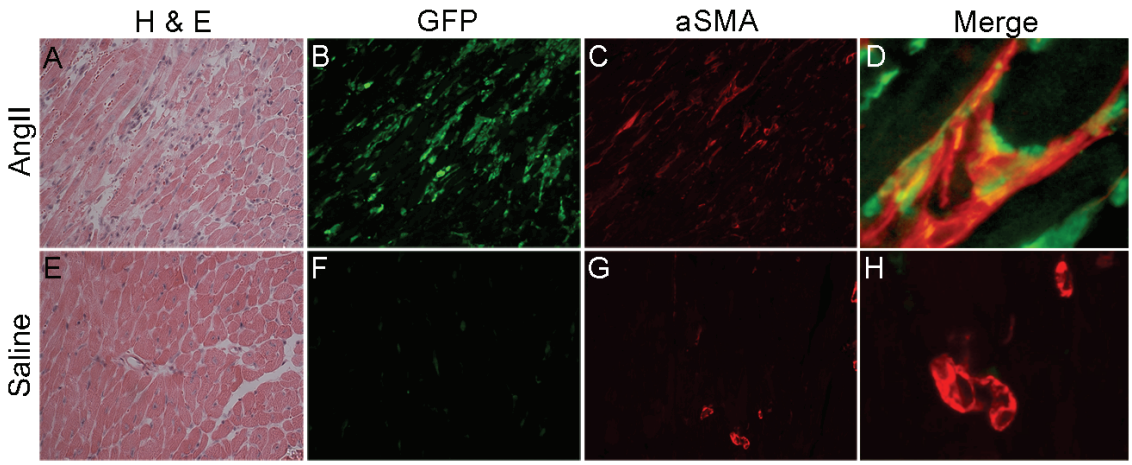

Figure 5.1 Fibrocyte Infiltration

Chimeric animals with transplanted GFP+ bone marrow cells received saline (A, B, C, D) or AngII for 3d (E, F, G, H). Areas containing infiltrating cells were identified by H&E stain (A, E) and characterized by immunofluorescent staining for GFP (B, F) and αSMA (C, G). Merged images of green and red channels show dual staining indicating GFP+/αSMA+ cells in the area of infiltration (D, H). Images were captured at 25X and 100X, with representative images shown. n=3.

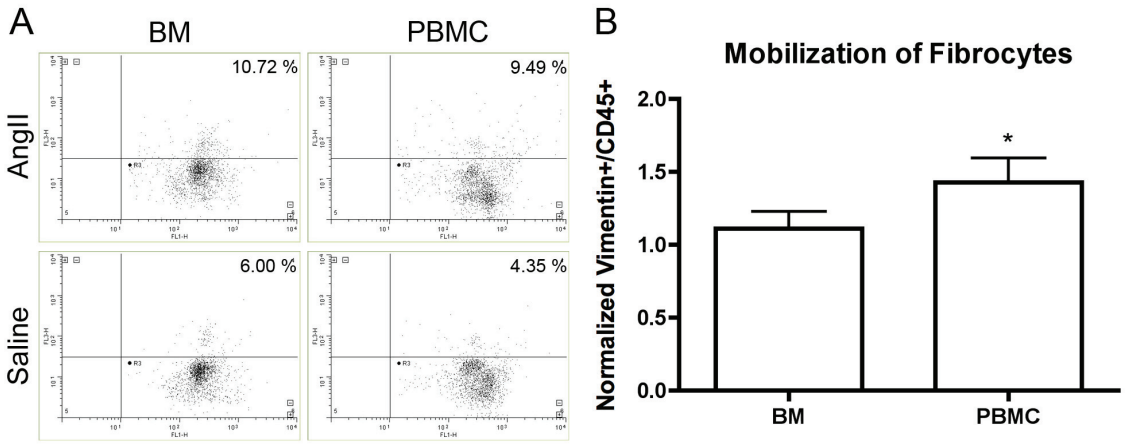

Figure 5.2 Fibrocyte Mobilization

Animals received saline as a control or AngII for 3d and bone marrow (BM) and peripheral blood mononuclear cells (PBMCs) were isolated for assessment of CD45 and vimentin presense by flow cytometry (A). Quantification of relative levels of vimentin+ cells within the CD45+ population in bone marrow and peripheral blood is shown (B). n=5; *$p<0.05$.

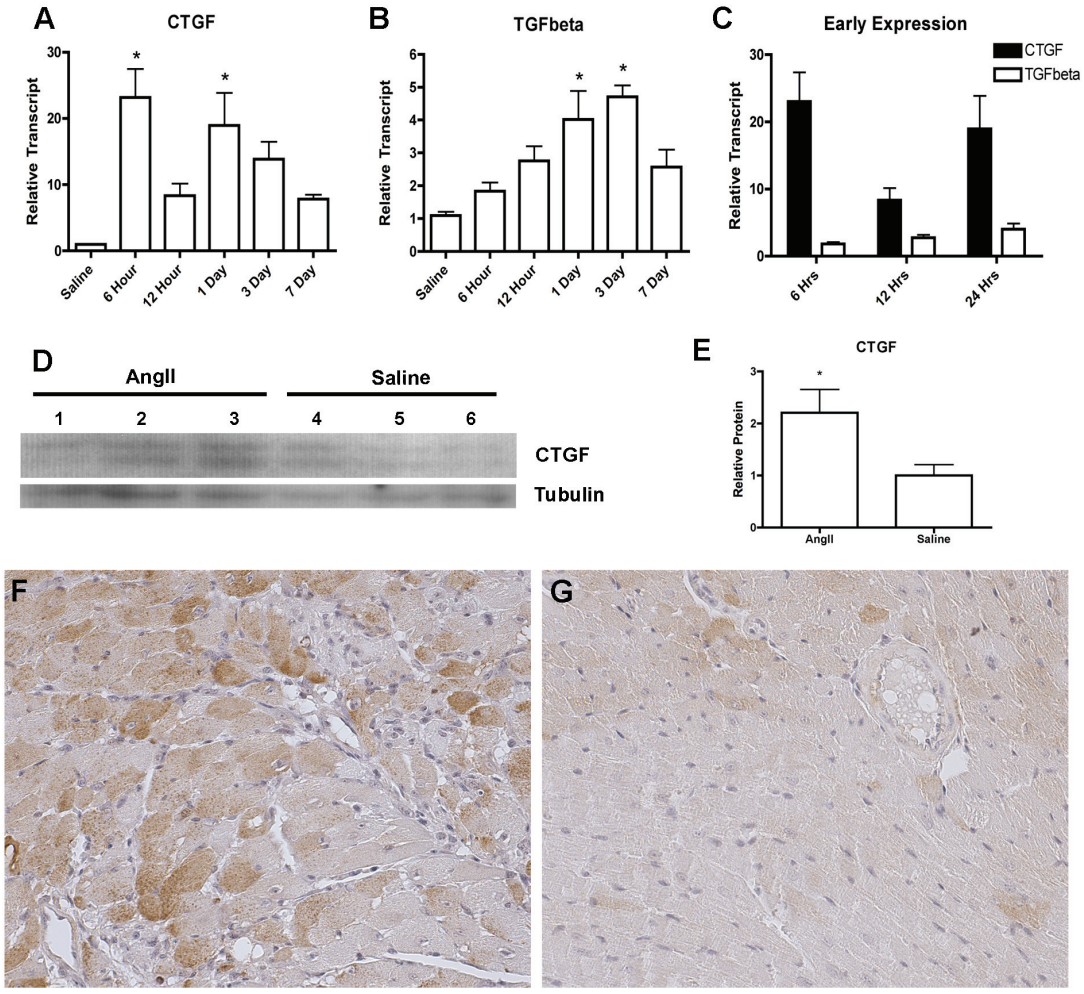

Figure 5.3 CTGF and TGFβ Production

qRT-PCR was used to assess myocardial expression for CTGF (A), TGFβ (B) and the early expression compared (C). Transcript levels are reported relative to housekeeping gene ribosomal 18S (n=8). Immunoblotting was used to determine CTGF and β-tubulin protein production in whole myocardium. A representative blot with 3 samples in each experimental group (AngII; lanes 1-3 and saline; lanes 4-6) is shown (D). CTGF protein was semi-quantified relative to the housekeeping protein β-tubulin (E) (n=6). Immunohistochemistry was used to localize CTGF within the myocardium.

Representative sections from animals treated with AngII for 3d (F) or saline as a control (G) are shown. Images were captured at 40x. *$p<0.05$.

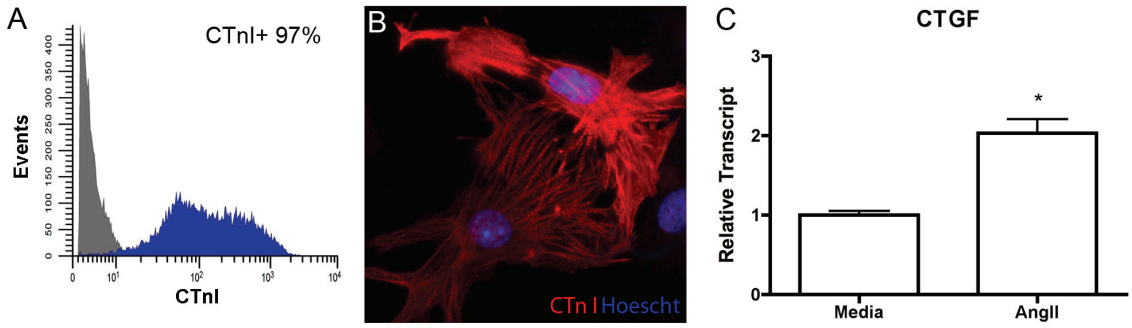

Figure 5.4 Cardiomyocytes Produce CTGF

Cardiomyocytes were isolated from neonatal mice. Purity was assessed using CTnI staining by flow cytometry (A) and immunofluoresence with nuclei counterstained with Hoescht (B). Cultured cardiomyoctes were stimulated with AngII or saline control for 6hr. CTGF mRNA expression was assessed by qRT-PCR and compared to the housekeeping gene 18S (C). Images were captured at 63x. n=8; *p<0.05.

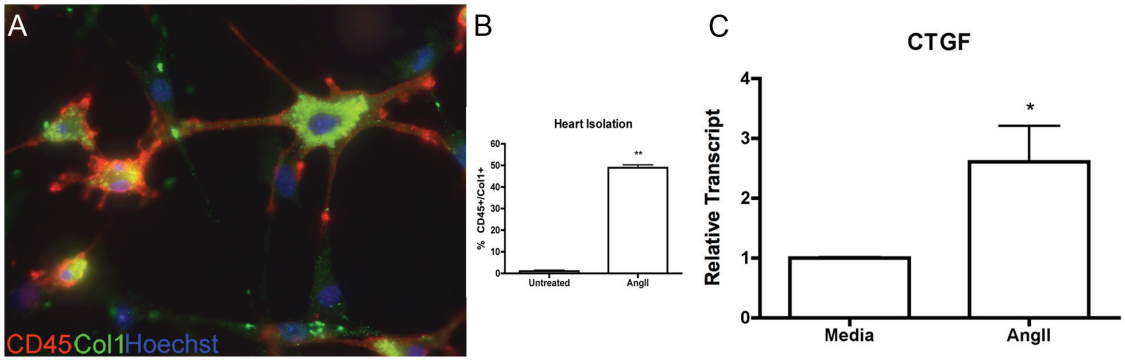

Figure 5.5 Isolated Fibrocytes Produce CTGF

Fibrocytes were isolated from the myocardium of mice exposed to AngII for 3d. Purity was assessed by immunofluoresent staining for CD45+/ColI+ with nuclei counterstained with Hoescht (A). Purity was quantified by calculating the percentage of CD45+/ColI+ cells relative to the total number of nuclei (B). Isolated fibrocytes were stimulated with AngII or saline control for 6hr. CTGF mRNA expression was assessed by qRT-PCR and compared to the housekeeping gene 18S (C). Images were captured at 63x. n=5; *p<0.05, **p<0.01.

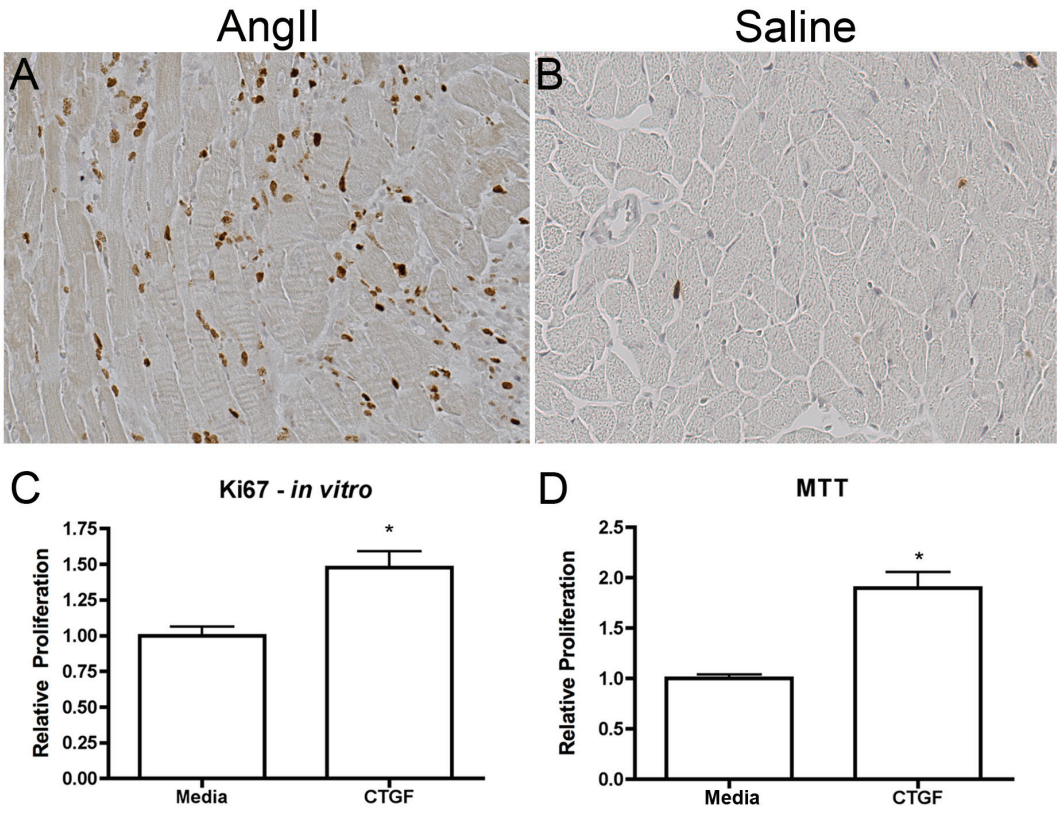

Figure 5.6 Fibrocytes Proliferate in Response to CTGF

Immunohistochemistry was used to identify Ki67 positive cells within the myocardium of animals exposed to AngII (A) or saline control (B) for 3d. Isolated fibrocytes were exposed to CTGF or vehicle control for 24hr. Proliferation was assessed by counting cells positive for immunofluorescent staining of Ki67 relative to the number of nuclei in 5 fields of view per sample captured at 25x (C) and MTT assay (D). Representative images were captured at 40x. n=6; *$p<0.05$.

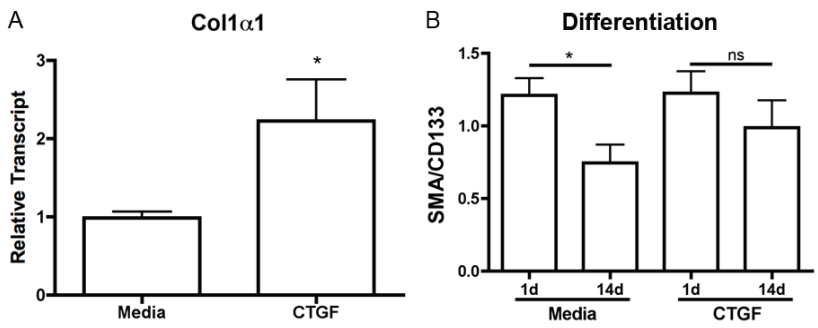

Figure 5.7 Fibrocytes Differentiate/ECM is Produced in Response to CTGF

Isolated fibrocytes were exposed to AngII, CTGF or vehicle control for 6hr. The COL1A1 transcript expression was assessed by qRT-PCR relative to housekeeping gene 18S (A) (n=6). PBMCs were enriched for fibrocytes in media containing CTGF or vehicle control and maintained in culture for 1 or 14d. Immunofluorescent staining for αSMA and CD133 was done and the area of positive staining was normalized to the total number of nuclei positive and reported as a ratio of αSMA/CD133 staining from 5 fields of view per sample captured at 25x. n=4; *$p<0.05$.

CHAPTER 6

MYOCARDIAL MIGRATION BY FIBROBLAST PROGENITOR CELLS IS BLOOD PRESSURE DEPENDENT IN A MODEL OF ANGII MYOCARDIAL FIBROSIS

NL Rosin, MJ Sopel*, A Falkenham**, TL Myers**, JF Légaré**

Hypertension Research.2012. epub:doi: 10.1038/hr.2011.217

* Author contributions are clearly outlined in Appendix 2.

6.1 Abstract

Introduction: Activation of the renin angiotensin system (RAS) is believed to promote myocardial fibrosis. However, it is unclear if these physiological responses result from chronic hemodynamic stress or via direct cellular signaling. *Methods*: Male C57B/6 mice were randomly assigned to receive AngII (2.0mg/kg/min), AngII+Hydralazine (6.9mg/kg/min), or saline (control) via osmotic pumps for 7d. Blood pressure was measured via non-invasive plethysmography. Hearts were harvested and processed for analysis. Cellular infiltration and collagen deposition were analyzed using histologic staining. Molecular mediators were assessed using quantitative RT-PCR. *Results*: As previously described, animals that receive AngII developed hypertension and multifocal cellular infiltration by $SMA^{+}/CD133^{+}$ fibroblast progenitors followed by collagen deposition. The co-administration of hydralazine with AngII completely inhibited the hypertensive effects of AngII ($p \leq 0.01$), resulted in minimal cellular infiltration and minimal collagen deposition. These findings were in the context of persistent RAS system activation seen by elevation in serum aldosterone levels in AngII and hydralazine+AngII animals when compared to saline. At the molecular level, infusion of AngII resulted in the significant upregulation of pro-fibrotic factors (CTGF-7.8±0.7 fold), pro-inflammatory mediators (TNFα-4.6±0.8 fold; IL-1β-6.4±2.6 fold) and chemokines (CCL2-3.8±1.0 fold; CXCL12-3.2±0.4 fold), which were inhibited when hydralazine was also infused. *Conclusions:* We provide evidence that myocardial infiltration by fibroblast progenitor cells and resulting fibrosis secondary to AngII can be prevented by the addition of hydralazine. Furthermore the beneficial effects of hydralazine were observed

while maintaining RAS activation suggesting that the mechanism of fibrosis is blood pressure dependent.

6.2 Introduction

There is growing evidence that the renin-angiotensin system (RAS), specifically angiotensin II (AngII), is implicated in the development of myocardial fibrosis, a common pathological feature of many cardiovascular conditions (5, 81, 282, 283). RAS activation and increased levels of AngII can be seen in patients with cardiovascular diseases that include atherosclerosis, hypertension, cardiac hypertrophy and heart failure (5, 20, 21). Conversely, inhibition of RAS activation with angiotensin receptor blockade has been shown to significantly improve patient survival and limit the progression of cardiac remodeling and heart failure (186).

Investigations in small animals have confirmed that AngII exposure can result in myocardial fibrosis (7, 11, 12, 187, 191, 193, 194, 284). Such experiments have supported a direct relationship between RAS activation via AngII and fibrosis. As such, animal models of fibrosis using AngII have proven very helpful in understanding some of the molecular events leading to the development of fibrosis. However, AngII is also a potent vasoconstrictor capable of significant hypertension (HTN) making it difficult to dissociate the effects of HTN versus AngII on the myocardium. In fact the mechanism responsible for remodeling as a result of HTN or RAS activation has been a longstanding debate (11, 285).

Using a mouse model of AngII infusion, our laboratory has been able to characterize the early molecular and cellular events occurring in the myocardium within 1 week of exposure to AngII. We have shown that animals exposed to AngII develop hypertension and early infiltration (1d) by fibroblast progenitor cells called fibrocytes (214). We, and others, have also provided evidence that strategies that limit the migration of fibrocytes inhibits the development of fibrosis supporting an effector role for these cells.

In the present manuscript we have utilized our experience with AngII infusion model to better characterize early events in the development of fibrosis. Specifically we evaluated the effects of RAS activation in the absence of hypertension using the anti-hypertensive drug hydralazine, which acts on smooth muscle cells as a vasodilator independent of the RAS system.

6.3 Materials and Methods

6.3.1 Animals

All work was approved by Dalhousie University's *University Committee on Laboratory Animals*. Male C57BL/6 mice ranging from 7 to 8 wk of age were purchased from Jackson Laboratory (Bar Harbour, ME) and were housed within the Medical Sciences Animal Care Facility at Dalhousie University. Mice were provided food and water *ad libitum* for 1 wk prior to experimentation. Animals were anesthetized with isoflurane (Baxter Healthcare Corp., New Providence, NJ) in oxygen delivered by a Fortec vaporizer. When surgical levels of anesthesia were reached a 1-2 cm mid-scapular skin incision was made and a mini osmotic pump (Alzet, Palo Alto, CA) was inserted subcutaneously. The incision was closed using 7mm wound clips. Animals were

randomly assigned to receive; AngII (n=10, 2.0 µg/kg/min, Sigma Aldrich, Oakville ON), AngII and hydralazine (n=4, 6.9 µg/kg/min, Sigma Aldrich) or a vehicle control of saline (n=10). The pumps remained in for 7d during which the animals were provided with food and water *ad libitum* and observed for signs of morbidity. Prior to euthanization, blood pressure measurements were taken via the Coda2 non-invasive cuff system (Kent Scientific, Torrington, CT) for a minimum of 5 consecutive measurements per animal. Experience in our laboratory and findings from others have shown that blood pressure measurements taken at completion of the experiment reflect changes that have been stable over several days supporting our approach to measure blood pressure at 7 d (286, 287). Animals were then anesthetized, blood was collected and the hearts were harvested and divided along the short axis into 3 portions including the base, middle and apical sections. The base portion was processed for histological examination while the other two portions were snap frozen immediately for molecular analysis.

6.3.2 ELISA for Aldosterone

Collected blood was allowed to clot at room temperature and the serum was collected after the sample was centrifuged at 600g for 10min. Samples were aliquoted and stored at -80°C until required for ELISA assay. Serum aldosterone levels were assessed using a standard ELISA kit (Cayman Chemical Company, Ann Arbor, MI) as per manufacturers instructions. Briefly, serum samples were diluted 1:4 and plated out in triplicates along with recommended controls. The plate was covered and incubated for 18hrs at 4°C. The plate was then developed for 1.5hrs while shaking and then read at 420nm. Total concentrations for each sample were calculated, averaged and compared between groups.

6.3.3 Histological Analysis

Hearts were fixed in 10% formalin, paraffin embedded and serially sectioned (5μm). Basic myocardial histology and cellular infiltration were examined using heart cross-sections stained with H&E. A blinded observer quantified Infiltrating cells by counting the number of grids affected within an image of an entire heart cross section at 5x magnification (1 section per animal) based on a previously published grid-scoring method, to quantify the degree of cellular infiltration between groups (214).

6.3.4 Collagen Deposition

Collagen detection was accomplished using Sirius red and fast green stains, and quantified as previously described (214). Briefly, slides were examined under a microscope with the 10X objective and areas of collagen deposition were captured with a digital camera. Image analysis software was used to quantify the amount of tissue positive for Sirius red. Four images per sections from each individual animal were averaged and experimental groups compared to control animals.

6.3.5 Immunohistochemistry

Immunohistochemistry for CD133 (Abcam), a-smooth muscle actin (SMA; Sigma), and Ki67 (Sigma) was performed as previously described (214). Briefly, endogenous peroxidases and non-specific staining were blocked to prevent non-specific staining. Sections were incubated with the relevant antibody followed by the relevant biotin-conjugated secondary antibody (Vector, Burlington, ON, Canada). The antibody complexes were then conjugated to an Avidin-biotin complex (Vecstastain ABC kit; Vector) and developed using 3,3' diaminobenzidine as the chromogen (DAB,

DakoCytomation). Light microscopy was performed; pictures were captured and analyzed in Adobe Photoshop 5.0.

6.3.6 Relative Quantitative Polymerase Chain Reaction (qRT-PCR)

Using the TRIzol reagent (Gibco-BRL, Gaithersburg, MD), RNA was isolated from the snap frozen myocardium as per the manufacturer's protocol. First strand cDNA was synthesized from 1 μg of total RNA using iScript cDNA Synthesis Kit (Biorad. Hercules, CA).

Relative quantitative RT-PCR (qRT-PCR) was completed using 12.5 ng of input cDNA with 0.5 μM of each of the forward and reverse primers and 1x iQ SYBR Green Supermix (Bio-Rad) was subjected to qRT-PCR using iQ Multicolour Real-Time PCR Detection System thermocycler (Bio-Rad). Standard curves, for efficiency, and no-template control samples were run along with the samples during thermocycling. A melting curve was performed after thermocycling was complete to ensure target specificity. The primers were designed against the mRNA sequence of selected growth factor or cytokine and shown in table 6.1. Expression was normalized to the 18S ribosomal gene using the Pfaffl method.

6.3.7 *In Vitro* – Primary Fibroblast Isolation and Proliferation Assay

Mouse skin fibroblasts were isolated from ear clippings. Clippings were mechanically diced and enzymatically digested with Collagenase type II (1.63mg/mL in Dulbeco's modified essential media) for 30min at 37^{o}C with 5% CO_2 (Invitrogen, Burrlington ON). Isolated cells were plated on 0.1% gelatin (Sigma) coated tissue culture flasks and

allowed to grow to 80% confluence prior to use. All assays were done using isolated cells before 5 passages.

BrdU assay for assessment of relative proliferation was completed according to the manufacturer's protocol (Millipore, Billerica MA). In brief, primary fibroblasts were plated on 96-well culture plates, allowed to adhere overnight and serum starved for 24 hours prior to treatment. Cells were then treated with either saline as a control, AngII (100nM), Hydralazine (40nM) or AngII + Hydralazine for 6 hours, at which point BrdU reagent was added to the culture plate. After 24 hours from the time of treatment plates were fixed, dried and stored at 4^{o}C until analysis. Plates were then incubated with primary anti-BrdU antibody, washed, incubated with secondary biotin conjugated anti-goat antibody, washed, incubated with substrate then stopped and read at 490nm.

6.3.8 Statistical Analysis

One-way ANOVA tests were completed on all quantitative data using the Newman Keuls post-test to compare the experimental groups to the saline control. Our level of significance was set as $p \leq 0.05$. All statistical calculations were computed using GraphPad Prism 4 software.

6.4 Results

6.4.1 Model Establishment

Animals were randomly assigned to 3 experimental groups and infused with: a) AngII (2.0 μg/kg/min, n=10); b) AngII with Hydralazine (6.9 mg/kg/min; n=4); or c) saline

(control, n=10). Infusion of AngII, a known vasoconstrictor, resulted in a significant increase in mean arterial blood pressure when compared to saline control (Fig. 6.1). Co-administration of AngII with Hydralazine allowed normalization of the blood pressure to levels similar to saline control animals (Fig. 6.1A). Furthermore, hydralazine also inhibited the myocardial hypertrophic effects of AngII as AngII+hydralazine animals had a significantly lower heart wt/body wt ratio (Fig. 6.1B), which was comparable to saline controls (AngII (6.7 ± 0.3mg/g), AngII+Hydralazine (5.7 ± 0.2mg/g), Saline: (5.2 ± 0.2mg/g)). Serum levels of aldosterone were evaluated using a standard ELISA and showed that AngII and AngII+hydralazine had elevation in serum aldosterone levels when compared to saline controls though significance was not reached (Fig. 6.1C). Taken together our findings suggest that the hypertensive effects of AngII can be controlled with the anti-hypertensive hydralazine while maintaining RAS activation creating a model to look at the early cellular and molecular events occurring in these animals.

6.4.2 Myocardial Fibrosis

The degree of myocardial fibrosis in experimental animals was determined by quantifying the collagen depositions within the myocardium using heart sections stained with Sirius red as previously described (214). AngII infusion resulted in multi-focal areas of extensive collagen deposition compared to saline infused control animals ($p < 0.01$; Fig. 6.2 A,B). When Hydralazine was also infused, there was a significant reduction in collagen deposition evident within the myocardium that approached levels seen in saline control expressed as a percent surface of an area of myocardium affected ($p < 0.01$; Fig. 6.2 C,D). These findings were confirmed by showing significant transcript

up-regulation for collagen-1 in AngII animals (103.0 $\pm$ 36.2 fold) with levels returning to baseline when hydralazine was co-administered ($p<0.01$; Fig. 6.2 E).

6.4.3 Cellular Infiltration

Previous work from our laboratory has shown that myocardial fibrosis is temporally preceded by infiltration of fibroblast progenitor cells within the myocardium (214). In the present experiments, AngII exposure resulted in multi-focal areas of cellular infiltration and myocyte loss when compared to saline control (Fig. 6.3 A,B). When animals were given AngII in combination with hydralazine minimal cellular infiltration could be identified after 7d of exposure (Fig. 6.3 C). We have adapted a grid-scoring method to quantify the degree of cellular infiltration between groups confirming that significant myocardial cellular infiltration is evident in AngII exposed animals and this is inhibited by hydralazine ($p < 0.01$; Fig. 6.3D). Cells seen infiltrating the myocardium were mononuclear in appearance with no evident polymorphonuclear cells. Immunohistochemistry was used to confirm that a significant proportion of the cells seen in AngII exposed animals were $SMA^+/CD133^+$ fibrocytes as previously published (Fig 6.4) (214). In contrast, animals that received both AngII and hydralazine had minimal infiltration by $SMA^+/CD133^+$ cells. Taken together our findings confirm that myocardial fibrosis is dependent on the accumulation of $SMA^+/CD133^+$ fibrocytes prior to ECM deposition and that this observation is blood pressure dependent given that hydralazine can inhibit this response.

6.4.4 Myocardial Pro-Fibrotic Cytokine Environment

Transcript levels of a well-known pro-fibrotic factor, connective tissue growth factor (CTGF) were significantly increased after AngII exposure (7.8±0.8 fold) in the myocardium at 7d ($p=0.008$; Fig 6.5). The co-administration of AngII with Hydralazine resulted in a significant reduction in CTGF back to baseline levels seen in saline control animals (Fig 6.5). Similar findings were observed for the pro-inflammatory cytokines TNFa (4.6±0.8 fold) and IL1b (6.4±2.6 fold) in animals receiving AngII and return to baseline in animals co-administered AngII+hydralazine ($p<0.05$; Fig. 6.5).

6.4.5 Myocardial Chemokine Expression Associated with Fibrocyte Migration

To investigate factors in the environmental milieu that may be recruiting the infiltrating cells we used relative qRT-PCR to assess the transcript levels of chemotactic cytokine for fibroblast progenitor cells, CXCL12 and CCL2 (60, 219). There was a significant increase in CXCL12 mRNA (3.2±0.4 fold; $p=0.008$) expression compared to the baseline expression of the normalized housekeeping gene in the myocardium of animals exposed to AngII at 7d (Fig. 6.6). Similarly there was a significant increase in CCL2 mRNA expression in the myocardium of AngII exposed animals (3.8±1.0 fold; $p=0.015$). The addition of hydralazine resulted in complete inhibition in the up-regulation in CXCL12 and CCL2 in the myocardium to levels seen in control animals (Fig. 6.6).

6.4.6 Effect of Hydralazine at the Cellular Level

The effects of hydralazine, other than those resulting from vasodilation and blood pressure reduction were also investigated. We first looked at the induction of the transcription factor hypoxia inducible factor 1 (HIF1), which has been suggested as a

down-stream effector of hydralazine. Transcript levels, measured by qRT-PCR were significantly increased after 7d of AngII exposure (5.0±0.8 fold; p=0.016), however when hydralazine was administered in combination with AngII, the level of HIF1 were not elevated but were similar to baseline levels seen in control animals (Fig. 6.7).

Previous work by us has shown that in areas of myocardial infiltration by fibrocytes a significant number of these cells are proliferating (214). We therefore investigated the effects of hydralazine on proliferation both in-vivo and in-vitro. As previously described infiltrating $SMA^{+}/CD133^{+}$ cells were shown to have a high proliferative index as demonstrated by strong positivity for Ki67 after AngII exposure. In contrast, animals that received both AngII and hydralazine had a significant reduction in the positivity for Ki67 suggesting that hydralazine may affect proliferation of fibrocytes (Fig 6.8). To confirm these findings we used an *in vitro* assay with primary fibroblasts looking at the relative proliferation of primary fibroblast cultures as determined by BrdU incorporation. Our *in-vitro* findings suggested a significant reduction from saline (30.6%) in the relative proliferation of fibroblasts after hydralazine exposure with or without AngII (Fig. 6.8). Similar findings were obtained with MTT assay (results not shown). Taken together, hydralazine may have some effects at the cellular level, which could modulate the development of fibrosis and are independent of blood pressure reduction.

6.5 Discussion

AngII infusion models have been well described and are known to result in increased blood pressure, myocardial hypertrophy and a characteristic ECM deposition within the

myocardium typical of myocardial fibrosis (60, 88, 288). In the present mouse model used, the physiological response to AngII resulted in blood pressure elevation with the early development of myocardial hypertrophy within 7 days of exposure. Using this model we then attempted to create a situation in which RAS upregulation via AngII infusion was maintained without the resulting hypertension by the addition of hydralazine.

Hydralazine was chosen based on its anti-hypertensive properties that result in lower blood pressure in a dose dependent manner while not acting on AngII receptors (289, 290). In animals that received AngII+hydralazine, RAS upregulation was demonstrated by evidence of significant serum elevation in aldosterone levels a downstream mediator and marker of RAS activation. Our primary observation using this model was that the addition of hydralazine to AngII resulted in normalization of blood pressure and inhibition of fibrosis normally seen in animals receiving AngII. Taken together, AngII and its effects on promoting myocardial fibrosis appear at least in part blood pressure dependent.

Work from our laboratory and others have recently identified bone marrow derived fibroblast progenitor cells as the primary cells recruited to the myocardium prior to the development of fibrosis (24, 214). We were able to show minimal infiltration by $SMA^{+}/CD133^{+}$ fibrocytes in animals receiving AngII+hydralazine when compared to animals receiving AngII. These findings support a direct relationship between cell migration and the development of fibrosis. Characterizing fully the mechanism by which

AngII results in myocardial fibrosis extends well beyond the scope of this manuscript. However, using our model in which RAS up-regulation was maintained without hypertension we did explore key pathways characteristically described as potentially being involved in promoting fibrogenesis. We have chosen to look at CTGF as a pro-fibrotic cytokine based on evidence that it is produced by cardiomyocytes providing a direct mechanism by which AngII act directly on myocardium and promote a pro-fibrotic environment. AngII has been shown to increase CTGF expression within the myocardium and specifically in cardiomyocyte in-vitro (260, 264). CTGF also appears to be capable of inducing both pro-fibrotic and pro-inflammatory gene expression in cultured cardiomyocytes (291). In fact CTGF has been suggested to be the primary mediator of AngII-induced myocardial fibrosis (265). Our findings suggest that CTGF that is significantly up-regulated in AngII exposed animals was completely inhibited by the administration of hydralazine. Similar findings were observed with classically described pro-inflammatory cytokines TNFa and IL1b. While we provide no direct evidence that hydralazine inhibits the production of these cytokines we provide strong evidence of an association between early fibrocyte migration and pro-fibrotic cytokine production in the myocardium.

Interactions between chemokines and their respective receptors have emerged as key mechanisms in the directed migration of leukocytes and also fibrocytes (87, 292-295). Fibrocytes have been traditionally shown to express the chemokine receptors CCR7 and CXCR4 (208, 218, 220). Recently, Haudek et al. was able to show that CCR2 plays a critical role in regulating fibrocyte migration in a model of myocardial fibrosis (24).

Using $CCR2^{-/-}$ animals, they were able to show a significant reduction in AngII dependent fibroblast progenitor cell migration (fibrocytes) and a reduction in fibrosis. In the present manuscript we did not attempt to modulate fibrocyte migration using specific blockade of chemokines. However, our findings support previous work by others that have suggested a key role for CXCL12 and CCL2 in regulating fibrocyte migration and accumulation (24).

It is generally assumed that fibroblasts and myofibroblasts are the cells responsible for ECM deposition. As such there is a large body of literature that supports the direct effects of AngII, via the AT1 receptor that can promote fibroblast proliferation, myofibroblast differentiation and fibrosis (191-194). We provide evidence that AngII interaction with its receptor may be sufficient but not necessary to result in fibrosis. Our findings are in keeping with others that have suggested that the effects of AngII on fibrosis are blood pressure dependent (260, 289, 290). Some have even suggested that blood pressure can affect the migration of fibrocytes ($CD45^{+}/SMA^{+}$) into the myocardium but were also unable to provide a definitive mechanism (290). In contrast transgenic mice that over-express AT1a receptor and develop hypertrophy and fibrosis do so without developing hypertension emphasizing the multifactorial pathways capable of promoting ECM deposition and fibrosis (296)**.** However their findings were based on transgenic mice that have abnormal RAS regulation based on over-expression of only the AT1 receptor. Data from spontaneously hypertensive models suggest that hydralazine was unable to inhibit fully the development of fibrosis but these findings can be explained by mechanisms independent of RAS activation (297).

In contrast to our findings in the present manuscript, there are examples in the literature where a reduction in blood pressure to normo-tensive levels did not abrogate organ damage, suggesting that fibrosis may under certain circumstances be blood pressure independent (297, 298). However, some of these studies had other important differences that one should take into consideration, such as the presence of metabolic syndrome using genetically mutated mouse, where obesity, dietary supplementation, glucose intolerance and hyperinsulinemia likely contributed to end organ damage (297). The same can be said for a model combining aldosterone administration, uninephrectomy and a high salt diet, in which increased load on the remaining kidney likely contributed to organ damage (298). Furthermore, hydralazine has traditionally been administered in the drinking water, whereas in the current study we have used a more direct administration of hydralazine through an osmotic mini-pump, providing a constant dosage over time (298, 299). While not tested, our approach may have resulted in a potentially higher effective dose as the drug is delivered more directly to the circulation.

Some experimental studies have shown a beneficial effect of mineralocorticoid antagonist in reducing myocardial fibrosis that was suggested to be independent of blood pressure effects. These have been explained by reductions in myocardial oxidative stress suggesting that oxidative stress may be the common pathway by which AngII activation and hypertension can lead to myocardial fibrosis (300, 301). While we did not specifically look at oxidative stress, our findings would suggest that aldosterone up-regulation may not be sufficient to result in fibrosis given the absence of fibrosis in

AngII+hydralazine animals who did have increased levels of aldosterone in their serum. Finally one needs to consider mechanisms of action of hydralazine other than its anti-hypertensive effects that may have resulted in its beneficial role in reducing fibrosis. One of these mechanism has recently been suggested in which hydralazine may be able to induce hypoxia-inducible factor-1 (HIF-1) which in turn can effect multiple genes as a transcription factor that mediates adaptive responses in response to injury such as ischemia (302, 303). Our findings support a significant up-regulation of HIF-1 with AngII exposure, however when co-administered with hydralazine there was a return of HIF-1 to baseline levels. Using our data it is not possible to conclude that hydralazine is any direct effect on HIF-1. We can only conclude that in animals without hypertension or myocardial histologic changes that are receiving AngII + hydralazine there appears to be no significant up-regulation in the mRNA of HIF-1.

In the present manuscript we attempted to separate RAS activation from hypertension in trying to identify potential mechanisms for the development of myocardial fibrosis. The reason for this is that the downstream effects of RAS activation leading to myocardial fibrosis are not fully characterized. Clinical trial published to date using RAS blocking agents, such as angiotensin receptor blockers and angiotensin converting enzyme inhibitors, have established a clear benefit for patients with significant reductions in the number of adverse cardiac events (11, 186). This is in contrast to clinical studies that have used hydralazine and achieved similar reduction in blood pressure, but failed to offer the same clinical benefit as RAS inhibition (304-306). In the present manuscript we provide no explanation for this discrepancy. Taken together, this would suggest that

blood pressure reduction might not be the sole factor influencing myocardial events such as fibrosis. Data obtained in the present study would support the notion that while fibrosis appears in part dependent on blood pressure elevation, the anti-fibrotic properties of hydralazine may extend beyond its anti-hypertensive effects. We observed a reduction in fibrocytes or fibroblast proliferation in response to hydralazine both *in vivo* and *in vitro*. Although discerning the cellular mechanism responsible for this anti-proliferative response is beyond the scope of this manuscript, this suggests that regulation other than the vasodilator effects of hydralazine should be considered.

In summary, we provide evidence that the effects of AngII on the development of myocardial fibrosis, appears to be at least in part blood pressure dependent. While we also provide evidence that blood pressure elevation seems necessary for early fibrocyte migration and the development of a pro-fibrotic environment the mechanisms for this is unclear at present.

6.6 Acknowledgements

The present work was supported in part by a grant from the Nova Scotia Health Research Foundation (#42311) and the Canadian Institute of Health Research (#44122).

Table 6.1 Primer Sequences of Target Genes

Gene Symbol	Forward Primer	Reverse Primer
CCL2	CCAGCCAACTCTCACTGAAGC	AGCTCTCCAGCCTACTCATTGG
Col1a1	GTGGAGGGAGTTTACACGAAGC	GTGGAGGGAGTTTACACGAAGC
CTGF	TCAACCTCAGACACTGGTTTCG	TAGAGCAGGTCTGTCTGCAAGC
CXCL12	GTAGAATGGAGCCAGACCATCC	ATTCGATCAGAGCCCATAGAGC
IL1β	TCCTCGGCCAAGACAGGTCGCT	CCCCCACACGTTGACAGCTAGGT
TNFα	TCTCATGCACCACCATCAAGGACT	ACCACTCTCCCTTTGCAGAACTCA
HIF-1	AACAGTCCCTCTGTAGTTGTGG	TAGCGACAAAGTGCATAAAACC
18S	TCAACTTTCGATGGTAGTCGCCGT	TCCTTGGATGTGGTAGCCGTTTCT

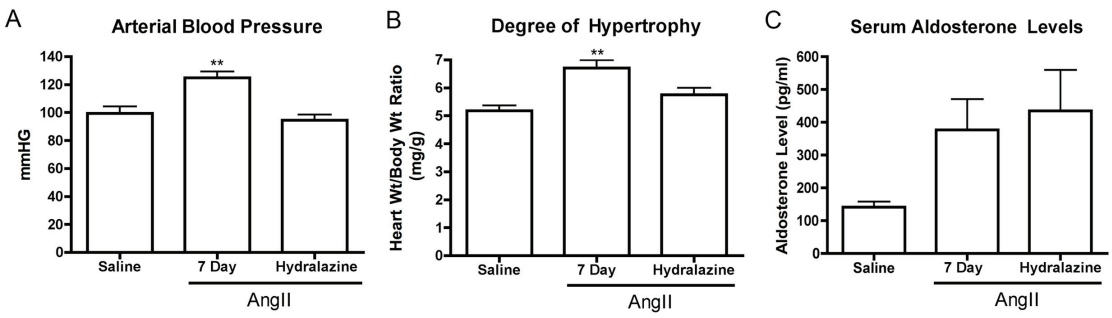

Figure 6.1 Establishing the Model

Hemodynamic measurements were taken via tail cuff (7d) and compared between groups with systolic blood pressure findings shown as mean±SD (A). Cardiac mass index was expressed as heart weight/body weight ratio at 7d (B). Serum levels at 7d of aldosterone were measured by ELISA and expressed as pg/ml (C). **$p<0.01$.

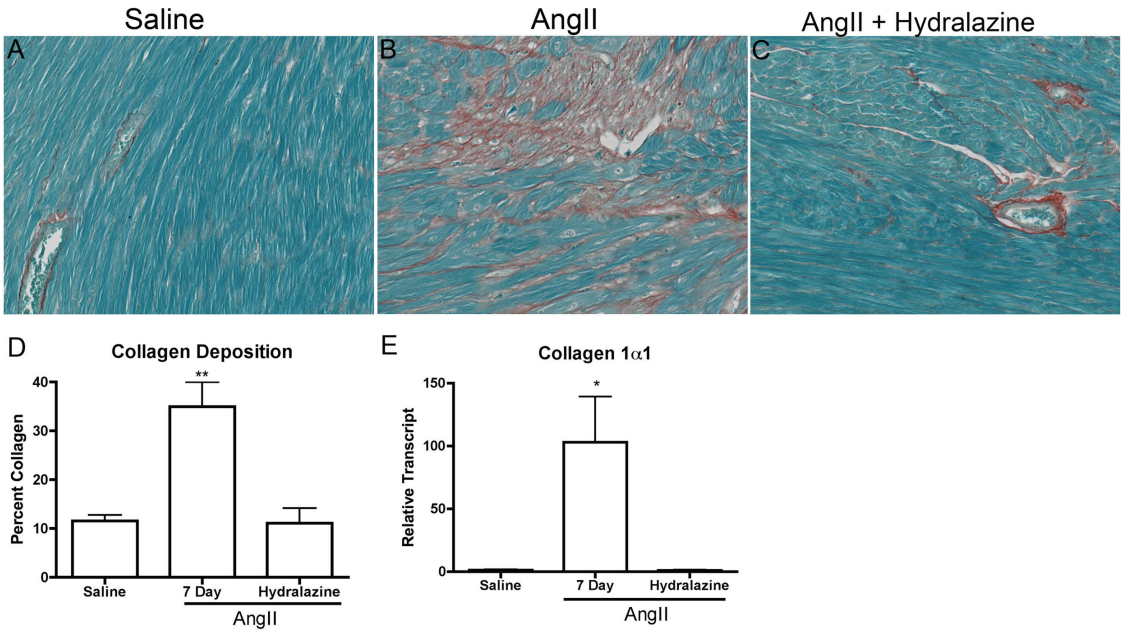

Figure 6.2 Myocardial Fibrosis

Collagen deposition in heart sections from experimental groups was assessed using a standardized Sirius red and fast green stain. Representative sections are shown from control animals (A), 7d AngII exposed animals (B), and 7d AngII+hydralazine exposed animals (C). Collagen in the heart sections was quantified using image analysis software and expressed as the percent area affected (D). Collagen deposition was also quantified using whole heart extracts and processed for qRT-PCR for the pro-Collagen-1 (E). Images were captured at 25X. **$p<0.01$, *$p<0.05$.

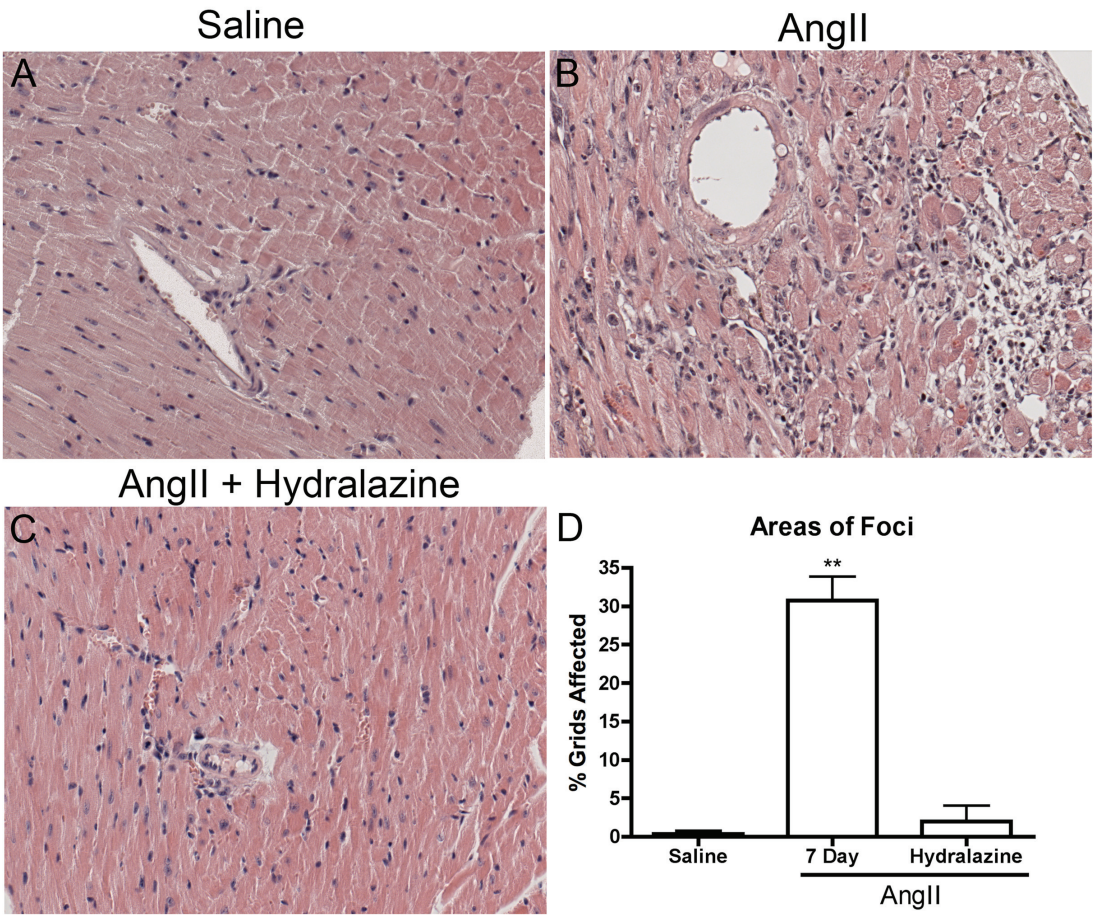

Figure 6.3 Cellular Infiltration

Hearts stained with H&E from control animals receiving saline (A), AngII for 7d (B) or AngII+hydralazine for 7d (C). Quantification of infiltrating cells was performed using a modified grid analysis technique comparing the number of grids affected from a representative cross section of the myocardium (heart) taken at low power (5x magnification) from each group (D). Images were captured at 25X. **p<0.01.

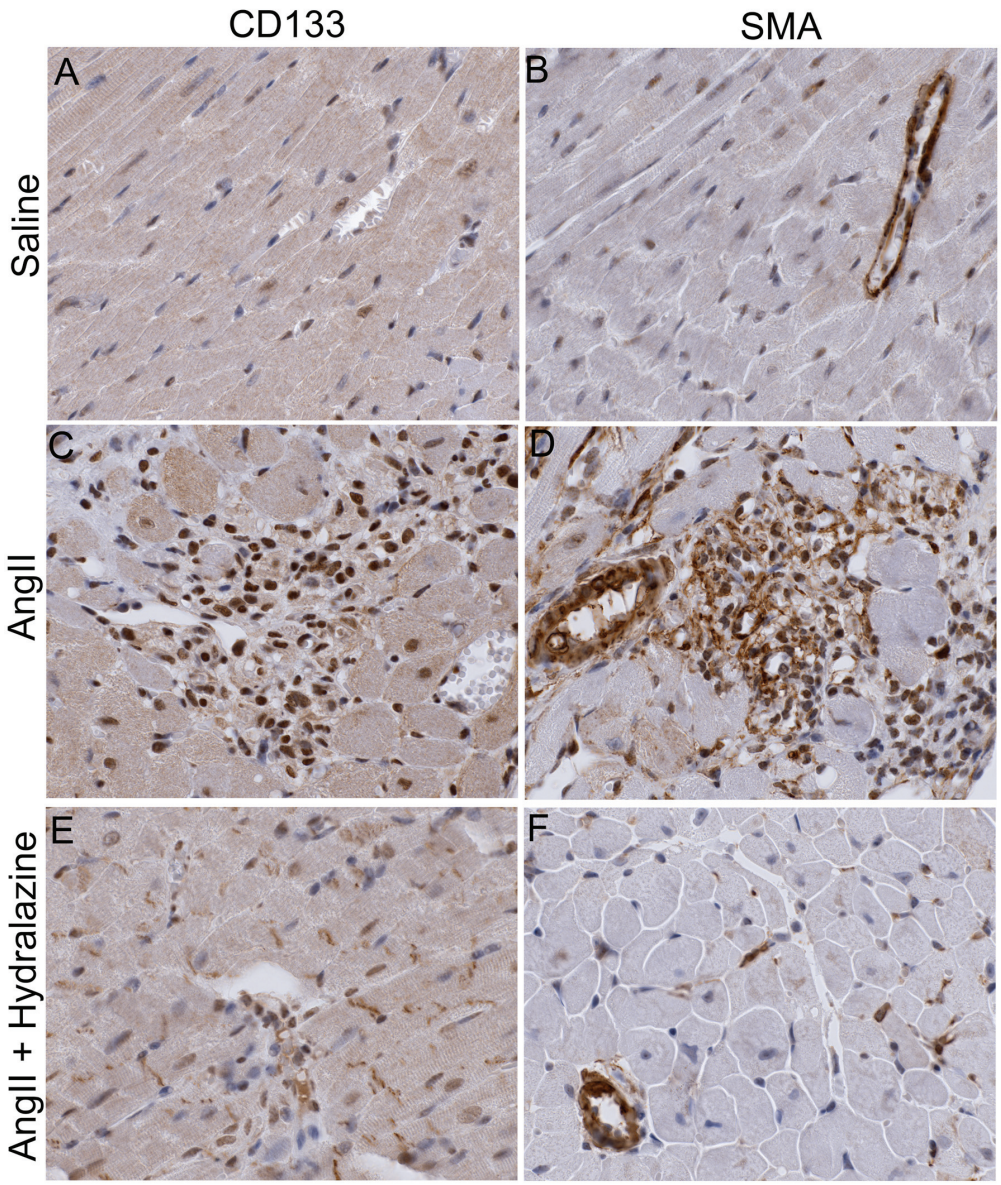

Figure 6.4 Immunohistochemistry Staining

Immunohistochemistry for CD133 (A, C, E) and SMA (B, D, F) was used to identify positive cellular infiltrate in heart sections. Representative sections from control animals receiving saline (A, B), AngII for 7d (C, D) and AngII+hydralazine for 7d (E, F) are shown. Images were captured at 63X.

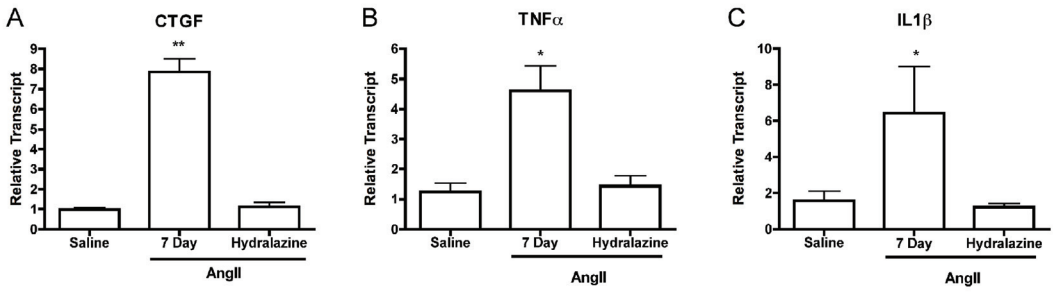

Figure 6.5 Pro-Fibrotic Micro-Environment

qRT-PCR was used to assess myocardial expression for CTGF (A), TNFa (B) and IL-1b (C) transcript levels relative to housekeeping gene. **p<0.01, *p<0.05.

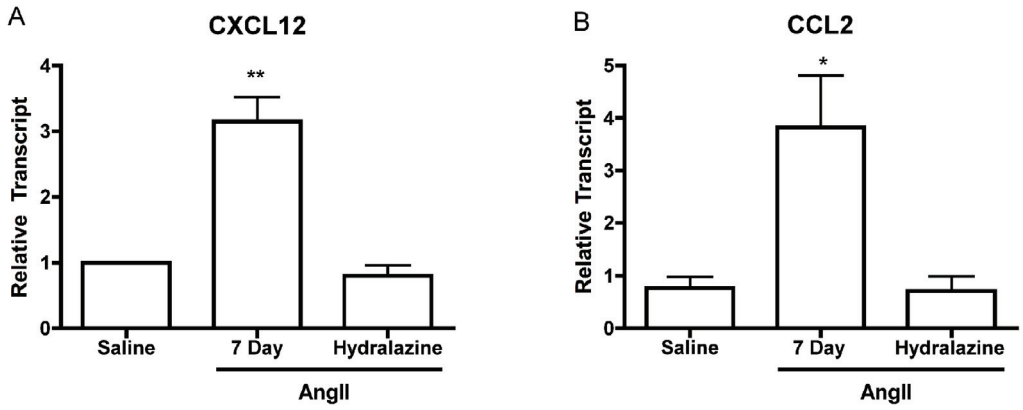

Figure 6.6 Chemokine Expression

qRT-PCR was used to assess myocardial expression of CXCL12 (A) and CCL2 (B) transcript levels relative to housekeeping gene (E). **p<0.01, *p<0.05.

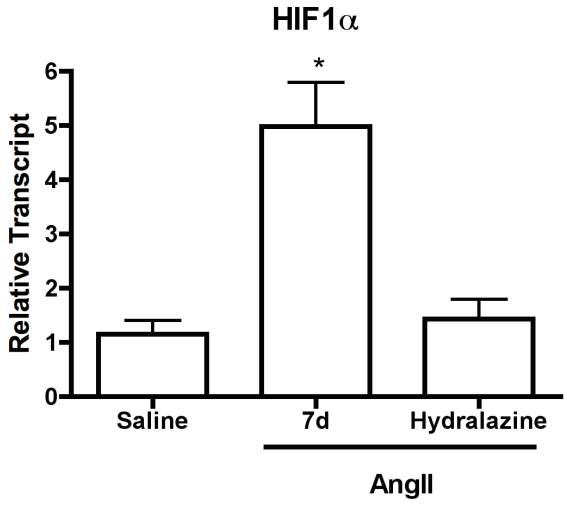

Figure 6.7 Transcription Factor Expression

qRT-PCR was used to assess myocardial expression of HIF-1 transcript level relative to housekeeping gene. *$p<0.05$.

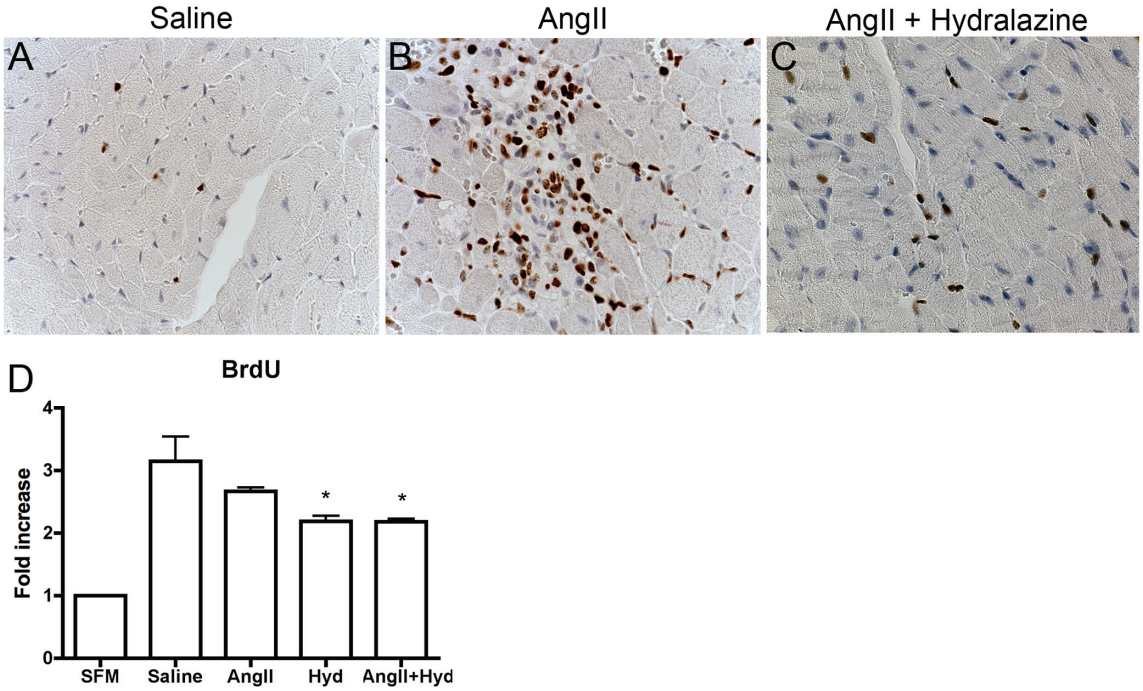

Figure 6.8 Cellular Effects of Hydralazine

Immunohistochemistry for Ki67 was used to illustrate the proliferative index of infiltrating fibrocytes. Representative sections from animals receiving saline (A), AngII (B) or AngII + Hyd (C) are shown. Images were captured at 63x. The BrdU assay for proliferation was used on primarily isolated fibroblasts after exposure to; Saline, AngII, Hydralazine (Hyd), or AngII + Hyd (D). Relative proliferation was expressed as fold increase compared to serum free media (SFM). *$p<0.05$.

CHAPTER 7

TREATMENT WITH ACTIVATED PROTEIN C (APC) IS PROTECTIVE DURING THE DEVELOPMENT OF MYOCARDIAL FIBROSIS

MJ Sopel*, NL Rosin, A Falkenham**, TL Mycrs **, M Bezuhly**, CT Exmon**, TDG Lee, RS Liwski, JF Légaré**

Submitted to Cardiovascular Research, March 30th, 2012 – Rejected May 2012

Resubmitted to PLoS One, June 5th, 2012

In revision – July 10th, 2012

* Author contributions are clearly outlined in Appendix 2.

7.1 Abstract

Introduction: Myocardial fibrosis contributes to the development of heart failure. Activated Protein C (aPC) is a circulating anticoagulant with anti-inflammatory and cytoprotective properties. Using a model of myocardial fibrosis second to Angiotensin II (AngII) infusion, we investigated the novel therapeutic function aPC in the development of fibrosis. *Methods and Results:* C57Bl/6 and Tie2-EPCR mice were infused with AngII (2.0μg/kg/min), AngII and aPC (0.4μg/kg/min) or saline for 3d. Hearts were harvested and processed for analysis or used for cellular isolation. Basic histology and collagen deposition were assessed using histologic stains. Transcript levels of molecular mediators were analyzed by quantitative RT-PCR. Mice infused with AngII exhibited multifocal areas of myocardial cellular infiltration associated with significant collagen deposition compared to saline control animals ($p<0.01$). AngII-aPC infusion inhibited this cellular infiltration and the corresponding collagen deposition. AngII-aPC infusion also inhibited significant expression of the pro-fibrotic cytokines TGF-β1, CTGF and PDGF found in AngII only infused animals ($p<0.05$). aPC signals through its receptor, EPCR. Using Tie2-EPCR animals, where endothelial cells over-express EPCR and exhibit enhanced aPC-EPCR signaling, no significant reduction in cellular infiltration or fibrosis was evident with AngII infusion suggesting aPC-mediate protection is endothelial cell independent. Isolated infiltrating cells expressed significant EPCR transcripts suggesting a direct effect on infiltrating cells. *Conclusions:* This data indicates that aPC treatment abrogates the fibrogenic response to AngII. aPC does not appear to confer protection by stimulating the endothelium but by acting directly on the infiltrating cells, potentially inhibiting migration or activation.

7.2 Introduction

Myocardial fibrosis is a common sequelae associated with many cardiovascular diseases and is characterized by the accumulation of excess extracellular (ECM) proteins within the myocardial tissues (5). While initially the ECM deposition occurs in response to injury and is beneficial, it can become pathologic (5). The lack of regression in this ECM deposition in the tissue is the hallmark of myocardial fibrosis that ultimately results in irreversible organ failure (5). Current pharmacological agents used to treat cardiovascular disease do not abrogate or reverse myocardial fibrosis (307).

The etiology of myocardial fibrosis is multifactorial. It is associated with cellular and structural changes including the recruitment/proliferation of effector cells, apoptosis of myocytes and the accumulation and rearrangement of structural fibers (5, 214, 308). Using the well-established AngII infusion model of myocardial fibrosis, we have previously investigated the early events in this process (214, 228). Infusion of AngII in this model results in rapid infiltration of fibroblast progenitor cells, termed fibrocytes. Fibrocytes, which are a progenitor cell type originating from an early monocyte lineage, can produce both pro-inflammatory mediators as well as pro-fibrotic factors (24, 214, 228). They are believed to be capable of bridging an initial inflammatory response to a later corresponding fibrotic response (221, 222). Fibrocyte infiltration is followed by a loss of functional myocytes and an accumulation of extracellular matrix proteins within the myocardial tissue resulting in the development of myocardial fibrosis (24, 214, 308).

In a mouse model of bleomycin induced lung fibrosis, where fibrocytes have been shown to be a key effector cell, administration of activated Protein C (aPC) decreased cellular infiltration and reduced tissue fibrosis (196, 309). aPC is a serine protease that acts as a naturally produced anticoagulant by cleaving Factor Va and VIIIa, which inhibits thrombin formation (310). Recently, aPC has been shown to have anti-inflammatory and cytoprotective activities as well (311-313). The administration of aPC confers protection against sepsis and ischemia/reperfusion injury in kidney, skeletal muscle, skin grafts and myocardium (311, 313-318). These protective effects are believed to be due to the decreased vascular expression of cellular adhesion molecules; downregulation of pro-inflammatory mediator expression; the improvement of microvascular circulation and endothelial barrier function; and upregulation of survival signaling pathways (130, 319-322). aPC also appears to have direct beneficial effects on the myocardium such that individuals with a genetic defect within the aPC signaling pathway have an increased risk of cardiovascular events including myocardial infarcts (323, 324). However, the benefits of aPC have yet to be tested in models of myocardial fibrosis in the absence of ischemia reperfusion.

These data suggested to us that aPC administration might modulate the myocardial response to elevated circulating AngII and potentially confer protection against the development of fibrosis secondary to AngII exposure.

7.3 Materials and Methods

7.3.1 Animals

All work was performed in accordance with the Canadian Council on Animal Care and was approved by Dalhousie University's University Committee on Laboratory Animals (REB #2007-1534). Male C57BL/6 (Jackson Laboratory; Bar Harbour, ME) and Tie2-EPCR (generously provided by Dr. Charles Esmon, University of Oklahoma Health Science Centre, OK) mice ranging from 8-9wk old. Mice were provided food and water *ad libitum* for at least 1wk prior to experimentation. Animals were anesthetized with isoflurane (Baxter Healthcare Corp., New Providence, NJ) in oxygen delivered by a Fortec vaporizer. When surgical levels of anesthesia were reached a 1-2cm mid-scapular skin incision was made and a mini osmotic pump (Alzet, Palo Alto, CA) was inserted subcutaneously. The incision was closed using 7mm wound clips. Animals were randomly assigned to receive AngII (2.0 μg/kg/min, Sigma Aldrich, Oakville ON), AngII and aPC (0.4μg/kg/min, Sigma Aldrich), AngII and Heparin (200U/kg bolus injection at initiation and 70U/kg/hr, MedXL, Montreal, QC) or a vehicle control of saline. The pumps remained in for 3d during which the animals were provided with food and water *ad libitum* and observed for signs of morbidity. Prior to euthanization, blood pressure measurements were taken via the Coda2 non-invasive cuff system (Kent Scientific, Torrington, CT) for a minimum of 5 consecutive measurements per animal. Animals were then anesthetized with isoflurane again and animals were sacrificed via exsanguination. Hearts were harvested and processed for cellular isolation or histologic and molecular analysis. Hearts intended for histologic and molecular analysis were divided along the short axis into 3 portions including the base, middle and apical sections.

The base portion was processed for histological examination while the other two portions were snap frozen immediately for molecular analysis. Due to overlapping experimental groups previously published (214), some historical samples from AngII and saline infused animals were used for this study to compare to new experimental groups. Additional animals were added to saline and AngII experimental groups to ensure experimental reproducibility.

7.3.2 Cellular Isolation and Culture

Infiltrating cells were isolated from excised heart of AngII infused animals as previously stated (214). Cellular isolates were incubated at 37°C with 5% CO_2 for 3d, after which all non-adherent cellular debris was removed and fresh media was supplied for an additional day. Cells were washed with sterile PBS and fixed for histologic staining or lysed using TRIzol (Gibco). Coverslips were stored at 4°C until stained and lysed samples were stored at 80°C until RNA isolation could be completed.

7.3.3 Histologic Analysis

Hearts were fixed in 10% formalin, paraffin embedded and serially sectioned (5μm). Basic myocardial histology and cellular infiltration were examined using heart cross-sections stained with H&E. A blinded observer quantified infiltrating cells by counting mononuclear cells evident in between myocytes and around vessels in 5 fields of view at 25x magnification per animal.

7.3.4 Collagen Deposition

Collagen detection was accomplished using Sirius red and fast green stains. Images of entire cross-sections of myocardium where compiled from images taken at 5X

magnification. Using Adobe Photoshop CS5, red pixels were positively selected and summed for a total number of red (collagen) pixels. Subsequently, all non-background pixels were summed for a total number of heart pixels. The total collagen pixels were divided by the total heart pixels to provide a semi-quantitative measurement of the percent of the heart affected by fibrosis. To avoid measuring discrepancies between staining, the same red colour palette was used to select red pixels.

7.3.5 TUNEL

Apoptosis was detected on 5μm paraffin embedded heart sections using a commercially available terminal deoxynucleotide transferase-mediated dUTP nick-end labeling (TUNEL) assay (Chemicon, Billerica, MA). Assay was completed as per manufacturers instructions. Five images from a heart section from each animal were viewed with the 25X objective. An observer blinded to the treatment group counted the number of TUNEL positive cells in each image, and the mean number of cells per image for each experimental group was compared to the control group.

7.3.6 Immunofluorescence Staining

Isolated cells were grown on coverslips and then fixed in 4% paraformaldahyde, permeabilized with 0.03% Triton X-100, blocked against non-specific antibody binding with 10% normal goat serum and stained for CD45 (BD Biosciences, Mississauga, ON) and Collagen type 1 (Rockland Inc, Gilbertsville, PA). Antibodies were detected using anti-host specific Alexa fluorescently labeled secondary antibodies (Invitrogen).

7.3.7 RNA Isolation and cDNA Synthesis

Using the TRIzol reagent (Gibco), RNA was isolated from the snap frozen myocardium as per the manufacturer's protocol. First strand cDNA was synthesized from 1 μg of total RNA using iScript cDNA Synthesis Kit (Biorad. Hercules, CA).

7.3.8 Conventional Reverse Transcription-Polymerase Chain Reaction (RT-PCR)

Conventional RT-PCR was completed using 12.5ng of input cDNA with 0.5μM of each of the forward and reverse primers and 10uL of REDExtract-N-Amp PCR Ready Mix (Sigma) that was subjected to conventional RT-PCR using an iCycler (BioRad). Experimental samples were run along with a sample containing no template cDNA to ensure reagents were contamination free. All samples were run on a 1% agarose gel and were visualized using ethidium bromide and UV imaging conducted using an AlphaImager (Alpha Innotech, San Leanardo, CA). An image of PCR products was produced for analysis. The primers were designed against the mRNA sequence of endothelial protein C receptor (EPCR) (forward: 5'-GCCCTTTGTAACTCCGATGG-3'; reverse: 5'-GGAGGATGGTGACGTTTTGG-3'); and 18S ribosomal RNA (forward: 5'-TCAACTTTCGATGGTAGTCGCCGT-3'; reverse: 5'-TCCTTGGATGTGGTAGCCGTTTCT-3')

7.3.9 Relative Quantitative RT-PCR

Relative quantitative RT-PCR (qRT-PCR) was completed using 12.5ng of input cDNA with 0.5μM of each of the forward and reverse primers and 1x iQ SYBR Green Supermix (Bio-Rad) was subjected to qRT-PCR using an iQ Multicolour Real-Time PCR Detection System thermocycler (Bio-Rad). Standard curves, for efficiency, and no-template control

samples were run along with the samples during thermocycling. A melting curve was performed after thermocycling was complete to ensure target specificity. The primers were designed against the mRNA sequence of connective tissue growth factor (CTGF) (forward: 5'-TCAACCTCAGACACTGGTTTCG-3'; reverse: 5'-TAGAGCAGGTCTGTCTGCAAGC-3'); transforming growth factor β1 (TGF-β1) (forward: 5'-GGTCTCCCAAGGAAAGGTAGG-3'; reverse: 5'-CTCTTGAGTCCCTCGCATCC-3'), platelet derived growth factor (PDGF) (forward: 5'-TTAAGGACTTGACCCTGCTTCC-3'; reverse: 5'-GCATCTGCCTGAAGTGTGTACC-3'); collagen 1α1 (forward: 5'-CAACAGTCGCTTCACCTACAGC-3'; reverse: 5'-GTGGAGGGAGTTTACACGAAGC-3'); B-cell lymphoma 2 (Bcl-2) (forward: CCAGCGTGTGTGTGCAAGTGTAAA-3'; reverse: 5'-ACACTCCGGCTTCACTGAGAATGT-3'); Bcl-2 associated X protein (Bax) (forward: 5'-tggttgccctcttctactttgc-3'; reverse: 5'-CATCTTCTTCCAGATGGTGAGC-3'); and 18S, as stated above. Expression was normalization to the 18S ribosomal gene using the Pfaffl method.

7.3.10 Statistical Analysis

One-way ANOVA tests were completed on all quantitative data using the Bonferonni post-test to compare the all the experimental groups in multi-treatment experiments. A students T-test was used to compare an experimental group to a control group if there was only one experimental group. Our level of significance was set as $p \leq 0.05$. All statistical calculations were computed using GraphPad Prism 4 software.

7.4 Results

7.4.1 Hemodynamic Measurements

To assess the impact of aPC treatment in a model of myocardial fibrosis secondary to AngII infusion, we assigned animals to 3 experimental groups. Animals were infused with: a) AngII (2.0 μg/kg/min, n=11); b) AngII with aPC (0.4 μg/kg/min; n=6); or c) saline (control, n=12). Infusion of AngII, a known vasoconstrictor, resulted in a significant increase in mean arterial blood pressure when compared to saline control (126.2±3.5 mmHg and 99.3±5.1mmHg respectively; $p < 0.01$; Fig. S7.1). Co-administration of AngII with aPC did not prevent the increase in blood pressure (115.7±5.8; $p < 0.05$; Fig. S7.1).

7.4.2 Cellular Infiltration

Myocardial fibrosis is associated with a significant cellular component which we assessed using H&E stained myocardial cross-sections from each of our experimental groups. While normal myocardial histology was observed in saline controls, cellular infiltration was evident within the myocardial tissue from AngII infused animals (Fig 7.1A, B). Little cellular infiltration was found in the myocardium of AngII-aPC infused animals, which appeared similar to saline controls (Fig. 7.1C). This observation was confirmed by quantification of cellular infiltration that indicated significant cellular infiltration in AngII infused animals compared to controls (63.1±9.7cells/field of view (FOV) and 3.3±1.9cells/FOV; $p < 0.05$; Fig. 7.1D). No significant cellular infiltration was detected in AngII-aPC treated animals when compared to saline control (14.48±5.8cells/FOV; Fig. 7.1D).

7.4.3 Myocardial Fibrosis

To assess whether the cellular infiltration was accompanied by fibrosis, the degree of myocardial fibrosis in experimental animals was determined by staining myocardial cross-sections with Sirius red. Excess collagen (red) deposition, beyond levels seen in saline controls, was evident within multi-focal areas of the myocardium from AngII infused animals (Fig. 7.2A,B). However, Collagen levels in AngII-aPC infused animals appeared similar to saline controls (Fig. 7.2C). Quantification of collagen validated our observation of significant collagen deposition in AngII infused animals, which was significantly inhibited by the coadministration of aPC (saline: 5.7±1.7%; AngII:16.5±2.2%; AngII-aPC: 5.2±1.1%; $p < 0.01$, Fig. 7.2D). Transcript levels of pro-collagen1α1, assessed by qRT-PCR, appeared decreased in AngII-aPC infused animals compared to animals infused with AngII alone, however, statistical significance was not reached (Fig 7.2E). Taken together, aPC treatment inhibited AngII-induced collagen production and deposition.

7.4.4 Pro-Fibrotic Factors

The transcript levels of well-known fibrotic factors were assessed by qRT-PCR to determine if their expression levels were altered by aPC treatment in this fibrotic model. We assessed TGF-β1, CTGF and PDGF transcript levels because they have previously been shown to be increased in response to AngII infusion and are believed to promote the initiation and progression of fibrosis (214, 325). All three pro-fibrotic factors where significantly increased in AngII infused animals (TGF-β1: 4.7±0.3 fold; CTGF: 13.8±4.0 fold; PDGF: 6.3±1.8 fold) but not when aPC was infused with AngII (Fig. 7.3). In fact,

both CTGF and PDGF levels were measured at control levels when aPC was co-infused suggesting that aPC can abrogate AngII mediated upregulation of pro-fibrotic factors.

7.4.5 The Effect of aPC on the Endothelium

aPC is believed to mediate many of its anti-inflammatory and cytoprotective effects by engagement of EPCR on the endothelium, which inhibits endothelial cell activation and promotes endothelial barrier function (130, 319, 326). To evaluate the role of the endothelium in aPC-mediated inhibition of AngII induced myocardial fibrosis, Tie2-EPCR transgenic mice that overexpress EPCR on endothelial cells, were used. These animals have been previously shown to have decreased expression of cellular adhesion molecules on the endothelium (23, 322). These mice have been shown to be significantly resistance to endotoxin-induced death as well as cancer metastasis (23, 322). Interestingly, AngII-treated Tie2-EPCR mice developed significant myocardial cellular infiltration as well as collagen deposition when compared to wild type, saline treated animals (Fig. 7.4A). Taken together, this data suggests that aPC does not appear to elicit its protective effects on the myocardium (fibrosis reduction) via activation of the EPCR on the endothelium. In support of our observation in Tie2-EPCR mice, we showed no statistically significant effects of aPC stimulation in wild type mice on the expression levels of the cellular adhesion molecules, P-selectin, E-selectin and ICAM-1, within our experimental groups (Fig 7.4B). These adhesion molecules are normally expressed on endothelial cells and are used as markers of activation.

7.4.6 Apoptosis

aPC is known to have cytoprotective properties that arise from its inhibition of apoptotic signaling pathways (320). We quantified the extent of cell death by apoptosis between experimental groups using a TUNEL stain. We did not find a significant number of TUNEL positive cells within the myocardium of AngII infused animals when compared to saline control (data not shown). We then assessed the transcript levels of the pro-survival molecule, Bcl-2, and the pro-apoptosis molecule, Bax, to determine if the ratio of these two apoptosis regulators deviated from that of our saline controls. We found no significant differences in the Bcl-2/Bax ratio in any of our experimental groups (Fig. 7.5A). This data suggests that apoptosis is not a significant contributor to the fibrotic process at this time point and therefore, aPCs cytoprotective effects do not appear to play a significant role in the initial stages of myocardial fibrosis.

7.4.7 Effects of Angicoagulation on Fibrosis Development

aPC is best known for its role in the coagulation pathway where it inhibits the production of thrombin by cleaving upstream mediators required for its generation, promoting anticoagulation (310). To determine if the beneficial effect of aPC on fibrosis development in our experiments resulted from anticoagulant activities we co-infused AngII with heparin (n=3), an anticoagulant which also reduces thrombin levels (327). In animals infused with AngII and heparin, significant cellular infiltration and fibrosis were still evident, suggesting that the anticoagulant activities of aPC are likely not responsible for inhibiting the development of myocardial fibrosis (Fig. 7.5B).

7.4.8 EPCR Expression on Infiltrating Cells

EPCR expression has been found on several subsets of circulating leukocytes and as such, these cells are also capable of responding to elevated circulating aPC (328, 329). With a lack of benefit seen with AngII infusion in Tie2-EPCR mice, we don't believe the endothelial cells are the main cell type conferring protection against AngII-mediated fibrosis. As such, we wanted to investigate if fibrocytes, a circulating leukocyte, express EPCR and are capable of responding to aPC stimulation. Infiltrating fibrocytes were isolated out of the hearts of 3d AngII infused animals as previously described (214). After 3 days in culture, immunofluorescence for CD45 and collagen 1 expression was used to elucidate their phenotype. Approximately 50% of isolated cells were $CD45^{+}$/$Collagen^{+}$, indicative of a fibrocyte rich population (Fig. 7.6A). We also assessed the expression level of EPCR on isolated infiltrating cells via conventional RT-PCR to determine if they may directly respond to increased circulating aPC levels. We found substantial levels of EPCR transcripts within isolated cells (FC) as well as our control native myocardium (HRT; Fig. 7.6). This data confirms that these cells do express EPCR and could be directly affected by increased levels of circulating aPC.

7.5 Discussion

Initially known as a vasoconstrictor, AngII has more recently been shown to be a pro-fibrotic molecule. It is involved in the development of myocardial fibrosis both clinically and in animal models (5, 24, 214). AngII infusion in mice has therefore become a well-established model used to study myocardial fibrosis. Using this model we have previously demonstrated that AngII results in significant early cellular infiltration (1d) by fibroblasts progenitor cells (fibrocytes) followed by corresponding deposition of

extracellular matrix proteins by 3d (214, 228). We, and others, have therefore been able to use this model of fibrosis to study early mediators of the fibrotic process in an effort to identify potential interventions.

In this study we demonstrate that aPC protects against the development of myocardial fibrosis secondary to AngII exposure. We provide novel evidence that aPC inhibits the previously described fibrocyte accumulation followed by collagen deposition seen with AngII infusion. Furthermore, we show a corresponding inhibition of expression of pro-fibrotic mediators, specifically TGF-β1, CTGF and PDGF, with aPC treatment. While aPC appears to counteract the pro-fibrotic effects of AngII, the animals that received AngII and aPC were still hypertensive, suggesting that the beneficial effects of aPC are blood pressure independent. Our findings support previous work demonstrating that aPC administration during a myocardial ischemic insult results in reduced scarring and improved function, though the mechanisms by which this occurs have not been elucidated (317, 321).

We have previously established that fibrosis is temporally preceded by myocardial infiltration of fibrocytes, that are likely responsible for the development of fibrosis (214). Work by others has demonstrated a link between fibrocyte accumulation and fibrosis by using strategies that reduced fibrocyte migration and consequently decreased fibrosis (24, 219). In our model of myocardial fibrosis, administration of aPC blocked fibrocyte infiltration normally associated with AngII exposure. This inhibition in cellular recruitment does not appear to be in response to decreased expression of cellular

adhesion molecules normally expressed on endothelial cells. We were unable to show any significant differences in mRNA expression levels for P-selectin, E-selectin or ICAM in heart homogenates of the different experimental groups. It is possible that an increase in transcript levels of cellular adhesion molecules may have been masked by a dilution of their specific transcript levels in the endothelium by the overwhelming amount of transcripts from other cell types within the myocardium.

We sought to isolate the effects of aPC on the endothelium, as endothelial cells represent the point of entry for circulating fibrocytes into the myocardium. We used Tie2-EPCR mice, which over express the EPCR on the endothelium, creating an animal in which there is increased endogenous aPC-EPCR signaling. However, Tie2-EPCR mice that received exogenous AngII still developed significant cellular infiltration and corresponding fibrosis within the myocardium. Taken together, our data suggests that the mechanisms responsible for aPCs anti-fibrotic effects do not appear to be mediated through EPCR signaling on endothelium.

A mechanism by which aPC might be cardioprotecitve may relate to its cytoprotective and anti-apoptotic signaling capabilities. In the present study we were unable to demonstrate significant apoptosis within the myocardium of AngII infused animals by TUNEL staining and we could not show a difference in the ratio of pro-survival and pro-apoptosis mediators, Bcl-2/Bax, in animals that received AngII+aPC. While this data does not rule out a cytoprotective effect of aPC within this model at a different time

point, it did not appear to be the key mechanism by which aPC confers its initial anti-fibrotic effects.

Though there is little evidence that the protective effects of aPC are mediated by its anticoagulative properties, there is some evidence suggesting that anticoagulation can be protective in hypertension (330). To address this limitation we infused mice with AngII along with an alternative anticoagulant, heparin. We found that AngII infused mice that also received heparin showed similar cellular infiltration and fibrotic sequelae as those that receive AngII alone. Our findings indicate that the anticoagulant properties of aPC are an unlikely mechanism providing its protection effects.

Though this study shows that aPC administration is effective in counteracting the fibrotic effects that occur secondary to AngII infusion, it does not appear to be mediated by the classic signaling effects of systemic aPC administration. Our findings suggest that aPC had no effect on endothelial cells, did not reduce apoptosis and that its effects were not dependent on its anticoagulation properties. The beneficial effects of aPC seemed to be mediated by a reduction in cellular infiltration and a reduction in myocardial pro-fibrotic mediator production (CTGF, PDGF and TGF-β1). It is likely that aPC is mediating these effects by directly stimulating a cell type other than endothelial cells that is involved in the development of myocardial fibrosis. EPCR expression has been found in monocytes, the lineage from which fibrocytes originate, and myofibroblasts, the phenotype that fibrocytes differentiate into (331, 332). We provide novel evidence suggesting that fibrocytes themselves express EPCR and could directly respond to aPC. Interestingly,

aPC has been shown to directly inhibit monocyte activation and migration in the presence of potent stimulators, including TNFα and CCL2, respectively (328, 333). It is therefore possible that systemic administration of aPC may have a direct and similar effect on circulating fibrocytes and may inhibit their activation and recruitment into the myocardium. This potential mechanism intuitively explains the decreased cellular infiltration within the heart. Furthermore, fibrocytes are known to produce pro-fibrotic mediators when recruited into tissue and if aPC does inhibits their recruitment and/or activation, this would address the significant reduction of the pro-fibrotic factors in the myocardium seen when aPC is added to our model of myocardial fibrosis. Further work is required to understand the effect of aPC on fibrocytes and the effect of aPC on the heart in the presence of fibrotic stimuli.

Myocardial fibrosis is part of the continuum that eventually contributes to the development of chronic heart failure (5). Even with current medical interventions, the prognosis for patients with heart failure is not always promising, forcing researchers to consider new therapies (334). Knowledge gained from the present study on the beneficial effects of aPC may offer some insight into novel approaches to reduce the burden of cardiovascular diseases.

7.6 Funding

This work was supported by a grant from the Nova Scotia Health Research Foundation (#42311 to J.F.L.); the Canadian Institute of Health Research (#44122 to J.F.L.); and an investigator initiated research grant from Astellas (#43742 to R.S.L.).

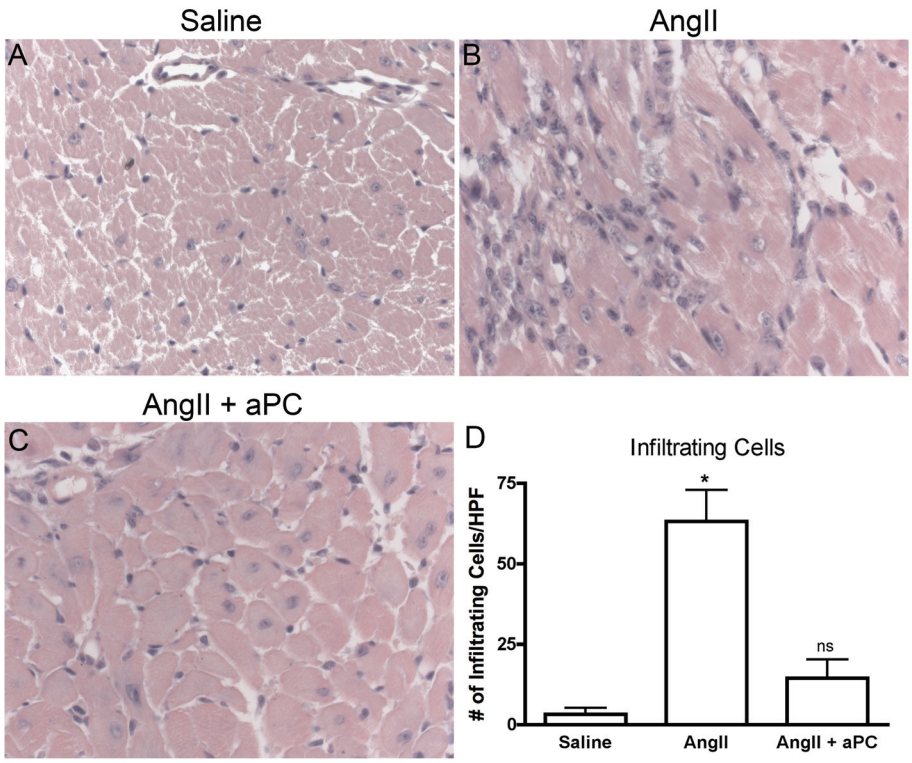

Figure 7.1 Cellular Infiltration

Representative images of hearts sections stained with H&E from animal infused with saline (A), AngII (B) and AngII and aPC (C). AngII infusion was associated with evident mononuclear cellular infiltration within the interstitial and perivascular tissues while little cellular infiltration was evident when aPC was also infused. Infiltrating cell counts were completed to quantify this observation within an average of 5 field of views/heart (D). Images were taken at 40x magnification.

* $p<0.05$

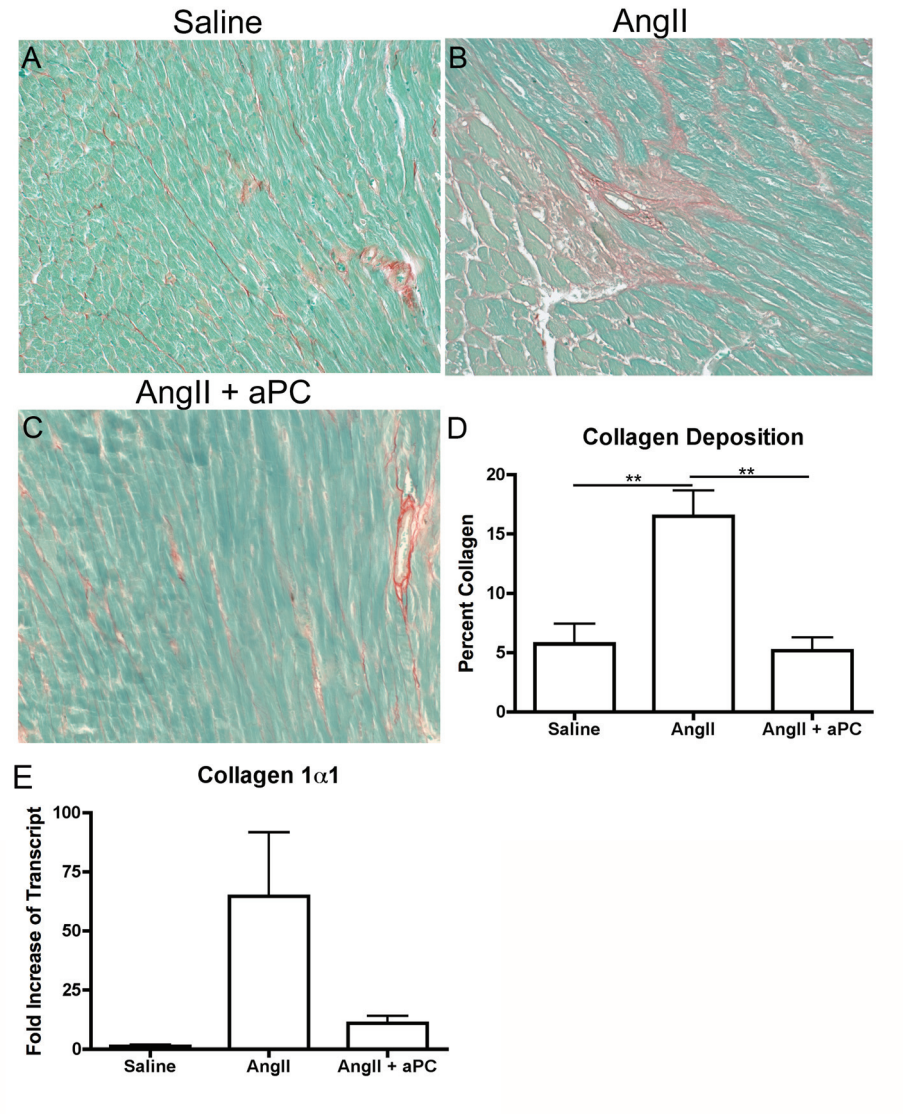

Figure 7.2 Collagen Deposition

Myocardial collagen content was assessed as an indicator of fibrosis. Collagen was initially assessed using myocardial sections stained with Sirius red and fast green where collagen is stained red and the counter stain is green. Representative images of sections from animals infused with saline (A), AngII (B) and AngII and aPC (C). Collagen content of Sirius red stained sections was semi-quantitatively assessed by completing red pixel measurements compared to total pixel content to derive a percent collagen content

within a cross section of heart (D). qRT-PCR was completed to assess pro-collagen1α1 transcript levels within the different experimental groups (E). Images were taken at 25x magnification $**p<0.01$

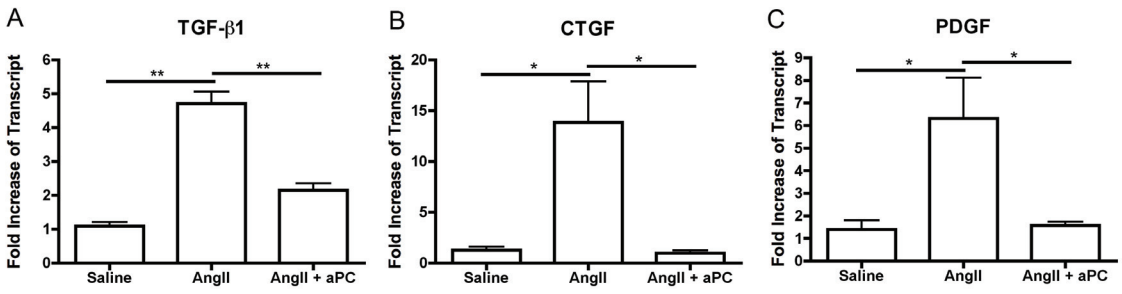

Figure 7.3 Pro-Fibrotic Mediators

The transcript levels of different pro-fibrotic mediators were assessed using qRT-PCR from whole heart samples. TGF-β1, CTGF and PDGF transcript levels were significantly elevated in animals exposed to only AngII but transcript levels were significantly less when aPC was also infused. * $p<0.05$ ** $p<0.01$

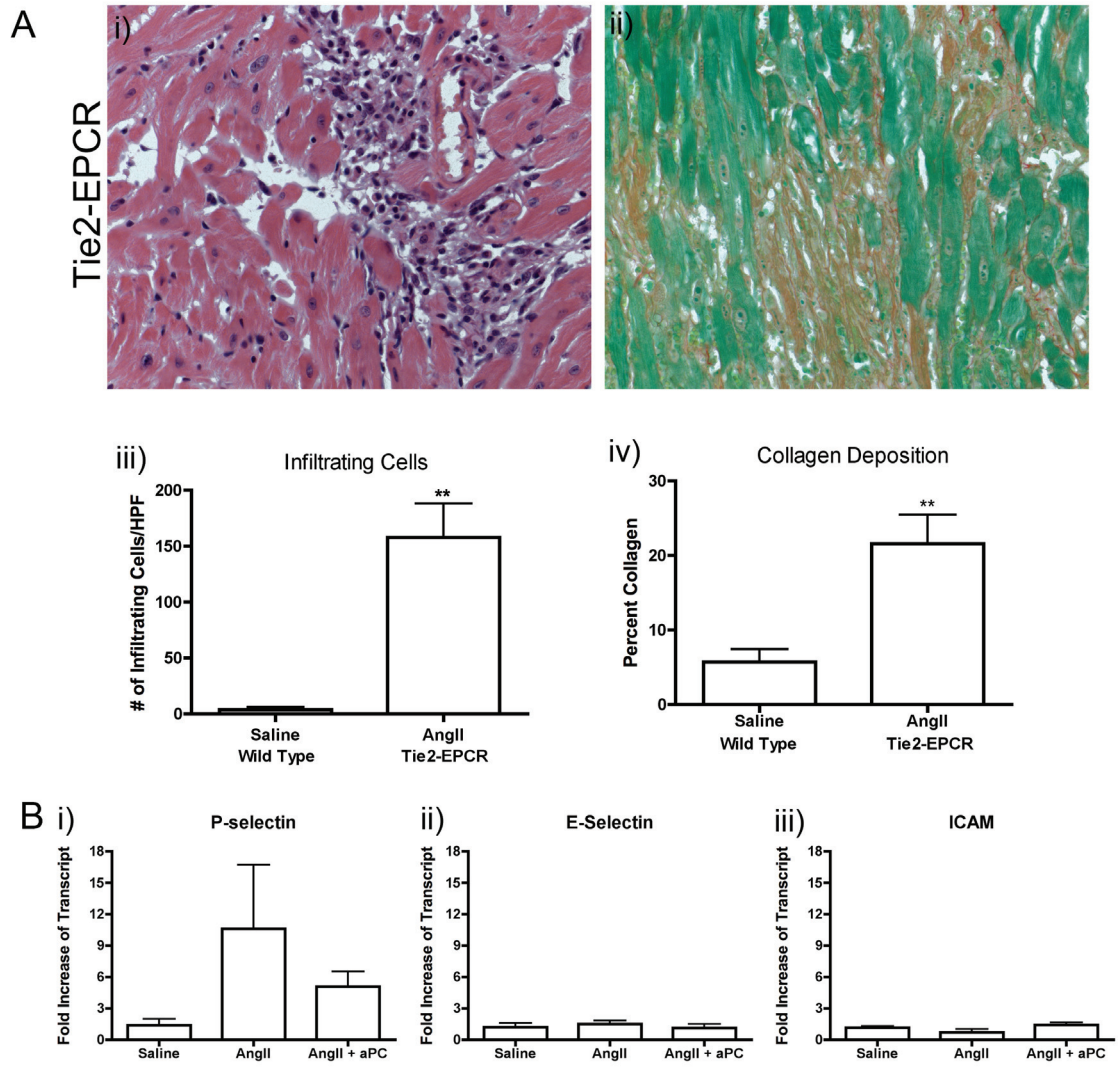

Figure 7.4 Endothelial Cell Activation

AngII was infused in Tie2-EPCR mice that have excess expression of the aPC receptor within endothelial cells and as such have chronically downregulated endothelial cell activation (A). Cellular infiltration and collagen deposition, as measured by H&E (Ai) and Sirius red (Aii) staining respectively, were still evident within AngII infused Tie2-EPCR animals. Quantification of both cellular infiltration and collagen content

demonstrated a significant increase beyond the levels of saline controls in wild type animals (Aiii, Aiv). The transcript levels of cellular adhesion molecules, including P-selectin (Bi), E-selectin (Bii) and ICAM (Biii), were assessed using qRT-PCR analysis of whole heart samples. No significant change was measured in the level of cellular adhesion molecule transcript levels in either experimental group compared to controls (B). Images were taken at 40x magnification. * $p<0.05$ ** $p<0.01$

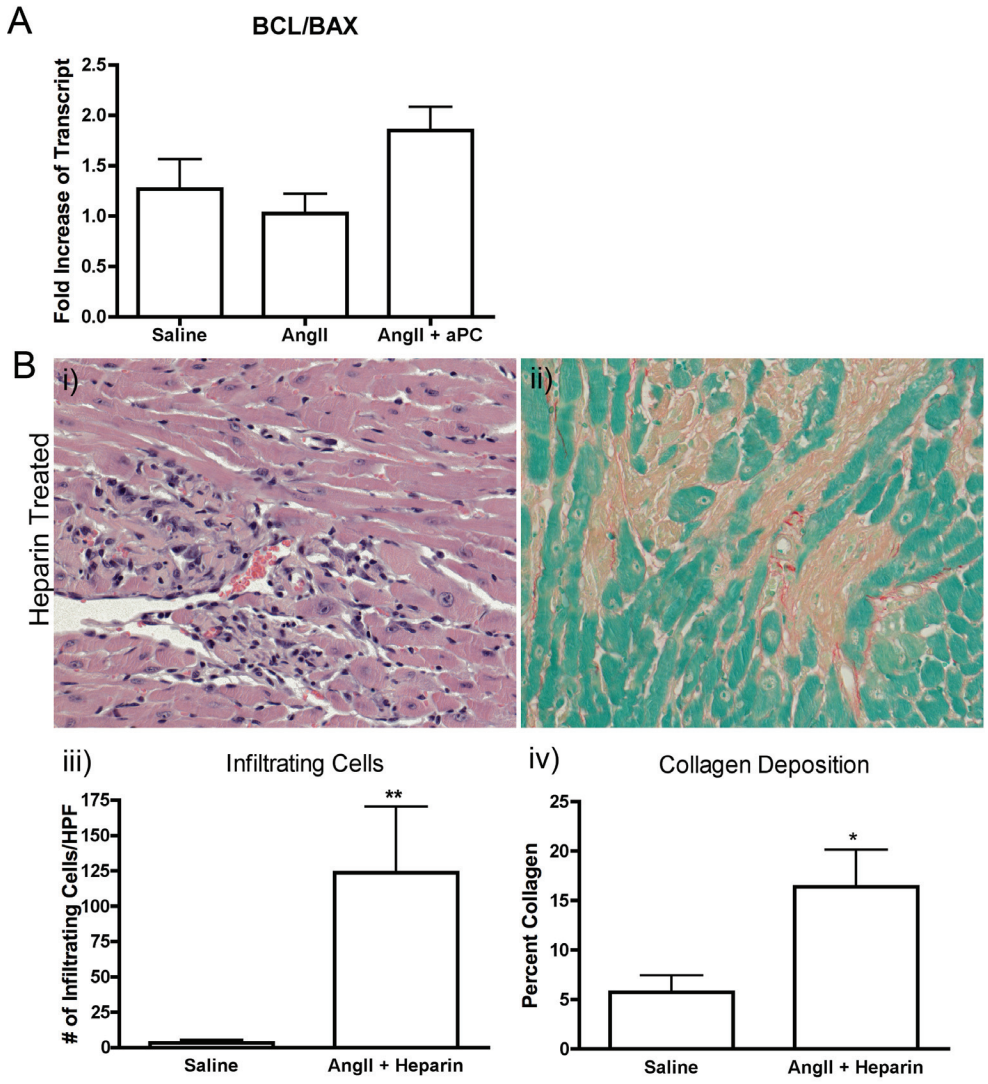

Figure 7.5 Putative Mechanism of Action of aPC

Transcript levels of the pro-survival factor Bcl-2 and the pro-apoptotic factor Bax were measured by qRT-PCR and a ratio of the two genes were generated for each animal assessed from each experimental group (A). No significant difference in the Bcl-2/Bax ratio was measured. To assess the effect of anticoagulation in this model, animals were infused with both AngII and heparin to determine the effects of anticoagulation within our fibrotic model (B). Cellular infiltration and collagen deposition, as measured by

H&E (Bi) and Sirius red (Bii) staining respectively, were still evident within the myocardium of animals infused with AngII and heparin. Quantification of both cellular infiltration (Biii) and collagen content (Biv) demonstrated a significant increase beyond the levels of saline controls. Images were taken at 40x magnification.

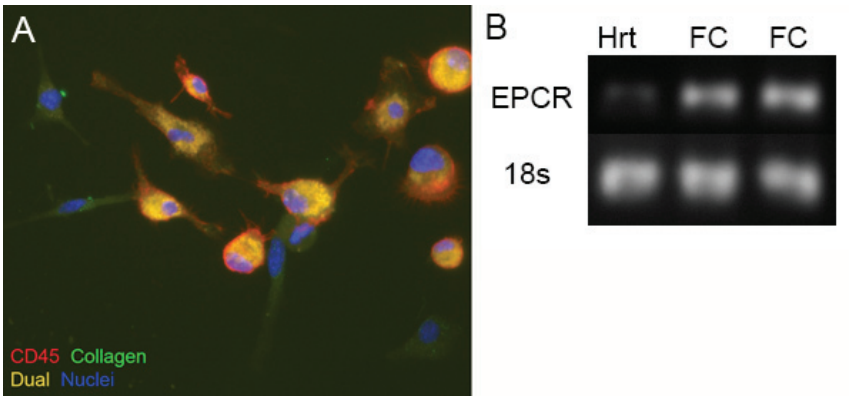

Figure 7.6 EPCR Expression on Infiltrating Cells

Conventional RT-PCR was used to analyze the expression of EPCR in Fibrocytes (FC, n=2) isolated from AngII infused hearts. Significant EPCR expression was detected in isolated cells as well as faint expression in a sample of whole heart (HRT). 18s was used as a housekeeping gene to ensure equal loading between samples.

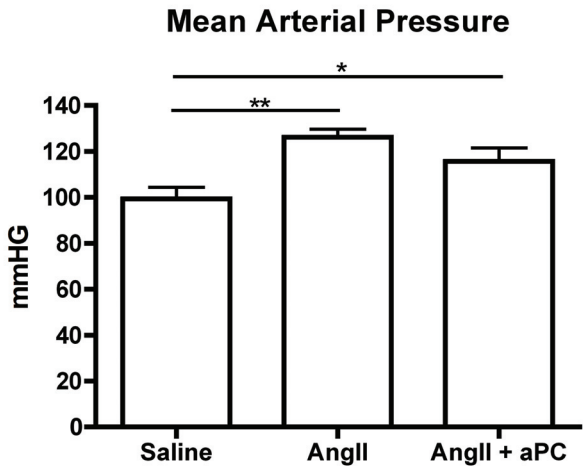

Figure S7.1 Hemodynamic Measurements

AngII infusion after 3d was associated with a significant increase in the mean arterial pressure (mmHG) of mice as measured by a non-invasive tail cuff system. Co-infusion with aPC did not significantly alter the AngII induced hypertension. * $p<0.05$ ** $p<0.01$

CHAPTER 8 – CIRCULATING FIBROCYTE LEVELS IN PATIENTS WITH ISCHEMIC HEART DISEASE

Preliminary Findings

[*] Contributing individuals are clearly outlined in Appendix 2.

8.1 Introduction

Ischemic heart disease (IHD), characterized by impaired blood flow to cardiac tissue, constitutes by far the predominant cause of myocardial injury leading to fibrosis and heart failure (335-337). Coronary artery bypass grafting (CABG) surgery is a common treatment option offered to patients with IHD to alleviate disease symptoms and improve outcomes. It has previously been established that CABG with cardiopulmonary bypass (CPB) promotes the mobilization of early progenitor cells out of the bone marrow and into the circulation (338, 339). While most studies have examined the mobilization of endothelial progenitor cells (EPCs) other progenitor lineages exist and are likely pertinent to tissue repair. Fibroblast progenitor cells, or fibrocytes, are a bone marrow derived progenitor cell type that is found in the circulation (340). Fibrocytes rapidly migrate into injured tissues and are believed to differentiate into a myofibroblast-like cell type (214, 228, 340). These cells are believed to contribute to both healthy repair as well as pathologic fibrosis. Circulating fibrocyte levels are not well established in patients with IHD or in the progenitor population mobilized after CABG surgery.

Using animal models, fibrocytes have been shown to infiltrate into the myocardium prior to the development of myocardial fibrosis and have been shown to be a key effector cell driving this process (24, 214, 219, 228, 229). Fibrocytes are derived from a monocyte progenitor lineage and have customarily been identified by staining for markers of either progenitor cells (CD34) or hematopoietic cells (CD45/CDllb) in combination with a mesenchymal cell marker (collagen) (85, 208, 209, 341). These cells have been shown to produce several pro-fibrotic factors as well as ECM proteins and are therefore able to

directly contribute to the fibrotic process (201, 211, 221, 342-345). In other fibrotic disease states, including lung fibrosis and burn healing, patients have been shown to have elevated levels of circulating fibrocytes (346-348), however this has never been characterized in IHD patients undergoing CABG surgery.

Many patients with IHD present clinically with established myocardial injury in which a reparative process has already been initiated within the myocardium (349). This repair process is characterized by the deposition of extracellular matrix (ECM) proteins within the cardiac tissue. Though initially beneficial, excess deposition of ECM proteins can eventually replace healthy myocardial tissue and become a pathologic fibrotic process (2). This progressive ventricular remodeling characterized by fibrosis can eventually impair organ function, thus contributing to the development of heart failure (3). While current therapies for IHD aim to prevent further damage to the cardiac tissue, myocardial fibrosis is not believed to efficiently resolve. Therefore, better understanding of the biologic components of fibrosis is necessary to develop therapeutic targets to specifically inhibit this process when it becomes pathologic.

We hypothesized that the level of circulating fibrocytes in patients with IHD would be elevated compared to healthy controls and that CABG surgery with CPB would promote further fibrocyte mobilization.

8.2 Methods

8.2.1 Study Design and Patients

Between November 2011 and March 2012, patients requiring elective CABG surgery at the Queen Elizabeth II Health Science Center were prospectively recruited for this study. Informed consent was obtained according the Capital Health Guidelines from the Research Ethics Review Board (REB # CDHA-RS/2011-146). The inclusion criteria for this study consisted of any patient undergoing isolated CABG surgery. The exclusion criteria included any patient requiring urgent surgery, requiring concomitant procedure or had a recent history of myocardial infarction (<2 weeks). Healthy volunteers were also recruited for the study as controls and informed consent was also acquired from these individual.

8.2.2 Surgical Procedure

A median sternotomy was performed in all patients. CABG surgery with CPB was performed in a standardized fashion using ascending aortic cannulation and 2-stage venous cannulation of the right atrium. Intermittent cold blood cardioplegia was delivered antegrade via the aortic root. The choice of conduits and/or construction of composite grafts was based on surgeon preferences rather than fixed criteria. Arterial conduits were harvested with minimal trauma (non-skeletonized internal-mammary-artery graft) and all treated with either a Papaverine® solution or nitroglycerine/calcium channel blocker (Verapamil®) solution prior to use.

8.2.3 Postoperative Management

All postoperative cardiac surgery patients were taken to a dedicated cardiovascular intensive care unit (CVICU). Patients discharged from the CVICU were transferred to an intermediate care or general care ward under the care of the same team. All patients were monitored continuously for a minimum of 24h.

8.2.4 Blood Sampling for Progenitor Cell Assessment

Each blood sample was obtained in an EDTA-K_2 tube and was thoroughly inverted to ensure complete anti-coagulation. Blood samples were taken from the arterial line of patients shortly after it was inserted prior to surgery (Pre-CABG), 1h after patient was taken off CPB (1h-post CABG) or 6h after CPB (6h-post CABG). A maximum of 10ml was taken at each time point from patients. Healthy controls provided a one-time donation of approximately 30ml.

8.2.5 PBMC Isolation and Culture

Peripheral blood mononuclear cells (PBMC) were isolated as previously reported (350). Briefly, blood was diluted with an equal volume of Dulbecco's phosphate buffered saline (DPBS; Gibco, Life Technologies, Burlington, ON) containing 2% fetal bovine serum (FBS). PBMCs were then isolated using Ficoll-Paque density centrifugation. Isolated cells were plated out at $1x10^6$/well on coverslips in a 6-well culture plate or $8x10^6$/T75 flask. All culture dishes and coverslips had been pre-coated with 0.01% sterile gelatin. Cells were cultured in Roswell Park Memorial Institute 1640 (RPMI) media (Givco, Life Technologies) supplemented with 10% heat-inactivated fetal calf serum, 2mM L-glutamate, 100μg/ml streptomycin and 100U/ml Penicillin for 1d, 3d or 10d at 37°C with

5% CO_2. Non-adherent debris was aspirated after 3d in culture and media was replenished at regular intervals. Cells were then fixed in 4% paraformaldehyde for histology studies or processed for flow cytometry.

8.2.6 Flow Cytometry

Fresh blood samples were standardized by transferring 100ul of blood into each sample tube for analysis. Total white blood cells (WBC) were then isolated from samples using BD Pharm Lysis (BD Bioscience, San Jose, CA) as per manufacturer's protocol. Samples allocated for intracellular marker staining (collagen) were permeabilized using a Cytofix/Cytoperm kit (BD Bioscience) as per manufacturer's protocol. All samples were incubated with a human F_c receptor block (Miltenyi Biotech, Cambridge, MA) prior to antibody staining. Permeabilized cells were then incubated with mouse anti-Collagen-1 antibody (Millipore, Billerica, MA) followed by a Fitc-conjugate anti-mouse secondary. The samples were then incubated with an aPC conjugated mouse anti-CD45 antibody (BC Bioscience). Remaining samples, not permeabilized, were incubated with a Fitc-conjugated anti-CD34 antibody (BD Bioscience). Isotype and negative controls were completed along side experimental staining to control for non-specific binding. Samples were fixed in a 0.4% formaldehyde solution and stored at 4°C until analysis. Samples were measured using a FACScalibur Flow Cytometer (BD Bioscience) and analysized using WinList 5.0 software.

Cultured PBMCs in a T75 flask were detached using trypsin after 10d of culture. Cells were permeabilized with Cytofix/Cytoperm kit and incubated with a human F_c receptor

block (Miltenyi). Cells were then incubated with mouse anti-Collagen-1 (Millipore) antibody followed by a Fitc-conjugate anti-mouse secondary. Samples were fixed in a 0.4% formaldehyde solution and stored at 4°C until analysis.

8.2.7 Immunofluorescent Staining

Cultured cells fixed on coverslips were stained for Collagen-1 and CD45. Cells were exposed to PBS with 0.1% triton, which was also used in subsequent incubations and washes. Cells were incubated with 10% normal goat serum to block non-specific protein binding. Cells were incubated with rabbit anti-Collagen-1 (Rockland Immunochemicals, Gilbertsville, PA) and mouse anti-CD45 (BD Bioscience). This was followed by incubation with host specific secondary antibodies. Hoechst was used to identify intact nuclei. Cells were visualized and pictures were taken using a AxioCam HRc (Carl Zeiss) and analyzed using Adobe Photoshop 5.0. Five random fields of views at 20x magnification were captured from each coverslip. Adherent cells were counted and averaged per subject.

8.2.8 Statistical Analysis

Data is provided as mean ± SEM. A students T test was used to compare between healthy control individuals and CABG patients at baseline (pre-CABG). A one-way ANOVA was used to compare CABG patients prior to their surgery to the time points after their surgery.

8.3 Results

8.3.1 Study Participant Characteristics

The study population included six CABG surgery patients and five healthy volunteers. Patients enrolled in the study were only male, though females were not excluded, and their average age was 69 ± 6 years. The control group contained two males and three females who had the average age of 49 ± 7 years. All patients underwent CABG to treat 3-vessel coronary artery disease and one patient also received a mitral valve repair due to intra-operative findings of severe mitral insufficiency. Prior to surgery, 67% of patients were being treated with ACE inhibitors, 17% of patients were on an angiotensin receptor blocker regimen and 17% of patients were not on either treatment. No history of cardiovascular disease was reported in any of our control individuals.

8.3.2 Circulating Progenitor Cells

It has previously been reported that CABG surgery promotes mobilization of progenitor cells (338, 339). To confirm this, we assessed CD34 expression, a marker of immature progenitor cells, on circulating leukocytes prior to and after CABG surgery. We found a slight increase in $CD34^+$ cells at baseline in patients with IHD compared to healthy controls (Fig. 7.1; pre-CABG: 1.38 ± 1.05%; Control: 0.01 ± 0.01%). The number of $CD34^+$ cells did increase after CABG surgery and peaked at 1h post-CABG (Fig. 8.1; 1h post: 6.01 ± 2.81%; 6h post: 0.49 ± 0.04%).

8.3.3 Circulating Fibrocytes

Fibrocytes have previously been reported as collagen expressing cells in circulation (221, 340, 351). As such, we aimed to report circulating fibrocyte levels by measuring

$CD45^+/Collagen^+$ cells by flow cytometry in freshly isolated total leukocytes. We were able to detected $CD45^+/Collagen^+$ in each of our experimental groups (Fig. 8.2; Control: 0.04 ± 0.01%; pre: 0.03 ± 0.02%; 1h post: 0.04 ± 0.03%; 6h post: 0.03 ± 0.01%). A statistically significant difference could not be detected between our experimental groups and as such the circulating population did not appear to change between healthy controls and IHD patients prior to surgery. CABG surgery also did not appear to have an effect on $CD45^+/collagen^+$ cell levels in circulation.

8.3.4 Fibrocytes in Culture

Others have previously reported that culturing isolated PBMCs over time will select for, and enrich, fibrocytes from the circulation by promoting further differentiation of this cell type (85, 196, 253, 344). Therefore, to assess the phenotypic changes of these cells over time we cultured isolated PBMCs for 1d, 3d or 10d. We analyzed collagen expression by flow cytometry and found that after 1 day in culture, a minimal number of cells were $collagen^+$ (Fig. 8.3; 1d: 0.20 ± 0.09%). This finding supported our initial flow cytometry data from freshly isolated leukocytes. However, collagen expression significantly increased over time in the remaining viable cells in culture (Fig. 8.3; 3d: 52.8 ± 13.7%; 10d: 83.9 ± 7.5%; 1d vs. 10d: $p \leq 0.01$). This data was confirmed by immunofluorescent staining on fixed cells (1d and 3d data not shown). Cells were largely found to be $CD45^+/Collagen^+$ after 10d in culture, an observation found in both patients and control subjects (Fig. 8.4).

We then assessed the number of cells that remained in culture after 10d to determine if the resulting population differed between our experimental groups. There was an apparent increase in the number of cells viable in cultures obtained from CABG patients in comparison to healthy controls. A statistically significant difference was confirmed by cell number quantification (Fig. 8.3; pre-CABG: 15.6 ±1.4 cells/FOV; control: 6.0 ± 2.4 cells/FOV; $p \leq 0.01$). This finding suggests that circulating cells from patients with IHD have enhanced potential to differentiate into fibrocytes in culture. Furthermore, we found a positive trend that this potential for fibrocyte differentiation was further increased in patients, 6h after CABG surgery (Fig. 8.3; 6h post: 22.37 ± 6.20 cells/FOV), though it did not reach statistical difference. This data suggests that not only do patients with IHD have enhanced potential of circulating leukocytes to differentiate into fibrocytes, a yet to be identified stimuli provided by CABG surgery appears to promote this potential further.

8.3.5 Physiologic Variables Associated with CABG Surgery

Both surgical procedures and patient tolerance of the surgery varies between cases and several measures are recorded during and after the procedure in order to aid in predicting outcomes. Patients were on cardiopulmonary bypass for an average of 105 ± 6 min, varying from 88 min up to 123 min. The average clamp time for patients was 75 ± 7 min, with the minimum time being 56 min and the max being 105 min. Troponin T levels are continuously monitored over time as an indicator of cardiac injury and the average peak troponin was 0.52 ± 0.16 ng/ml and ranged from 0.05 ng/ml to 1.170 ng/ml. While a correlation study comparing these variables to the average number of cells in culture after 10d has yet to be completed, this analysis would indicate if an increase in cultured fibrocytes correlates with a surgical variable.

8.4 Discussion

The aim of this paper was to assess circulating fibrocyte levels in patients with IHD compared to healthy controls and determine if CABG surgery is a stimulus capable of mobilization of circulating fibrocytes. Patients with IHD typically exhibit ventricular remodeling characterized by fibrosis and as such, we believed that they would have elevated levels of circulating fibrocytes (349). We were able to detect a slight increase in the circulating progenitor population, determined by CD34 expression, in IHD patients compared to healthy controls. However, we found that fibrocytes, as defined by collagen expression, did not compose a large proportion of circulating cells (0.03%) in patients and did not statistically differ from the levels measured in healthy individuals (0.04%). Furthermore, while we detected an increase in $CD34^+$ progenitor cells after CABG surgery, there was no statistical difference in the level of circulating $CD45^+collagen^+$ cell population after surgery. This data suggests that $collagen^+$ circulating leukocytes are a very small population and don't appear to change in IHD patients or after CABG surgery.

Currently, the evidence for fibrocytes, defined as $collagen^+$ cells, in circulation is inconsistent. Some of the initial studies, which were instrumental in elucidating fibrocytes as an effector cell in the healing process, are widely quoted as defining fibrocytes composing approximately 0.5% of circulating WBCs (221, 340). However, to the best of our knowledge this analysis is derived from studies in which cells are grown in culture over time and the percent is then extrapolated from later findings. Recently, Fang and colleagues (2012) were able to detect collagen positivity in approximately 0.1% of freshly isolated WBCs via flow cytometetry (351). Alternatively, other groups have

reported circulating fibrocytes by analyzing subsets of PBMCs that were further processed to select for non-adherant non-T cell (NANT) population (347, 352). These groups report that that fibrocytes consist of approximately 7% of this NANT population, however it is not clear as to what percentage of total WBCs this converts to and what, if any effect, the isolation process has on the resulting cell population. Interestingly, Bellini and Mattoli suggest in a review that fibrocytes, as defined by collagen expression, may not exist in circulation but that this population arises from a less differentiated progenitor population that is collagen$^-$ (208). To support this statement they reference several papers that examine fibrocyte characteristics and function but do not address this population in freshly isolated blood but only after culture (85, 341, 348, 353, 354). Yeager and colleagues (2012), identified fibrocytes by labeling freshly isolated WBCs with pro-collagen rather than highly processed collagen-1, which was expressed in 0.2% of WBCs in healthy individuals (355). Therefore, a consensus has yet to be reached regarding if cells in circulation express mature collagen and if so, what percent of WBC they compose.

In our study, we measured an average of 0.03% of circulating cells were characteristic of a fibrocyte phenotype. Furthermore, this population did not vary between healthy individuals and patients with IHD. This is at least 10-fold less than what others have reported. However, in our experience, accurately labeling for intracellular collagen for flow cytometry is technically challenging which could contribute to the variation seen in the literature. Our flow cytometry for collagen was consistently positive in fibroblast controls (data not shown) and was able to differentiate degree of collagen positivity

between fresh WBC (<0.1%) and 10d cultured PBMCs (>80%). Furthermore, our flow cytometry data was confirmed using immunofluorescent staining.

While we were unable to identify a large population of collagen$^+$ cells in circulation, we were able to select for a population in culture that became collagen$^+$ over time. After 10d in culture, more than 80% of the remaining viable and adherent cells were expressing collagen. This indicates that a circulating population has the potential to express and secrete extracellular matrix proteins. This likely would translate into an early monocyte progenitor cell migrating into tissue and undergoing a differentiation into a fibrocyte *in vivo*. Interestingly, we were able to culture 2-fold more fibrocytes in samples taken from patients with IHD at baseline compare to healthy controls. This suggests that there may be more progenitor cells in circulation that have the potential to become fibrocytes. The increase in CD34$^+$ cell in circulation, even at baseline, supports this theory. Alternatively, the active fibrotic process occurring in patients with IHD may have resulted in the increase of circulating mediators, such as TGFβ, which could have 'primed' these cells and increased their proliferation capacity (356). Nevertheless, the increase presence of fibrocytes likely contributes to the ongoing fibrosis once they are recruited to the myocardium.

CABG with CPB has previously been shown to increase mobilization of progenitor cells out of the bone marrow and into circulation (338, 339). We were able to replicate this finding by showing a peak increase in CD34$^+$ cells 1h after surgery. While this early increase in progenitor cells is likely attributed to neutrophils and monocytes, we did find

an increase of fibrocytes in culture from samples take 6h after surgery. This increase is likely promoted by the vascular trauma induced by CABG and CPB, which would prompt a healing response (357). It has been previously shown that CABG with CPB mobilizes endothelial progenitor cells, however this is the first study that suggests it also increases the circulating levels of a progenitor population with fibrocytes potential as well.

This data suggests that a circulating cell type can produce ECM proteins and thus potentially contribute to myocardial fibrosis. Fibrocytes have been shown to home to fibrotic tissue and infiltrate rapidly after an insult in rodent models of injury and fibrosis (196, 340). Furthermore, inhibition of fibrocyte infiltration or differentiation ameliorates scar formation in rodent models, suggesting a significant role for these cells (24, 229, 231, 358). However, there is yet to be definitive evidence that these cells actively cause fibrosis, just correlatory evidence suggesting a role. While this study shows an increase in these cells, we have yet to provide evidence that they secrete molecular mediators that promote fibrosis or actively contribute to myocardial fibrosis. However, this study can act as a basis to design future studies to further dissect the role and the mechanisms by which these cells contribute to myocardial fibrosis.

In this study we provide evidence that there is an increase in cells that have the potential to become fibrocytes in circulation of patients with IHD. It is our belief that these cells likely contribute to myocardial fibrosis once they are recruited to the fibrotic tissue. While further work is required to understand the exact role of these cells, their activation

and trafficking are mechanisms that can potentially be exploited for therapeutic interventions targeted to the fibrotic process in the future.

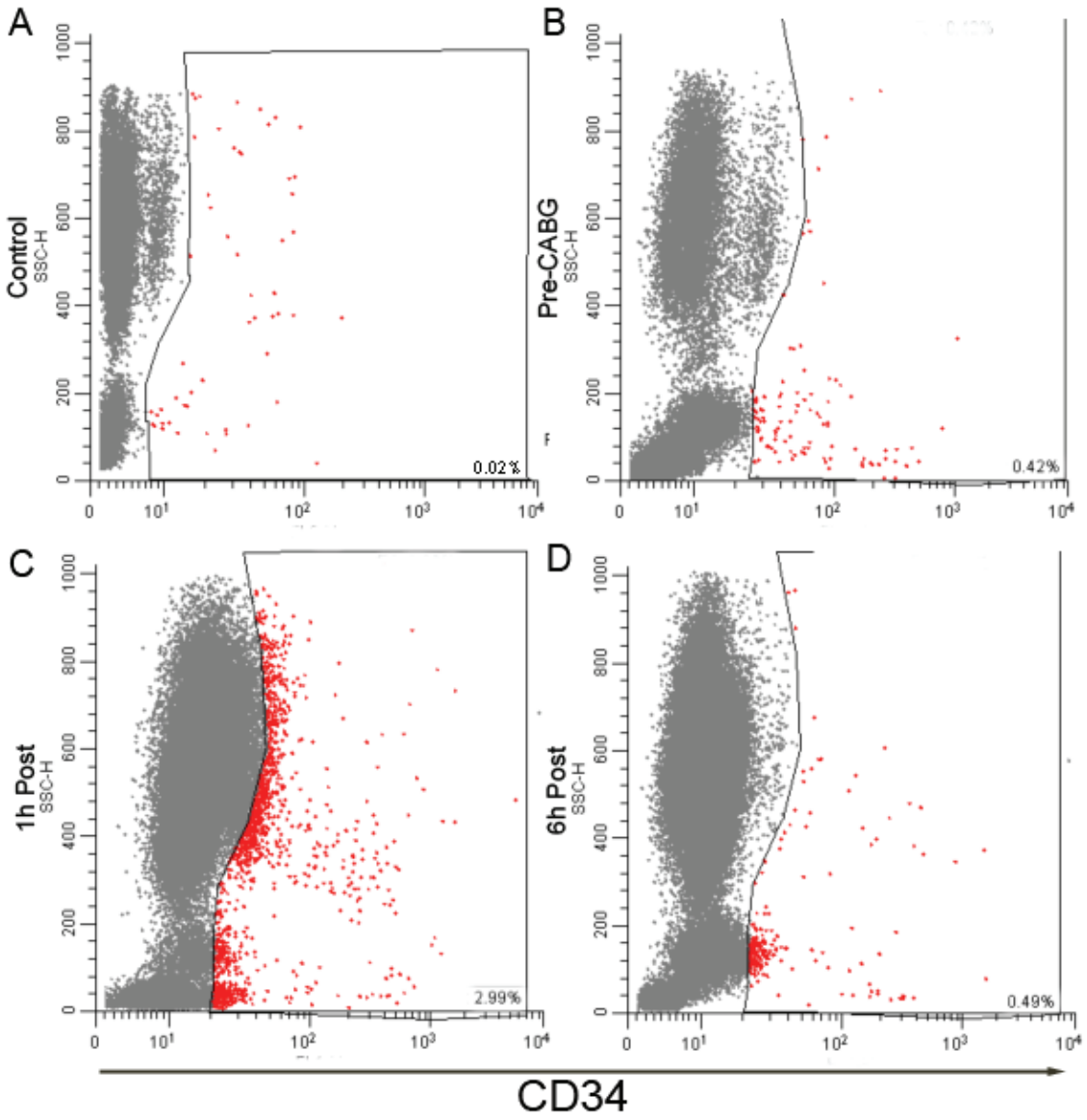

Figure 8.1 CD34$^+$ Cells in Circulation

Representative flow cytometry analysis of freshly isolated WBCs for CD34 expression in samples obtained from control individuals (A) and patients pre-CABG (B), 1hr post-CABG (C) and 6h post-CABG (D). Fluorescence is displayed on the x axis while SSC is displayed on the y-axis. Positive staining beyond isotype measurements is evident within the gated area.

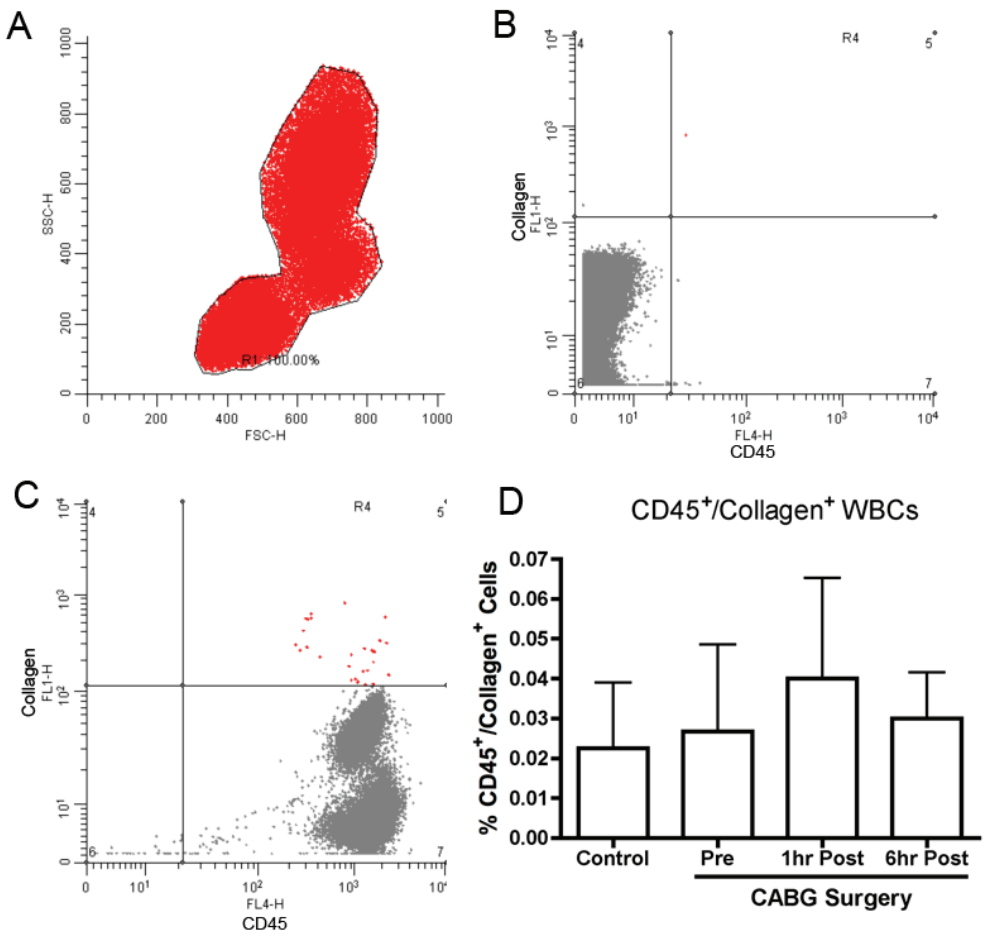

Figure 8.2 Fibrocytes in Circulation

Circulating fibrocytes were assessed in freshly isolated WBCs using flow cytometry for CD45 (x-axis) and collagen (y-axis). A representative plot showing forward scatter (FSC – x-axis) and side scatter (SSC – y-axis) of measured cells and the gate that was used to analyze total blood leukocytes (A). We ran isotype controls with all of our experimental samples to ensure that we were accounting for non-specific antibody binding. A representative plot of an isotype control for our Collagen illustrates that non-specific binding of antibody lays within our gated areas (B). An individual and representative analysis of a sample obtained from a control individual is displayed in a scatter plot

where $CD45^+$/$collagen^+$ cells are evident in the top right hand corner of the plot (C). The percent of $CD45^+$/$collagen^+$ in WBCs from each experimental group was averaged to examine trends (D).

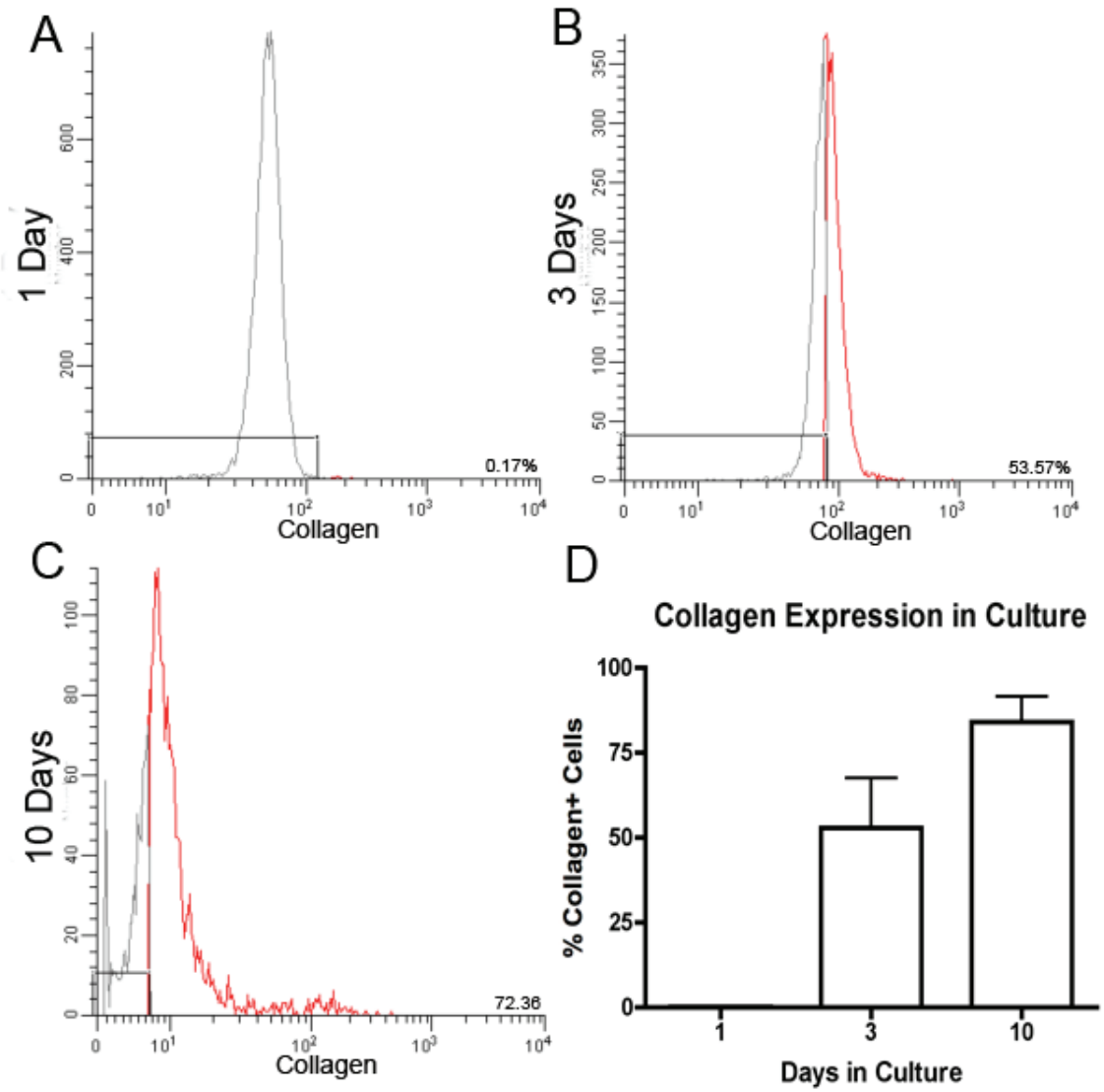

Figure 8.3 Collagen Expression in Culture

PBMCs, were cultured for 1d (A), 3d (B) or 10d (C) and were analysized for collagen expression by flow cytometry. Percent of positive cells, beyond isotype are indicated by red in the histogram. Average collagen measured after indicated culture time is represented in graph where the experimental groups are collapsed into time points (D).

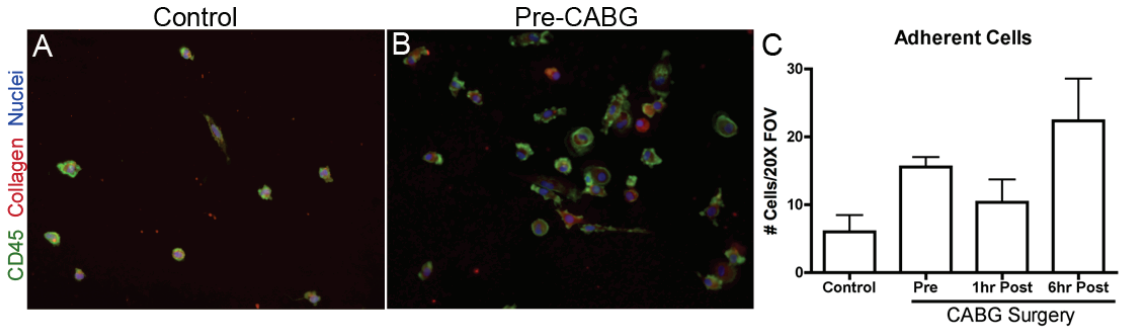

Figure 8.4 Fibrocyte Counts in Culture

Cells isolated from control individuals (A) and ischemic heart disease patients at baseline (B) were cultured for 10d and fixed for immunofluorescent staining. Cells were stained for CD45 (green), collagen (red) and nuclei (blue). Average cell counts from 5 random FOV at 20x magnification were used to quantify cell counts between groups (C).

CHAPTER 9 – DISCUSSION

9.1 Primary Findings

The aim of this study was to investigate the early cellular and molecular mediators that promote the development of myocardial fibrosis. We found a population of bone marrow derived cells that infiltrated the myocardium prior to significant ECM protein deposition in a model of myocardial fibrosis secondary to AngII infusion. We identified this initial infiltrating cell type as a population of fibroblast progenitor cells, termed fibrocytes. We then undertook experimentation to determine the factors that recruit fibrocytes into the myocardium and what molecular mediators this cell type produced in response to fibrotic stimuli. We determined the role of hypertension as a physiologic stimulus to myocardial injury, cellular infiltration and fibrosis in our model. We also assessed the beneficial effects of a novel therapeutic intervention, aPC, on the development of myocardial fibrosis and determined that it potentially confers protection by acting directly on fibrocytes in circulation. Lastly, we measured the level of fibrocytes in the circulation of patients with ischemic heart disease to begin to assess their potential involvement in myocardial fibrosis in humans.

9.2 Characterization of Fibrocyte Phenotype

To date, fibrocytes have been identified using immuno-based assays labeling for a panel of cell markers expressed by this mesenchymal progenitor cell type. Fibrocytes are a relatively newly characterized cell type and identification markers are still being characterized. Currently, a panel of markers is required as no one cell-specific marker has been proposed and verified as a fibrocyte marker. Most investigators use a combination

of progenitor cell marker (CD133/CD34) and/or leukocyte markers (CD45/CDllb/CD68) with mesenchymal markers (Coll/Vimentin/αSMA) to identify fibrocytes (markers used in these studies are outlined in Appendix 1 Table A1) (208). However, the cellular expression of these markers differs depending on the degree of fibrocyte differentiation (344). Fibrocytes are believed to start off with a phenotype similar to a monocyte, the lineage from which they are derived, and differentiate into an αSMA^+ myofibroblast-like mesenchymal cell type in a fibrotic microenvironment (85, 88, 196, 209, 221, 253, 343, 353). Prior to the work presented here, these cells had been implicated in models of lung, skin and liver fibrosis but at the initiation of this project had not been shown to infiltrate the fibrotic myocardium (196, 210, 211, 255, 359, 360).

It has long been appreciated that circulating leukocytes infiltrate into the myocardium during the development of myocardial fibrosis (59, 61, 101, 361). However, in the absence of ischemia, the infiltration was largely believed to consist of monocytes (identified by the expression of cell specific markers). Using a model of AngII infusion, others have characterized the infiltrating population as expressing markers of leukocytes (CD45) (362), monocytes (CD11b/MAC-1, CD107b/MAC-3, F4/80, CD68/ED-1) (7, 12, 189, 362, 363), and some reports of T-cell (CD3) (362). There has also been evidence of an increased fibroblast/myofibroblast population after AngII infusion (362, 364). While Campbell and colleages (1995) suggest that there is a mixed population of monocytes and fibroblasts they do not provide data for the presence of monocytes nor do they provide any dual staining (365). Similar data has been reported in other models of non-ischemic cardiomyopathies including aldosterone infusion (171, 366) and aortic constriction

models (367-369). These studies looked at individual markers of leukocytes, monocytes, T cells and fibroblasts but did not consider a progenitor cell type with a heterogenous phenotype. Prior to our studies there was no evidence to suggest that the infiltrating cells were not leukocytes, or monocytes to be specific, but during the time that our work was being completed a handful of manuscripts were published implicating a fibroblast progenitor cell type in the pathogenesis of chronic heart failure and ischemic myopathies (60, 88, 219, 360). These were the first studies to suggest that the phenotype of the infiltrating cells during the development of myocardial fibrosis may not be completely elucidated.

Initially we turned to the AngII infusion model of myocardial fibrosis to further characterize the mechanisms of cellular infiltration and manipulate the cellular response during myocardial fibrosis but had difficulty replicating previously reported evidence. In an attempt to characterize the evident population of infiltrating cells, we initially stained for a panel of leukocyte markers and found few cells positive for these markers after 7 days of AngII infusion, at which time we can demonstrate extensive myocardial fibrosis. This data conflicted the previous paradigm that the majority of the infiltrating cells were monocytes. Furthermore, a former Masters student within our lab, Dr. Adam Oxner, investigated the pro-inflammatory effects of AngII on purified monocytes *in vitro* and found conflicting results in the secreted cytokine profiles elicited (350). Specifically, we found that AngII-treated monocytes expressed IL-6, a pleiotropic mediator, but not TNF-α, a highly pro-inflammatory mediator, suggesting that monocytes do not upregulate a strictly pro-inflammatory response to AngII. This data also suggests that classically

derived, pro-inflammatory monocytes may not be the main infiltrating effector cell type in the heart in response to AngII exposure.

To fully elucidate the phenotype of the infiltrating cell population we completed a panel of histologic analysis for cell specific markers. We initially stained for markers indicative of resident cells within the heart. Though the heart constitutively contains mast cells, we did not observe many by toludine blue staining nor did we see an increase with AngII infusion (data not shown). We did find an increase in markers associated with the endothelium, including vWF and laminin (data not shown); however, we did not see a significant increase in endothelial cells within areas of cellular infiltration using a Tie2-GFP transgenic mouse strain. This data suggested to us that there was an increase in many matrix proteins, including those typically supporting the vasculature, within the heart. However, aberrant angiogensis did not appear to be driving the fibrotic process evident within AngII infused animals. We also investigated the presence of smooth muscle cells and myofibroblasts by completing immunohistochemistry assay for αSMA stain and found a large population of cells with a spindle morphology that was αSMA^{+} within areas of cellular infiltration, indicative of myofibroblasts. Lastly, we wanted to assess the origin of the infiltrating population to determine if they were bone marrow derived and to assess this we completed immunohistochemistry for CD133, a hematopoietic progenitor marker. We found a significant population of CD133 positive cells within the areas of cellular infiltration. The considerable number of cells positive for both αSMA and CD133 prompted us to do a dual label for the two markers and we were able to identify a population of $CD133^{+}/\alpha SMA^{+}$ cells within our AngII exposed

hearts. This suggested to us that a significant proportion of the cellular infiltration consisted of fibroblast progenitor cells. While these cells expressed a hematopoietic progenitor cell marker (CD133), suggesting they were bone marrow derived, we wanted to confirm their origin. Using a GFP bone marrow chimera mouse model, we confirmed that a large proportion of the infiltrating cells were of bone marrow origin. Thus, in our model of myocardial fibrosis, we observed significant cellular infiltration prior to the development of myocardial fibrosis where the infiltrating population appeared to largely consist of a bone marrow-derived fibroblast progenitor cell type. Haudek and colleagues (2010) corroborated this data when they too provided evidence that fibrocytes are a key infiltrating cell type in AngII-mediated myocardial fibrosis (24).

We used an *in vitro* culture system to further characterize this infiltrating cell type using cells isolated from AngII exposed hearts. Using an adapted cell isolation technique, we were able to culture a significant population of cells out of AngII exposed hearts and a much smaller population from naïve, untreated hearts. Isolated cells from an AngII heart were found to be both $CD133^{+}/\alpha SMA^{+}$ and $CD45^{+}/collagen^{+}$, suggesting a fibrocyte phenotype. Cells from naïve hearts were only positive for the mesenchymal markers, indicative of a fibroblast population. The fibrocyte-rich cultures were found to produce collagen mRNA when stimulated with AngII and CTGF, providing evidence that these cells respond to pro-fibrotic stimuli by upregulating ECM production. We also found that stimulating these cells with AngII upregulated the pro-fibrotic factors CTGF and TGFβ (Appendix 1 – Fig. A1). Furthermore, stimulation with TGFβ upregulated mRNA transcript levels of CTGF as well (Appendix 1 – Fig. A1). Therefore our infiltrating

population can be cultured and appears to respond to pro-fibrotic stimuli by upregulating other pro-fibrotic factors and ECM proteins suggesting a functional role for these cells in orchestrating a fibrotic response.

9.3 Fibrocyte Differentiation

Fibrocytes are believed to be an early progenitor cell that is capable of differentiating into multiple lineages depending on the microenvironment (370, 371). Circulating fibrocytes are phenotypically similar to monocytes, as they are derived from the same lineage (85, 88, 209, 353). Therefore, they express high levels of leukocyte markers and progenitor cell markers but express low or negligible levels of mesenchymal markers (196, 209, 253). Exposure to a fibrotic milieu, including factors such as TGF- β, endothelin-1, and basic Fibroblast Growth Factor (bFGF), promotes fibrocyte differentiation into a ECM producing mesenchymal cells (85, 196, 344, 345, 372). Thus, after extravasation into fibrotic tissue, expression of leukocyte and progenitor cell markers continue to decrease while mesenchymal markers are significantly upregulated (85, 196, 221, 253, 343). Fibrocytes are believed to terminally differentiate into an αSMA^+ myofibroblast-like mesenchymal cell type in a fibrotic setting.

In the course of my work we have attempted to analyze fibrocyte development to better characterize the life cycle of this cell type. Others have suggested that fibrocytes, characterized by collagen expression, consist of approximately 0.5% of circulating cells (221, 340). In our studies we were unable to measure a population of collagen expressing cells in isolated WBCs that reached even the small proportion of the circulating

population previously reported. The number of circulating Coll$^+$ cells was even maintained in patients with ischemic heart disease. In our hands, we detected approximately 0.03% of total circulating WBCs were Coll$^+$ cells by flow cytometry. Furthermore, no collagen staining was evident using immunofluorescent staining on freshly isolated cells cytospun and fixed on slides (data not shown). We also assessed the expression of CD105 and vimentin, two putative fibrocyte markers, in circulating human WBCs using flow cytometetry and found neither marker was explicitly expressed on a distinct population (data not shown). However, vimentin appeared to be a useful marker in assessing fibrocytes in circulation in mice, as we were able to demonstrate an increase in circulating vimentin$^+$ cells after AngII infusion compared to controls. Many of the other reports that have postulated collagen expression in circulating fibrocytes analysed collagen in cultured cells and extrapolated its expression in the originating cell type (221, 340, 373). Interestingly, while we were unable to show a similar level of Coll$^+$ cells in circulation were able to show that a population of cells in circulation possessed the potential to become Coll$^+$, replicating the earlier work done to assess circulating fibrocyte levels. Data from this work suggests that a very small percentage circulating leukocytes express processed collagen but a population in circulation can differentiate into and ECM producing cell when exposed to the appropriate conditions.

Many potential fibrocyte markers, including collagen, are maintained within the cell cytoplasm and identifying them by flow cytometry requires permeabilization of the cells prior to staining. Permeabilization alters cell morphology and increases the potential for non-specific antibody binding, making this technique increasingly challenging and prone

to misinterpretation. Indeed in our hands, isotype controls for different collagen antibodies provided a positive signal equal to or greater than experimental positive controls. We chose the antibody that we used for flow cytometry after thorough testing in which our flow cytometry for collagen was consistently positive in fibroblast controls (data not shown). We were also able to differentiate degree of collagen positivity between fresh WBC (<0.1%) and 10d cultured PBMCs (>80%). In these assays, we did detect positive measurements with our isotype control but the positivity reported for actual experimental samples was measured beyond that of our isotype controls. Furthermore, our flow cytometry data was confirmed using immunofluorescent staining. We believe that we have the measurements we have provided for collagen expression by flow cytometry represent true findings and not artifacts derived from cell processing.

We investigated fibrocyte differentiation *in vivo* using our mouse model and characterizing the cells at different time points. We assessed the phenotype of the infiltrating cell phenotype after only 3d of AngII infusion and identified a population of $CD45^+/\alpha SMA^+$ cells within the myocardium. However, after 7d of AngII infusion, when extensive myocardial fibrosis is evident, few cells were found to be positive for CD45. Interestingly, both CD133 and CD68 (ED-1) expression were maintained until 7d as evident by the $CD133^+/\alpha SMA^+$ population in mice and the $ED\text{-}1^+/\alpha SMA^+$ population in rats. While this data doesn't clearly elucidate the exact phenotype differentiation of fibrocytes *in vivo* over time, it does provide supporting evidence that fibrocytes start off with primarily a monocyte phenotype and then differentiate over time into a cell type with a largely mesenchymal cell phenotype. The varying phenotypes of this progenitor

cell makes it technically challenging to identify fibrocytes, which has likely resulted in underestimating their involvement in many disease processes.

We, and others, have studied the differentiation of fibrocytes both *in vivo* and *in vitro* but cannot conclusively state that these cells differentiate into myofibroblasts. We can provide evidence that fibrocytes become αSMA^+ cells that can secrete fibrogenic factors and ECM proteins when in a pro-fibrotic microenvironment (85, 88, 196, 209, 221, 253, 343, 353). While these are properties similar to those of myofibroblasts, no one has yet to do a functional comparison between activated resident fibroblasts and fibrocytes. However, exact specification of the terminal cell type of fibrocyte differentiation is less important than their functional properties. Studies that attempt to prevent fibrocyte infiltration, by either chemokine blockade or inhibition of differentiation, result in improved pathology and ameliorated scar formation (24, 229, 231, 358). Therefore fibrocyte infiltration appears to promote fibrosis.

9.4 Fibrocyte Chemotaxis

In an attempt to understand the chemotactic factors responsible for recruiting fibrocytes into the fibrotic myocardium, we undertook a series of experiments that would effectively interfere with chemokine signaling previously believed essential for fibrocyte recruitment. Both CCL2/MCP-1 and CXCL12/SDF-1α have been implicated as essential chemotactic factors for fibrocyte migration. Indeed, others have shown that isolated fibrocytes migrated to both CCL2/MCP-1 and CXCL12/SDF-1α in *in vitro* migration assays (91, 196, 201, 374). The blockade of either chemokine-induced signaling in *in*

vivo models of lung and myocardial fibrosis appeared to inhibit infiltrating cell accumulation and decrease tissue ECM accumulation (24, 229, 231, 358). Our experiments confirmed that fibrocytes express the appropriate receptors for both chemokines (CCR2-CCL2/MCP-1 and CXCR4-CXCL12/SDF-1α). We also provided data that $CD133^+$ expressing progenitor cells within the PBMC population migrate to both CCL2/MCP-1 and CXCL12/SDF-1α. However, inhibition of CCL2/MCP-1, CXCL12/SDF-1α or both chemokines was not sufficient to abrogate the initial fibrocyte infiltration into the myocardium. This data indicates that, while fibrocytes can migrate to either chemokine, neither CCL2/MCP-1 or CXCL12/SDF-1α are the essential chemotactic signal required for fibrocyte migration. Alternatively, CCL21-CCR7 signaling has been shown to be a key mechanism for recruiting fibrocytes in models of wound healing and renal fibrosis, though we have yet to examine this chemotactic pathway in our model (85, 218).

Interestingly, while CCL2/MCP-1 blockade was insufficient to inhibit initial fibrocyte migration it did confer a degree of protection to the fibrotic heart. This data suggests that CCL2/MCP-1 signaling may, in itself, contribute to fibrosis. Indeed, CCL2/MCP-1 has been reported to promote fibroblast activation, proliferation and ECM protein production increasing their fibrogenic function (93). Another possibility is that CCL2/MCP-1 is required to recruit and/or activate another cell type that is key in maintaining the accumulating fibrocyte population and stimulate their fibrogenic effects. Monocytes/macrophages are a possible candidate for this stimulatory role, as CCL2/MCP-1 is a potent monocyte chemoattractant. Macrophages are capable of

producing pro-fibrotic mediators (TGF-β/PDGF) that may be essential in maintaining an active fibrocyte/myofibroblast population and in their absence the recruited cells may succumb to apoptosis rather than survive and proliferate (375). More evidence is required to understand the role of CCL2/MCP-1 in promoting myocardial fibrosis.

Cellular infiltration requires interaction of circulating cells with the endothelium (via cell adhesion molecules) to slow, tether and facilitate extravasation into the tissue. Since fibrocytes are derived from a monocyte lineage, it would be a logical assumption that they may use the same adhesion molecules for diapedesis. Engagement of selectins on the endothelial surface tethers monocytes and induces them to roll along the vessel (376). Monocyte arrest requires engagement of their α4β1 (VLA-4) and αLβ2 (LFA-1) surface integrins to their endothelial ligands, VCAM-1 and ICAM-1 respectively (377). Interestingly, in an attempt to inhibit cellular infiltration we used blocking antibodies against α4 or β2 and still saw significant CD68 (ED-1) positive cellular infiltration in the myocardium (Appendix 1 - Fig A2). In these same animals, dermal LPS injection was used as a monocyte migration control and the blocking antibodies significantly inhibited the infiltration of CD68 (ED-1) positive cells into LPS injection sites, similar to published results (101). This data suggests that the infiltrating cell population (fibrocytes) likely use alternative adhesion molecules to traffic into tissues. This was further supported by our findings that ICAM-1 mRNA expression, nor the mRNA levels of any other adhesion molecule tested, does not significantly change in our model; however, this only reflects the transcript levels and not the protein expression or molecule activation state of the individual adhesion molecules. While Pillings and colleagues

identified the expression of several adhesion molecules present on the cell surface of isolated fibrocytes(353), there is still a lack of functional studies determining which adhesion molecules are required for fibrocyte migration.

9.5 The Role of Fibrocytes in Promoting Fibrosis

While fibrocytes were described several decades ago (378), they have only recently been implicated in fibrotic processes. Fibrocyte infiltration has been demonstrated in models of skin, lung, liver, kidney and heart fibrosis (24, 196, 211, 343). Inhibition of fibrocyte migration or differentiation results in ameliorated scar formation and improved organ function (60, 231, 235, 237, 238, 379). These data suggest that fibrocyte infiltration and differentiation directly promote fibrosis.

While it is believed that fibrocytes are directly fibrogenic, the factors that this cell type produces that propagate healing and fibrosis are still being elucidated. Fibrocytes have been shown capable of responding to fibrotic stimuli including AngII, TGF-β, endothelin-1, bFGF and PDGF (201, 211, 344). Our studies also show that fibrocytes can respond to CTGF stimulation as well. Many of these factors, including CTGF, promote fibrocyte differentiation into an αSMA expressing cell type and cellular proliferation (85, 344, 345, 359, 380). In response to stimulation with pro-fibrotic factors, isolated fibrocytes have been shown to secrete TGF-β, bFGF, PDGF and our data also suggests CTGF, thus creating a positive feedback loop for maintenance of cell survival and fibrogenic activity (211, 221, 342, 345). Furthermore, fibrocytes also produce ECM proteins, including collagen and fibronectin, which illustrates how they directly

contribute to the scarring process (201, 211, 343, 344). Additionally, fibrocytes have been shown to secrete MMPs including MMP-2, MMP-8 and MMP-9 (342, 374). In the presence of TGF-β, an increase in the activation state of MMP-2 and MMP-9 can be detected in fibrocyte cultures indicating that they also contribute to the active remodeling of the ECM during fibrosis (374). Taken together, this data support an effector role for fibrocytes in the initiation and propagation of fibrosis.

Fibrocytes are also believed to contribute to tissue injury by promoting the initial inflammation. Fibrocytes secrete pro-inflammatory cytokines including IL-1, TNF-α and IL-8, which promote tissue inflammation(221, 342). Disorders that are T-cell mediated, such as autoimmune disease, may be indirectly promoted by fibrocytes as they are capable of presenting antigens to T cells in the context of Class II and Class I MHC (381, 382). Therefore, fibrocyte-mediated activation of T cells can propagate chronic inflammation, while also contributing to the corresponding fibrosis associated with these diseases (381, 382). Others have indicated a role for lymphocytes in AngII mediated vascular remodeling(383). We investigated the role of lymphocytes within our model of myocardial fibrosis by infusing immunodificient RAG-1 knockout animals, which lack functional T and B cells, and found no appreciable difference in cellular infiltration or fibrosis after 7 days of AngII infusion (Appendix 1 – Fig. A3). While the adaptive immunity aspect of fibrocyte function may not be directly contributing to myocardial fibrosis in our model, these cells still might be contributing to the early inflammation by producing inflammatory mediators.

While the data above provides evidence that fibrocytes promote fibrosis, their effector role has yet to be explicitly proven. Studies have been completed that strongly implicate fibrocyte recruitment and differentiation as key mechanisms driving fibrosis. Phillips and colleagues (2004) provided evidence that fibrocytes home to fibrotic tissue by injecting differentiated human fibrocytes into SCID mice undergoing bleomycin induced lung fibrosis. They detected human fibrocytes within the injured lung tissue suggesting that fibrocytes are specifically recruited to fibrotic tissues. Other investigators tried to inhibit fibrocyte recruitment by inhibiting chemokine signaling, including CCL2/MCP-1, CXCL12/SDF-1α or CCL21, in various models of fibrosis. These studies showed reduced, though not abrogated, fibrocyte recruitment and corresponding decreases in organ fibrosis (24, 229, 231, 358). Pilling and colleagues (2003) discovered that fibrocyte differentiation was impeded by exposure to serum amyloid P (SAP) (353). SAP was later found to confer protection in various models of fibrosis in which SAP was believed to inhibit fibrocyte recruitment and differentiation, suggesting that fibrocytes differentiation is essential in the development of fibrosis (60, 247, 353, 379). We showed that aPC treatment inhibited cellular infiltration, potentially by acting on circulating fibrocytes, which conferred protection against AngII-mediated myocardial fibrosis. Taken together, this data shows that fibrocytes are specifically recruited to sites of fibrosis and if their infiltration or differentiation is inhibited the resulting fibrosis is ameliorated. However, no evidence has yet to definitively show that fibrocytes explicitly cause fibrosis.

A study could be designed to address the causal role of fibrocytes in fibrosis. In theory, one could deplete a wild type mouse of monocytes, potentially using lipid-encapsulated clodrinate disodium, and then exposed the mice to fibrotic stimuli, such as AngII infusion. The resulting fibrosis could later be assessed and if the disease process was inhibited then that would provide evidence suggesting that monocytes are an important effector population. If monocyte depletion was effective, then differentiated fibrocytes, grown in culture from the same mouse strain, could then be injected into these mice after the initiation of the fibrogenic stimulus. It would still be difficult to completely assess function of fibrocytes in this study because the macrophage depletion treatment would have to stop, as to not potentially inhibit fibrocyte function. Therefore while the isolated fibrocytes would be supplemented in to this system and be the only initial circulating monocyte-like cell the, the endogenous monocyte population would be capable of replenishing itself. However, fibrocytes should be the primary early infiltrators and could be tracked either by deriving them from a GFP^+ mouse strain or by labeling them with a tracking dye such as CFSE. If fibrosis is then induced by the replenished fibrocyte in these previously monocyte depleted animals than that would provide evidence of a causal role for fibrocytes in the initiation of fibrosis.

9.6 Hypertension as a Fibrotic Stimulus

It has long been established that chronic hypertension promotes myocardial fibrosis and remodeling. Theoretically, hypertension induces myocardial stress and pressure-overload injury that then stimulates cellular infiltration and corresponding fibrosis. There has been some debate in the literature regarding the role of AngII in hypertension-mediated fibrosis. The vasoactive properties of AngII promote hypertension when serum levels are

elevated but there is also evidence that AngII has fibrogenic properties that are pressure-independent (5). Our studies using various anti-hypertensive therapies inhibited the development of myocardial fibrosis, supporting hypertension as a physiologic fibrotic stimulus. We used methods to block AngII-specific signaling as well as RAS-independent methods to inhibit hypertension, which not only inhibited ECM deposition but also inhibited fibrocyte infiltration and pro-fibrotic/inflammatory mediator expression. This data suggests that the influx of fibrocytes and other effector cells as well as the resulting fibrosis is, in part, hypertension dependent in an AngII infusion model. Interestingly, in our study using aPC as a therapeutic intervention, AngII-mediated hypertension was preserved during aPC treatment but the treatment still conferred protection against AngII-mediated fibrosis. Though we believe that aPC may circumvent the fibrotic effects on the heart in this model not by inhibiting hypertension but by directly acting on fibrocytes. However, this data would suggest that hypertension alone is not a sufficient enough stimulus to induce myocardial fibrosis. To further complicate our understanding of the role of hypertension in myocardial fibrosis, the use of anti-hypertensive agents clinically shows minimal benefit as a sole therapeutic intervention in many cardiovascular diseases (304-306). Anti-hypertensives are typically used in combination with other drugs, such as ACE inhibitors and/or β-blockers to maximize benefit. This data indicates that inhibiting hypertension is not sufficient to inhibit the progression of myocardial remodeling, including fibrosis. While conflicting, this evidence suggests that there are both pressure-independent and -dependent mechanisms that drive bothmyocardial fibrosis and the recruitment of fibrocytes.

9.7 Novel Anti-Fibrotic Therapeutics

As no current therapies currently exist that effectively target the pathologic fibrotic response evident in many cardiovascular diseases, we investigated the effect of a potential novel therapeutic for the treatment of fibrosis. We treated animals receiving AngII with a concurrent aPC infusion. In this study, we observed that aPC inhibited the infiltration of fibrocytes, the deposition of excess ECM proteins and the upregulation of pro-fibrotic and inflammatory mediators. However, we found that aPC did not mediate these beneficial effects through its well-established pro-survival or anti-coagulant properties. Furthermore, much of the protective effects of aPC were thought to be mediated by the stimulation of endothelial EPCR signaling; however, we found no supporting evidence for this in our model when we increased the endogenous endothelial aPC-EPCR signaling using transgenic mice that overexpress EPCR in endothelial cells. We could only speculate that aPC has direct inhibitory effect of the infiltrating fibrocytes. We detected EPCR transcript expression in fibrocyte rich cultures suggesting that they are capable of responding to aPC directly. The inhibitory effect of aPC on fibrocytes is supported by evidence suggesting that EPCR signaling inhibits monocyte chemotaxis and activation (328, 333). It is therefore plausible that aPC would confer similar effects on circulating fibrocytes as they are derived from the same monocyte progenitor population. This suggests that aPC may directly inhibit fibrocyte infiltration, activation and potentially differentiation. Thus aPC treatment may directly target the fibrogenic properties of this cell type, and as such, fibrosis itself.

The development of an anti-fibrotic treatment option would be a useful tool for clinicians treating patients with cardiovascular disease. By increasing myocardial stiffness, fibrosis can directly promote heart failure. However, fibrosis is also a putative reparative process that is initiated to compensate for cardiac injury. Studies have shown that if the fibrotic process is completely inhibited, then the muscular walls of the heart may not be able to sustain hemodynamic pressure after significant injury. This has been shown to promote ventricular rupture in animal models of myocardial fibrosis (384). Fibrocytes represent a unique avenue of potential therapy. Since fibrocytes infiltrate into tissues from circulation, inhibition of their recruitment, shouldn't disturb other processes that are essential to the maintenace of function in the heart. For example, inhibition of fibrocyte recruitment improves late scar formation in models of myocardial fibrosis but does not completely abrogate it because resident fibroblasts are still functional within the cardiac tissue. Therefore the heart is still capable of producing the ECM required to reinforcing the muscular structure, allowing the heart to endure increased hemodynamic pressure but the process may not become excessive. Inhibiting fibrocyte recruitment is also attractive because they appear to infiltrate tissues using different adhesion molecules and chemoattractant signals than other leukocytes. It is therefore possible that they may be targeted for inhibition while other leukocyte subsets, including monocytes, would not be affected, minimizing detrimental side effects of treatment. Therefore, if the appropriate lifestyle alterations could be made in combination with a suitable drug regimen developed to inhibit injurious physiologic stimuli (hypertension, clot formation, cholesterolemia), an anti-fibrotic agent such as a fibrocyte inhibitor would work well in this disease management scenario. Together, this regimen would be able to decrease the

initial injurious stimuli as well as the downstream fibrotic pathways, thus promoting preserved cardiac integrity and function. Furthermore, an anti-fibrotic intervention would be useful in treating patients receiving cardiotoxic drugs, such as establish chemotherapy treatments. In this scenario, individuals endure a non-ischemic myocardial insult and the use of a drug that inhibits cellular infiltration, corresponding fibrosis and potentially promotes cytoprotective signaling pathways would be an effective prophylactic treatment. The use of anti-fibrotic drugs clinically could be monitored using serum assays for Troponin T, a marker of myocardial damage, and perhaps serum CTGF, a putative fibrosis biomarker, in combination with regular imaging studies to monitor wall thickness and contraction. This would allow clinicians to monitor cardiac damage, degree of fibrosis, contractility and risk of free wall rupture.

9.8 Translating Basic Research into a Clinical Scenario

To assess the role of fibrocytes in complex clinical cases of myocardial fibrosis, we investigated the levels of circulating fibrocytes in patients with ischemic heart disease. We recruited patients that were scheduled for elective CABG surgery, as these patients initially present with established myocardial injury in which the reparative process would have already been initiated. We assessed baseline fibrocyte levels in circulation and investigated whether surgical trauma altered this level of fibrocytes. We detected a very small and unchanging population of collagen expressing circulating leukocytes. However, we were able to discern a population of circulating leukocytes with the potential to become an ECM producing cell. A population originating from the total isolated PBMCs remained viable in culture and developed became $CD45^{+}/Coll^{+}$, indicating that this population has the potential to develop into a fibrocyte phenotype.

From this data we can hypothesize that once this circulating population is recruited into tissue the cells likely differentiate into a classically described fibrocyte phenotype and actively produces ECM proteins to contribute to fibrosis. This circulating population appeared to be larger at baseline in patients with ischemic heart disease compared to healthy control subjects by assessing the number of $CD45^{+}/Coll^{+}$ evident in culture. Furthermore, this population appeared to be enhanced in patients 6 hours after CABG surgery suggesting that the surgical trauma promoted the mobilization of this progenitor cell type from bone marrow. These data support a potential function for fibrocytes in patients with ischemic heart disease.

9.9 Conclusion

We have effectively shown that a population of cells infiltrate into the myocardium prior to the deposition of extracellular matrix in a model of hypertensive-mediated cardiac remodeling. We have provided a phenotypic description of this infiltrating cell population and were one of the first groups to identify them as fibroblast progenitor cells, or fibrocytes. We have identified that CCL2/MCP-1 and/or CXCL12/SDF-1α do not appear to be required for recruitment of fibrocytes into the fibrotic heart, though they likely have alternative functional effects in the fibrotic process. We have shown that isolated fibrocytes produce pro-fibrotic factors, including CTGF and TGF-β, and the ECM protein collagen, suggesting that these cells can directly contribute to pathologic fibrosis. We identified aPC as a novel therapeutic agent that can inhibit cellular infiltration and fibrosis within the heart, potentially by having direct action on infiltrating fibrocytes. Lastly, we provide evidence that patients with ischemic heart disease have an increased circulating fibrocyte levels, compared to controls, which likely contribute to

myocardial fibrosis once recruited to the fibrotic cardiac tissue. Taken together, these data provide a significant contribution to our understanding of the mechanisms driving myocardial fibrosis.

The current state of our knowledge of myocardial fibrosis is expansive, however, there is a paucity of evidence relating to the early events responsible for initiating the development of fibrosis. Given this, our experimentation was designed to elucidate the effector cells and the early molecular signaling events promoting the initiation of fibrosis within the heart. We have provided pivotal data that addresses this important subject. Further elucidation of the early events of myocardial fibrosis will provide a more substantive foundation upon which to build effective experimentation into the development of anti-fibrotic therapies. This will allow clinicians to better tailor current therapeutic regimens, and potentially provide a larger armamentarium of therapeutic modalities for their patients.

REFERENCES

1 Canada H. Tracking Heart Disease and Stroke in Canada; 2009.

2 Wynn TA. Cellular and molecular mechanisms of fibrosis. *The Journal of Pathology* 2008; 214(2):199-210.

3 Berk BC, Fujiwara K, Lehoux S. ECM remodeling in hypertensive heart disease. *J Clin Invest* 2007; 117(3):568-575.

4 Hinglais N, Heudes D, Nicoletti A, Mandet C, Laurent M, Bariety J*, et al.* Colocalization of myocardial fibrosis and inflammatory cells in rats. *Laboratory investigation; a journal of technical methods and pathology* 1994; 70(2):286-294.

5 Kim S, Iwao H. Molecular and Cellular Mechanisms of Angiotensin II-Mediated Cardiovascular and Renal Diseases. *Pharmacol Rev* 2000; 52(1):11-34.

6 Kis K, Liu X, Hagood JS. Myofibroblast differentiation and survival in fibrotic disease. *Expert Reviews in Molecular Medicine* 2011; 13.

7 Liu J, Yang F, Yang X-P, Jankowski M, Pagano PJ. NAD(P)H Oxidase Mediates Angiotensin II-Induced Vascular Macrophage Infiltration and Medial Hypertrophy. *Arterioscler Thromb Vasc Biol* 2003; 23(5):776-782.

8 Chen Y, Arrigo A-P, Currie RW. Heat shock treatment suppresses angiotensin II-induced activation of NF-{kappa}B pathway and heart inflammation: a role for IKK depletion by heat shock? *Am J Physiol Heart Circ Physiol* 2004; 287(3):H1104-1114.

9 Sunderkotter C, Nikolic T, Dillon MJ, van Rooijen N, Stehling M, Drevets DA*, et al.* Subpopulations of Mouse Blood Monocytes Differ in Maturation Stage and Inflammatory Response. *J Immunol* 2004; 172(7):4410-4417.

10 Tacke F, Randolph GJ. Migratory fate and differentiation of blood monocyte subsets. *Immunobiology* 2006; 211(6-8):609-618.

11 Billet S, Aguilar F, Baudry C, Clauser E. Role of angiotensin II AT1 receptor activation in cardiovascular diseases. *Kidney Int* 2008; 74(11):1379-1384.

12 Li H-L, She Z-G, Li T-B, Wang A-B, Yang Q, Wei Y-S*, et al.* Overexpression of Myofibrillogenesis Regulator-1 Aggravates Cardiac Hypertrophy Induced by Angiotensin II in Mice. *Hypertension* 2007; 49(6):1399-1408.

13 Clauser E, Bouhnik J, Coezy E, Corvol P, Menard J. Synthesis and release of immunoreactive angiotensinogen by rat liver slices. *Endocrinology* 1983; 112(4):1188-1193.

14 Carey RM, Geary KM, Hunt MK, Ramos SP, Forbes MS, Inagami T*, et al.* Identification of individual renocortical cells that secrete renin. *American Journal of Physiology - Renal Physiology* 1990; 258(3):F649-F659.

15 Morris BJ, Catanzaro DF. Biosynthesis of preprorenin and intracellular conversion of prorenin to renin. *Clin Exp Pharmacol Physiol* 1981; 8(5):441-445.

16 Persson PB. Renin: origin, secretion and synthesis. *The Journal of Physiology* 2003; 552(3):667-671.

17 Laliberte F, Laliberte MF, Alhenc-Gelas F, Chevillard C. Cellular and subcellular immunohistochemical localization of angiotensin-converting enzyme in the rat adrenal gland. *Lab Invest* 1987; 56(4):364-371.

18 Kaschina E, Unger T. Angiotensin AT1/AT2 receptors: regulation, signalling and function. *Blood Press* 2003; 12(2):70-88.

19 Champman BJ, Books DP, Munday KA. Half-Life of Angiotensin II in the Concious and Barbituate-Anaethetized Rat *British Journal of Anaesthesia* 1980; 52(4):389-393.

20 Brasier AR, Recinos A, III, Eledrisi MS. Vascular Inflammation and the Renin-Angiotensin System. *Arterioscler Thromb Vasc Biol* 2002; 22(8):1257-1266.

21 Zhao Q, Ishibashi M, Hiasa K, Tan C, Takeshita A, Egashira K. Essential role of vascular endothelial growth factor in angiotensin II-induced vascular inflammation and remodeling. *Hypertension* 2004; 44(3):264-270.

22 Garg R, Yusuf S. Overview of randomized trials of angiotensin-converting enzyme inhibitors on mortality and morbidity in patients with heart failure. Collaborative Group on ACE Inhibitor Trials. *JAMA* 1995; 273(18):1450-1456.

23 Li W, Zheng X, Gu J, Hunter J, Ferrell GL, Lupu F*, et al.* Overexpressing endothelial cell protein C receptor alters the hemostatic balance and protects mice from endotoxin. *Journal of Thrombosis and Haemostasis* 2005; 3(7):1351-1359.

24 Haudek SB, Cheng J, Du J, Wang Y, Hermosillo-Rodriguez J, Trial J*, et al.* Monocytic fibroblast precursors mediate fibrosis in angiotensin-II-induced cardiac hypertrophy. *Journal of Molecular and Cellular Cardiology* 2010; 49(3):499-507.

25 Malpas SC, Groom AS, Head GA. Baroreflex Control of Heart Rate and Cardiac Hypertrophy in Angiotensin II¬ñInduced Hypertension in Rabbits. *Hypertension* 1997; 29(6):1284-1290.

26 Leri A, Fiordaliso F, Setoguchi M, Limana F, Bishopric NH, Kajstura J*, et al.* Inhibition of p53 Function Prevents Renin-Angiotensin System Activation and Stretch-Mediated Myocyte Apoptosis. *The American Journal of Pathology* 2000; 157(3):843-857.

27 Georgiopoulou VV, Kalogeropoulos AP, Raggi P, Butler J. Prevention, diagnosis, and treatment of hypertensive heart disease. *Cardiol Clin* 2010; 28(4):675-691.

28 Kranzhofer R, Schmidt J, Pfeiffer CAH, Hagl S, Libby P, Kubler W. Angiotensin Induces Inflammatory Activation of Human Vascular Smooth Muscle Cells. *Arterioscler Thromb Vasc Biol* 1999; 19(7):1623-1629.

29 Muller DN, Dechend R, Mervaala EM, Park JK, Schmidt F, Fiebeler A*, et al.* NF-kappaB inhibition ameliorates angiotensin II-induced inflammatory damage in rats. *Hypertension* 2000; 35(1 Pt 2):193-201.

30 Ruiz-Ortega M, Lorenzo O, Ruperez M, Blanco J, Egido J. Systemic Infusion of Angiotensin II into Normal Rats Activates Nuclear Factor-{{kappa}}B and AP-1 in the Kidney : Role of AT1 and AT2 Receptors. *Am J Pathol* 2001; 158(5):1743-1756.

31 Sadoshima J. Cytokine Actions of Angiotensin II. *Circ Res* 2000; 86(12):1187-1189.

32 Suzuki Y, Ruiz-Ortega M, Lorenzo O, Ruperez M, Esteban V, Egido J. Inflammation and angiotensin II. *The International Journal of Biochemistry & Cell Biology* 2003; 35(6):881-900.

33 Heitzer T, Schlinzig T, Krohn K, Meinertz T, Münzel T. Endothelial Dysfunction, Oxidative Stress, and Risk of Cardiovascular Events in Patients With Coronary Artery Disease. *Circulation* 2001; 104(22):2673-2678.

34 Sarkar S, Vellaichamy E, Young D, Sen S. Influence of cytokines and growth factors in ANG II-mediated collagen upregulation by fibroblasts in rats: role of myocytes. *American Journal of Physiology - Heart and Circulatory Physiology* 2004; 287(1):H107-H117.

35 Eguchi S, Numaguchi K, Iwasaki H, Matsumoto T, Yamakawa T, Utsunomiya H*, et al.* Calcium-dependent Epidermal Growth Factor Receptor Transactivation Mediates the Angiotensin II-induced Mitogen-activated Protein Kinase Activation in Vascular Smooth Muscle Cells. *Journal of Biological Chemistry* 1998; 273(15):8890-8896.

36 Ko WC, Hong CY, Hou SM, Lin CH, Ong ET, Lee CF*, et al.* Elevated Expression of Connective Tissue Growth Factor in Human Atrial Fibrillation and Angiotensin II-Treated Cardiomyocytes. *Circ J* 2011; 75(7):1592-1600.

37 Lopez B, Gonzalez A, Diez J. Role of matrix metalloproteinases in hypertension-associated cardiac fibrosis. *Curr Opin Nephrol Hypertens* 2004; 13(2):197-204.

38 Gajarsa J, Kloner R. Left ventricular remodeling in the post-infarction heart: a review of cellular, molecular mechanisms, and therapeutic modalities. *Heart Failure Reviews* 2011; 16(1):13-21.

39 Fomovsky GM, Thomopoulos S, Holmes JW. Contribution of extracellular matrix to the mechanical properties of the heart. *Journal of Molecular and Cellular Cardiology* 2010; 48(3):490-496.

40 Rossi MA. Pathologic fibrosis and connective tissue matrix in left ventricular hypertrophy due to chronic arterial hypertension in humans. *J Hypertens* 1998; 16(7):1031-1041.

41 Karl T W. Cardiac interstitium in health and disease: The fibrillar collagen network. *Journal of the American College of Cardiology* 1989; 13(7):1637-1652.

42 Heymans S, Schroen B, Vermeersch P, Milting H, Gao F, Kassner A*, et al.* Increased Cardiac Expression of Tissue Inhibitor of Metalloproteinase-1 and Tissue Inhibitor of Metalloproteinase-2 Is Related to Cardiac Fibrosis and Dysfunction in the Chronic Pressure-Overloaded Human Heart. *Circulation* 2005; 112(8):1136-1144.

43 Ali IU. Structural analysis of fibronectin and its collagen-binding fragment from several cell lines. *Proceedings of the National Academy of Sciences* 1984; 81(1):28-32.

44 Imanaka-Yoshida K, Enomoto-Iwamoto M, Yoshida T, Sakakura T. Vinculin, talin, integrin α6β1 and laminin can serve as components of attachment complex mediating contraction force transmission from cardiomyocytes to extracellular matrix. *Cell Motility and the Cytoskeleton* 1999; 42(1):1-11.

45 Wu X, Sun Z, Foskett A, Trzeciakowski JP, Meininger GA, Muthuchamy M. Cardiomyocyte contractile status is associated with differences in fibronectin and integrin interactions. *Am J Physiol Heart Circ Physiol* 2010; 298(6):H2071-2081.

46 Nawata J, Ohno I, Isoyama S, Suzuki J, Miura S, Ikeda J*, et al.* Differential expression of α1, α3 and α5 integrin subunits in acute and chronic stages of myocardial infarction in rats. *Cardiovascular Research* 1999; 43(2):371-381.

47 Shai S-Y, Harpf AE, Babbitt CJ, Jordan MC, Fishbein MC, Chen J*, et al.* Cardiac Myocyte-Specific Excision of the Beta1 Integrin Gene Results in Myocardial Fibrosis and Cardiac Failure. *Circulation Research* 2002; 90(4):458-464.

48 Ayada Y, Kusachi S, Murakami T, Hirohata S, Takemoto S, Komatsubara I*, et al.* Increase expression of biglycan mRNA in pressure-overloaded rat heart *Clinical and Experimental Hypertension* 2001; 23(8):633-643.

49 Grimm D, Huber M, Jabusch HC, Shakibaei M, Fredersdorf S, Paul M*, et al.* Extracellular Matrix Proteins in Cardiac Fibroblasts Derived from Rat Hearts with Chronic Pressure Overload: Effects of Beta-receptor Blockade. *Journal of Molecular and Cellular Cardiology* 2001; 33(3):487-501.

50 Laser M, Willey CD, Jiang W, Cooper G, Menick DR, Zile MR*, et al.* Integrin Activation and Focal Complex Formation in Cardiac Hypertrophy. *Journal of Biological Chemistry* 2000; 275(45):35624-35630.

51 Yamamoto K, Kusachi S, Ninomiya Y, Murakami M, Doi M, Takeda K*, et al.* Increase in the Expression of Biglycan mRNA Expression Co-localized Closely with that of Type I Collagen mRNA in the Infarct Zone After Experimentally-Induced Myocardial Infarction in Rats. *Journal of Molecular and Cellular Cardiology* 1998; 30(9):1749-1756.

52 Raspanti M, Viola M, Forlino A, Tenni R, Gruppi C, Tira ME. Glycosaminoglycans show a specific periodic interaction with type I collagen fibrils. *Journal of Structural Biology* 2008; 164(1):134-139.

53 Koli K, Saharinen J, Hyytiäinen M, Carita P, Keski-Oja J. Latency, activation, and binding proteins of TGF-β. *Microscopy Research and Technique* 2001; 52(4):354-362.

54 Tamaoki M, Imanaka-Yoshida K, Yokoyama K, Nishioka T, Inada H, Hiroe M*, et al.* Tenascin-C Regulates Recruitment of Myofibroblasts during Tissue Repair after Myocardial Injury. *The American Journal of Pathology* 2005; 167(1):71-80.

55 Zhou B, von Gise A, Ma Q, Hu YW, Pu WT. Genetic fate mapping demonstrates contribution of epicardium-derived cells to the annulus fibrosis of the mammalian heart. *Dev Biol* 2010; 338(2):251-261.

56 Huebener P, Abou-Khamis T, Zymek P, Bujak M, Ying X, Chatila K*, et al.* CD44 Is Critically Involved in Infarct Healing by Regulating the Inflammatory and Fibrotic Response. *The Journal of Immunology* 2008; 180(4):2625-2633.

57 Brower GL, Gardner JD, Forman MF, Murray DB, Voloshenyuk T, Levick SP*, et al.* The relationship between myocardial extracellular matrix remodeling and ventricular function. *European Journal of Cardio-Thoracic Surgery* 2006; 30(4):604-610.

58 Hutchinson KR, Stewart JA, Jr., Lucchesi PA. Extracellular matrix remodeling during the progression of volume overload-induced heart failure. *J Mol Cell Cardiol* 2009; 48(3):564-569.

59 Fujisawa G, Dilley R, Fullerton MJ, Funder JW. Experimental Cardiac Fibrosis: Differential Time Course of Responses to Mineralocorticoid-Salt Administration. *Endocrinology* 2001; 142(8):3625-3631.

60 Haudek SB, Xia Y, Huebener P, Lee JM, Carlson S, Crawford JR*, et al.* Bone marrow-derived fibroblast precursors mediate ischemic cardiomyopathy in mice. *Proc Natl Acad Sci U S A* 2006; 103(48):18284-18289.

61 Mann DLMD. Mechanisms and Models in Heart Failure: A Combinatorial Approach. *Circulation* 1999; 100(9):999-1008.

62 Brancato SK, Albina JE. Wound Macrophages as Key Regulators of Repair: Origin, Phenotype, and Function. *The American Journal of Pathology* 2010; 178(1):19-25.

63 Koh TJ, DiPietro LA. Inflammation and wound healing: the role of the macrophage. *Expert Reviews in Molecular Medicine* 2011; 13.

64 van Amerongen MJ, Harmsen MC, van Rooijen N, Petersen AH, van Luyn MJA. Macrophage Depletion Impairs Wound Healing and Increases Left Ventricular Remodeling after Myocardial Injury in Mice. *The American Journal of Pathology* 2007; 170(3):818-829.

65 Hanania R, Song Sun H, Xu K, Pustylnik S, Jeganathan S, Harrison RE. Classically Activated Macrophages Use Stable Microtubules for Matrix Metalloproteinase-9 (MMP-9) Secretion. *Journal of Biological Chemistry* 2012; 287(11):8468-8483.

66 Pellicoro A, Aucott RL, Ramachandran P, Robson AJ, Fallowfield JA, Snowdon VK*, et al.* Elastin accumulation is regulated at the level of degradation by macrophage metalloelastase (MMP-12) during experimental liver fibrosis. *Hepatology* 2011.

67 Mirza R, DiPietro LA, Koh TJ. Selective and Specific Macrophage Ablation Is Detrimental to Wound Healing in Mice. *The American Journal of Pathology* 2009; 175(6):2454-2462.

68 Goldsmith EC, Hoffman A, Morales MO, Potts JD, Price RL, McFadden A*, et al.* Organization of fibroblasts in the heart. *Developmental Dynamics* 2004; 230(4):787-794.

69 Kakkar R, Lee RT. Intramyocardial Fibroblast Myocyte Communication. *Circulation Research* 2010; 106(1):47-57.

70 Santiago J-J, Dangerfield AL, Rattan SG, Bathe KL, Cunnington RH, Raizman JE*, et al.* Cardiac fibroblast to myofibroblast differentiation in vivo and in vitro: Expression of focal adhesion components in neonatal and adult rat ventricular myofibroblasts. *Developmental Dynamics* 2010; 239(6):1573-1584.

71 Vasquez C, Benamer N, Morley GE. The Cardiac Fibroblast: Functional and Electrophysiological Considerations in Healthy and Diseased Hearts. *Journal of Cardiovascular Pharmacology* 2011; 57(4):380-388

72 Liu J, Wang Y, Pan Q, Su Y, Zhang Z, Han J*, et al.* Wntβ-catenin pathway forms a negative feedback loop during TGFβ- induced human normal skin fibroblast-to-myofibroblast transition. *Journal of Dermatological Science* 2012; 65(1):38-49.

73 Cucoranu I, Clempus R, Dikalova A, Phelan PJ, Ariyan S, Dikalov S*, et al.* NAD(P)H Oxidase 4 Mediates Transforming Growth Factor-β1-Induced Differentiation of Cardiac Fibroblasts Into Myofibroblasts. *Circulation Research* 2005; 97(9):900-907.

74 Dalla Costa AP, Clemente CFMZ, Carvalho HF, Carvalheira JB, Nadruz W, Franchini KG. FAK mediates the activation of cardiac fibroblasts induced by mechanical stress through regulation of the mTOR complex. *Cardiovascular Research* 2010; 86(3):421-431.

75 Galie PA, Russell MW, Westfall MV, Stegemann JP. Interstitial fluid flow and cyclic strain differentially regulate cardiac fibroblast activation via AT1R and TGF-β. *Experimental Cell Research* 2012; 318(1):75-84.

76 Kennedy L, Liu S, Shi-wen X, Chen Y, Eastwood M, Carter DE*, et al.* CCN2 is necessary for the function of mouse embryonic fibroblasts. *Experimental Cell Research* 2007; 313(5):952-964.

77 Leask A. Potential Therapeutic Targets for Cardiac Fibrosis: TGF{beta}, Angiotensin, Endothelin, CCN2, and PDGF, Partners in Fibroblast Activation. *Circ Res* 2010; 106(11):1675-1680.

78 Olson ER, Naugle JE, Zhang X, Bomser JA, Meszaros JG. Inhibition of cardiac fibroblast proliferation and myofibroblast differentiation by resveratrol. *American Journal of Physiology - Heart and Circulatory Physiology* 2005; 288(3):H1131-H1138.

79 van den Borne SWM, van de Schans VAM, Strzelecka AE, Vervoort-Peters HTM, Lijnen PM, Cleutjens JPM*, et al.* Mouse strain determines the outcome of wound healing after myocardial infarction. *Cardiovascular Research* 2009; 84(2):273-282.

80 Jin D, Takai S, Sugiyama T, Hayashi T, Fukumoto M, Oku H*, et al.* Long-term angiotensin II blockade may improve not only hyperglycemia but also age-associated cardiac fibrosis. *J Pharmacol Sci* 2009; 109(2):275-284.

81 Towbin JA. Scarring in the heart--a reversible phenomenon? *N Engl J Med* 2007; 357(17):1767-1768.

82 Aisagbonhi O, Rai M, Ryzhov S, Atria N, Feoktistov I, Hatzopoulos AK. Experimental myocardial infarction triggers canonical Wnt signaling and endothelial-to-mesenchymal transition. *Disease Models & Mechanisms* 2011; 4(4):469-483.

83 Widyantoro B, Emoto N, Nakayama K, Anggrahini DW, Adiarto S, Iwasa N*, et al.* Endothelial Cell,ÄìDerived Endothelin-1 Promotes Cardiac Fibrosis in Diabetic Hearts Through Stimulation of Endothelial-to-Mesenchymal Transition. *Circulation* 2010; 121(22):2407-2418.

84 Rajkumar V, Howell K, Csiszar K, Denton C, Black C, Abraham D. Shared expression of phenotypic markers in systemic sclerosis indicates a convergence of pericytes and fibroblasts to a myofibroblast lineage in fibrosis. *Arthritis Research & Therapy* 2005; 7(5):R1113 - R1123.

85 Abe R, Donnelly SC, Peng T, Bucala R, Metz CN. Peripheral Blood Fibrocytes: Differentiation Pathway and Migration to Wound Sites. *J Immunol* 2001; 166(12):7556-7562.

86 Iwano M, Plieth D, Danoff TM, Xue C, Okada H, Neilson EG. Evidence that fibroblasts derive from epithelium during tissue fibrosis. *J Clin Invest* 2002; 110(3):341-350.

87 Sallusto F, Mackay CR. Chemoattractants and their receptors in homeostasis and inflammation. *Curr Opin Immunol* 2004; 16(6):724-731.

88 Haudek SB, Trial J, Xia Y, Gupta D, Pilling D, Entman ML. Fc receptor engagement mediates differentiation of cardiac fibroblast precursor cells. *Proceedings of the National Academy of Sciences* 2008; 105(29):10179-10184.

89 Tamura Y, Matsumura K, Sano M, Tabata H, Kimura K, Ieda M*, et al.* Neural Crest-Derived Stem Cells Migrate and Differentiate Into Cardiomyocytes After Myocardial Infarction. *Arteriosclerosis, Thrombosis, and Vascular Biology* 2011; 31(3):582-589.

90 Deshmane SL, Kremlev S, Amini S, Sawaya BE. Monocyte chemoattractant protein-1 (MCP-1): an overview. *J Interferon Cytokine Res* 2009; 29(6):313-326.

91 Ekert J, Murray L, Das A, Sheng H, Giles-Komar J, Rycyzyn M. Chemokine (C-C motif) ligand 2 mediates direct and indirect fibrotic responses in human and murine cultured fibrocytes. *Fibrogenesis & Tissue Repair* 2011; 4(1):23.

92 Wang JM, Hishinuma A, Oppenheim JJ, Matsushima K. Studies of binding and internalization of human recombinant monocyte chemotactic and activating factor (MCAF) by monocytic cells. *Cytokine* 1993; 5(3):264-275.

93 Gharaee-Kermani M, Denholm EM, Phan SH. Costimulation of Fibroblast Collagen and Transforming Growth Factor β Gene Expression by Monocyte Chemoattractant Protein-1 via Specific Receptors. *Journal of Biological Chemistry* 1996; 271(30):17779-17784.

94 Tarzami ST, Calderon TM, Deguzman A, Lopez L, Kitsis RN, Berman JW. MCP-1/CCL2 protects cardiac myocytes from hypoxia-induced apoptosis by a G(alphai)-independent pathway. *Biochemical and Biophysical Research Communications* 2005; 335(4):1008-1016.

95 Chen X-L, Grey JY, Thomas S, Qiu F-H, Medford RM, Wasserman MA*, et al.* Sphingosine kinase-1 mediates TNF-α-induced MCP-1 gene expression in endothelial cells: upregulation by oscillatory flow. *American Journal of Physiology - Heart and Circulatory Physiology* 2004; 287(4):H1452-H1458.

96 Zhan Y, Kim S, Izumi Y, Izumiya Y, Nakao T, Miyazaki H*, et al.* Role of JNK, p38, and ERK in Platelet-Derived Growth Factor‚ÄìInduced Vascular Proliferation, Migration, and Gene Expression. *Arteriosclerosis, Thrombosis, and Vascular Biology* 2003; 23(5):795-801.

97 Rollins BJ, Yoshimura T, Leonard EJ, Pober JS. Cytokine-activated human endothelial cells synthesize and secrete a monocyte chemoattractant, MCP-1/JE. *Am J Pathol* 1990; 136(6):1229-1233.

98 Lakshminarayanan V, Lewallen M, Frangogiannis NG, Evans AJ, Wedin KE, Michael LH*, et al.* Reactive Oxygen Intermediates Induce Monocyte Chemotactic Protein-1 in Vascular Endothelium after Brief Ischemia. *The American Journal of Pathology* 2001; 159(4):1301-1311.

99 de Lemos JA, Morrow DA, Sabatine MS, Murphy SA, Gibson CM, Antman EM*, et al.* Association Between Plasma Levels of Monocyte Chemoattractant Protein-1 and Long-Term Clinical Outcomes in Patients With Acute Coronary Syndromes. *Circulation* 2003; 107(5):690-695.

100 Murakami Y, Kurosaki K, Matsui K, Shimada K, Ikeda U. Serum MCP-1 and VEGF Levels are not Affected by Inhibition of the Renin-Angiotensin System in Patients with Acute Myocardial Infarction. *Cardiovascular Drugs and Therapy* 2003; 17(3):249-255.

101 Sopel M, Ma I, Gelinas L, Oxner A, Myers T, Legare JF. Integrins and monocyte migration to the ischemic myocardium. *J Invest Surg* 2010; 23(2):79-86.

102 Dewald O, Zymek P, Winkelmann K, Koerting A, Ren G, Abou-Khamis T*, et al.* CCL2/Monocyte Chemoattractant Protein-1 Regulates Inflammatory Responses Critical to Healing Myocardial Infarcts. *Circulation Research* 2005; 96(8):881-889.

103 Hayashidani S, Tsutsui H, Shiomi T, Ikeuchi M, Matsusaka H, Suematsu N*, et al.* Anti-Monocyte Chemoattractant Protein-1 Gene Therapy Attenuates Left Ventricular Remodeling and Failure After Experimental Myocardial Infarction. *Circulation* 2003; 108(17):2134-2140.

104 Frangogiannis NG, Dewald O, Xia Y, Ren G, Haudek S, Leucker T*, et al.* Critical Role of Monocyte Chemoattractant Protein-1/CC Chemokine Ligand 2 in the Pathogenesis of Ischemic Cardiomyopathy. *Circulation* 2007; 115(5):584-592.

105 Abbott JD, Huang Y, Liu D, Hickey R, Krause DS, Giordano FJ. Stromal Cell‚ÄìDerived Factor-1Œ± Plays a Critical Role in Stem Cell Recruitment to the Heart After Myocardial Infarction but Is Not Sufficient to Induce Homing in the Absence of Injury. *Circulation* 2004; 110(21):3300-3305.

106 Askari AT, Unzek S, Popovic ZB, Goldman CK, Forudi F, Kiedrowski M*, et al.* Effect of stromal-cell-derived factor 1 on stem-cell homing and tissue regeneration in ischaemic cardiomyopathy. *The Lancet* 2003; 362(9385):697-703.

107 Chu P-Y, Zatta A, Kiriazis H, Chin-Dusting J, Du X-J, Marshall T*, et al.* CXCR4 Antagonism Attenuates the Cardiorenal Consequences of Mineralocorticoid Excess / Clinical Perspective. *Circulation: Heart Failure* 2011; 4(5):651-658.

108 Saxena A, Fish JE, White MD, Yu S, Smyth JWP, Shaw RM*, et al.* Stromal Cell-Derived Factor-1α Is Cardioprotective After Myocardial Infarction. *Circulation* 2008; 117(17):2224-2231.

109 Kucia M, Jankowski K, Reca R, Wysoczynski M, Bandura L, Allendorf D*, et al.* CXCR4–SDF-1 Signalling, Locomotion, Chemotaxis and Adhesion. *Journal of Molecular Histology* 2004; 35(3):233-245.

110 Hu X, Dai S, Wu W-J, Tan W, Zhu X, Mu J*, et al.* Stromal Cell-Derived Factor-1α Confers Protection Against Myocardial Ischemia/Reperfusion Injury. *Circulation* 2007; 116(6):654-663.

111 Misao Y, Takemura G, Arai M, Ohno T, Onogi H, Takahashi T*, et al.* Importance of recruitment of bone marrow-derived CXCR4+ cells in post-infarct cardiac repair mediated by G-CSF. *Cardiovascular Research* 2006; 71(3):455-465.

112 Tang J, Wang J, Song H, Huang Y, Yang J, Kong X*, et al.* Adenovirus-mediated stromal cell-derived factor-1 alpha gene transfer improves cardiac structure and function after experimental myocardial infarction through angiogenic and antifibrotic actions. *Molecular Biology Reports* 2010; 37(4):1957-1969.

113 Tang YL, Zhu W, Cheng M, Chen L, Zhang J, Sun T*, et al.* Hypoxic Preconditioning Enhances the Benefit of Cardiac Progenitor Cell Therapy for Treatment of Myocardial Infarction by Inducing CXCR4 Expression. *Circulation Research* 2009; 104(10):1209-1216.

114 Sasaki T, Fukazawa R, Ogawa S, Kanno S, Nitta T, Ochi M*, et al.* Stromal cell-derived factor-1α improves infarcted heart function through angiogenesis in mice. *Pediatrics International* 2007; 49(6):966-971.

115 Segers VFM, Tokunou T, Higgins LJ, MacGillivray C, Gannon J, Lee RT. Local Delivery of Protease-Resistant Stromal Cell Derived Factor-1 for Stem Cell Recruitment After Myocardial Infarction. *Circulation* 2007; 116(15):1683-1692.

116 Zhang M, Mal N, Kiedrowski M, Chacko M, Askari AT, Popovic ZB*, et al.* SDF-1 expression by mesenchymal stem cells results in trophic support of cardiac myocytes after myocardial infarction. *The FASEB Journal* 2007; 21(12):3197-3207.

117 Ghadge SK, Mühlstedt S, Pzcelik C, Bader M. SDF-1α as a therapeutic stem cell homing factor in myocardial infarction. *Pharmacology & Therapeutics* 2011; 129(1):97-108.

118 Pyo RT, Sui J, Dhume A, Palomeque J, Blaxall BC, Diaz G*, et al.* CXCR4 modulates contractility in adult cardiac myocytes. *Journal of Molecular and Cellular Cardiology* 2006; 41(5):834-844.

119 Chen J, Chemaly E, Liang L, Kho C, Lee A, Park J*, et al.* Effects of CXCR4 Gene Transfer on Cardiac Function After Ischemia-Reperfusion Injury. *The American Journal of Pathology* 2010; 176(4):1705-1715.

120 Hedayat M, Mahmoudi MJ, Rose NR, Rezaei N. Proinflammatory cytokines in heart failure: double-edged swords. *Heart Fail Rev* 2010; 15(6):543-562.

121 Blum A, Sclarovsky S, Rehavia E, Shohat B. Levels of T-lymphocyte subpopulations, interleukin-1β and soluble interleukin-2 receptor in acute myocardial infarction. *American Heart Journal* 1994; 127(5):1226-1230.

122 Torre-Amione G, Kapadia S, Benedict C, Oral H, Young JB, Mann DL. Proinflammatory cytokine levels in patients with depressed left ventricular ejection fraction: A report from the studies of left ventricular dysfunction (SOLVD). *Journal of the American College of Cardiology* 1996; 27(5):1201-1206.

123 Hao K, Hanawa H, Ding L, Ota Y, Yoshida K, Toba K*, et al.* Free heme is a danger signal inducing expression of proinflammatory proteins in cultured cells derived from normal rat hearts. *Molecular Immunology* 2011; 48(9-10):1191-1202.

124 Honsho S, Nishikawa S, Amano K, Zen K, Adachi Y, Kishita E*, et al.* Pressure-Mediated Hypertrophy and Mechanical Stretch Induces IL-1 Release and Subsequent IGF-1 Generation to Maintain Compensative Hypertrophy by Affecting Akt and JNK Pathways. *Circulation Research* 2009; 105(11):1149-1158.

125 Bujak M, Dobaczewski M, Chatila K, Mendoza LH, Li N, Reddy A*, et al.* Interleukin-1 Receptor Type I Signaling Critically Regulates Infarct Healing and Cardiac Remodeling. *The American Journal of Pathology* 2008; 173(1):57-67.

126 Dinarello CA, Cannon JG, Wolff SM, Bernheim HA, Beutler B, Cerami A*, et al.* Tumor necrosis factor (cachectin) is an endogenous pyrogen and induces production of interleukin 1. *J Exp Med* 1986; 163(6):1433-1450.

127 Chandrasekar B, Colston JT, de la Rosa SD, Rao PP, Freeman GL. TNF-α and H2O2 induce IL-18 and IL-18R beta expression in cardiomyocytes via NF-κB activation. *Biochemical and Biophysical Research Communications* 2003; 303(4):1152-1158.

128 Godambe SA, Chaplin DD, Bellone CJ. Regulation of IL-1 gene expression: Differential responsiveness of murine macrophage lines. *Cytokine* 1993; 5(4):327-335.

129 Libby P, Ordovas JM, Auger KR, Robbins AH, Birinyi LK, Dinarello CA. Endotoxin and tumor necrosis factor induce interleukin-1 gene expression in adult human vascular endothelial cells. *Am J Pathol* 1986; 124(2):179-185.

130 Hoffmann JN, Vollmar B, Laschke MW, Inthorn D, Fertmann J, Schildberg FW*, et al.* Microhemodynamic and cellular mechanisms of activated protein C action during endotoxemia. *Crit Care Med* 2004; 32(4):1011-1017.

131 Levine B, Kalman J, Mayer L, Fillit HM, Packer M. Elevated Circulating Levels of Tumor Necrosis Factor in Severe Chronic Heart Failure. *New England Journal of Medicine* 1990; 323(4):236-241.

132 Aukrust P, Ueland T, Lien E, Bendtzen K, Müller F, Andreassen AK*, et al.* Cytokine network in congestive heart failure secondary to ischemic or idiopathic dilated cardiomyopathy. *The American Journal of Cardiology* 1999; 83(3):376-382.

133 Cesari M, Penninx BWJH, Newman AB, Kritchevsky SB, Nicklas BJ, Sutton-Tyrrell K*, et al.* Inflammatory Markers and Onset of Cardiovascular Events. *Circulation* 2003; 108(19):2317-2322.

134 Vasan RS, Sullivan LM, Roubenoff R, Dinarello CA, Harris T, Benjamin EJ*, et al.* Inflammatory Markers and Risk of Heart Failure in Elderly Subjects Without Prior Myocardial Infarction. *Circulation* 2003; 107(11):1486-1491.

135 Ghezzi P, Dinarello CA, Bianchi M, Rosandich ME, Repine JE, White CW. Hypoxia increases production of interleukin-1 and tumor necrosis factor by human mononuclear cells. *Cytokine* 1991; 3(3):189-194.

136 Palmieri EA, Benincasa G, Di Rella F, Casaburi C, Monti MG, De Simone G*, et al.* Differential expression of TNF-alpha, IL-6, and IGF-1 by graded mechanical stress in normal rat myocardium. *American Journal of Physiology - Heart and Circulatory Physiology* 2002; 282(3):H926-H934.

137 Shivakumar K, Sollott SJ, Sangeetha M, Sapna S, Ziman B, Wang S*, et al.* Paracrine effects of hypoxic fibroblast-derived factors on the MPT-ROS threshold and viability of adult rat cardiac myocytes. *American Journal of Physiology - Heart and Circulatory Physiology* 2008; 294(6):H2653-H2658.

138 Hofmann U, Heuer S, Meder K, Boehler J, Lange V, Quaschning T*, et al.* The proinflammatory cytokines TNF-α and IL-1β impair economy of contraction in human myocardium. *Cytokine* 2007; 39(3):157-162.

139 Bozkurt B, Kribbs SB, Clubb FJ, Michael LH, Didenko VV, Hornsby PJ*, et al.* Pathophysiologically Relevant Concentrations of Tumor Necrosis Factor-Œ± Promote Progressive Left Ventricular Dysfunction and Remodeling in Rats. *Circulation* 1998; 97(14):1382-1391.

140 Dallas SL, Rosser JL, Mundy GR, Bonewald LF. Proteolysis of Latent Transforming Growth Factor-beta (TGF-β)-binding Protein-1 by Osteoclasts. *Journal of Biological Chemistry* 2002; 277(24):21352-21360.

141 Biernacka A, Dobaczewski M, Frangogiannis NG. TGF-β signaling in fibrosis. *Growth Factors* 2011; 29(5):196-202.

142 Kim J-S, Kim J-G, Moon M-Y, Jeon C-Y, Won H-Y, Kim H-J*, et al.* Transforming growth factor-β regulates macrophage migration via RhoA. *Blood* 2006; 108(6):1821-1829.

143 Kitamura M. Identification of an inhibitor targeting macrophage production of monocyte chemoattractant protein-1 as TGF-beta 1. *The Journal of Immunology* 1997; 159(3):1404-1411.

144 Desmouliére A, Geinoz A, Gabbiani F, Gabbiani G. Transforming growth factor-beta 1 induces alpha-smooth muscle actin expression in granulation tissue myofibroblasts and in quiescent and growing cultured fibroblasts. *The Journal of Cell Biology* 1993; 122(1):103-111.

145 Koitabashi N, Danner T, Zaiman AL, Pinto YM, Rowell J, Mankowski J*, et al.* Pivotal role of cardiomyocyte TGF-β signaling in the murine pathological response to sustained pressure overload. *The Journal of Clinical Investigation* 2011; 121(6):2301-2312.

146 Kobayashi T, Inoue T, Okada H, Kikuta T, Kanno Y, Nishida T*, et al.* Connective tissue growth factor mediates the profibrotic effects of transforming growth factor-β produced by tubular epithelial cells in response to high glucose. *Clinical and Experimental Nephrology* 2005; 9(2):114-121.

147 Nakerakanti SS, Bujor AM, Trojanowska M. CCN2 Is Required for the TGF-β Induced Activation of Smad1 - Erk1/2 Signaling Network. *PLoS One* 2011; 6(7):e21911.

148 Deten A, Hölzl A, Leicht M, Barth W, Zimmer H-G. Changes in Extracellular Matrix and in Transforming Growth Factor Beta Isoforms After Coronary Artery Ligation in Rats. *Journal of Molecular and Cellular Cardiology* 2001; 33(6):1191-1207.

149 Huntgeburth M, Tiemann K, Shahverdyan R, Schlūter K-D, Schreckenberg R, Gross M-L*, et al.* Transforming Growth Factor β, Oppositely Regulates the Hypertrophic and Contractile Response to β-Adrenergic Stimulation in the Heart. *PLoS One* 2011; 6(11):e26628.

150 Li J-M, Brooks G. Differential Protein Expression and Subcellular Distribution of TGFβ1, β2 and β3 in Cardiomyocytes During Pressure Overload-induced Hypertrophy. *Journal of Molecular and Cellular Cardiology* 1997; 29(8):2213-2224.

151 Pauschinger M, Knopf D, Petschauer S, Doerner A, Poller W, Schwimmbeck PL*, et al.* Dilated Cardiomyopathy Is Associated With Significant Changes in Collagen Type I/III ratio. *Circulation* 1999; 99(21):2750-2756.

152 Dobaczewski M, Chen W, Frangogiannis NG. Transforming growth factor (TGF)-beta signaling in cardiac remodeling. *J Mol Cell Cardiol* 2011; 51(4):600-606.

153 Daniels A, van Bilsen M, Goldschmeding R, van der Vusse GJ, van Nieuwenhoven FA. Connective tissue growth factor and cardiac fibrosis. *Acta Physiol (Oxf)* 2009; 195(3):321-338.

154 Yang M, Huang H, Li J, Li D, Wang H. Tyrosine phosphorylation of the LDL receptor-related protein (LRP) and activation of the ERK pathway are required for connective tissue growth factor to potentiate myofibroblast differentiation. *The FASEB Journal* 2004; 18(15):1920-1921.

155 Mercurio S, Latinkic B, Itasaki N, Krumlauf R, Smith JC. Connective-tissue growth factor modulates WNT signalling and interacts with the WNT receptor complex. *Development* 2004; 131(9):2137-2147.

156 Huang XR, Chung ACK, Yang F, Yue W, Deng C, Lau CP*, et al.* Smad3 Mediates Cardiac Inflammation and Fibrosis in Angiotensin II,ÄìInduced Hypertensive Cardiac Remodeling. *Hypertension* 2010; 55(5):1165-1171.

157 Mori T, Kawara S, Shinozaki M, Hayashi N, Kakinuma T, Igarashi A*, et al.* Role and interaction of connective tissue growth factor with transforming growth factor-β in persistent fibrosis: A mouse fibrosis model. *Journal of Cellular Physiology* 1999; 181(1):153-159.

158 Yang F, Chung ACK, Huang XR, Lan HY. Angiotensin II Induces Connective Tissue Growth Factor and Collagen I Expression via Transforming Growth Factor,ÄìŒ≤,ÄìDependent and ,ÄìIndependent Smad Pathways. *Hypertension* 2009; 54(4):877-884.

159 Koitabashi N, Arai M, Kogure S, Niwano K, Watanabe A, Aoki Y*, et al.* Increased Connective Tissue Growth Factor Relative to Brain Natriuretic Peptide as a Determinant of Myocardial Fibrosis. *Hypertension* 2007; 49(5):1120-1127.

160 Vallon V, Wyatt A, Klingel K, Huang D, Hussain A, Berchtold S*, et al.* SGK1-dependent cardiac CTGF formation and fibrosis following DOCA treatment. *Journal of Molecular Medicine* 2006; 84(5):396-404.

161 Hayata N, Fujio Y, Yamamoto Y, Iwakura T, Obana M, Takai M*, et al.* Connective tissue growth factor induces cardiac hypertrophy through Akt signaling. *Biochemical and Biophysical Research Communications* 2008; 370(2):274-278.

162 Grotendorst GR. Connective tissue growth factor: a mediator of TGF-β action on fibroblasts. *Cytokine & Growth Factor Reviews* 1997; 8(3):171-179.

163 Dean RG, Balding LC, Candido R, Burns WC, Cao Z, Twigg SM*, et al.* Connective Tissue Growth Factor and Cardiac Fibrosis after Myocardial Infarction. *Journal of Histochemistry & Cytochemistry* 2005; 53(10):1245-1256.

164 Finckenberg P, Inkinen K, Ahonen J, Merasto S, Louhelainen M, Vapaatalo H*, et al.* Angiotensin II Induces Connective Tissue Growth Factor Gene Expression via Calcineurin-Dependent Pathways. *The American Journal of Pathology* 2003; 163(1):355-366.

165 González A, López B, Ravassa S, Beaumont J, Arias T, Hermida N*, et al.* Biochemical markers of myocardial remodelling in hypertensive heart disease. *Cardiovascular Research* 2009; 81(3):509-518.

166 Hye-Ryong Shim A, Liu H, Focia PJ, Chen X, Lin PC, He X. Structures of a platelet-derived growth factor/propeptide complex and a platelet-derived growth factor/receptor complex. *Proceedings of the National Academy of Sciences* 2010; 107(25):11307-11312.

167 Zhao W, Zhao T, Huang V, Chen Y, Ahokas RA, Sun Y. Platelet-derived growth factor involvement in myocardial remodeling following infarction. *Journal of Molecular and Cellular Cardiology* 2011; 51(5):830-838.

168 Tangkijvanich P, Santiskulvong C, Melton AC, Rozengurt E, Yee HF. p38 MAP kinase mediates platelet-derived growth factor-stimulated migration of hepatic myofibroblasts. *Journal of Cellular Physiology* 2002; 191(3):351-361.

169 Thommen R, Humar R, Misevic G, Pepper MS, Hahn AWA, John M*, et al.* PDGF-BB increases endothelial migration and cord movements during angiogenesis in vitro. *Journal of Cellular Biochemistry* 1997; 64(3):403-413.

170 Uutela M, Wirzenius M, Paavonen K, Rajantie I, He Y, Karpanen T*, et al.* PDGF-D induces macrophage recruitment, increased interstitial pressure, and blood vessel maturation during angiogenesis. *Blood* 2004; 104(10):3198-3204.

171 Yoshida M, Sakuma J, Hayashi S, Abe K, Saito I, Harada S*, et al.* A histologically distinctive interstitial pneumonia induced by overexpression of the interleukin 6, transforming growth factor beta 1, or platelet-derived growth factor B gene. *Proceedings of the National Academy of Sciences* 1995; 92(21):9570-9574.

172 Younai S, Venters G, Vu S, Nichter L, Nimni ME, Tuan TL. Role of growth factors in scar contraction: an in vitro analysis. *Ann Plast Surg* 1996; 36(5):495-501.

173 Pontén A, Li X, Thorén P, Aase K, Sjöblom T, Östman A*, et al.* Transgenic Overexpression of Platelet-Derived Growth Factor-C in the Mouse Heart Induces Cardiac Fibrosis, Hypertrophy, and Dilated Cardiomyopathy. *The American Journal of Pathology* 2003; 163(2):673-682.

174 Chintalgattu V, Ai D, Langley RR, Zhang J, Bankson JA, Shih TL*, et al.* Cardiomyocyte PDGFR-β signaling is an essential component of the mouse cardiac response to load-induced stress. *The Journal of Clinical Investigation* 2010; 120(2):472-484.

175 Chu TF, Rupnick MA, Kerkela R, Dallabrida SM, Zurakowski D, Nguyen L*, et al.* Cardiotoxicity associated with tyrosine kinase inhibitor sunitinib. *The Lancet* 2007; 370(9604):2011-2019.

176 Wang Z, Kong D, Banerjee S, Li Y, Adsay NV, Abbruzzese J*, et al.* Down-regulation of Platelet-Derived Growth Factor-D Inhibits Cell Growth and Angiogenesis through Inactivation of Notch-1 and Nuclear Factor-κB Signaling. *Cancer Research* 2007; 67(23):11377-11385.

177 Vantler M, Karikkineth BC, Naito H, Tiburcy M, Didié M, Nose M*, et al.* PDGF-BB protects cardiomyocytes from apoptosis and improves contractile function of engineered heart tissue. *Journal of Molecular and Cellular Cardiology* 2010; 48(6):1316-1323.

178 Porter KE, Turner NA. Cardiac fibroblasts: At the heart of myocardial remodeling. *Pharmacology & Therapeutics* 2009; 123(2):255-278.

179 Simoons ML, Windecker S. Chronic stable coronary artery disease: drugs vs. revascularization. *European Heart Journal* 2010; 31(5):530-541.

180 Buja LM. Myocardial ischemia and reperfusion injury. *Cardiovascular Pathology* 2005; 14(4):170-175.

181 Suwaidi JA, Hamasaki S, Higano ST, Nishimura RA, Holmes DR, Lerman A. Long-Term Follow-Up of Patients With Mild Coronary Artery Disease and Endothelial Dysfunction. *Circulation* 2000; 101(9):948-954.

182 Smith SC, Allen J, Blair SN, Bonow RO, Brass LM, Fonarow GC*, et al.* AHA/ACC Guidelines for Secondary Prevention for Patients With Coronary and Other Atherosclerotic Vascular Disease: 2006 Update. *Circulation* 2006; 113(19):2363-2372.

183 Vaartjes I, Hoes AW, Reitsma JB, de Bruin A, Grobbee DE, Mosterd A*, et al.* Age- and gender-specific risk of death after first hospitalization for heart failure. *BMC Public Health* 2010; 10(1):637.

184 King SB, 3rd, Marshall JJ, Tummala PE. Revascularization for coronary artery disease: stents versus bypass surgery. *Annu Rev Med* 2010; 61:199-213.

185 Ptaszek LM, Mansour M, Ruskin JN, Chien KR. Towards regenerative therapy for cardiac disease. *The Lancet* 2012; 379(9819):933-942.

186 Schmieder RE, Hilgers KF, Schlaich MP, Schmidt BM. Renin-angiotensin system and cardiovascular risk. *Lancet* 2007; 369(9568):1208-1219.

187 Harada K, Komuro I, Shiojima I, Hayashi D, Kudoh S, Mizuno T*, et al.* Pressure Overload Induces Cardiac Hypertrophy in Angiotensin II Type 1A Receptor Knockout Mice. *Circulation* 1998; 97(19):1952-1959.

188 Kawano S, Kubota T, Monden Y, Tsutsumi T, Inoue T, Kawamura N*, et al.* Blockade of NF-kappaB improves cardiac function and survival after myocardial infarction. *Am J Physiol Heart Circ Physiol* 2006; 291(3):H1337-1344.

189 Kiarash A, Pagano PJ, Tayeh M, Rhaleb N-E, Carretero OA. Upregulated Expression of Rat Heart Intercellular Adhesion Molecule-1 in Angiotensin II- but Not Phenylephrine- Induced Hypertension. *Hypertension* 2001; 37(1):58-65.

190 Liu F, Levin MD, Petrenko NB, Lu MM, Wang T, Yuan LJ*, et al.* Histone-deacetylase inhibition reverses atrial arrhythmia inducibility and fibrosis in cardiac hypertrophy independent of angiotensin. *J Mol Cell Cardiol* 2008; 45(6):715-723.

191 Crabos M, Roth M, Hahn AW, Erne P. Characterization of angiotensin II receptors in cultured adult rat cardiac fibroblasts. Coupling to signaling systems and gene expression. *J Clin Invest* 1994; 93(6):2372-2378.

192 Dostal DE, Booz GW, Baker KM. Angiotensin II signalling pathways in cardiac fibroblasts: conventional versus novel mechanisms in mediating cardiac growth and function. *Mol Cell Biochem* 1996; 157(1-2):15-21.

193 Sadoshima J, Izumo S. Molecular characterization of angiotensin II--induced hypertrophy of cardiac myocytes and hyperplasia of cardiac fibroblasts. Critical role of the AT1 receptor subtype. *Circ Res* 1993; 73(3):413-423.

194 Zhou G, Kandala JC, Tyagi SC, Katwa LC, Weber KT. Effects of angiotensin II and aldosterone on collagen gene expression and protein turnover in cardiac fibroblasts. *Mol Cell Biochem* 1996; 154(2):171-178.

195 Phan SH. Fibroblast phenotypes in pulmonary fibrosis. *Am J Respir Cell Mol Biol* 2003; 29(3 Suppl):S87-92.

196 Phillips RJ, Burdick MD, Hong K, Lutz MA, Murray LA, Xue YY*, et al.* Circulating fibrocytes traffic to the lungs in response to CXCL12 and mediate fibrosis. *J Clin Invest* 2004; 114(3):438-446.

197 Zeisberg EM, Tarnavski O, Zeisberg M, Dorfman AL, McMullen JR, Gustafsson E*, et al.* Endothelial-to-mesenchymal transition contributes to cardiac fibrosis. *Nat Med* 2007; 13(8):952-961.

198 Endo J, Sano M, Fujita J, Hayashida K, Yuasa S, Aoyama N*, et al.* Bone Marrow-Derived Cells Are Involved in the Pathogenesis of Cardiac Hypertrophy in Response to Pressure Overload. *Circulation* 2007; 116(10):1176-1184.

199 Underwood RA, Gibran NS, Muffley LA, Usui ML, Olerud JE. Color subtractive-computer-assisted image analysis for quantification of cutaneous nerves in a diabetic mouse model. *J Histochem Cytochem* 2001; 49(10):1285-1291.

200 Frid MG, Brunetti JA, Burke DL, Carpenter TC, Davie NJ, Reeves JT*, et al.* Hypoxia-Induced Pulmonary Vascular Remodeling Requires Recruitment of Circulating Mesenchymal Precursors of a Monocyte/Macrophage Lineage. *Am J Pathol* 2006; 168(2):659-669.

201 Moore BB, Kolodsick JE, Thannickal VJ, Cooke K, Moore TA, Hogaboam C*, et al.* CCR2-Mediated Recruitment of Fibrocytes to the Alveolar Space after Fibrotic Injury. *Am J Pathol* 2005; 166(3):675-684.

202 Varda-Bloom N, Leor J, Ohad DG, Hasin Y, Amar M, Fixler R*, et al.* Cytotoxic T Lymphocytes Are Activated Following Myocardial Infarction and Can Recognize and Kill Healthy Myocytes In Vitro. *Journal of Molecular and Cellular Cardiology* 2000; 32(12):2141-2149.

203 Zamilpa R, Lindsey ML. Extracellular matrix turnover and signaling during cardiac remodeling following MI: Causes and consequences. *Journal of Molecular and Cellular Cardiology* 2010; 48(3):558-563.

204 Alexis D, Christine C, Giulio G. Tissue repair, contraction, and the myofibroblast. *Wound Repair and Regeneration* 2005; 13(1):7-12.

205 Reininger AJ. VWF attributes - impact on thrombus formation. *Thrombosis Research* 2008; 122(Supplement 4):S9-S13.

206 Handgretinger R, Gordon PR, Leimig T, Chen X, B‹Hring H-JR, Niethammer D*, et al.* Biology and Plasticity of CD133+ Hematopoietic Stem Cells. *Annals of the New York Academy of Sciences* 2003; 996(Hematopoeitic Stem Cells 2002: Genetics and Function: Fourth International Symposium):141-151.

207 Mohle R, Bautz F, Rafii S, Moore MAS, Brugger W, Kanz L. The Chemokine Receptor CXCR-4 Is Expressed on CD34+ Hematopoietic Progenitors and Leukemic Cells and Mediates Transendothelial Migration Induced by Stromal Cell-Derived Factor-1. *Blood* 1998; 91(12):4523-4530.

208 Bellini A, Mattoli S. The role of the fibrocyte, a bone marrow-derived mesenchymal progenitor, in reactive and reparative fibroses. *Lab Invest* 2007; 87(9):858-870.

209 Bucala R. Circulating Fibrocytes: Cellular Basis for NSF. *Journal of the American College of Radiology* 2008; 5(1):36-39.

210 Moreno M, Ramalho LN, Sancho-Bru P, Ruiz-Ortega M, Ramalho F, Abraldes JG*, et al.* Atorvastatin attenuates angiotensin II-induced inflammatory actions in the liver. *Am J Physiol Gastrointest Liver Physiol* 2009; 296(2):G147-156.

211 Sakai N, Wada T, Matsushima K, Bucala R, Iwai M, Horiuchi M*, et al.* The renin-angiotensin system contributes to renal fibrosis through regulation of fibrocytes. *Journal of Hypertension* 2008; 26(4):780-790.

212 Pinzani M, Rombouts K. Liver fibrosis: from the bench to clinical targets. *Digestive and Liver Disease* 2004; 36(4):231-242.

213 Swartz RD. Idiopathic Retroperitoneal Fibrosis: A Review of the Pathogenesis and Approaches to Treatment. *American Journal of Kidney Diseases* 2009; 54(3):546-553.

214 Sopel MJ, Rosin NL, Lee TDG, Legare J-F. Myocardial fibrosis in response to Angiotensin II is preceded by the recruitment of mesenchymal progenitor cells. *Lab Invest* 2010; 23(2):79-86.

215 Hart-Matyas M, Nejat S, Jordan JL, Hirsch GM, Lee TDG. IFN-[gamma] and Fas/FasL pathways cooperate to induce medial cell loss and neointimal lesion formation in allograft vasculopathy. *Transplant Immunology* 2010; 22(3-4):157-164.

216 Hellemans J, Mortier G, De Paepe A, Speleman F, Vandesompele J. qBase relative quantification framework and software for management and automated analysis of real-time quantitative PCR data. *Genome Biol* 2007; 8(2):R19.

217 Hong KM, Burdick MD, Phillips RJ, Heber D, Strieter RM. Characterization of human fibrocytes as circulating adipocyte progenitors and the formation of human adipose tissue in SCID mice. *FASEB J* 2005; 19(14):2029-2031.

218 Sakai N, Wada T, Yokoyama H, Lipp M, Ueha S, Matsushima K*, et al.* Secondary lymphoid tissue chemokine (SLC/CCL21)/CCR7 signaling regulates fibrocytes in renal fibrosis. *Proc Natl Acad Sci U S A* 2006; 103(38):14098-14103.

219 Chu PY, Mariani J, Finch S, McMullen JR, Sadoshima J, Marshall T*, et al.* Bone Marrow-Derived Cells Contribute to Fibrosis in the Chronically Failing Heart. *Am J Pathol* 2010; 176(4):1735-1742.

220 Keeley EC, Mehrad B, Strieter RM. The role of circulating mesenchymal progenitor cells (fibrocytes) in the pathogenesis of fibrotic disorders. *Thromb Haemost* 2009; 101(4):613-618.

221 Chesney J, Metz C, Stavitsky AB, Bacher M, Bucala R. Regulated production of type I collagen and inflammatory cytokines by peripheral blood fibrocytes. *J Immunol* 1998; 160(1):419-425.

222 Quan TE, Cowper S, Wu SP, Bockenstedt LK, Bucala R. Circulating fibrocytes: collagen-secreting cells of the peripheral blood. *Int J Biochem Cell Biol* 2004; 36(4):598-606.

223 Segers VF, Lee RT. Stem-cell therapy for cardiac disease. *Nature* 2008; 451(7181):937-942.

224 Collins JM, Russell B. Stem cell therapy for cardiac repair. *J Cardiovasc Nurs* 2009; 24(2):93-97.

225 Joggerst SJ, Hatzopoulos AK. Stem cell therapy for cardiac repair: benefits and barriers. *Expert Rev Mol Med* 2009; 11:e20.

226 Passier R, van Laake LW, Mummery CL. Stem-cell-based therapy and lessons from the heart. *Nature* 2008; 453(7193):322-329.

227 Rosin NL, Sopel M, Falkenham A, Myers TL, Legare JF. Myocardial migration by fibroblast progenitor cells is blood pressure dependent in a model of angII myocardial fibrosis. *Hypertens Res* 2012; 35(4):449-456.

228 Sopel M, Falkenham A, Oxner A, Ma I, Lee TD, Legare JF. Fibroblast progenitor cells are recruited into the myocardium prior to the development of myocardial fibrosis. *Int J Exp Pathol* 2012; 93(2):115-124.

229 Xu J, Lin SC, Chen J, Miao Y, Taffet GE, Entman ML*, et al.* CCR2 mediates the uptake of bone marrow-derived fibroblast precursors in angiotensin II-induced cardiac fibrosis. *Am J Physiol Heart Circ Physiol* 2011; 301(2):H538-547.

230 Mehrad B, Burdick MD, Strieter RM. Fibrocyte CXCR4 regulation as a therapeutic target in pulmonary fibrosis. *The International Journal of Biochemistry & Cell Biology* 2009; 41(8-9):1708-1718.

231 Song JS, Kang CM, Kang HH, Yoon HK, Kim YK, Kim KH*, et al.* Inhibitory effect of CXC chemokine receptor 4 antagonist AMD3100 on bleomycin induced murine pulmonary fibrosis. *Exp Mol Med* 2010; 42(6):465-472.

232 Leone AM, Rutella S, Bonanno G, Contemi AM, de Ritis DG, Giannico MB*, et al.* Endogenous G-CSF and CD34+ cell mobilization after acute myocardial infarction. *Int J Cardiol* 2006; 111(2):202-208.

233 Ma N, Stamm C, Kaminski A, Li W, Kleine HD, Muller-Hilke B*, et al.* Human cord blood cells induce angiogenesis following myocardial infarction in NOD/scid-mice. *Cardiovasc Res* 2005; 66(1):45-54.

234 Yamani MH, Ratliff NB, Cook DJ, Tuzcu EM, Yu Y, Hobbs R*, et al.* Peritransplant ischemic injury is associated with up-regulation of stromal cell-derived factor-1. *J Am Coll Cardiol* 2005; 46(6):1029-1035.

235 Moore BB, Paine R, 3rd, Christensen PJ, Moore TA, Sitterding S, Ngan R*, et al.* Protection from pulmonary fibrosis in the absence of CCR2 signaling. *J Immunol* 2001; 167(8):4368-4377.

236 Sakai N, Wada T, Furuichi K, Shimizu K, Kokubo S, Hara A*, et al.* MCP-1/CCR2-dependent loop for fibrogenesis in human peripheral CD14-positive monocytes. *J Leukoc Biol* 2006; 79(3):555-563.

237 Seki E, de Minicis S, Inokuchi S, Taura K, Miyai K, van Rooijen N*, et al.* CCR2 promotes hepatic fibrosis in mice. *Hepatology* 2009; 50(1):185-197.

238 Kitagawa K, Wada T, Furuichi K, Hashimoto H, Ishiwata Y, Asano M*, et al.* Blockade of CCR2 ameliorates progressive fibrosis in kidney. *Am J Pathol* 2004; 165(1):237-246.

239 Levesque JP, Hendy J, Takamatsu Y, Simmons PJ, Bendall LJ. Disruption of the CXCR4/CXCL12 chemotactic interaction during hematopoietic stem cell mobilization induced by GCSF or cyclophosphamide. *J Clin Invest* 2003; 111(2):187-196.

240 Dai S, Yuan F, Mu J, Li C, Chen N, Guo S*, et al.* Chronic AMD3100 antagonism of SDF-1alpha-CXCR4 exacerbates cardiac dysfunction and remodeling after myocardial infarction. *J Mol Cell Cardiol* 2010; 49(4):587-597.

241 Rosenberg HF. Cytokines and fibrocyte differentiation -- altering the balance: an interview with Dr. Darrell Pilling. Interview by Helene F. Rosenberg. *J Leukoc Biol* 2008; 83(6):1334-1335.

242 De Clercq E. Recent advances on the use of the CXCR4 antagonist plerixafor (AMD3100, Mozobil) and potential of other CXCR4 antagonists as stem cell mobilizers. *Pharmacol Ther* 2010; 128(3):509-518.

243 De Falco E, Porcelli D, Torella AR, Straino S, Iachininoto MG, Orlandi A*, et al.* SDF-1 involvement in endothelial phenotype and ischemia-induced recruitment of bone marrow progenitor cells. *Blood* 2004; 104(12):3472-3482.

244 Suuronen EJ, Price J, Veinot JP, Ascah K, Kapila V, Guo XW*, et al.* Comparative effects of mesenchymal progenitor cells, endothelial progenitor cells, or their combination on myocardial infarct regeneration and cardiac function. *J Thorac Cardiovasc Surg* 2007; 134(5):1249-1258.

245 Zhuang Y, Chen X, Xu M, Zhang LY, Xiang F. Chemokine stromal cell-derived factor 1/CXCL12 increases homing of mesenchymal stem cells to injured myocardium and neovascularization following myocardial infarction. *Chin Med J (Engl)* 2009; 122(2):183-187.

246 Devine SM, Flomenberg N, Vesole DH, Liesveld J, Weisdorf D, Badel K*, et al.* Rapid mobilization of CD34+ cells following administration of the CXCR4 antagonist AMD3100 to patients with multiple myeloma and non-Hodgkin's lymphoma. *J Clin Oncol* 2004; 22(6):1095-1102.

247 Murray LA, Chen Q, Kramer MS, Hesson DP, Argentieri RL, Peng X*, et al.* TGF-beta driven lung fibrosis is macrophage dependent and blocked by Serum amyloid P. *Int J Biochem Cell Biol* 2011; 43(1):154-162.

248 Gurtner GC, Werner S, Barrandon Y, Longaker MT. Wound repair and regeneration. *Nature* 2008; 453(7193):314-321.

249 Sun Y. Intracardiac renin-angiotensin system and myocardial repair/remodeling following infarction. *J Mol Cell Cardiol* 2009; 48(3):483-489.

250 Mervaala E, Muller DN, Schmidt F, Park J-K, Gross V, Bader M*, et al.* Blood Pressure-Independent Effects in Rats With Human Renin and Angiotensinogen Genes. *Hypertension* 2000; 35(2):587-594.

251 Kai H, Kudo H, Takayama N, Yasuoka S, Kajimoto H, Imaizumi T. Large blood pressure variability and hypertensive cardiac remodeling--role of cardiac inflammation. *Circ J* 2009; 73(12):2198-2203.

252 Sun Y. Myocardial repair/remodelling following infarction: roles of local factors. *Cardiovasc Res* 2009; 81(3):482-490.

253 Pilling D, Fan T, Huang D, Kaul B, Gomer RH. Identification of markers that distinguish monocyte-derived fibrocytes from monocytes, macrophages, and fibroblasts. *PLoS One* 2009; 4(10):e7475.

254 Andersson-Sjoland A, de Alba CG, Nihlberg K, Becerril C, Ramirez R, Pardo A*, et al.* Fibrocytes are a potential source of lung fibroblasts in idiopathic pulmonary fibrosis. *Int J Biochem Cell Biol* 2008; 40(10):2129-2140.

255 Kisseleva T, Uchinami H, Feirt N, Quintana-Bustamante O, Segovia JC, Schwabe RF*, et al.* Bone marrow-derived fibrocytes participate in pathogenesis of liver fibrosis. *J Hepatol* 2006; 45(3):429-438.

256 Roderfeld M, Rath T, Voswinckel R, Dierkes C, Dietrich H, Zahner D*, et al.* Bone marrow transplantation demonstrates medullar origin of CD34+ fibrocytes and ameliorates hepatic fibrosis in Abcb4-/- mice. *Hepatology* 2010; 51(1):267-276.

257 Wang JF, Jiao H, Stewart TL, Shankowsky HA, Scott PG, Tredget EE. Fibrocytes from burn patients regulate the activities of fibroblasts. *Wound Repair Regen* 2007; 15(1):113-121.

258 Rosenkranz S. TGF-beta1 and angiotensin networking in cardiac remodeling. *Cardiovasc Res* 2004; 63(3):423-432.

259 Ruiz-Ortega M, Rodriguez-Vita J, Sanchez-Lopez E, Carvajal G, Egido J. TGF-beta signaling in vascular fibrosis. *Cardiovasc Res* 2007; 74(2):196-206.

260 Chen MM, Lam A, Abraham JA, Schreiner GF, Joly AH. CTGF expression is induced by TGF- beta in cardiac fibroblasts and cardiac myocytes: a potential role in heart fibrosis. *J Mol Cell Cardiol* 2000; 32(10):1805-1819.

261 Sonnylal S, Shi-Wen X, Leoni P, Naff K, Van Pelt CS, Nakamura H*, et al.* Selective expression of connective tissue growth factor in fibroblasts in vivo promotes systemic tissue fibrosis. *Arthritis Rheum* 2010; 62(5):1523-1532.

262 Shi-Wen X, Leask A, Abraham D. Regulation and function of connective tissue growth factor/CCN2 in tissue repair, scarring and fibrosis. *Cytokine Growth Factor Rev* 2008; 19(2):133-144.

263 Wang GW, Kang YJ. Inhibition of doxorubicin toxicity in cultured neonatal mouse cardiomyocytes with elevated metallothionein levels. *J Pharmacol Exp Ther* 1999; 288(3):938-944.

264 He Z, Way KJ, Arikawa E, Chou E, Opland DM, Clermont A*, et al.* Differential regulation of angiotensin II-induced expression of connective tissue growth factor by protein kinase C isoforms in the myocardium. *J Biol Chem* 2005; 280(16):15719-15726.

265 Ruperez M, Lorenzo O, Blanco-Colio LM, Esteban V, Egido J, Ruiz-Ortega M. Connective tissue growth factor is a mediator of angiotensin II-induced fibrosis. *Circulation* 2003; 108(12):1499-1505.

266 Suzuki J, Matsubara H, Urakami M, Inada M. Rat angiotensin II (type 1A) receptor mRNA regulation and subtype expression in myocardial growth and hypertrophy. *Circ Res* 1993; 73(3):439-447.

267 Bradham DM, Igarashi A, Potter RL, Grotendorst GR. Connective tissue growth factor: a cysteine-rich mitogen secreted by human vascular endothelial cells is related to the SRC-induced immediate early gene product CEF-10. *J Cell Biol* 1991; 114(6):1285-1294.

268 Igarashi A, Okochi H, Bradham DM, Grotendorst GR. Regulation of connective tissue growth factor gene expression in human skin fibroblasts and during wound repair. *Mol Biol Cell* 1993; 4(6):637-645.

269 Wang Q, Usinger W, Nichols B, Gray J, Xu L, Seeley TW*, et al.* Cooperative interaction of CTGF and TGF-beta in animal models of fibrotic disease. *Fibrogenesis Tissue Repair* 2011; 4(1):4.

270 Ahmed MS, ÿie E, Vinge LE, Yndestad A, ÿystein Andersen G, Andersson Y*, et al.* Connective tissue growth factor--a novel mediator of angiotensin II-stimulated cardiac fibroblast activation in heart failure in rats. *Journal of Molecular and Cellular Cardiology* 2004; 36(3):393-404.

271 Grotendorst GR, Duncan MR. Individual domains of connective tissue growth factor regulate fibroblast proliferation and myofibroblast differentiation. *FASEB J* 2005; 19(7):729-738.

272 Garrett Q, Khaw PT, Blalock TD, Schultz GS, Grotendorst GR, Daniels JT. Involvement of CTGF in TGF-beta1-stimulation of myofibroblast differentiation and collagen matrix contraction in the presence of mechanical stress. *Invest Ophthalmol Vis Sci* 2004; 45(4):1109-1116.

273 Lee CH, Shah B, Moioli EK, Mao JJ. CTGF directs fibroblast differentiation from human mesenchymal stem/stromal cells and defines connective tissue healing in a rodent injury model. *J Clin Invest* 2010; 120(9):3340-3349.

274 Zhang W, Liu HT. MAPK signal pathways in the regulation of cell proliferation in mammalian cells. *Cell Res* 2002; 12(1):9-18.

275 Sanchez-Lopez E, Rayego S, Rodrigues-Diez R, Rodriguez JS, Rodriguez-Vita J, Carvajal G*, et al.* CTGF promotes inflammatory cell infiltration of the renal interstitium by activating NF-kappaB. *J Am Soc Nephrol* 2009; 20(7):1513-1526.

276 Reunanen N, Foschi M, Han J, Kahari VM. Activation of extracellular signal-regulated kinase 1/2 inhibits type I collagen expression by human skin fibroblasts. *J Biol Chem* 2000; 275(44):34634-34639.

277 Ikawa Y, Ng PS, Endo K, Kondo M, Chujo S, Ishida W*, et al.* Neutralizing monoclonal antibody to human connective tissue growth factor ameliorates transforming growth factor-beta-induced mouse fibrosis. *J Cell Physiol* 2008; 216(3):680-687.

278 Wang X, Wu G, Gou L, Liu Z, Fan X, Wu L*, et al.* A novel single-chain-Fv antibody against connective tissue growth factor attenuates bleomycin-induced pulmonary fibrosis in mice. *Respirology* 2011; 16(3):500-507.

279 Yokoi H, Mukoyama M, Nagae T, Mori K, Suganami T, Sawai K*, et al.* Reduction in connective tissue growth factor by antisense treatment ameliorates renal tubulointerstitial fibrosis. *J Am Soc Nephrol* 2004; 15(6):1430-1440.

280 Adler SG, Schwartz S, Williams ME, Arauz-Pacheco C, Bolton WK, Lee T*, et al.* Phase 1 study of anti-CTGF monoclonal antibody in patients with diabetes and microalbuminuria. *Clin J Am Soc Nephrol* 2010; 5(8):1420-1428.

281 Brigstock DR. Strategies for blocking the fibrogenic actions of connective tissue growth factor (CCN2): From pharmacological inhibition in vitro to targeted siRNA therapy in vivo. *J Cell Commun Signal* 2009; 3(1):5-18.

282 de Resende MM, Kauser K, Mill JG. Regulation of cardiac and renal mineralocorticoid receptor expression by captopril following myocardial infarction in rats. *Life Sciences* 2006; 78(26):3066-3073.

283 Ishiyama Y, Gallagher PE, Averill DB, Tallant EA, Brosnihan KB, Ferrario CM. Upregulation of Angiotensin-Converting Enzyme 2 After Myocardial Infarction by Blockade of Angiotensin II Receptors. *Hypertension* 2004; 43(5):970-976.

284 Dostal DE, Rothblum KN, Chernin MI, Cooper GR, Baker KM. Intracardiac detection of angiotensinogen and renin: a localized renin-angiotensin system in neonatal rat heart. *Am J Physiol* 1992; 263(4 Pt 1):C838-850.

285 Mehta PK, Griendling KK. Angiotensin II cell signaling: physiological and pathological effects in the cardiovascular system. *Am J Physiol Cell Physiol* 2007; 292(1):C82-97.

286 Inaba S, Iwai M, Furuno M, Kanno H, Senba I, Okayama H*, et al.* Temporary treatment with AT1 receptor blocker, valsartan, from early stage of hypertension prevented vascular remodeling. *Am J Hypertens* 2011; 24(5):550-556.

287 Li C, Salisbury R, Ely D. Hydralazine Reverses Stress-Induced Elevations in Blood Pressure, Angiotensin II, Testosterone, and Coronary Pathology in a Social Colony Model. *ISRN Pathology* 2011.

288 Castano AP, Lin SL, Surowy T, Nowlin BT, Turlapati SA, Patel T*, et al.* Serum amyloid P inhibits fibrosis through Fc gamma R-dependent monocyte-macrophage regulation in vivo. *Sci Transl Med* 2009; 1(5):5ra13.

289 Marvar PJ, Thabet SR, Guzik TJ, Lob HE, McCann LA, Weyand C*, et al.* Central and peripheral mechanisms of T-lymphocyte activation and vascular inflammation produced by angiotensin II-induced hypertension. *Circ Res* 2010; 107(2):263-270.

290 Qi G, Jia L, Li Y, Bian Y, Cheng J, Li H*, et al.* Angiotensin II infusion-induced inflammation, monocytic fibroblast precursor infiltration, and cardiac fibrosis are pressure dependent. *Cardiovasc Toxicol* 2011; 11(2):157-167.

291 Wang X, McLennan SV, Allen TJ, Twigg SM. Regulation of pro-inflammatory and pro-fibrotic factors by CCN2/CTGF in H9c2 cardiomyocytes. *J Cell Commun Signal* 2010; 4(1):15-23.

292 Frenette PS, Wagner DD. Adhesion molecules--Part II: Blood vessels and blood cells. *N Engl J Med* 1996; 335(1):43-45.

293 Frenette PS, Wagner DD. Adhesion molecules--Part 1. *N Engl J Med* 1996; 334(23):1526-1529.

294 Luster AD. Chemokines--chemotactic cytokines that mediate inflammation. *N Engl J Med* 1998; 338(7):436-445.

295 Olson TS, Ley K. Chemokines and chemokine receptors in leukocyte trafficking. *Am J Physiol Regul Integr Comp Physiol* 2002; 283(1):R7-28.

296 Paradis P, Dali-Youcef N, Paradis FW, Thibault G, Nemer M. Overexpression of angiotensin II type I receptor in cardiomyocytes induces cardiac hypertrophy and remodeling. *Proc Natl Acad Sci U S A* 2000; 97(2):931-936.

297 Watanabe D, Tanabe A, Naruse M, Morikawa S, Ezaki T, Takano K. Renoprotective effects of an angiotensin II receptor blocker in experimental model rats with hypertension and metabolic disorders. *Hypertens Res* 2009; 32(9):807-815.

298 Shibata S, Nagase M, Yoshida S, Kawachi H, Fujita T. Podocyte as the target for aldosterone: roles of oxidative stress and Sgk1. *Hypertension* 2007; 49(2):355-364.

299 Cheng XW, Okumura K, Kuzuya M, Jin Z, Nagata K, Obata K*, et al.* Mechanism of diastolic stiffening of the failing myocardium and its prevention by angiotensin receptor and calcium channel blockers. *J Cardiovasc Pharmacol* 2009; 54(1):47-56.

300 Habibi J, DeMarco VG, Ma L, Pulakat L, Rainey WE, Whaley-Connell AT*, et al.* Mineralocorticoid receptor blockade improves diastolic function independent of blood pressure reduction in a transgenic model of RAAS overexpression. *Am J Physiol Heart Circ Physiol* 2011; 300(4):H1484-1491.

301 Nagata K, Obata K, Xu J, Ichihara S, Noda A, Kimata H*, et al.* Mineralocorticoid receptor antagonism attenuates cardiac hypertrophy and failure in low-aldosterone hypertensive rats. *Hypertension* 2006; 47(4):656-664.

302 Knowles HJ, Tian YM, Mole DR, Harris AL. Novel mechanism of action for hydralazine: induction of hypoxia-inducible factor-1alpha, vascular endothelial growth factor, and angiogenesis by inhibition of prolyl hydroxylases. *Circ Res* 2004; 95(2):162-169.

303 Rey S, Semenza GL. Hypoxia-inducible factor-1-dependent mechanisms of vascularization and vascular remodelling. *Cardiovasc Res* 2010; 86(2):236-242.

304 Greenberg B, Massie B, Bristow JD, Cheitlin M, Siemienczuk D, Topic N*, et al.* Long-term vasodilator therapy of chronic aortic insufficiency. A randomized double-blinded, placebo-controlled clinical trial. *Circulation* 1988; 78(1):92-103.

305 Lin M, Chiang HT, Lin SL, Chang MS, Chiang BN, Kuo HW*, et al.* Vasodilator therapy in chronic asymptomatic aortic regurgitation: enalapril versus hydralazine therapy. *J Am Coll Cardiol* 1994; 24(4):1046-1053.

306 Schmieder RE, Schlaich MP, Klingbeil AU, Martus P. Update on reversal of left ventricular hypertrophy in essential hypertension (a meta-analysis of all randomized double-blind studies until December 1996). *Nephrol Dial Transplant* 1998; 13(3):564-569.

307 Marian AJ. Experimental therapies in hypertrophic cardiomyopathy. *J Cardiovasc Transl Res* 2009; 2(4):483-492.

308 Fabris B, Candido R, Bortoletto M, Zentilin L, Sandri M, Fior F*, et al.* Dose and time-dependent apoptotic effects by angiotensin II infusion on left ventricular cardiomyocytes. *J Hypertens* 2007; 25(7):1481-1490.

309 Yasui H, Gabazza EÄ, Tamaki S, Kobayashi T, Hataji O, Yuda H*, et al.* Intratracheal Administration of Activated Protein C Inhibits Bleomycin-induced Lung Fibrosis in the Mouse. *American Journal of Respiratory and Critical Care Medicine* 2001; 163(7):1660-1668.

310 Kisiel W, Canfield WM, Ericsson LH, Davie EW. Anticoagulant properties of bovine plasma protein C following activation by thrombin. *Biochemistry* 1977; 16(26):5824-5831.

311 Bezuhly M, Morris SF, Juskevicius R, Currie RW, West KA, Liwski RS. Activated protein C improves ischemic flap survival and modulates proangiogenic and antiinflammatory gene expression. *Plast Reconstr Surg* 2009; 123(2):502-515.

312 Neyrinck AP, Liu KD, Howard JP, Matthay MA. Protective mechanisms of activated protein C in severe inflammatory disorders. *Br J Pharmacol* 2009; 158(4):1034-1047.

313 Bernard GR, Vincent J-L, Laterre P-F, LaRosa SP, Dhainaut J-F, Lopez-Rodriguez A*, et al.* Efficacy and Safety of Recombinant Human Activated Protein C for Severe Sepsis. *New England Journal of Medicine* 2001; 344(10):699-709.

314 Bernard GR, Margolis BD, Shanies HM, Ely EW, Wheeler AP, Levy H*, et al.* Extended evaluation of recombinant human activated protein C United States Trial (ENHANCE US): a single-arm, phase 3B, multicenter study of drotrecogin alfa (activated) in severe sepsis. *Chest* 2004; 125(6):2206-2216.

315 Dillon JP, Laing AJ, Cahill RA, O'Brien GC, Street JT, Wang JH*, et al.* Activated protein C attenuates acute ischaemia reperfusion injury in skeletal muscle. *J Orthop Res* 2005; 23(6):1454-1459.

316 Mizutani A, Okajima K, Uchiba M, Noguchi T. Activated protein C reduces ischemia/reperfusion-induced renal injury in rats by inhibiting leukocyte activation. *Blood* 2000; 95(12):3781-3787.

317 Pirat B, Muderrisoglu H, Unal MT, Ozdemir H, Yildirir A, Yucel M*, et al.* Recombinant human-activated protein C inhibits cardiomyocyte apoptosis in a rat model of myocardial ischemia-reperfusion. *Coron Artery Dis* 2007; 18(1):61-66.

318 Vincent JL, Bernard GR, Beale R, Doig C, Putensen C, Dhainaut JF*, et al.* Drotrecogin alfa (activated) treatment in severe sepsis from the global open-label trial ENHANCE: further evidence for survival and safety and implications for early treatment. *Crit Care Med* 2005; 33(10):2266-2277.

319 Minhas N, Xue M, Fukudome K, Jackson CJ. Activated protein C utilizes the angiopoietin/Tie2 axis to promote endothelial barrier function. *The FASEB Journal* 2010; 24(3):873-881.

320 Cheng T, Liu D, Griffin JH, Fernandez JA, Castellino F, Rosen ED*, et al.* Activated protein C blocks p53-mediated apoptosis in ischemic human brain endothelium and is neuroprotective. *Nat Med* 2003; 9(3):338-342.

321 Ding JW, Tong XH, Yang J, Liu ZQ, Zhang Y, Li S*, et al.* Activated protein C protects myocardium via activation of anti-apoptotic pathways of survival in ischemia-reperfused rat heart. *J Korean Med Sci* 2010; 25(11):1609-1615.

322 Bezuhly M, Cullen R, Esmon CT, Morris SF, West KA, Johnston B*, et al.* Role of activated protein C and its receptor in inhibition of tumor metastasis. *Blood* 2009; 113(14):3371-3374.

323 Ireland H, Kunz G, Kyriakoulis K, Stubbs PJ, Lane DA. Thrombomodulin gene mutations associated with myocardial infarction. *Circulation* 1997; 96(1):15-18.

324 Samani NJ, Lodwick D, Martin D, Kimber P. Resistance to activated protein C and risk of premature myocardial infarction. *Lancet* 1994; 344(8938):1709-1710.

325 Kelly DJ, Cox AJ, Gow RM, Zhang Y, Kemp BE, Gilbert RE. Platelet-Derived Growth Factor Receptor Transactivation Mediates the Trophic Effects of Angiotensin II In Vivo. *Hypertension* 2004; 44(2):195-202.

326 Esmon CT. The endothelial protein C receptor. *Current Opinion in Hematology* 2006; 13(5):382-385

327 Lindahl U, Backstrom G, Hook M, Thunberg L, Fransson LA, Linker A. Structure of the antithrombin-binding site in heparin. *Proc Natl Acad Sci U S A* 1979; 76(7):3198-3202.

328 Pereira C, Schaer DJ, Bachli EB, Kurrer MO, Schoedon G. Wnt5A/CaMKII signaling contributes to the inflammatory response of macrophages and is a target for the antiinflammatory action of activated protein C and interleukin-10. *Arterioscler Thromb Vasc Biol* 2008; 28(3):504-510.

329 Sturn DH, Kaneider NC, Feistritzer C, Djanani A, Fukudome K, Wiedermann CJ. Expression and function of the endothelial protein C receptor in human neutrophils. *Blood* 2003; 102(4):1499-1505.

330 van Sluis GL, Brüggemann LW, Esmon CT, Kamphuisen PW, Richel DJ, Büller HR*, et al.* Endogenous activated protein C is essential for immune-mediated cancer cell elimination from the circulation. *Cancer letters* 2011; 306(1):106-110.

331 Galligan L, Livingstone W, Volkov Y, Hokamp K, Murphy C, Lawler M*, et al.* Characterization of protein C receptor expression in monocytes. *Br J Haematol* 2001; 115(2):408-414.

332 Gillibert-Duplantier J, Rullier A, Neaud V, Kisiel W, Rosenbaum J. Liver myofibroblasts activate protein C and respond to activated protein C. *World J Gastroenterol* 2010; 16(2):210-216.

333 Xue M, March L, Sambrook PN, Fukudome K, Jackson CJ. Endothelial protein C receptor is overexpressed in rheumatoid arthritic (RA) synovium and mediates the anti-inflammatory effects of activated protein C in RA monocytes. *Ann Rheum Dis* 2007; 66(12):1574-1580.

334 Doughty RN, Rodgers A, Sharpe N, MacMahon S. Effects of beta-blocker therapy on mortality in patients with heart failure. A systematic overview of randomized controlled trials. *Eur Heart J* 1997; 18(4):560-565.

335 Nadal-Ginard B, Kajstura J, Leri A, Anversa P. Myocyte death, growth, and regeneration in cardiac hypertrophy and failure. *Circ Res* 2003; 92(2):139-150.

336 Pfeffer JM, Pfeffer MA, Fletcher PJ, Braunwald E. Progressive ventricular remodeling in rat with myocardial infarction. *Am J Physiol* 1991; 260(5 Pt 2):H1406-1414.

337 Pfeffer MA, Braunwald E. Ventricular remodeling after myocardial infarction. Experimental observations and clinical implications. *Circulation* 1990; 81(4):1161-1172.

338 Gill M, Dias S, Hattori K, Rivera ML, Hicklin D, Witte L*, et al.* Vascular Trauma Induces Rapid but Transient Mobilization of VEGFR2+AC133+ Endothelial Precursor Cells. *Circulation Research* 2001; 88(2):167-174.

339 Sun Y, Yi D, Wang Y, Zheng R, Sun G, Wang J*, et al.* Age-dependent mobilization of circulating endothelial progenitor cells in infants and young children undergoing cardiac surgery with cardiopulmonary bypass. *Cytokine* 2009; 47(3):206-213.

340 Bucala R, Spiegel LA, Chesney J, Hogan M, Cerami A. Circulating fibrocytes define a new leukocyte subpopulation that mediates tissue repair. *Mol Med* 1994; 1(1):71-81.

341 Pilling D, Tucker NM, Gomer RH. Aggregated IgG inhibits the differentiation of human fibrocytes. *J Leukoc Biol* 2006; 79(6):1242-1251.

342 Hartlapp I, Abe R, Saeed RW, Peng T, Voelter W, Bucala R*, et al.* Fibrocytes induce an angiogenic phenotype in cultured endothelial cells and promote angiogenesis in vivo. *FASEB J* 2001; 15(12):2215-2224.

343 Kao H-K, Chen B, Murphy GF, Li Q, Orgill DP, Guo L. Peripheral Blood Fibrocytes: Enhancement of Wound Healing by Cell Proliferation, Re-Epithelialization, Contraction, and Angiogenesis. *Annals of Surgery* 2011; 254(6):1066-1074

344 Schmidt M, Sun G, Stacey MA, Mori L, Mattoli S. Identification of Circulating Fibrocytes as Precursors of Bronchial Myofibroblasts in Asthma. *J Immunol* 2003; 171(1):380-389.

345 Vannella KM, McMillan TR, Charbeneau RP, Wilke CA, Thomas PE, Toews GB*, et al.* Cysteinyl Leukotrienes Are Autocrine and Paracrine Regulators of Fibrocyte Function. *J Immunol* 2007; 179(11):7883-7890.

346 Fujiwara A, Kobayashi H, Masuya M, Maruyama M, Nakamura S, Ibata H*, et al.* Correlation between circulating fibrocytes, and activity and progression of interstitial lung diseases. *Respirology* 2012; 17(4):693-698.

347 Wang C-H, Huang C-D, Lin H-C, Huang T-T, Lee K-Y, Lo Y-L*, et al.* Increased activation of fibrocytes in patients with chronic obstructive asthma through an epidermal growth factor receptor‚Äìdependent pathway. *Journal of Allergy and Clinical Immunology* 2012; (0).

348 Yang L, Scott PG, Giuffre J, Shankowsky HA, Ghahary A, Tredget EE. Peripheral blood fibrocytes from burn patients: identification and quantification of fibrocytes in adherent cells cultured from peripheral blood mononuclear cells. *Lab Invest* 2002; 82(9):1183-1192.

349 Gandhi PS, Goyal RK, Jain AR, Mallya BS, Gupta VM, Shah DS*, et al.* Beneficial effects of carvedilol as a concomitant therapy to angiotensin-converting enzyme inhibitor in patients with ischemic left ventricular systolic dysfunction. *Canadian Journal of Physiology & Pharmacology* 2007; 85(2):193-199.

350 Gelinas L, Falkenham A, Oxner A, Sopel M, Legare JF. Highly purified human peripheral blood monocytes produce IL-6 but not TNF{alpha} in response to angiotensin II. *J Renin Angiotensin Aldosterone Syst* 2011; 12(3):295-303.

351 Fang L, Moore X-L, Chan W, White DA, Chin-Dusting J, Dart AM. Decreased Fibrocyte Number is Associated with Atherosclerotic Plaque Instability in Man. *Cardiovascular Research* 2012.

352 Wang C-H, Huang C-D, Lin H-C, Lee K-Y, Lin S-M, Liu C-Y*, et al.* Increased Circulating Fibrocytes in Asthma with Chronic Airflow Obstruction. *American Journal of Respiratory and Critical Care Medicine* 2008; 178(6):583-591.

353 Pilling D, Buckley CD, Salmon M, Gomer RH. Inhibition of Fibrocyte Differentiation by Serum Amyloid P. *J Immunol* 2003; 171(10):5537-5546.

354 Varcoe RL, Mikhail M, Guiffre AK, Pennings G, Vicaretti M, Hawthorne WJ*, et al.* The role of the fibrocyte in intimal hyperplasia. *Journal of Thrombosis and Haemostasis* 2006; 4(5):1125-1133.

355 Yeager ME, Nguyen CM, Belchenko DD, Colvin KL, Takatsuki S, Ivy DD*, et al.* Circulating fibrocytes are increased in children and young adults with pulmonary hypertension. *Eur Respir J* 2012; 39(1):104-111.

356 Hein S, Arnon E, Kostin S, Schonburg M, Elsasser A, Polyakova V*, et al.* Progression From Compensated Hypertrophy to Failure in the Pressure-Overloaded Human Heart: Structural Deterioration and Compensatory Mechanisms. *Circulation* 2003; 107(7):984-991.

357 Butler J, Rocker GM, Westaby S. Inflammatory response to cardiopulmonary bypass. *The Annals of Thoracic Surgery* 1993; 55(2):552-559.

358 Sun L, Louie MC, Vannella KM, Wilke CA, LeVine AM, Moore BB*, et al.* New concepts of IL-10-induced lung fibrosis: fibrocyte recruitment and M2 activation in a CCL2/CCR2 axis. *American Journal of Physiology - Lung Cellular and Molecular Physiology* 2010; 300(3):L341-L353.

359 Mori L, Bellini A, Stacey MA, Schmidt M, Mattoli S. Fibrocytes contribute to the myofibroblast population in wounded skin and originate from the bone marrow. *Experimental Cell Research* 2005; 304(1):81-90.

360 Kania G, Blyszczuk P, Stein S, Valaperti A, Germano D, Dirnhofer S*, et al.* Heart-Infiltrating Prominin-1+/CD133+ Progenitor Cells Represent the Cellular Source of Transforming Growth Factor {beta}-Mediated Cardiac Fibrosis in Experimental Autoimmune Myocarditis. *Circ Res* 2009; 105(5):462-470.

361 Légaré J-F, Oxner A, Heimrath O, Issekutz T. Infiltration of polymorphonuclear cells into the post-ischaemic myocardium is dependent on β2 and α4 integrins. *International Journal of Experimental Pathology* 2007; 88(4):291-300.

362 Xiao HD, Fuchs S, Campbell DJ, Lewis W, Dudley Jr SC, Kasi VS*, et al.* Mice with Cardiac-Restricted Angiotensin-Converting Enzyme (ACE) Have Atrial Enlargement, Cardiac Arrhythmia, and Sudden Death. *The American Journal of Pathology* 2004; 165(3):1019-1032.

363 Rocha R, Martin-Berger CL, Yang P, Scherrer R, Delyani J, McMahon E. Selective Aldosterone Blockade Prevents Angiotensin II/Salt-Induced Vascular Inflammation in the Rat Heart. *Endocrinology* 2002; 143(12):4828-4836.

364 Campbell SE, Janicki JS, Weber KT. Temporal differences in fibroblast proliferation and phenotype expression in response to chronic administration of angiotensin II or aldosterone. *J Mol Cell Cardiol* 1995; 27:1545-1560.

365 Campbell SE, Janicki JS, Weber KT. Temporal differences in fibroblast proliferation and phenotype expression in response to chronic administration of angiotensin II or aldosterone. *Journal of Molecular and Cellular Cardiology* 1995; 27(8):1545-1560.

366 Rocha R, Rudolph AE, Frierdich GE. Aldosterone induces a vascular inflammatory phenotype in the rat heart. *Am J Physiol Heart Circ Physiol* 2002; 283:H1802-H1810.

367 Kai H, Mori T, Tokuda K, Takayama N, Tahara N, Takemiya K*, et al.* Pressure Overload-Induced Transient Oxidative Stress Mediates Perivascular Inflammation and Cardiac Fibrosis through Angiotensin II. *Hypertens Res* 2006; 29(9):711-718.

368 Tokuda K, Kai H, Kuwahara F, Yasukawa H, Tahara N, Kudo H*, et al.* Pressure-Independent Effects of Angiotensin II on Hypertensive Myocardial Fibrosis. *Hypertension* 2004; 43(2):499-503.

369 Xia Y, Lee K, Li N, Corbett D, Mendoza L, Frangogiannis N. Characterization of the inflammatory and fibrotic response in a mouse model of cardiac pressure overload. *Histochemistry and Cell Biology* 2009; 131(4):471-481.

370 Choi YH, Burdick MD, Strieter RM. Human circulating fibrocytes have the capacity to differentiate osteoblasts and chondrocytes. *The International Journal of Biochemistry & Cell Biology* 2010; 42(5):662-671.

371 Hong KM, Burdick MD, Phillips RJ, Heber D, Strieter RM. Characterization of human fibrocytes as circulating adipocyte progenitors and the formation of human adipose tissue in SCID mice. *The FASEB Journal* 2005; 19(14):2029-2031.

372 Yang L, Scott PG, Dodd C, Medina A, Jiao H, Shankowsky HA*, et al.* Identification of fibrocytes in postburn hypertrophic scar. *Wound Repair Regen* 2005; 13(4):398-404.

373 Douglas RS, Afifiyan NF, Hwang CJ, Chong K, Haider U, Richards P*, et al.* Increased Generation of Fibrocytes in Thyroid-Associated Ophthalmopathy. *Journal of Clinical Endocrinology & Metabolism* 2010; 95(1):430-438.

374 Garcia-de-Alba C, Becerril C, Ruiz V, Gonzalez Y, Reyes S, Garcia-Alvarez J*, et al.* Expression of Matrix Metalloproteases by Fibrocytes. Possible Role in Migration and Homing. *Am J Respir Crit Care Med* 2010:201001-200028OC.

375 Barrientos S, Stojadinovic O, Golinko MS, Brem H, Tomic-Canic M. Growth factors and cytokines in wound healing. *Wound Repair & Regeneration* 2008; 16(5):585-601.

376 Alon R, Chen S, Puri KD, Finger EB, Springer TA. The Kinetics of L-selectin Tethers and the Mechanics of Selectin-mediated Rolling. *The Journal of Cell Biology* 1997; 138(5):1169-1180.

377 Hyduk SJ, Cybulsky MI. Role of α4β1 Integrins in Chemokine-Induced Monocyte Arrest under Conditions of Shear Stress. *Microcirculation* 2009; 16(1):17-30.

378 Paul J. Establishment of Permanent Cell Strains from Human Adult Peripheral Blood. *Nature* 1958; 182(4638):808-808.

379 Pilling D, Roife D, Wang M, Ronkainen SD, Crawford JR, Travis EL*, et al.* Reduction of Bleomycin-Induced Pulmonary Fibrosis by Serum Amyloid P. *The Journal of Immunology* 2007; 179(6):4035-4044.

380 Oh SJ, Kurz H, Christ B, Wilting J. Platelet-derived growth factor-B induces transformation of fibrocytes into spindle-shaped myofibroblasts in vivo. *Histochemistry and Cell Biology* 1998; 109(4):349-357.

381 Chesney J, Bacher M, Bender A, Bucala R. The peripheral blood fibrocyte is a potent antigen-presenting cell capable of priming naive T cells in situ. *Proc Natl Acad Sci U S A* 1997; 94(12):6307-6312.

382 Balmelli C, Ruggli N, McCullough K, Summerfield A. Fibrocytes are potent stimulators of anti-virus cytotoxic T cells. *J Leukoc Biol* 2005; 77(6):923-933.

383 Guzik TJ, Hoch NE, Brown KA, McCann LA, Rahman A, Dikalov S*, et al.* Role of the T cell in the genesis of angiotensin II induced hypertension and vascular dysfunction. *J Exp Med* 2007; 204(10):2449-2460.

384 Jourdan-LeSaux C, Zhang J, Lindsey ML. Extracellular matrix roles during cardiac repair. *Life Sciences* 2010; 87(13,Äì14):391-400.

APPENDIX 1 – SUPPLEMENTARY FIGURES

Table A1: Cell Specific Markers used to Identify Fibrocytes

Progenitor	Leukocyte	Mesenchymal
CD133 GFP* CD34	CD45	αSMA Vimentin Collagen

Combination of these either a progenitor or a leukocyte marker with a mesenchymal marker was used to identifya fibrocyte phenotype in the above studies.

*GFP was used as a marker of bone marrow origin in GFP chimera animals and not specifically as a progenitor marker.

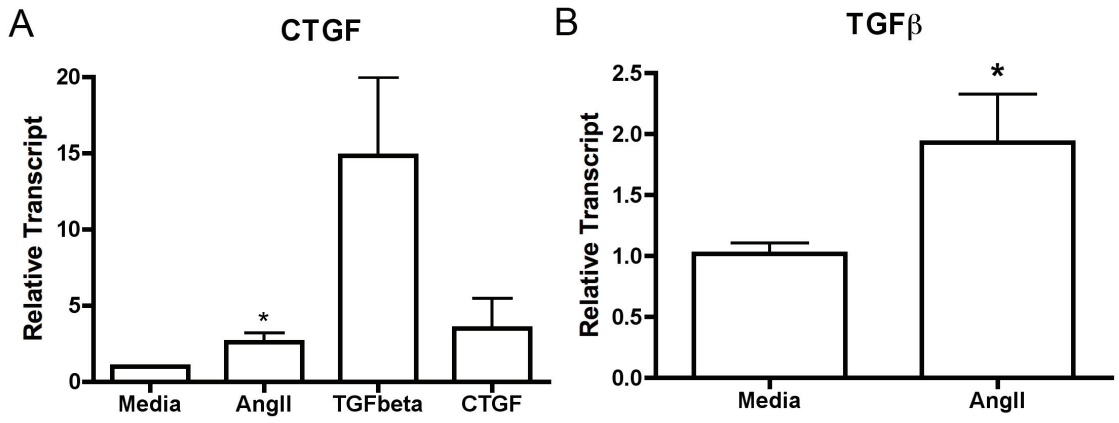

Figure A1 CTGF and TGFβ Expression by Cultured Fibrocytes

Preliminary data from studies stimulating *in vitro* cultures of fibrocyte rich populations isolated from AngII exposed hearts with various pro-fibrotic stimuli. AngII stimulation significantly increased CTGF and TGFβ transcript levels. TGFβ and CTGF also appear to increase transcript levels of CTGF but did not reach statistical difference. * $p \leq 0.05$

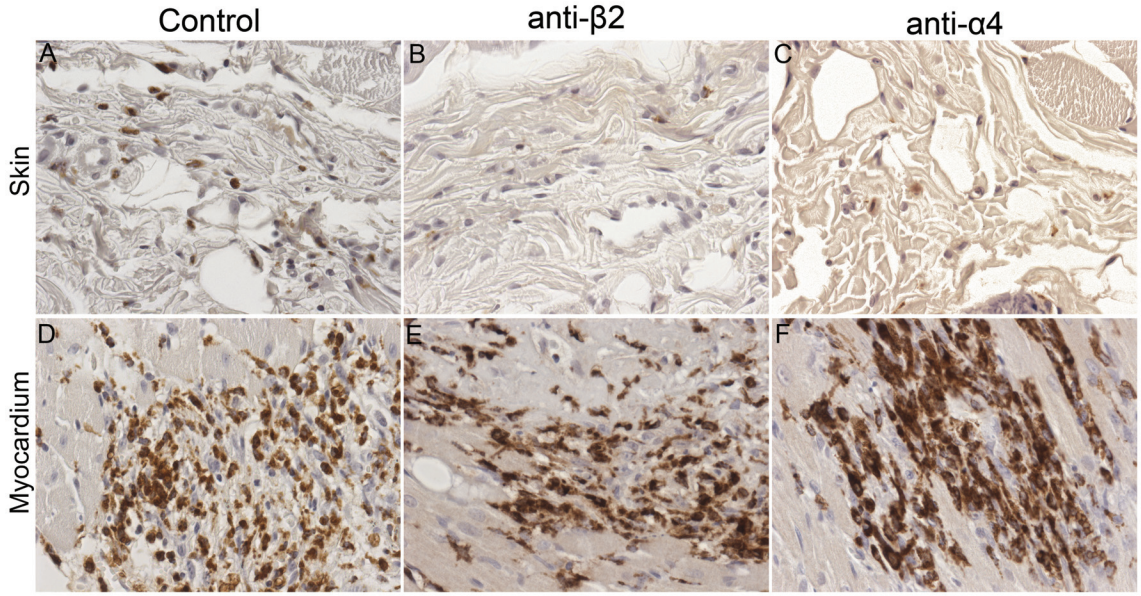

Figure A2 Blocking β2 and α4 Integrins during AngII Infusion

In an attempt to inhibit fibrocyte infiltration into the myocardium, we administered anti-2 and anti-α4 antibodies at the beginning of AngII treatment as previously shown {101). LPS was also injected into two dermal sites as a positive control for macrophage migration (A-C). Infiltration of ED-1 positive cells into the LPS injection sites is reduced when animals are given either blocking antibody (B, C) compared to animals treated with a non-specific antibody (A). This suggests that these antibodies partially inhibit infiltration of what is believe to be ED-1 macrophages and that they use β2 and α4 to traffick into tissue sites. However, infiltration of ED-1 positive cells into the heart is not inhibited by by either blocking antibody (D-E). This suggests that the infiltrating cells within the AngII exposed hearts, shown to be fibrocytes, do not appear to use β2 or α4 to extravasate into tissues. Note: The control heart presented has not been treated with a control antibody, but was only infused with AngII. It was in the opinion of this author

that the histology seen in myocardium of control antibody treated animal was not representative of typical cellular infiltration. Skin micrographs were taken at 20x magnification and micrgraphs of hearts were taken at 40x magnification.

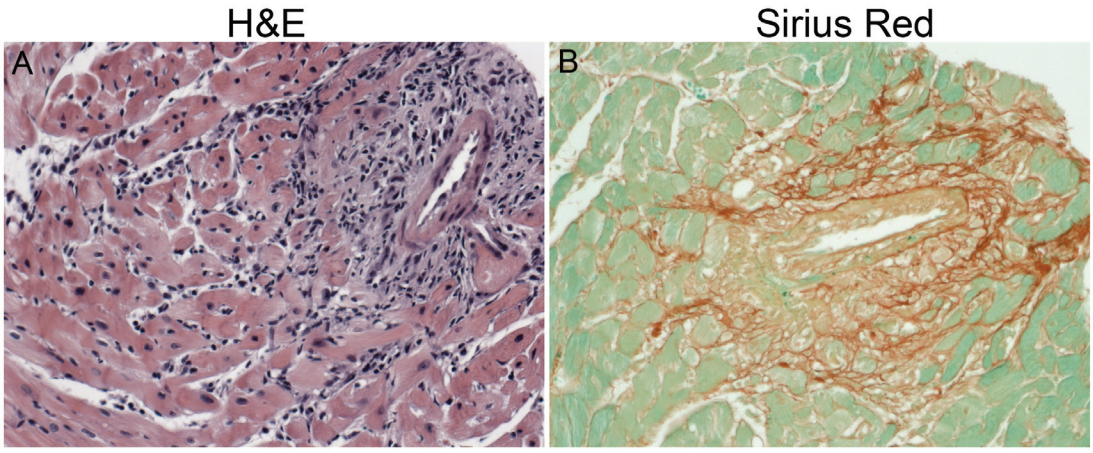

Figure A3 AngII Infusion in RAG KO Animals

AngII was infused into RAG knockout animals, which do not have function T or B cells, for 7d. Comparable cellular infiltration and fibrosis was evident in these animals by H&E (A) and Sirius Red (B) staining. This data suggests that T and B cells likely do not play a significant role in promoting AngII-mediated myocardial fibrosis. Images taken at 20x magnification.

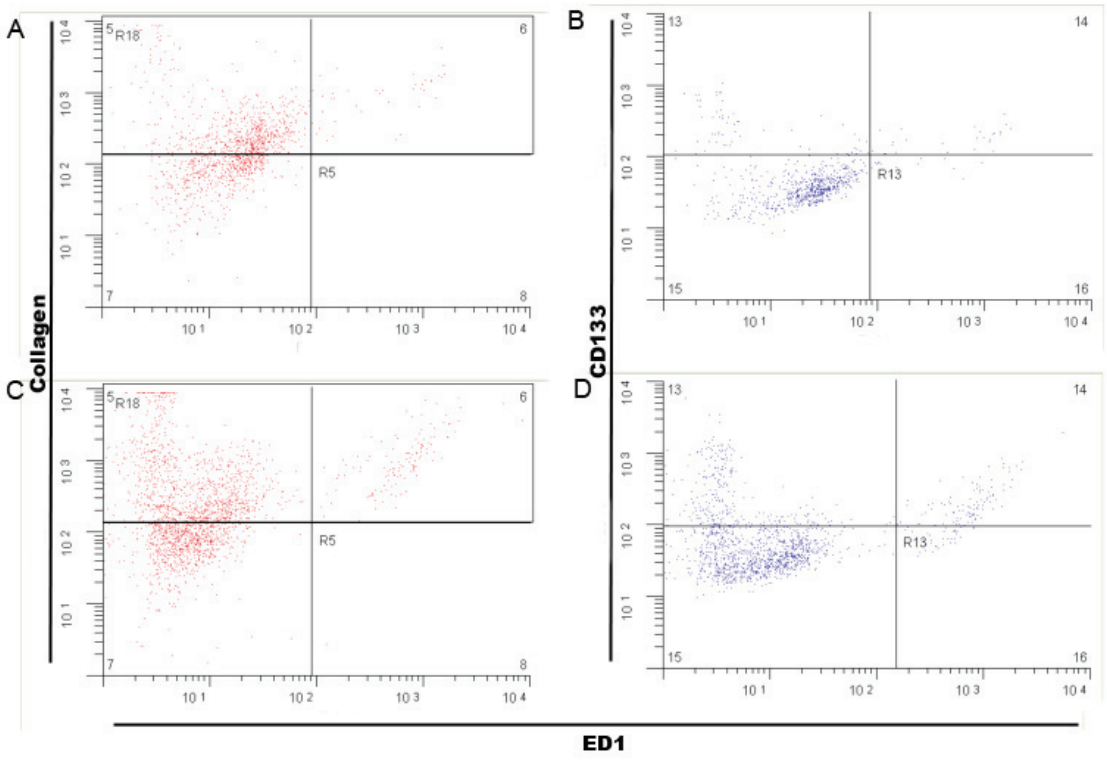

Figure A4 Dual Staining Scatterplot for Data Depicted in Figure 3.6

Representative scatterplots obtained by processing freshly isolated cells from the myocardium of naïve (A, B) and AngII exposed (C, D) animals. Dual staining for ED1 and Collagen (A, C) as well as ED1 and CD133 (B, D) are shown.

APPENDIX 2 – AUTHOR CONTRIBUTIONS FOR PRESENTED MANUSCRIPTS

Chapter 2 – Myocardial Fibrosis in Response to Angiotensin II is Preceded by the Recruitment of Mesenchymal Progenitor Cells

Author	Specific Contributions	Figures Provided
Mryanda Sopel	• Assisted with project design • Animal work including surgeries, blood pressure measurements, tissue harvesting and processing • Histologic staining, analysis and quantification • Immunohistochemistry and immunofluorescent staining and analysis (technical assistance from Tanya Myers) • Gene expression studies • Cell isolation, culture and analysis (technical assistance from Tanya Myers) • Analyzed data, constructed figures and wrote manuscript • Editted and submitted manuscript	2.1, 2.2, 2.3, 2.4, 2.5, 2.6, 2.7, 2.9
Nicole Rosin	• Generated GFP chimera animals and completed AngII infusion and analysis in these animals • Asissted with cell isolation protocol	2.8

Chapter 3 – Fibroblast Progenitor Cells are Recruited into the Myocardium Prior to the Development of Myocardial Fibrosis

Author	Specific Contributions	Figures Provided
Mryanda Sopel	• Assisted with project design • Animal work including surgeries, blood pressure measurements, tissue harvesting and processing • Histologic staining, analysis and quantification • Immunohistochemistry and immunofluorescent staining and analysis (technical assistance from Tanya Myers) • Cell isolation, culture and analysis (technical assistance from Tanya Myers) • Analyzed data, constructed figures and wrote manuscript • Editted and submitted manuscript	3.1, 3.4, 3.5, 3.6, 3.7, S3.1
Alec Falkenham	• Histologic staining • Assisted with Immunhistochemistry • Asissted with cell isolation protocol	
Adam Oxner	• Assisted with project design • Animal work including surgeries, blood pressure measurements, tissue harvesting and processing • Histologic staining, analysis and quantification • Provided ED-1 immunohistochemistry	3.2, 3.3
Irene Ma	• Gene expression studies	3.3

Chapter 4 – Fibroblast Progenitor Cell Migration to the AngII Exposed Myocardium is Not CXCL12- or CCL2-Dependent

Author	Specific Contributions	Figures Provided
Alec Falkenham	• Assisted with project design • Animal work including surgeries, blood pressure measurements, tissue harvesting and processing • Histologic staining, analysis and quantification • Immunohistochemistry and immunofluorescent staining and analysis (technical assistance from Tanya Myers) • Cell isolation, culture and analysis • Analyzed data, constructed figures and wrote manuscript • Editted and submitted manuscript	4.1, 4.2, 4.3, 4.4, 4.5, 4.6, 4.7, 4.8, S4.1, S4.2
Mryanda Sopel	• Histologic staining • Gene expression studies	4.1, 4.5
Nicole Rosin	• Assisted with migration studies • Gene expression studies	4.1, 4.5

Chapter 5 – The Regulation and Role of Connective Tissue Growth Factor in AngII Induced Myocardial Fibrosis

Author	Specific Contributions	Figures Provided
Nicole Rosin	• Assisted with project design • Animal work including surgeries, blood pressure measurements, tissue harvesting and processing • Histologic staining, analysis and quantification • Immunohistochemistry and immunofluorescent staining and analysis (technical assistance from Tanya Myers) • Cell isolation, culture and analysis • Analyzed data, constructed figures and wrote manuscript • Editted and submitted manuscript	5.1, 5.2, 5.3, 5.4, 5.5, 5.6, 5.7
Alec Falkenham	• Animal work including surgeries and tissue harvesting • Histologic staining • Assisted with cell isolation and analysis	5.4
Mryanda Sopel	• Animal work including surgeries and tissue harvesting • Assisted with migration studies • Gene expression studies (CTGF, TGFbeta) • Assisted with cell isolation	5.3

Chapter 6 – Myocardial Migration by Fibroblast Progenitor Cells is Blood Pressure Dependent in a Model of AngII Myocardial Fibrosis

Author	Specific Contributions	Figures Provided
Nicole Rosin	• Assisted with project design • Gene expression studies • Completed *in vitro* studies • Analyzed data, constructed figures and jointly wrote manuscript • Editted and submitted manuscript	6.2, 6.5, 6.6, 6.7, 6.8
Mryanda Sopel	• Assisted with project design • Animal work including surgeries, blood pressure measurements, tissue harvesting and processing • Histologic staining, analysis and quantification • Immunohistochemistry staining (technical assistance from Tanya Myers) • Assisted with cell isolation and analysis	6.1, 6.2, 6.3, 6.4
Alec Falkenham	• Assisted with the animal work including surgeries and tissue harvesting • Histologic staining	

Chapter 7 – Treatment with Activated Protein C (aPC) is Protective During the Development of Myocardial Fibrosis

Author	Specific Contributions	Figures Provided
Mryanda Sopel	• Assisted with project design • Animal work including surgeries, blood pressure measurements, tissue harvesting and processing • Histologic staining, analysis and quantification • Immunohistochemistry and immunofluorescent staining and analysis • Gene expression studies • Analyzed data, constructed figures and wrote manuscript • Editted and submitted manuscript	7.1, 7.2, 7.3, 7.4, 7.5
Nicole Rosin	• Completed cell isolation, culture and analysis • Assisted the gene expression study	7.6
Alec Falkenham	• Assisted with the animal work including surgeries and tissue harvesting • Histologic staining	

Chapter 8 – Circulating Fibrocyte Levels in Patients with Ischemic Heart Disease – Preliminary Findings

Author	Specific Contributions	Figures Provided
Mryanda Sopel	• Assisted with project design • Wrote Research Ethics Board submission • Aquired blood samples • Isolated WBC and processed for flow cytometry • Processed *in vitro* cultures • Preformed immunofluorescent staining • Analyzed data, constructed figures and wrote up results	8.1, 8.2, 8.3, 8.4,
Alec Falkenham	• Preformed most PBMC isolations and initiated *in vitro* cultures	

APPENDIX 3 – COPYRIGHT PERMISSION LETTERS

RightsLink®

Home | Account Info | Help

Title: Myocardial fibrosis in response to Angiotensin II is preceded by the recruitment of mesenchymal progenitor cells

Author: Mryanda J Sopel, Nicole L Rosin, Timothy DG Lee, Jean-Francois Légaré

Publication: Laboratory Investigation

Publisher: Nature Publishing Group

Date: Nov 29, 2010

Logged in as:
Mryanda Sopel
LOGOUT

Author Request

If you are the author of this content (or his/her designated agent) please read the following. If you are not the author of this content, please click the Back button and select an alternative Requestor Type to obtain a quick price or to place an order.

Ownership of copyright in the article remains with the Authors, and provided that, when reproducing the Contribution or extracts from it, the Authors acknowledge first and reference publication in the Journal, the Authors retain the following non-exclusive rights:

a) To reproduce the Contribution in whole or in part in any printed volume (book or thesis) of which they are the author(s).

b) They and any academic institution where they work at the time may reproduce the Contribution for the purpose of course teaching.

c) To reuse figures or tables created by them and contained in the Contribution in other works created by them.

d) To post a copy of the Contribution as accepted for publication after peer review (in Word or Text format) on the Author's own web site, or the Author's institutional repository, or the Author's funding body's archive, six months after publication of the printed or online edition of the Journal, provided that they also link to the Journal article on NPG's web site (eg through the DOI).

NPG encourages the self-archiving of the accepted version of your manuscript in your funding agency's or institution's repository, six months after publication. This policy complements the recently announced policies of the US National Institutes of Health, Wellcome Trust and other research funding bodies around the world. NPG recognises the efforts of funding bodies to increase access to the research they fund, and we strongly encourage authors to participate in such efforts.

Authors wishing to use the published version of their article for promotional use or on a web site must request in the normal way.

If you require further assistance please read NPG's online author reuse guidelines.

For full paper portion: Authors of original research papers published by NPG are encouraged to submit the author's version of the accepted, peer-reviewed manuscript to their relevant funding body's archive, for release six months after publication. In addition, authors are encouraged to archive their version of the manuscript in their institution's repositories (as well as their personal Web sites), also six months after original publication.

v2.0

BACK CLOSE WINDOW

If you require further assistance please read NPG's online author reuse guidelines.

For full paper portion: Authors of original research papers published by NPG are encouraged to submit the author's version of the accepted, peer-reviewed manuscript to their relevant funding body's archive, for release six months after publication. In addition, authors are encouraged to archive their version of the manuscript in their institution's repositories (as well as their personal Web sites), also six months after original publication.

v2.0

BACK CLOSE WINDOW

FW: Permission Request Form Canada

Permission Requests - UK <permissionsuk@wiley.com>

To: Adam Oxner <msopel@dal.ca>

Dear Mryanda Sopel,

Thank you for your email request.

Permission is granted for you to use the material requested for your thesis/dissertation subject to the usual acknowledgements and on the understanding that you will reapply for permission if you wish to distribute or publish your thesis/dissertation commercially.

Permission is granted solely for use in conjunction with the thesis, and the article may not be posted online separately.

Any third party material is expressly excluded from this permission. If any material appears within the article with credit to another source, authorisation from that source must be obtained.

Best Wishes

Verity Butler
Permissions Assistant
John Wiley & Sons Ltd.

Original Message